**U.S. DEPARTMENT OF COMMERCE**
**National Technical Information Service**

PB-260 478

# Studies of the Pressurized Fluidized-Bed Coal Combustion Process

**Exxon Research and Engineering Co, Linden, N J**

**Prepared for**

**Industrial Environmental Research Lab, Research Triangle Park, N C**

Sep 76

PB 260 478

EPA
U.S. Environmental Protection Agency
Office of Research and Development

Industrial Environmental Research
Laboratory
Research Triangle Park, N.C. 27711

EPA-600/7-76-011
September 1976

# STUDIES OF THE PRESSURIZED FLUIDIZED-BED COAL COMBUSTION PROCESS

Interagency
Energy-Environment
Research and Development
Program Report

REPRODUCED BY
NATIONAL TECHNICAL
INFORMATION SERVICE
U. S. DEPARTMENT OF COMMERCE
SPRINGFIELD, VA. 22161

## RESEARCH REPORTING SERIES

Research reports of the Office of Research and Development, U.S. Environmental Protection Agency, have been grouped into seven series. These seven broad categories were established to facilitate further development and application of environmental technology. Elimination of traditional grouping was consciously planned to foster technology transfer and a maximum interface in related fields. The seven series are:

1. Environmental Health Effects Research
2. Environmental Protection Technology
3. Ecological Research
4. Environmental Monitoring
5. Socioeconomic Environmental Studies
6. Scientific and Technical Assessment Reports (STAR)
7. Interagency Energy-Environment Research and Development

This report has been assigned to the INTERAGENCY ENERGY-ENVIRONMENT RESEARCH AND DEVELOPMENT series. Reports in this series result from the effort funded under the 17-agency Federal Energy/Environment Research and Development Program. These studies relate to EPA's mission to protect the public health and welfare from adverse effects of pollutants associated with energy systems. The goal of the Program is to assure the rapid development of domestic energy supplies in an environmentally--compatible manner by providing the necessary environmental data and control technology. Investigations include analyses of the transport of energy-related pollutants and their health and ecological effects; assessments of, and development of, control technologies for energy systems; and integrated assessments of a wide range of energy-related environmental issues.

## REVIEW NOTICE

This report has been reviewed by the participating Federal Agencies, and approved for publication. Approval does not signify that the contents necessarily reflect the views and policies of the Government, nor does mention of trade names or commercial products constitute endorsement or recommendation for use.

This document is available to the public through the National Technical Information Service, Springfield, Virginia 22161.

**TECHNICAL REPORT DATA**
*(Please read Instructions on the reverse before completing)*

| | | |
|---|---|---|
| 1. REPORT NO.<br>EPA-600/7-76-011 | 2. | 3. RECIPIENT'S ACCESSION NO.<br>PB-260 478 |
| 4. TITLE AND SUBTITLE STUDIES OF THE PRESSURIZED FLUIDIZED-BED COAL COMBUSTION PROCESS | | 5. REPORT DATE<br>September 1976<br>6. PERFORMING ORGANIZATION CODE |
| 7. AUTHOR(S) R. C. Hoke, R. R. Bertrand, M. S. Nutkis, D. D. Kinzler, L. A. Ruth, and M. W. Gregory | | 8. PERFORMING ORGANIZATION REPORT NO.<br>GRU. 15GFGS. 76 |
| 9. PERFORMING ORGANIZATION NAME AND ADDRESS<br>Exxon Research and Engineering Company<br>P.O. Box 8<br>Linden, New Jersey 07036 | | 10. PROGRAM ELEMENT NO.<br>EHE623A<br>11. CONTRACT/GRANT NO.<br>68-02-1312 and -1451 |
| 12. SPONSORING AGENCY NAME AND ADDRESS<br>EPA, Office of Research and Development<br>Industrial Environmental Research Laboratory<br>Research Triangle Park, NC 27711 | | 13. TYPE OF REPORT AND PERIOD COVERED<br>Phase; 8/73-8/75<br>14. SPONSORING AGENCY CODE<br>EPA-ORD |

15. SUPPLEMENTARY NOTES IERL-RTP project officer for this report is D. B. Henschel, Mail Drop 61, 919/549-8411 Ext 2825. APTD 1116 and EPA-650/2-74-001 (NTIS PB 210-246 and 231-374) are earlier EPA reports relating to this work.

16. ABSTRACT

The report gives results of studies of the environmental aspects of the pressurized fluidized-bed coal combustion (FBCC) process, using two experimental facilities: a new 218 kg coal/hr "miniplant" combustor (0.63 MW equivalent), and a 13 kg coal/hr "batch" combustion unit. Successful shakedown of the miniplant combustor culminated in a continuous 100-hr run. The miniplant combustor was operated at: coal rates up to 155 kg/hr (340 lb/hr), pressures up to 1020 kPa (10 atm), superficial velocities up to 3.2 m/s (10.5 ft/sec), temperatures up to 980C (1800F), and combustion intensities of 5 MW/cu m (480,000 Btu/hr-cu ft). Improvements in the coal feeding system and in the steam coil design were required to achieve these performance levels. Operating results from both facilities indicate that SO2 emissions can be controlled to meet current EPA New Source Performance Standards for coal-fired utility boilers with either limestone or dolomite sorbents. NOx emissions from pressurized FBCC can be controlled to 0.2 to 0.4 lb (as NO2)/million Btu (0.09-0.17 g/million J), compared to the current EPA standard of 0.7 lb/million Btu (0.30 g/million J). Particulate emissions cannot be controlled to the current EPA standard with two stages of conventional cyclones.

17. KEY WORDS AND DOCUMENT ANALYSIS

| a. DESCRIPTORS | | b. IDENTIFIERS/OPEN ENDED TERMS | c. COSATI Field/Group |
|---|---|---|---|
| Air Pollution | Fluidized-Bed Processors | Air Pollution Control | 13B |
| Desulfurization | Combustion | Stationary Sources | 07A, 07D |
| Flue Gases | | Fluidized-Bed Combustion | 21B |
| Limestone | | | 08G |
| Dolomite (Rock) | | | |
| Calcium Oxides | | Limestone-Based Desulfurization Process | 07B |

| | | |
|---|---|---|
| 18. DISTRIBUTION STATEMENT<br>Unlimited | 19. SECURITY CLASS *(This Report)*<br>Unclassified | 21. NO. OF PAGES<br>223 |
| | 20. SECURITY CLASS *(This page)*<br>Unclassified | 22. PRICE<br>#7.75 |

EPA Form 2220-1 (9-73)

PRICES SUBJECT TO CHANGE

EPA-600/7-76-011
September 1976

# STUDIES OF THE PRESSURIZED FLUIDIZED-BED COAL COMBUSTION PROCESS

by

R.C. Hoke, R.R. Bertrand, M.S. Nutkis,
D.D. Kinzler, L.A. Ruth, and M.W. Gregory

Exxon Research and Engineering Company
P.O. Box 8
Linden, New Jersey 07036

Contracts No. 68-02-1312 and -1451
Program Element No. EHE623A

EPA Project Officer: D. Bruce Henschel

Industrial Environmental Research Laboratory
Office of Energy, Minerals, and Industry
Research Triangle Park, NC 27711

Prepared for

U.S. ENVIRONMENTAL PROTECTION AGENCY
Office of Research and Development
Washington, DC 20460

i (a)

# ABSTRACT

The pressurized fluidized bed coal combustion process was studied in two experimental units including the new 2 MW (thermal) "miniplant" unit. The shakedown phase of the miniplant program was successfully completed, culminating in a continuous 100 hour demonstration run. The unit was operated at pressures up to 1020 kPa (10 atm), superficial velocities up to 3.2 m/s (10.5 ft/sec), temperatures up to 980°C (1800°F), coal feed rates up to 155 kg/hr (340 lbs/hr) and at combustion intensities of 5 MW/$m^3$ (480,000 BTU/hr $ft^3$). Improvements in the coal feeding system and in the steam coil design were required to achieve these performance levels.

Operating results from the miniplant and the older batch combustion unit indicate that $SO_2$ emissions can be controlled to levels meeting current EPA emission standards with either limestone or dolomite sorbents. However, dolomites are more effective and generally will require less sorbent to achieve the same level of $SO_2$ control. $NO_x$ emissions from pressurized fluidized bed coal combustion can be controlled to levels of 0.09 to 0.17 g (as $NO_2$)/MJ (0.2 to 0.4 lbs/MBTU). This compares to the current standard of 0.3 g (as $NO_2$)/MJ (0.7 lbs/MBTU). Control of particulate emissions to current standards cannot be achieved by two stages of conventional cyclones. A very efficient third stage particulate removal device will be required.

The miniplant and batch experimental units will be used in additional studies characterizing the environmental effects of the fluidized bed coal combustion process. This report was submitted in fulfillment of Contract Numbers 68-02-1312 and 68-02-1451 by Exxon Research and Engineering Company under the sponsorship of the Environmental Protection Agency. Work was completed in August, 1975.

# CONTENTS

**Page**

Abstract iii

List of Figures vi

List of Tables ix

Acknowledgements x

**Sections**

I Conclusions 1

II Recommendations 5

III Introduction 7

IV Miniplant Shakedown 10

- Equipment 10
- Materials 33
- Procedures 36
- Unit Performance 37
- Equipment Performance 41
- Combustion Results 73

V Batch Combustor Studies 80

- Equipment, Materials, Procedures 80
- Equipment and Technique Development 96
- Combustion Results 105

VI Discussion of Results 132

- $SO_2$ Emissions 132
- $NO_x$ Emissions 135
- Combustion Efficiency 135
- Heat Transfer Coefficients 139

VII References 140

VIII List of Publications and Patent Memoranda 141

## CONTENTS (CONTINUED)

Page

IX Appendix 143

- A. Materials of Construction 144
- B. Reports of Metallurgical Examinations 152
- C. Safety Consequences of a Steam-Coil Break 162
- D. Miniplant Alarms Annunciators 164
- E. Miniplant Data Logger Points 166
- F. Analytical Techniques 169
- G. Miniplant Run Summaries 170
- H. Batch Unit Run Summaries 198

## FIGURES

| No. | | Page |
|---|---|---|
| III-1 | Pressurized Fluidized Bed Coal Combustion System | 8 |
| IV-1 | Exxon Fluidized Bed Combustion Miniplant | 11 |
| IV-2 | Exxon Fluidized Bed Combustion Miniplant | 12 |
| IV-3 | Coal Feed System | 13 |
| IV-4 | Combustor Vessel | 15 |
| IV-5 | Combustor Vessel Lining | 16 |
| IV-6 | Combustor Preheat Burner | 18 |
| IV-7 | Combustor Fluidized Grid | 19 |
| IV-8 | Combustor Cooling Coils | 21 |
| IV-9 | Solids Pulse Pot | 22 |
| IV-10 | Solids Discharge Lockhopper | 23 |
| IV-11 | Combustor First Stage Cyclone | 25 |
| IV-12 | Combustor Second Stage Cyclone | 26 |
| IV-13 | Flue Gas Sampling System | 28 |
| IV-14 | Regenerator Vessel | 30 |
| IV-15 | Regenerator Cyclone | 32 |
| IV-16 | Coal Particle Size Distribution | 35 |
| IV-17 | Coal Feeder Orifice Assembly | 42 |
| IV-18 | Coal Flow Through a Tee | 44 |
| IV-19 | Combustor Temperature Control Schematic | 46 |
| IV-20 | Horizontal Cooling Coils | 47 |
| IV-21 | Horizontal Cooling Coils | 48 |
| IV-22 | Vertical Cooling Coils | 50 |
| IV-23 | Vertical Cooling Coils | 51 |
| IV-24 | Bed Temperature Profile - Horizontal Coils | 54 |
| IV-25 | Bed Temperature Profile - Vertical Coils | 55 |
| IV-26 | Damaged Horizontal Cooling Coils | 59 |
| IV-27 | Damaged Vertical Cooling Coils | 61 |
| IV-28 | Changes in Secondary Cyclone Dimensions | 65 |

## FIGURES (CONTINUED)

| No. |  | Page |
|---|---|---|
| IV-29 | Particle Size Distribution - Primary Cyclone Collection | 67 |
| IV-30 | Comparison of Particle Size Distribution for Solids Collected by Secondary Cyclone Before and After Modification | 68 |
| IV-31 | Ignitor - Pilot | 71 |
| IV-32 | $NO_x$ Emissions | 74 |
| IV-33 | Combustion Efficiency | 76 |
| V-1 | Batch Fluidized Bed Coal Combustion Unit | 81 |
| V-2 | Batch Fluidized Bed Coal Combustion Unit | 82 |
| V-3 | Petrocarb Coal Injector | 83 |
| V-4 | Combustor Vessel | 84 |
| V-5 | Fluidizing Grid | 86 |
| V-6 | Preheater Burner | 87 |
| V-7 | Location of Cooling Coils | 88 |
| V-8 | Coal Injector | 89 |
| V-9 | Flue Gas Sampling System | 91 |
| V-10 | Particle Size Distribution of Arkwright Coal | 92 |
| V-11 | Particle Size Distribution of Sorbents | 95 |
| V-12 | Coal Feeder Orifice Assembly | 99 |
| V-13 | Vertical Cooling Coil | 100 |
| V-14 | Comparison of Bed Temperature Profiles for Horizontal and Vertical Cooling Coils | 101 |
| V-15 | $SO_2$ Emissions - Limestone Sorbent | 106 |
| V-16 | $SO_2$ Emissions - Dolomite Sorbent | 107 |
| V-17 | $NO_x$ Emissions | 109 |
| V-18 | Particle Size Distribution - Overhead Samples | 120 |
| V-19 | Combustion Efficiency | 122 |
| V-20 | Comparison of Temperature Profiles - Wyoming and West Virginia Coal | 127 |

FIGURES (CONTINUED)

| No. | | Page |
|---|---|---|
| VI-1 | Comparison of $SO_2$ Removal Results - Limestone Sorbent | 133 |
| VI-2 | Comparison of $SO_2$ Emissions from Batch Unit and Argonne NL Study - Dolomite Sorbent | 134 |
| VI-3 | Comparison of $SO_2$ Emissions from Limestone and Dolomite Sorbents - Batch Unit Data | 136 |
| VI-4 | Comparison of $NO_x$ Emissions | 137 |
| VI-5 | Comparison of Combustion Efficiencies | 138 |

# TABLES

| No. | | Page |
|---|---|---|
| IV-1 | Miniplant Coal Analyses | 34 |
| IV-2 | Miniplant Fluidized Bed Combustion Test Conditions | 38 |
| IV-3 | Control of Operating Variables | 39 |
| IV-4 | Miniplant Cooling Coil Modifications | 52 |
| IV-5 | Miniplant Cooling Coil Damage | 58 |
| IV-6 | Miniplant Overall Heat Transfer Coefficient Measurements - Run 19.2 | 78 |
| IV-7 | Miniplant Overall Heat Transfer Coefficient Measurements - Runs 14.1, 14.2, 15.1 | 79 |
| V-1 | Coal Particle Size Distribution Penn-Rillton Co. Grind B-2 Specification | 93 |
| V-2 | Composition of Coals Used in Batch Fluidized Bed Coal Combustion Program | 93 |
| V-3 | Properties of Sorbents Used in Batch Fluidized Bed Coal Combustion Program | 94 |
| V-4 | Data for Run No. 3675-2C from Which Samples Were Analyzed for Trace Elements | 111 |
| V-5 | Elements Detected by Neutron Activation Analysis | 112 |
| V-6 | Neutron Activation Analysis - Upper Limits | 113 |
| V-7 | Material Balances for Typical Components | 115 |
| V-8 | Retention by Stone of Elements Present in Coal | 117 |
| V-9 | Comparison of Exxon and Argonne N.L. Data on Trace Element Recoveries | 118 |
| V-10 | Heat Transfer Coefficients (Bed to Tube) Measured During Coal Combustion | 124 |
| V-11 | Heat Transfer Coefficients Measured During Bed Pre-Heating | 125 |
| V-12 | Particle Size Distribution of Sulfated Sorbents | 128 |
| V-13 | Sulfur Balances for Batch Combustor | 129 |
| V-14 | Calcium Balances for Batch Combustor | 130 |

# ACKNOWLEDGEMENTS

The authors wish to express their appreciation to the many individuals who played major roles in the shakedown and operation of the FBC units at Exxon Research and Engineering Company. Specifically, we wish to acknowledge the efforts of V. J. Siminski, H. R. Silakowski, H. C. Bunje, T. C. Gaydos, R. E. Long, G. E. Walsh, D. T. Ferrughelli, E. Hellwege and J. E. Bond of the Government Research Laboratories. We also wish to acknowledge the efforts of personnel of the Mechanical Division, in particular R. A. Van Sweringen, E. C. Vath, S. Pampinto, T. Morrison, F. Huber, T. Artz, T. Morgan and E. Sullivan. A special acknowledgment goes to Mrs. N. Malinowsky who typed this report.

The personnel of the Industrial Environmental Research Laboratory of the E.P.A. have also been most helpful. We wish to express our gratitude for the help of D. B. Henschel the current EPA Project Office, S. L. Rakes, the previous Project Officer, P. P. Turner and R. P. Hangebrauck.

# SECTION I

# CONCLUSIONS

## MINIPLANT PERFORMANCE

The combustor section of the Exxon pressurized fluidized bed coal combustion miniplant is capable of operating at its basic design conditions with close control of operating variables.

Operation was demonstrated at pressures up to 1020 kPa (10 atm), superficial velocities up to 3.2 m/s (10.5 ft/sec), temperatures up to 980°C (1800°F) and combustion intensities of 5 $MW/m^3$ bed volume. Coal feed rates of 155 kg/hr and combustion heat release rates of 1.3 MW have been demonstrated to date. These are somewhat lower than specified in the design, but no difficulty is seen in operating at or above the design conditions.

Sustained operation of the combustor was demonstrated for a 100 hr. period.

## COMBUSTION RESULTS

The pressurized fluidized bed combustion (FBC) process is capable of meeting the current EPA standards for $SO_2$ and $NO_x$ emissions. Both limestone and dolomite are suitable sorbents under pressurized combustion conditions although dolomite is a more effective $SO_2$ sorbent, at least on a molar basis. A preliminary assessment of sorbent requirements based on data available to date indicates that the use of limestone will require a calcium to sulfur molar ratio of about 2.0 to 3.0 while dolomite use will require a calcium to sulfur ratio of about 1.0 to 1.5 under pressurized FBC operating conditions.

$NO_x$ emissions are in the range of 0.09 to 0.17 g (as $NO_2$)/MJ (0.2 to 0.4 lbs/M BTU) compared to the current emission standard of 0.3 g (as $NO_2$)/MJ (0.7 lbs/M BTU).

CO emissions are low, normally in the range of 150 to 250 ppm. Poor combustion conditions can cause an increase in CO emissions to levels exceeding 1000 ppm.

It is possible, with the two stage cyclone separator system used on the Exxon units, to reduce particulate emissions to the range of 0.5 to 0.9 $gm/m^3$ (0.2 to 0.4 gr/SCF). This is equivalent to 0.4 to 0.8 lb/M BTU and exceeds the emission standard of 0.1 lb/M BTU. More efficient cyclones could reduce these levels a bit further. However, even with improved cyclones, a third stage particulate removal device will be required to meet emission standards. The device will require a removal efficiency in the range of 75 to 99+%.

Once through carbon combustion efficiency ranges from 93 to 97% as the excess air level increases from 20 to 100%. Increasing the combustion efficiency to the target level of 98.5 to 99% will require recycle of carbon fines from the first stage cyclone to the combustor or to a carbon burnup cell.

Overall heat transfer coefficients between the fluidized bed and the steam coils ranges from 320 to 470 W/m$^2$ K (55 to 85 BTU/hr ft$^2$ °F) depending on the diameter of the cooling coils. Heat transfer coefficients measured in the miniplant at conditions fairly representative of those expected in utility size PFBC units range from 320 to 350 W/m$^2$ K (55 to 60 BTU/hr ft$^2$ °F).

Attrition rates measured for dolomites (Tymochtee, Pfizer No. 1337 and Baker) are much higher than those measured for Grove No. 1359 limestone. The attrition rate measured for Tymochtee dolomite varies with the batch. Most of the dolomite attrition occurs upon calcination during the heat up stage or the first few minutes of a run after coal combustion has begun.

Little difference is seen in the combustion of high sulfur, caking Eastern coal and low sulfur, noncaking Western subbituminous coal.

The batch and miniplant FBC units give comparable emission and combustion results despite a three-fold difference in diameter. (10 vs 32 cm)

## EQUIPMENT DEVELOPMENT AND PERFORMANCE

A number of equipment and design related problem areas were uncovered and overcome in the shakedown of the miniplant and batch units. Some of these problem areas are described below.

The use of a pneumatic transport coal injection system is feasible, but is sensitive to plugging and upsets. The injection system must be designed without any internal discontinuities such as sudden decreases in diameter to prevent plugging. In the coal feed systems used in the Exxon units, it is also necessary to use cooled injection probes with high velocity jets surrounding the inner coal/air core to prevent plugging and overheating at the probe outlet. With these modifications, the system performs satisfactorily. However, the successful operation of the system is dependent on close control of a fairly small pressure differential between the injector vessel and combustor. Disturbances in the pressure differential result in upsets in the coal feed.

The temperature distribution in the Exxon combustors is influenced by bed solids mixing rates. Closely packed horizontal cooling coils impede solids mixing rates and cause a sharp temperature gradient in the combustors. Use of vertically oriented coils which allow more rapid axial mixing of the solids is necessary to obtain fairly uniform temperatures. This factor must be considered in the design of larger units.

The cooling coils in the Exxon combustors were also subject to damage and distortion caused by mechanical stress. Damage usually occurred, or, at least, was more severe after the fluidized bed had agglomerated due to high temperature or a water leak into the bed. The coils in the miniplant, especially the horizontally oriented coils, were particularly subject to distortion which caused fracture of the tubes on several occasions. Vertical coils are less susceptible to damage than horizontal coils. The tubes showed no signs of corrosion as long as metal temperatures were kept low. It is important in larger units to protect the tubes from loss of coolant since the combination of the mechanical forces caused by the fluidized bed and high metal temperatures may cause tube damage. Injection of water into the bed caused by a tube break appears to result in agglomeration of the bed. No indications of steam-carbon reactions were noted when a water leak occurred. Calculations also indicate no significant reaction will occur.

Care must be exercised to prevent condensation of moisture in the flue gas cyclone diplegs during startup. If condensation occurs, solids in the diplegs plug, causing a backup of solids into the cyclone, rendering the cyclone inoperable. As long as the dipleg is dry, the pulsing system used to recycle solids from the first cyclone to the combustor works satisfactorily.

Erosion rates are high in the flue gas piping and valving system especially when the cyclones are not operating properly. A modified pressure control system was developed to function in the presence of high dust loading. A positive filtration system will be required to prevent damage to flue gas turbines in larger FBC units since failure of a cyclone could result in severe erosion damage in a very short time.

Combustor bed temperature must be up to about 650°C before feeding coal. At temperatures much below 650°C, the coal combustion efficiency is very poor, resulting in high carbon loadings and CO concentrations in the flue gas. This situation can also lead to burning of the coal above the bed and in the cyclones. Pressure and flow surges, especially during startup, can also result in burning in the cyclones.

Heat removal from a fluidized bed combustor is dependent primarily on the heat transfer surface area covered by the fluidized bed. The temperature difference between the bed and a steam/water cooling medium cannot be varied enough to have a significant effect on heat removal rates. Therefore, the fluidized bed temperature is controlled by the coal feed rate. If the expanded bed level is dropped to uncover heat transfer surface and thereby reduce the heat removal rates, the flue gas temperature will drop significantly. The heat transfer coefficients between the heat removal surface and the flue gas in the dilute phase above the expanded bed are fairly high, and a significant amount of heat will be extracted from the flue gas.

Care must be taken to obtain representative samples of flue gas for analysis. Condensation of water vapor, long residence time and exposure to metal surfaces can affect flue gas composition by decreasing $SO_2$ and increasing $SO_3$ concentrations.

## SECTION II

## RECOMMENDATIONS

Potential operating problems were uncovered during the shakedown of the miniplant combustor which should be considered in the design of larger fluidized bed combustion units. The steam coil design must permit free movement of the fluidized solids to obtain a uniform bed temperature. Vertical arrangement of the steam coils is inherently more conducive to free movement of the solids than horizontal coil configurations. Horizontal configurations cannot be ruled out, but the design of the coils should allow free movement of the solids. Damage to the coils can also readily occur if they are not properly supported. Horizontal coils are more susceptible to damage than vertical coils. Large scale tests of tube bundles should be made in "hot" combustors to assure the development of workable designs.

The pneumatic transport coal and sorbent feed system used on the Exxon pressurized FBC units is a workable system. However, it is susceptible to upsets and this should be considered in the design of coal feed systems for larger units. The design of the coal and sorbent transport system should minimize the opportunity for plugs to occur. Sudden decreases in pipe diameter should be avoided, instead, gradual changes using tapered connectors should be used. Multiple feed injection lines are desirable to minimize the impact of line plugging. Alternate feed lines should be provided to allow clean out of plugged lines. Gas flow through the coal and sorbent transport lines should be high enough not only to exceed the saltation velocity in the line, but also provide easier entry of the solids into the fluidized bed. An air-jacketed solids injection nozzle with high velocity air jets surrounding the coal/air core is recommended to assure adequate penetration of the coal into the fluidized bed combustor. Since the pneumatic transport system relies on a relatively constant pressure differential between the injector and the combustor to maintain steady coal flow, control systems must be designed to prevent the possibility of sudden changes in the pressure differential. Sudden changes in the pressure differential can result in temperature runaways and bed agglomeration, or back up of hot solids from the bed into the injector lines. Fast acting shut off systems must be used to shut off coal flow if either of these upsets develop.

Extremely high erosion rates will occur if the flue gas particulate loading and velocity are high. This situation could occur in the flue gas expansion turbine if a cyclone malfunctions. Therefore it is recommended that a positive filtration device be used between the cyclones and the gas turbine. The development of a continuous particulate concentration monitoring device is also recommended to prevent the possible occurrence of a sudden undetected increase of the particulate loading in the flue gas.

Special attention must be given to the start up of fluidized bed combustors. A heat up system is needed which will raise the bed temperature up to about 650°C while coolant is flowing through the steam coils. If coal is admitted to the combustor at lower temperatures, very poor combustion efficiency will occur which can lead to burning above the fluidized bed. Coolant flow is required to prevent damage to the steam coils during the heat up stage. Care must also be exercised during startup to prevent sudden flow surges during the period when the combustor is being brought up to operating pressure and flow. Flow surges can cause burning above the bed and in the cyclones. Steps must also be taken during startup to prevent condensation of moisture in lines which handle solids. If condensation occurs, the line will readily plug with wet solids. Such lines should be isolated or kept free of solids until the lines or the gas passing through them are hot enough to prevent condensation.

Since the miniplant combustor is now fully operational, it should be used in combustion and emissions related studies. It is capable of operating at conditions of high velocity, pressure and temperature in deep beds of sorbent with very high combustion intensities. It can be used to study the environmental effects of designs and operating conditions anticipated for larger units. It can also be used to test performance of subsystems. One very important area requiring further study is particulate control. The miniplant is capable of studying and evaluating particulate control devices under conditions closely approximating those expected in large FBC systems. Maximum use of the miniplant is planned in environmental characterization of the fluidized bed combustion process.

Although the miniplant is now fully operational, additional improvements can be made to certain components. It is recommended that a modified coal and sorbent feed system be installed with three feed lines. This will reduce the impact of plugs in the feed lines. Larger coal feed vessels are also recommended. These will reduce the frequency of the refilling operation which requires close attention to prevent upsets in the coal feed rate. Further modification of the vertical cooling coils now used in the miniplant is recommended to lengthen coil life.

It is also recommended that the study of sulfated sorbent regeneration be resumed. Additional regeneration studies should be made in the batch unit. Following the scheduled schakedown of the miniplant regenerator, a program should begin in the miniplant in which continuous combustion and regeneration can be studied over extended periods of time. Such regeneration studies are currently planned.

# SECTION III

# INTRODUCTION

The pressurized fluidized bed combustion of coal is a new combustion technique, which can reduce the emission of $SO_2$ and $NO_x$ from the burning of sulfur-containing coals to levels meeting EPA emission standards. This is done by using a suitable $SO_2$ sorbent such as limestone or dolomite as the fluidized bed material. In addition to emissions control, this technique has other potential advantages over conventional coal combustion systems which could result in a more efficient and less costly method of electric power generation. By immersing steam generating surfaces in the fluidized bed, the bed temperature can be maintained at low and uniform temperatures in the vicinity of 800 to 950°C. The lower temperatures decrease steam tube corrosion, allow the use of lower grade coals (since these temperatures are lower than ash slagging temperatures), and also decrease $NO_x$ emissions. Operation at elevated pressures, in the range of 600 to 1000 kPa, offers further advantages. The hot flue gas from a pressurized system can be expanded through a gas turbine, thereby increasing the power generating efficiency even further.

In the fluidized bed boiler, limestone or dolomite is calcined and reacts with $SO_2$ and oxygen in the flue gas to form $CaSO_4$ as shown in reaction (1).

$$CaO + SO_2 + 1/2O_2 \rightarrow CaSO_4 \qquad (1)$$

Fresh limestone or dolomite sorbent feed rates to the boiler can be reduced by regeneration of the sulfated sorbent to CaO and recycle of the regenerated sorbent back to the combustor. One regeneration system, studied by Exxon Research and Engineering Company in the past, is the so-called one step regeneration process in which sulfated sorbent is reduced to CaO in a separate vessel at a temperature of about 1100°C according to equation (2). $SO_2$ in the regenerator off gas is at a sufficiently high concentration to be recovered in a by-product sulfur plant.

$$CaSO_4 + \overset{CO}{H_2} \rightarrow CaO + SO_2 + \overset{CO_2}{H_2O} \qquad (2)$$

A diagram of the pressurized fluidized bed combustion and regeneration process is shown in Figure III-1.

Exxon Research and Engineering Company, under contract to the EPA, has built two pressurized fluidized bed combustion units to study the combustion and regeneration processes. The smaller of the two units, the batch unit, was built under contract CPA 70-19 and was described in

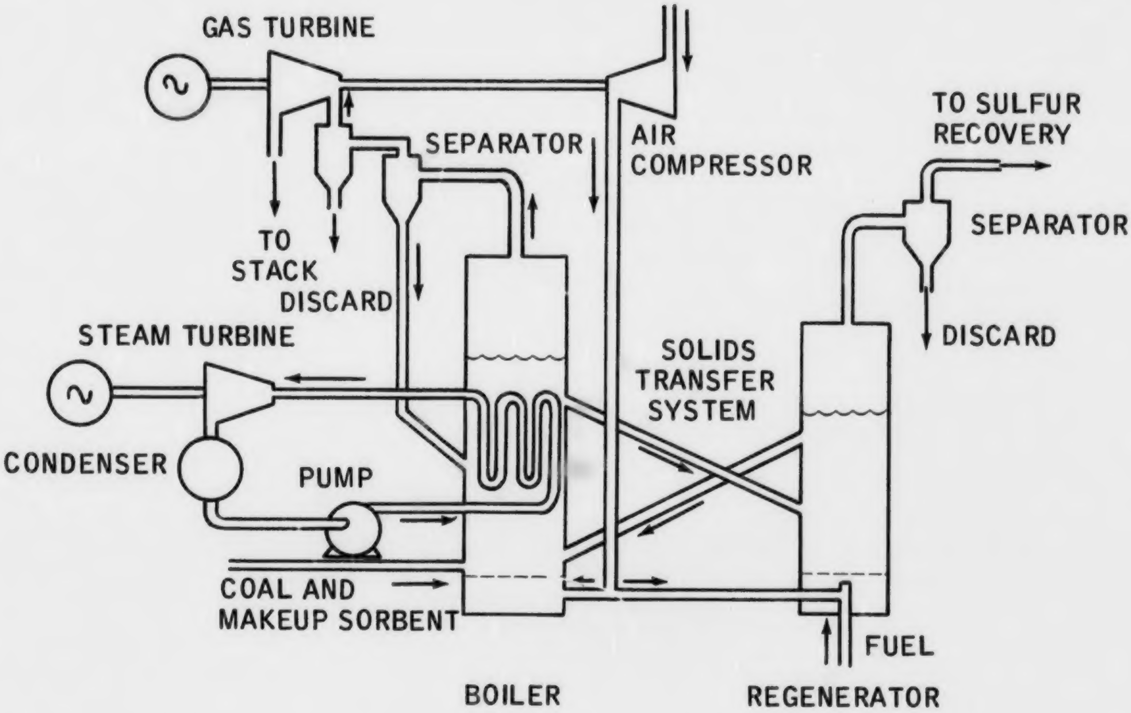
GAS TURBINE
AIR COMPRESSOR
TO SULFUR RECOVERY
SEPARATOR
TO STACK
DISCARD
SEPARATOR
DISCARD
STEAM TURBINE
SOLIDS TRANSFER SYSTEM
CONDENSER
PUMP
COAL AND MAKEUP SORBENT
FUEL
BOILER
REGENERATOR

Figure III-1

PRESSURIZED FLUIDIZED BED COAL COMBUSTION SYSTEM report EPA-650/2-74-001. That report also described the high pressure regeneration studies carried out in the unit and the initial coal combustion studies. The subsequent coal combustion studies carried out in the batch unit over the period August 1, 1973 to July 1, 1975 under Contracts CPA 70-19 and 68-02-1451 are described in this report. The program was aimed at the development of equipment and operating techniques, the study of the effect of process conditions on $SO_2$, $NO_x$ and CO emissions, the measurement of combustion efficiency, particulate and trace metal emissions and the measurement of heat transfer coefficients between the fluidized bed and steam tubes. Various coals and sorbents were also tested.

The larger unit, called the miniplant, was designed under EPA Contract CPA 70-19 and the design was described in a report to the EPA by Exxon Research and Engineering Company (1). The miniplant was built under Contract 68-02-0617. The shakedown of the combustor section of the miniplant was funded under Contract 68-02-1312. This report describes the combustor shakedown program which concluded in a 100 hr. continuous run. It includes a description of the miniplant, performance during the shakedown phase, equipment problems and corrective steps taken and combustion results. The combustion results cover measurement of $SO_2$, $NO_x$, and CO emissions, combustion efficiency and heat transfer coefficients made during the shakedown program. The shakedown period covered in this report is from October 1, 1973 to August 4, 1975.

# SECTION IV

# MINIPLANT SHAKEDOWN

## EQUIPMENT

The Exxon fluidized bed combustion miniplant is shown schematically in Figure IV-1. Figure IV-2 is a photograph of the unit. The miniplant consists of a refractory lined combustor vessel with provisions for continuous feeding of coal and fresh sorbent and continuous withdrawal of spent sorbent. A refractory lined regenerator vessel was built adjacent to the combustor and, when in operation, will provide for the continuous transfer of spent sorbent from the combustor to the regenerator and the continuous return of regenerated sorbent to the combustor. The combustor vessel is 9.75 metres high (32 ft.) lined to an internal diameter of 31.8 cm (12.5 in) and is capable of burning up to 218 kg/hr of coal (480 lbs/hr.). Cooling coils in the combustor remove the heat of combustion and maintain the bed temperature in the operating range of 800 to 1000°C (1470 to 1830°F). The maximum operating pressure is 1010 kPa (10 atm.); the maximum superficial velocity is 3 m/s(10 ft/sec). The regenerator vessel is 6.7 metres high (22 ft.) lined to an internal diameter of 21.6 cm (8.5 in.) and is capable of operating at temperatures up to 1100°C (2000°F) at 1000 kPa (10 atm) pressure.

The following discussion will focus in more detail on the major system components which include: 1) solids feeding system, 2) fluidized bed combustor with internal subcomponents, 3) combustor cyclones, 4) pressure control and flue gas discharge system, 5) flue gas sampling and analytical system, 6) process monitoring and data generation system, 7) combustor safety and alarm system, 8) fluidized bed regenerator system, and 9) miniplant support structure.

### Solids Feeding System

The solids feeding system, originally designed by Petrocarb, Inc. and subsequently modified by Exxon Research is illustrated in Figure IV-3. The system provides for uninterrupted solids feed (coal and limestone) from the primary injector to the combustor while allowing intermittent refilling of the primary injector (193 kg operating capacity) when its charge is reduced below 102 kg.

Solids in the primary injector are continuously aerated at a controlled pressure above that in the combustor. They exit the primary injector through a 1.3 cm diameter orifice and are pneumatically conveyed by a controlled stream of dry transport air through an s-shaped 1.3 cm I.D. stainless steel pipe leading into the combustor. A short segment of 1.3 cm I.D. rubber hose is used to connect the injector to the transport

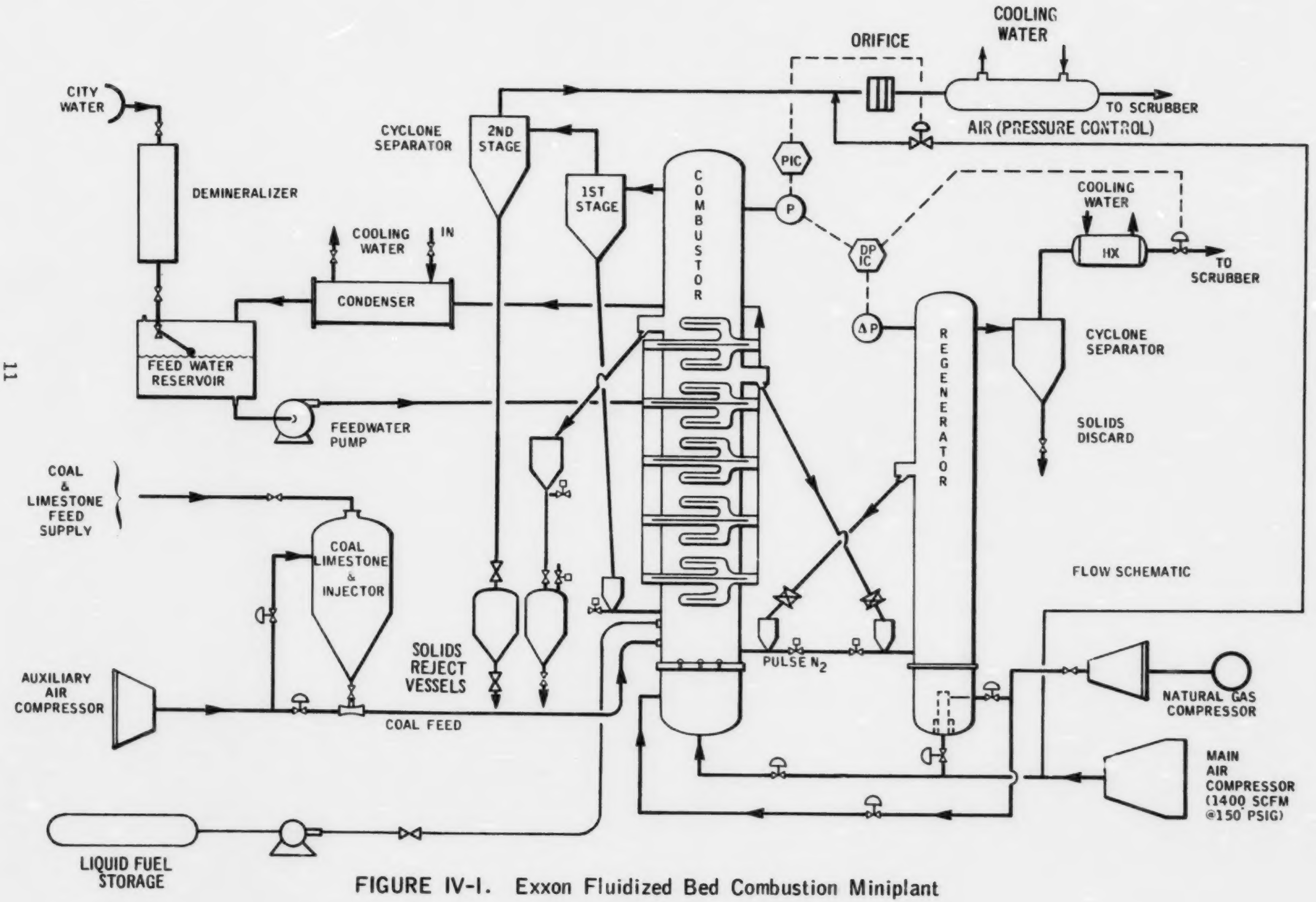
COOLING WATER
ORIFICE
TO SCRUBBER
AIR (PRESSURE CONTROL)
CITY WATER
CYCLONE SEPARATOR
2ND STAGE
1ST STAGE
C O M B U S T O R
PIC
P
DEMINERALIZER
DP IC
COOLING WATER
HX
TO SCRUBBER
COOLING WATER
IN
CONDENSER
ΔP
R E G E N E R A T O R
CYCLONE SEPARATOR
FEED WATER RESERVOIR
FEEDWATER PUMP
SOLIDS DISCARD
COAL & LIMESTONE FEED SUPPLY
COAL LIMESTONE & INJECTOR
FLOW SCHEMATIC
SOLIDS REJECT VESSELS
PULSE N2
AUXILIARY AIR COMPRESSOR
COAL FEED
NATURAL GAS COMPRESSOR
MAIN AIR COMPRESSOR (1400 SCFM @150 PSIG)
LIQUID FUEL STORAGE

FIGURE IV-I. Exxon Fluidized Bed Combustion Miniplant

FIGURE IV-2

EXXON FLUIDIZED BED COMBUSTION MINIPLANT

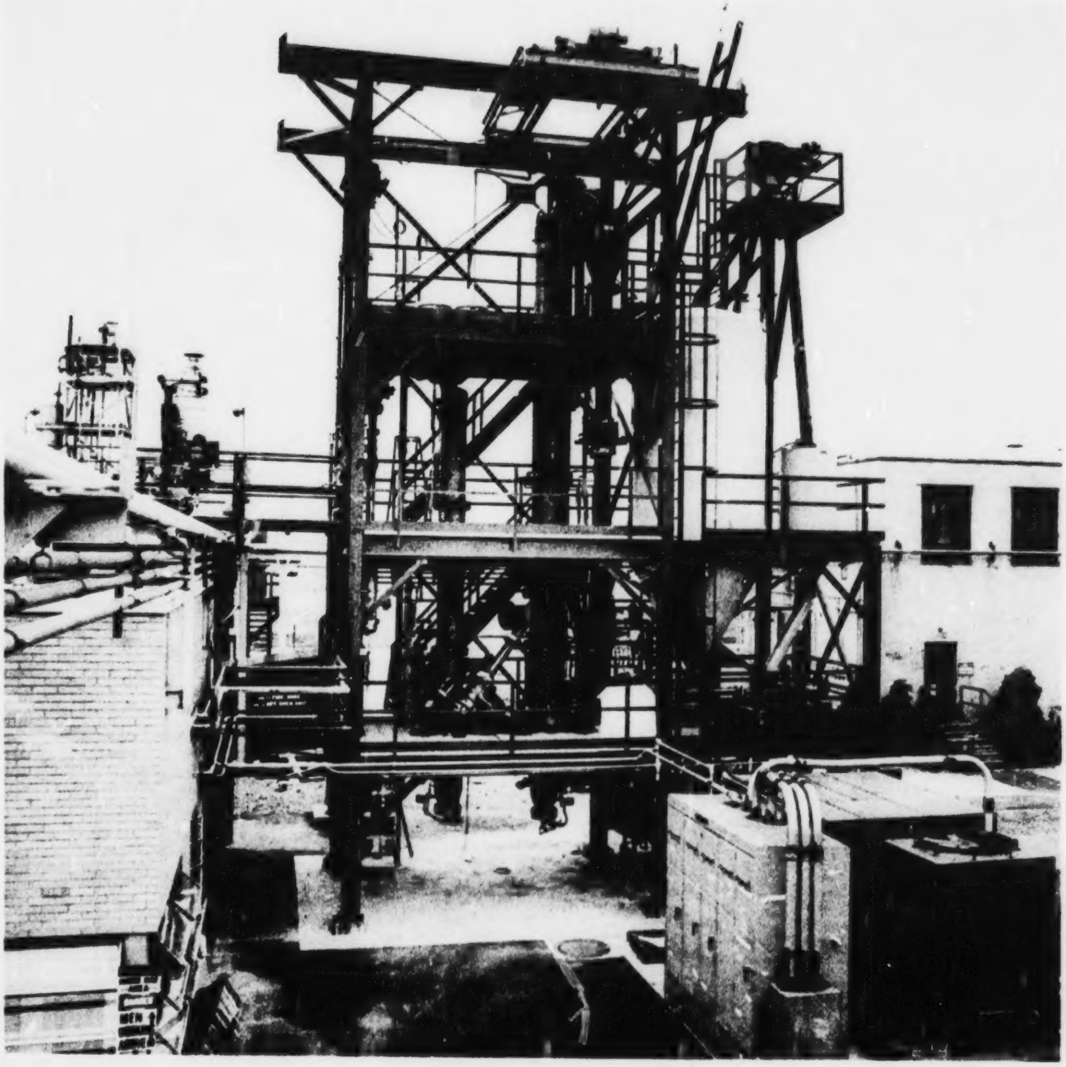

Figure IV-3

COAL & LIMESTONE FEED SYSTEM

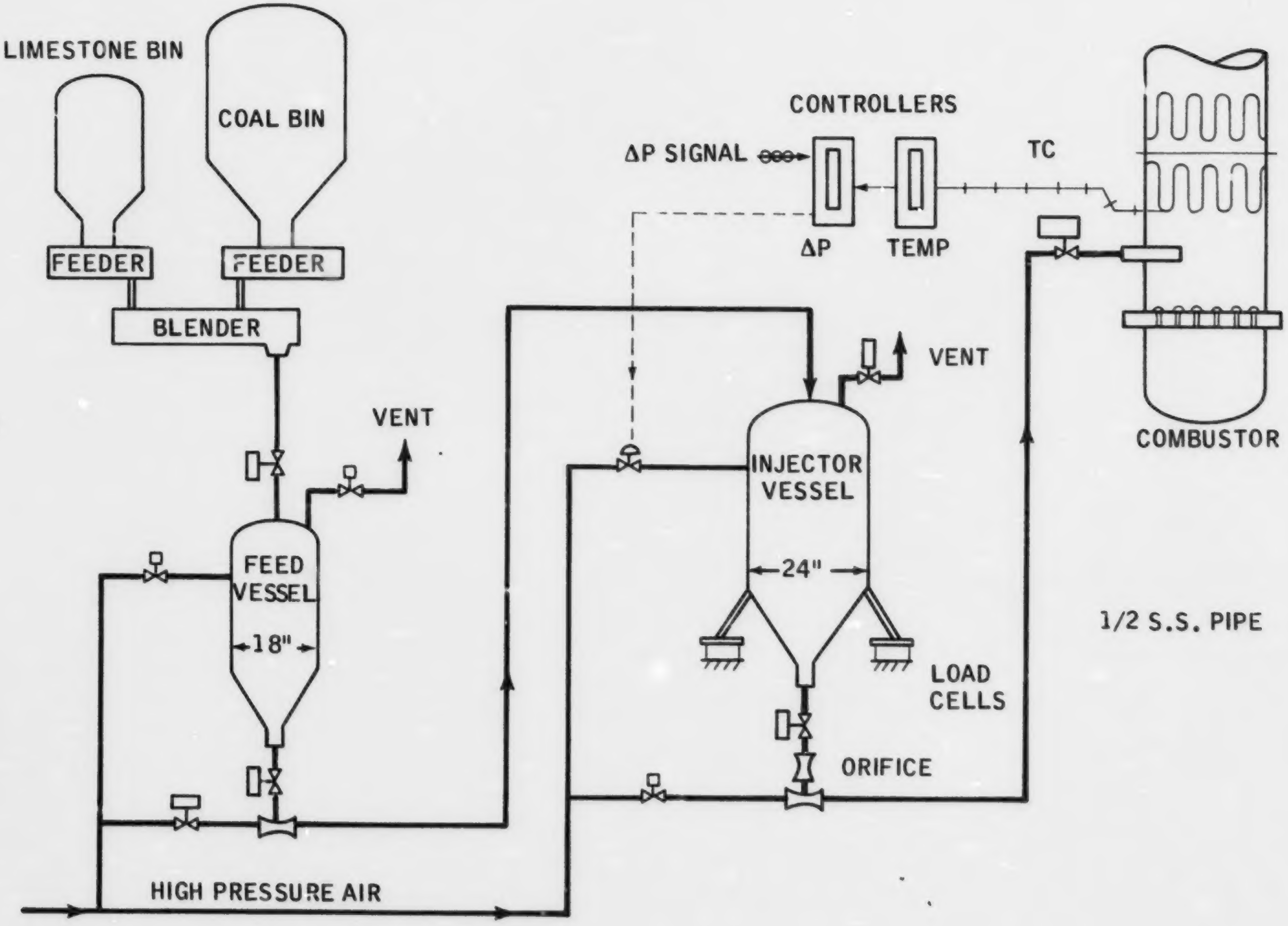
LIMESTONE BIN
COAL BIN
FEEDER
FEEDER
BLENDER
CONTROLLERS
ΔP SIGNAL
ΔP
TEMP
TC
COMBUSTOR
VENT
VENT
FEED VESSEL
18"
INJECTOR VESSEL
24"
LOAD CELLS
ORIFICE
1/2 S.S. PIPE
HIGH PRESSURE AIR

line in order not to interfere with operation of the load cells, located under the injector, which are used to monitor solids feed rate. Rate of solids feed is automatically controlled in order to maintain a specific operating temperature within the combustor. This is accomplished through a series of controls involving the pressure differential between the primary injector and combustor, the injector pressure, and the transport air flow rate. Final entry of solids into the combustor is through a 1.3 cm I.D. probe located 28 cm above the fluidizing grid and horizontally extending about 2.5 cm beyond the reactor wall. The tip of the probe includes ten 0.79 mm diameter holes which surround the solids feed opening. They are used to continuously inject an annular stream of sonic-velocity air to assist penetration of the solids feed into the fluidized bed and alleviate any tendency of the probe tip to become blocked with bed solids.

The remainder of the solids feeding system is involved in generating a specific feed ratio of coal to limestone, and refilling the primary injector in response to an appropriate weight demand signal. Crushed and sized coal and limestone are stored separately in 13.6 tonne and 1.8 tonne capacity storage bins, respectively. From here, they are screw-fed at a preselected ratio through a blender into the feed injector (91 kg operating capacity). Transfer from the feed injector to the primary injector is done penumatically.

Prior to initiation of a refilling operation, the primary injector, feed injector, and pair of solids storage bins remain isolated from each other. When the load cell under the primary injector detects a solids loading of less than 102 kg, 91 kg of solids are automatically transferred from the pressurized feed injector without interrupting feed to the combustor. Refilling is usually completed in about 5 minutes. After refilling, the feed injector is again isolated from the primary injector, vented, and filled with solids from the storage bins. The feed injector is again isolated and repressurized to await repetition of another cycle.

Process air for the solids feeding system is provided by an auxiliary air compressor with a rated capacity of 200 SCFM at 200 psig (5.6 standard $m^3$/min at 1380 kPa gauge). Prior to contacting solids, air is dried using a Pall Heatless Regenerative dryer.

## Fluidized Bed Combustor

The combustor consists of a 61.0 cm I.D. steel shell refractory lined with Grefco #75-28 Litecast to an actual internal diameter of 31.8 cm (see Figures IV-4 and IV-5). The 9.75 metre high unit is designed in flanged sections and contains various ports to allow for material entry

## FIGURE IV-4

## COMBUSTOR VESSEL

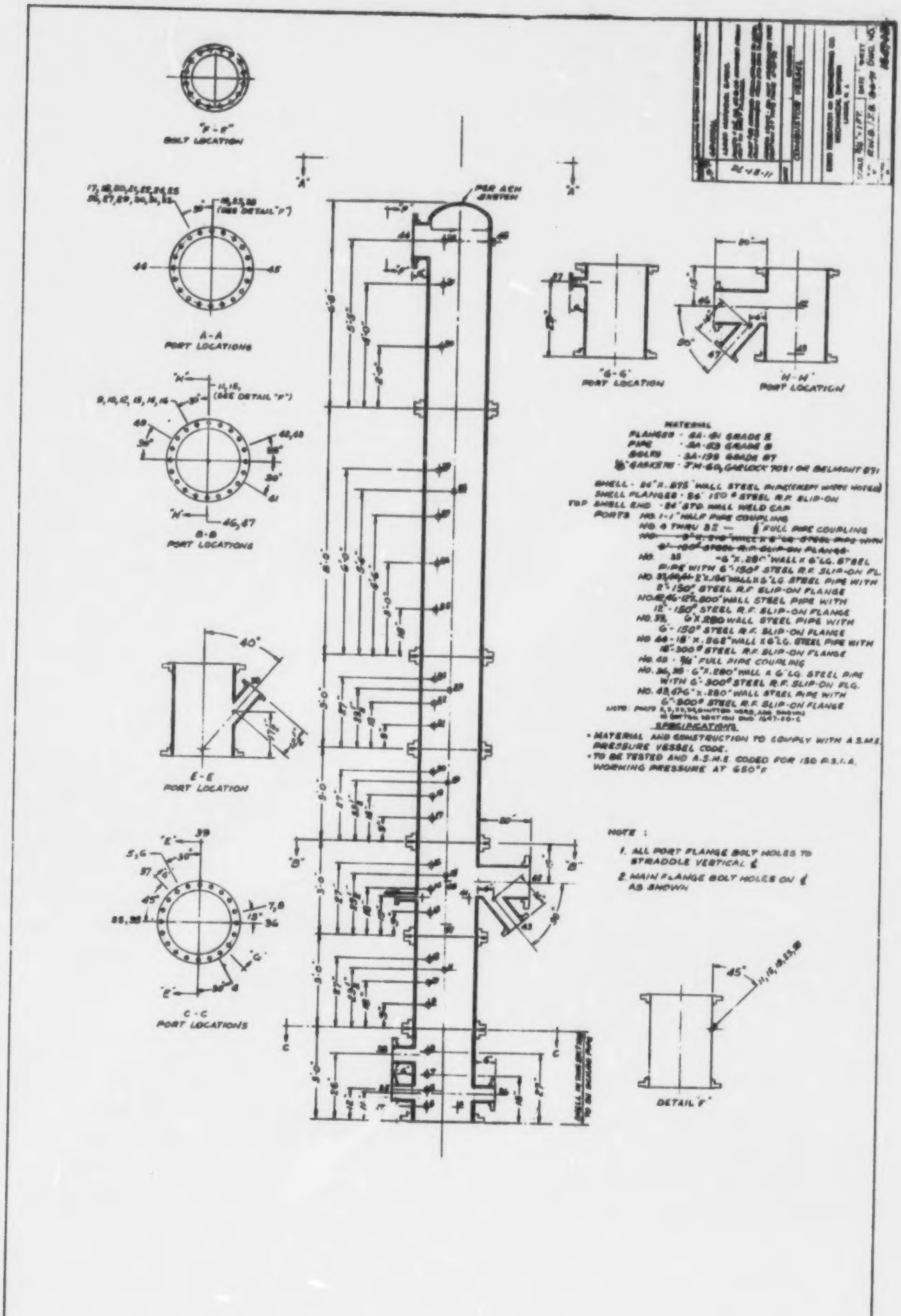
"F-F"
BOLT LOCATION
A-A
PORT LOCATIONS
B-B
PORT LOCATIONS
E-E
PORT LOCATION
C-C
PORT LOCATIONS
"G-G"
PORT LOCATION
"H-H"
PORT LOCATION
DETAIL "F"
PER ACH
SKETCH
MATERIAL
FLANGES - SA-181 GRADE II
PIPE - SA-53 GRADE B
BOLTS - SA-193 GRADE B7
⅛" GASKETS - JM-60, GARLOCK 7021 OR BELMONT 871
SHELL - 24" X .375" WALL STEEL PIPE (EXCEPT WHERE NOTED)
SHELL FLANGES - 24" 150 # STEEL R.F. SLIP-ON
TOP SHELL END - 24" STD. WALL WELD CAP
PORTS NO. 1-1" HALF PIPE COUPLING
NO. 4 THRU 32 — ½" FULL PIPE COUPLING
NO. 33 -6" X .280" WALL X 6" LG. STEEL PIPE WITH 6"-150# STEEL R.F. SLIP-ON FL.
2"-150# STEEL R.F. SLIP-ON FLANGE
12"-150# STEEL R.F. SLIP-ON FLANGE
6"-150# STEEL R.F. SLIP-ON FLANGE
NO. 44 - 16" X .562" WALL X 6" LG. STEEL PIPE WITH 16"-300# STEEL R.F. SLIP-ON FLANGE
NO. 45 - ¾" FULL PIPE COUPLING
WITH 6"-300# STEEL R.F. SLIP-ON FLG.
6"-300# STEEL R.F. SLIP-ON FLANGE
SPECIFICATIONS
• MATERIAL AND CONSTRUCTION TO COMPLY WITH A.S.M.E. PRESSURE VESSEL CODE.
• TO BE TESTED AND A.S.M.E. CODED FOR 150 P.S.I.A. WORKING PRESSURE AT 650°F
NOTE :
1. ALL PORT FLANGE BOLT HOLES TO STRADDLE VERTICAL ℄
2. MAIN FLANGE BOLT HOLES ON ℄ AS SHOWN
40°
45°
30°
90°

FIGURE IV-5

COMBUSTOR VESSEL LINING

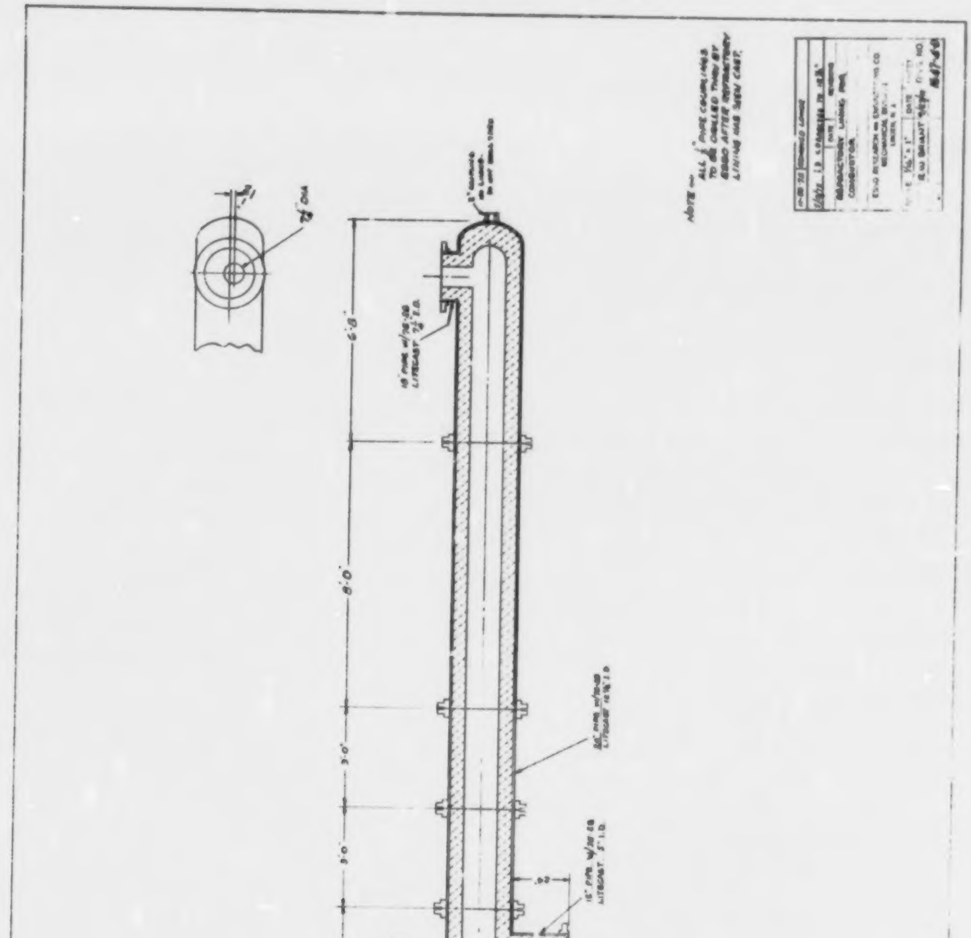

SECTION A-A
3'-0"
3'-0"
3'-0"
3'-0"
3'-0"
8'-0"
6'-8"
NOTE —
ALL ½" PIPE COUPLINGS TO BE DRILLED THRU BY
AFTER REFRACTORY LINING HAS BEEN CAST.
REFRACTORY LINING
COMBUSTOR

and discharge. Numerous taps are also provided along the length of the combustor to monitor both pressure and temperature. Currently pressure measurements are made at five locations: immediately below and above the fluidizing grid, at two points within the expanded bed, and at one location above the bed. Temperatures within the combustor are continuously measured via protected thermocouples at twelve vertical locations extending from 15.2 cm above the grid to the top of the unit, as well as at one point within the plenum below the grid. Combustion air to the unit is provided by the miniplant main air compressor having a capacity of 1400 SCFM at 150 psig (40 standard $m^3$/min at 1030 kPa gauge).

## Combustor Startup Burner

The bottom plenum section, where combustion air enters, also houses the burner used for initially preheating the limestone bed during unit startup. Fuel to the burner is provided by a natural gas compressor with a capacity of 20 SCFM at 200 psig (0.57 standard $m^3$/min at 1379 kPa gauge). The burner is shown schematically in Figure IV-6. A well-mixed stream of natural gas and air is ignited as it exits the nozzle using a flame generated by an auxiliary spark-fired pilot ignitor (see Section dealing with burner performance for more details regarding the pilot ignitor). The burner is water-cooled (both skin and cooling-water temperature are continuously monitored) and is designed to avoid flash-back during opera operation.

Once the fluidized bed temperature reaches 430°C, a liquid fuel (kerosene) system is used to heat the bed to the coal ignition temperature (>650°C). This system is also used to maintain bed temperature above 650°C should coal feeding be interrupted during normal combustor operation. Liquid fuel entry is at a point 15.2 cm above the combustor fluidizing grid. Injection is made through a 1.6 mm I.D. spray nozzle mounted within a 1.6 cm I.D. pipe resulting in a 0.76 mm annular spacing at the tip. Air flowing through the annulus provides cooling and creates a high velocity stream to insure penetration of the fuel into the bed as well as to avoid clogging of the nozzle.

## Combustor Fluidizing Grid

The combustor fluidizing grid, located 71 cm above the combustor bottom, separates the plenum from the main combustor chamber. The grid consists of a 1.3 cm thick X 69 cm diameter stainless steel plate containing 776 equally-spaced holes of 0.16 cm diameter within a 31.8 cm circle (see Figure IV-7). The design is such to give a grid pressure drop of approximate 30% of the total pressure drop across a 2.5-3.0 metre deep expanded bed. The unit is water-cooled with both the cooling water temperature and metal temperature continuously measured.

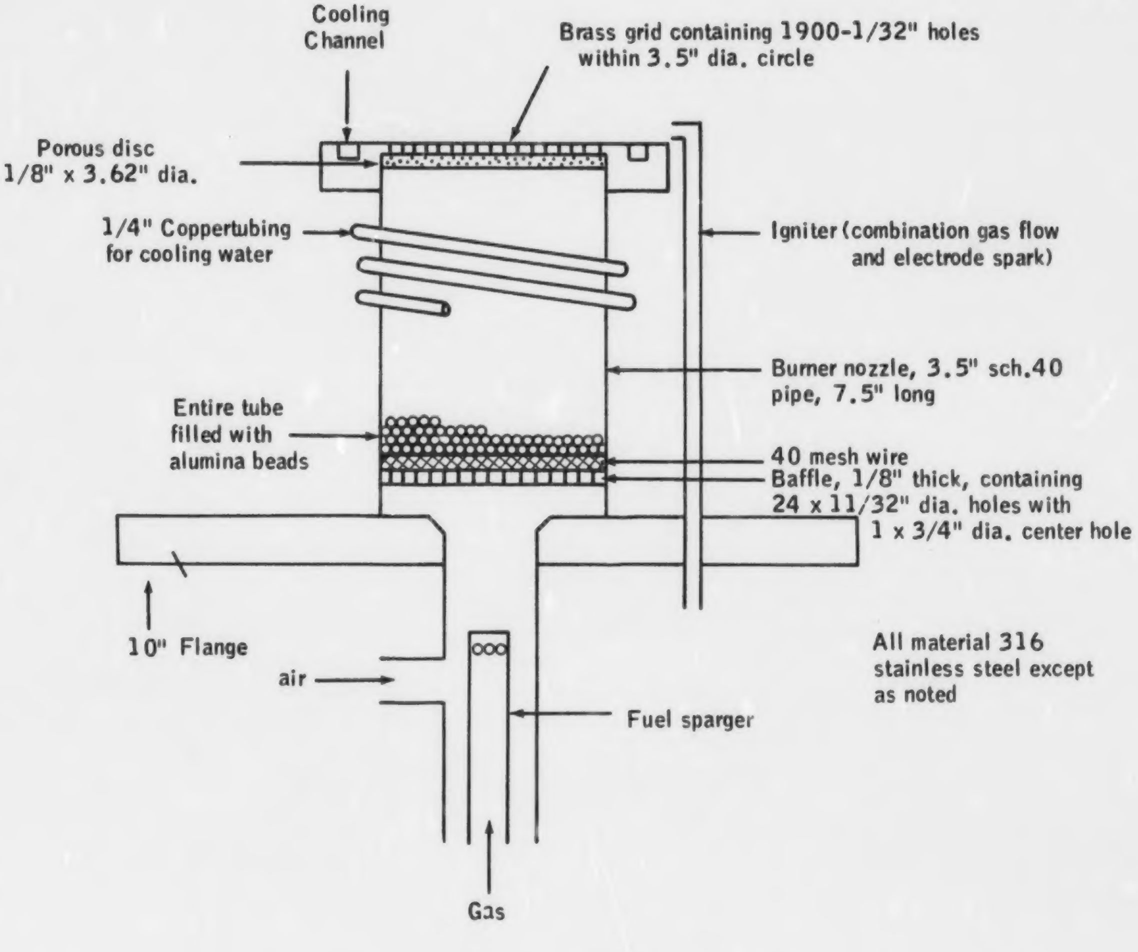
Cooling Channel
Brass grid containing 1900-1/32" holes within 3.5" dia. circle
Porous disc 1/8" x 3.62" dia.
1/4" Coppertubing for cooling water
Igniter (combination gas flow and electrode spark)
Burner nozzle, 3.5" sch.40 pipe, 7.5" long
Entire tube filled with alumina beads
40 mesh wire
Baffle, 1/8" thick, containing 24 x 11/32" dia. holes with 1 x 3/4" dia. center hole
10" Flange
All material 316 stainless steel except as noted
air
Fuel sparger
Gas

Figure IV-6 COMBUSTOR PREHEAT BURNER

FIGURE IV-7

COMBUSTOR FLUIDIZED GRID

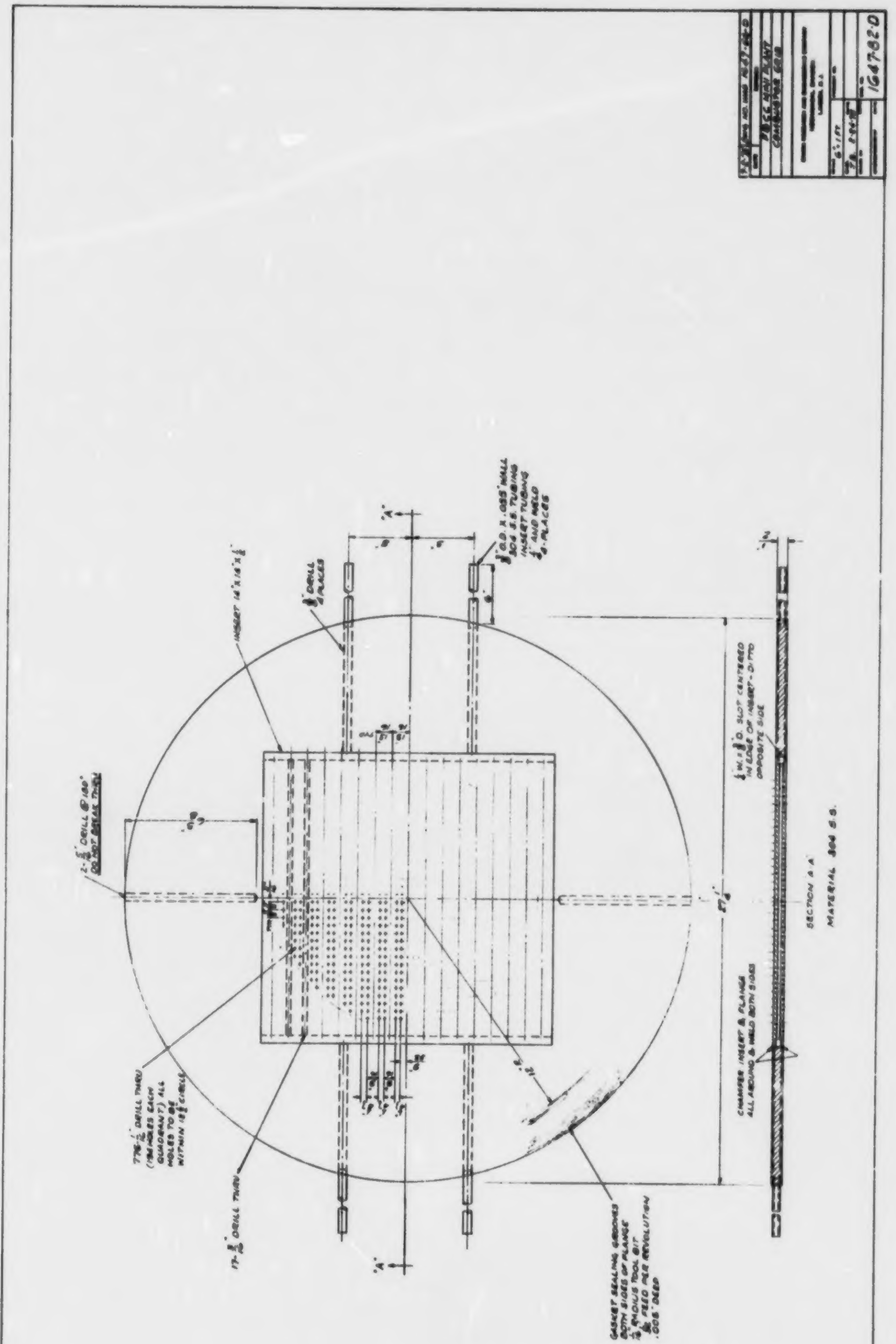
2-⅝" DRILL @ 180°
DO NOT BREAK THRU
INSERT 14"x14"x½"
⅜" DRILL 4 PLACES
⅜" O.D. X .035" WALL 304 S.S. TUBING INSERT TUBING ⅛" AND WELD
¼" W. x ⅜" D. SLOT CENTERED IN EDGE OF INSERT - DITTO OPPOSITE SIDE
SECTION A-A
MATERIAL 304 S.S.
CHAMFER INSERT & FLANGE ALL AROUND & WELD BOTH SIDES
776-1/32" DRILL THRU (194 HOLES EACH QUADRANT) ALL HOLES TO BE WITHIN 12½" CIRCLE
17-⅜" DRILL THRU
GASKET SEALING GROOVES BOTH SIDES OF FLANGE 1/16" RADIUS TOOL BIT 1/32 FEED PER REVOLUTION .005" DEEP
"A"
"A"
1G47820

## Combustor Cooling Coils

Heat removal from the combustor is provided by cooling coils located in discrete vertical zones above the grid. Each coil has a total surface area of 0.55 $m^2$ and consists of vertically-oriented loops constructed of 0.5 in Schedule 40 316 stainless steel pipe (Figure IV-8). A coolant distributor plate accommodates each pair of coils with one coil extending 45.7 cm above the plate while the other extends the same distance below. The plates, in turn, are sandwiched between combustor flanges located at 91.5 cm vertical increments beginning 91.5 cm above the fluidizing grid. Although there is provision for ten coils as shown in Figure IV-1, only four are currently installed and are located at the first two flanges above the grid.

Demineralized cooling water is pumped from a storage tank through the coils where it is partially vaporized. After exiting the combustor, the steam/water mixture flows through a condenser prior to return to the storage tank. Flow to each of the coils can be separately monitored and controlled. Cooling water exit temperature from each coil is also routinely recorded. In order to simplify measurement of heat transfer coefficients, it is also possible to increase the water flow to any one of the coils to prevent vaporization during the time of measurement.

## Combustor Solids Rejection and Transport

Solids rejection from the combustor is required to maintain a steady-state bed height whenever a mixture of coal and limestone is fed. Such rejection is accomplished through a port located 230 cm above the fluidizing grid. From here, solids flow by gravity through a 15.4 cm I.D. steel pipe, refractory lined to 5.1 cm, into a refractory-lined pulse pot (see Figure IV-9). Next, they are pneumatically transported by controlled nitrogen pulses to a pressurized lockhopper (Figure IV-10) from which they are periodically dumped into metal drums.

The full operational mode of the miniplant involves simultaneous operation of both the combustor and regenerator. In such a scheme, limestone would be continuously transferred from the combustor to the regenerator and back again after appropriate regeneration. Since regenerator shakedown has not been completed, such a transfer sequence has not been tested, nor have the final connections between both units been made. When such operation is carried out, solids transfer between both units will utilize pulse pots in a manner similar to that currently being used (and discussed above) for combustor solids rejection. Solids will exit the combustor through another port located 230 cm above the fluidizing grid and will return from the regenerator through a port located at the same height as the coal feeding point (28 cm above the fluidizing grid).

FIGURE IV-8

COMBUSTOR COOLING COILS

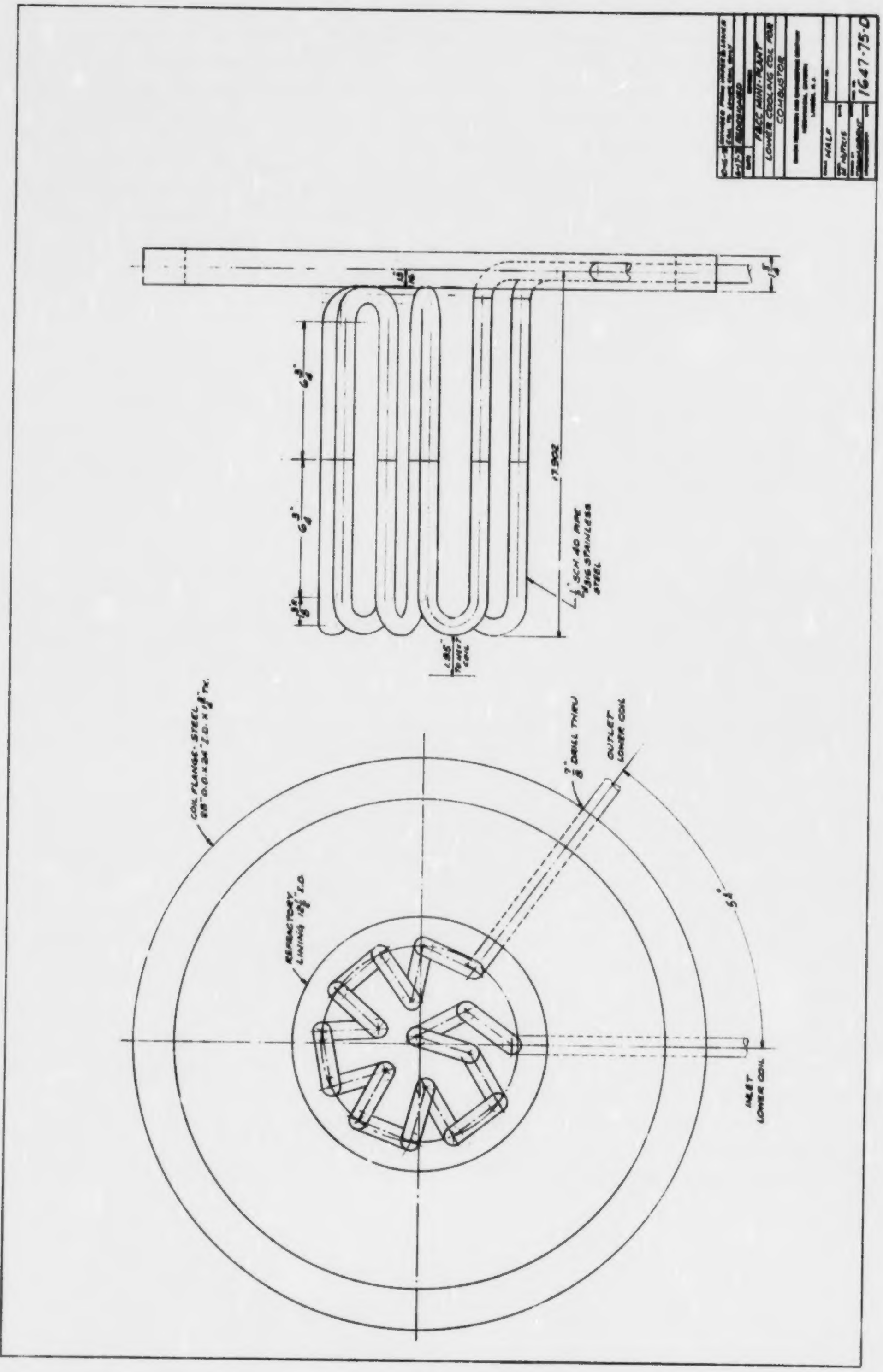
FREC MINI-PLANT
LOWER COOLING COIL FOR COMBUSTOR
HALF
1647-75-D
17.902
6 3/4"
6 3/4"
1/2" SCH 40 PIPE 316 STAINLESS STEEL
COIL FLANGE - STEEL 28" O.D. x 24" I.D. x 1 1/8" TK.
7/8" DRILL THRU
OUTLET LOWER COIL
REFRACTORY LINING 18 1/2" I.D
54°
INLET LOWER COIL

FIGURE IV-9

SOLIDS PULSE POT

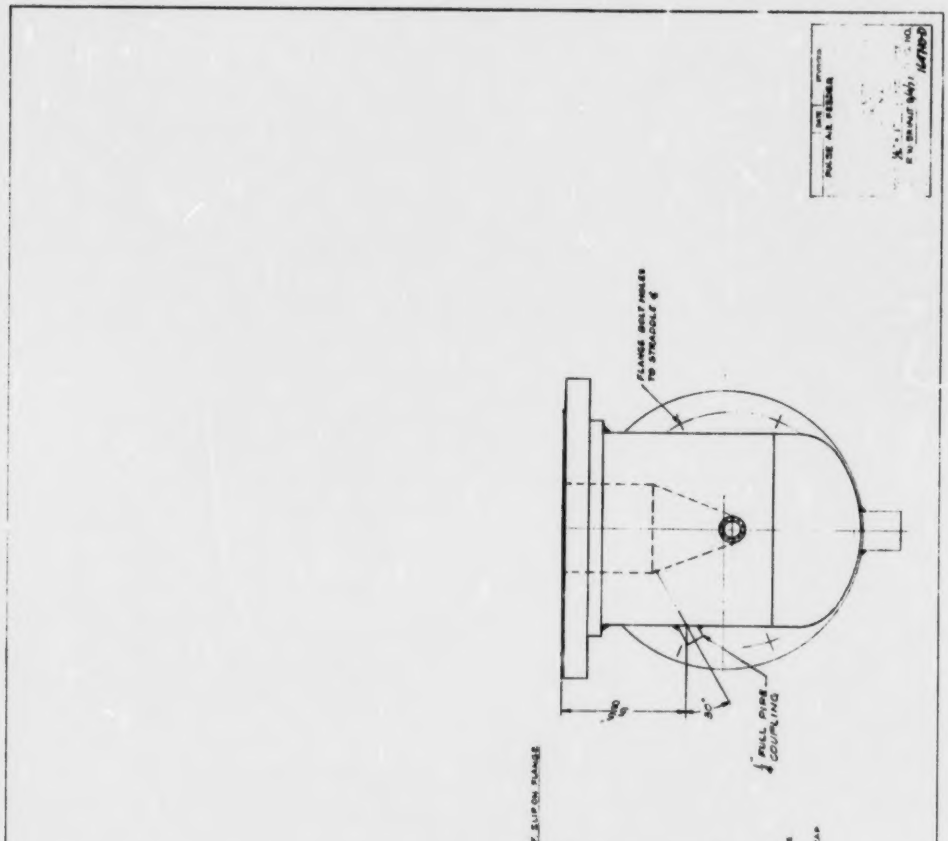
PULSE AIR FEEDER
DATE
NO.
FLANGE BOLT HOLES TO STRADDLE ℄
30°
1" FULL PIPE COUPLING
CAST REFRACTORY
1/2" FULL PIPE COUPLING
8 x .322 WALL PIPE
8 x .322 WALL WELD CAP
1" FULL PIPE COUPLING
4" DIA
6"x .280 WALL PIPE
11"
FLANGE BOLT HOLES TO STRADDLE ℄

FIGURE IV-10

SOLIDS DISCHARGE LOCKHOPPER

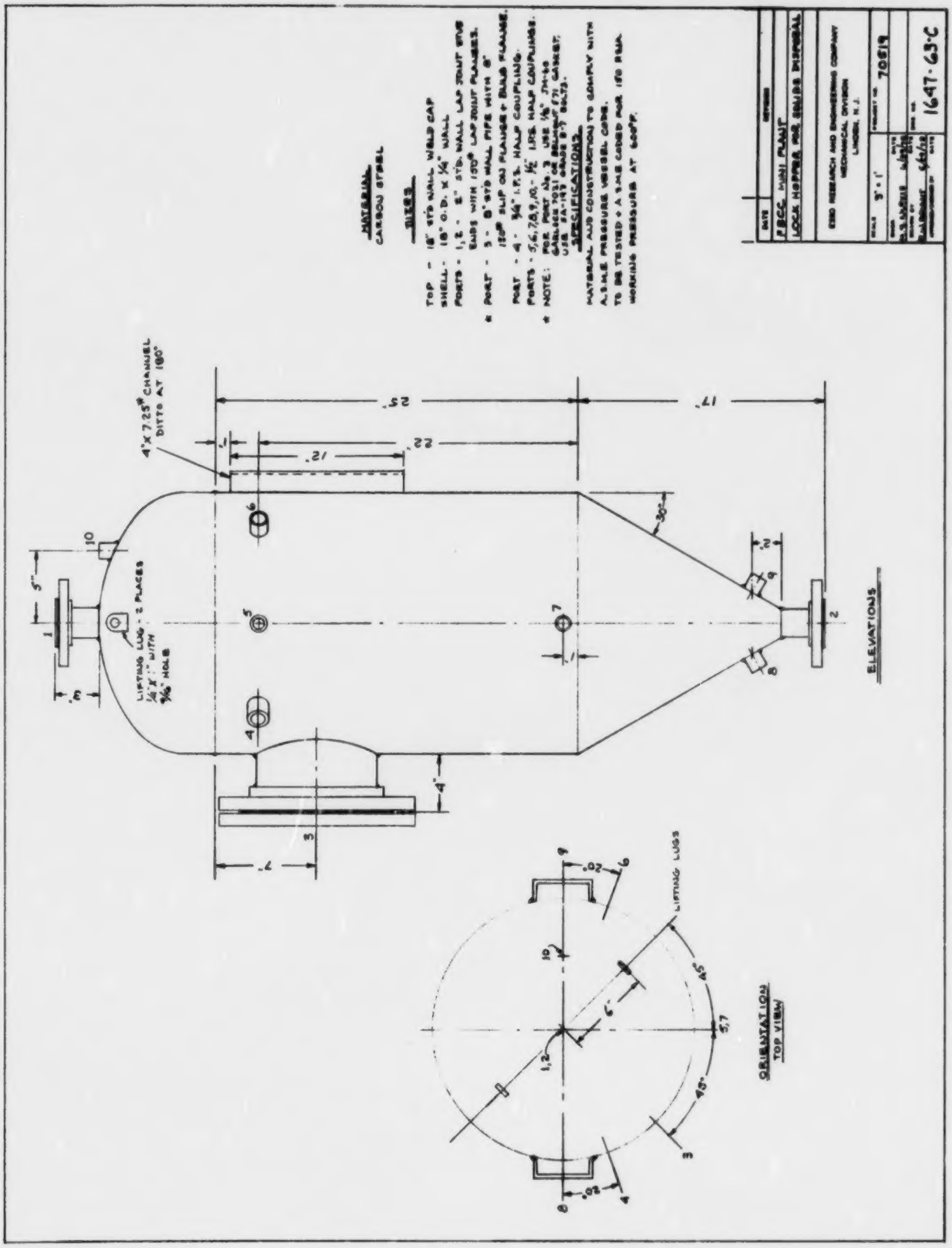
MATERIAL
CARBON STEEL
SIZES
TOP - 18" STD WALL WELD CAP
SHELL - 18" O.D. x 1/4" WALL
PORTS - 1,2 - 8" STD. WALL LAP JOINT STUB ENDS WITH 150# LAP JOINT FLANGES.
* PORT - 3 - 8" STD WALL PIPE WITH 8" 150# SLIP ON FLANGE + BLIND FLANGE.
PORT - 4 - 3/4" I.P.S. HALF COUPLING.
PORTS - 5,6,7,8,9,10 - 1/2" I.P.S. HALF COUPLINGS.
* NOTE: FOR PORT No. 3 USE 1/8" JM-60 GARLOCK 7021 OR BELMONT 171 GASKET; USE SA-193 GRADE B-7 BOLTS.
SPECIFICATIONS
MATERIAL AND CONSTRUCTION TO COMPLY WITH A.S.M.E PRESSURE VESSEL CODE.
TO BE TESTED + A.S.M.E CODED FOR 150 PSIA WORKING PRESSURE AT 600°F.
FBCC MINI PLANT
LOCK HOPPER FOR SOLIDS DISPOSAL
ESSO RESEARCH AND ENGINEERING COMPANY
MECHANICAL DIVISION
LINDEN, N.J.
3" = 1'
70519
1647-63-C
4" x 7.25# CHANNEL DITTO AT 180°
25"
22"
12"
1"
17"
30°
2"
5"
3"
LIFTING LUG - 2 PLACES 1/4" x 1" WITH 9/16" HOLE
4"
7"
1
2
3
4
5
6
7
8
9
10
ELEVATIONS
LIFTING LUGS
20°
45°
6"
1,2
5,7
ORIENTATION TOP VIEW

## Combustor Cyclones

Flue gas and entrained solids (flyash and limestone) exit the top of the combustor through a 45.7 cm I.D. steel pipe, refractory lined to 18.4 cm I.D., and enter a two-stage cyclone system (Figures IV-11 and IV-12). Both cyclones are refractory lined and designed to operate at combustor temperatures and pressures. Solids (primarily limestone) separated by the first stage cyclone drop through a 20.3 cm I.D. steel dipleg, refractory lined to 10.2 cm I.D., and enter a refractory-lined pulse pot (Figure IV-9). From here, they are pneumatically conveyed back to the combustor using controlled nitrogen pulses and enter at a point 66 cm above the fluidizing grid. Solids (primarily fly ash) escaping the primary cyclone pass through a 30.3 cm I.D. steel pipe, refractory lined to 14.5 cm I.D., and enter the more efficient second-stage cyclone where a finer distribution of solids is captured. Collected solids then pass through a 20.3 cm I.D. dipleg, refractory lined to 10.2 cm I.D., and enter a pressurized lockhopper (Figure IV-10) from which they are periodically dumped into metal drums. Although not yet installed, a Ducon granular bed filter with appropriate modifications will be placed after the second-stage cyclone to capture solids that manage to escape the cyclone separation system.

## Pressure Control and Flue Gas Discharge System

The technique used to control combustor pressure consists in dropping the system pressure across an appropriately sized ceramic coated nozzle located in the flue gas exit line. Back pressure is controlled by regulating the flow of a secondary air stream to the nozzle inlet.

After exiting the second-stage cyclone, flue gas passes through 20.3 cm I.D. steel pipe refractory lined to 10.2 cm I.D., and is expanded through a converging nozzle. The 2.5 cm thick nozzle consists of a conical-shaped entrance section with an initial diameter of 3.5 cm which converges at an angle of 30° over a distance of 1.0 cm to a 2.3 cm diameter cylindrical throat of 1.5 cm length. The nozzle is constructed of mild steel and is mounted in a carbon steel flange. The exposed surfaces of the nozzle and flange are covered by a 0.1 mm thick flame-sprayed coat of chromium carbide. In addition, a subcoat of nickel aluminide was flame sprayed to the base metal surfaces to provide a sound substrate for adherence of chromium carbide. Future plans call for the entire nozzle to be constructed of silicon carbide instead of coated metal as described above. Nozzle geometry will remain the same except that three different throat diameters will be used to achieve the correct combustion pressure over the range of operating variables planned.

The remainder of the combustor pressure control system is located 0.6 m upstream of the nozzle and consists of a secondary source of high pressure air which is metered through a 5.0 cm Kamyr ball valve equipped with

FIGURE IV-11

COMBUSTOR FIRST STAGE CYCLONE

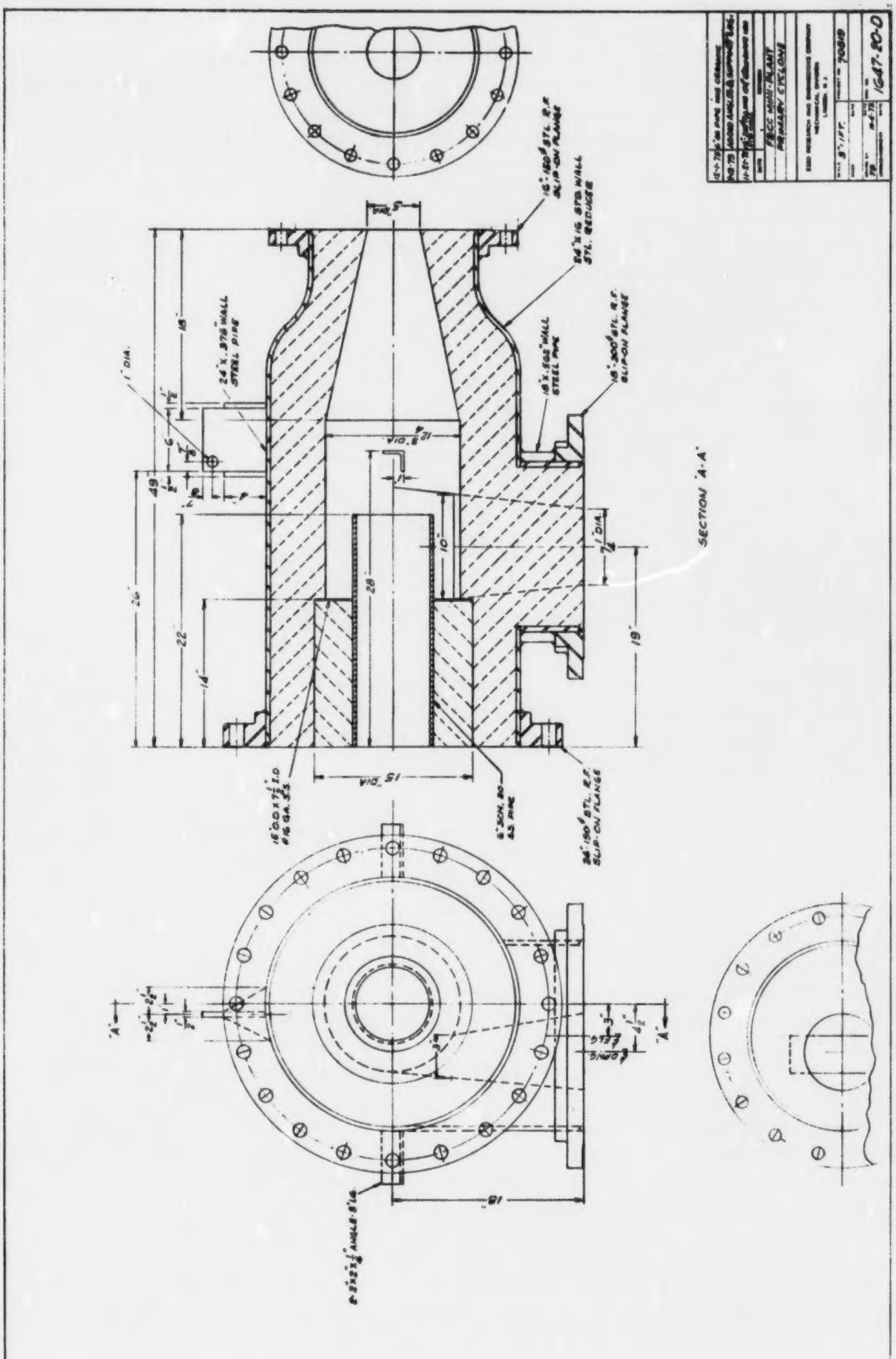

SECTION 'A-A'
24"x.375 WALL STEEL PIPE
1" DIA.
16"x.500 WALL STEEL PIPE
16" 300# STL. R.F. SLIP-ON FLANGE
24"x16 STD. WALL STL. REDUCER
24" 150# STL. R.F. SLIP-ON FLANGE
6" SCH. 80 S.S. PIPE
PRIMARY CYCLONE
1647-80-D

FIGURE IV-12

COMBUSTOR SECOND STAGE CYCLONE

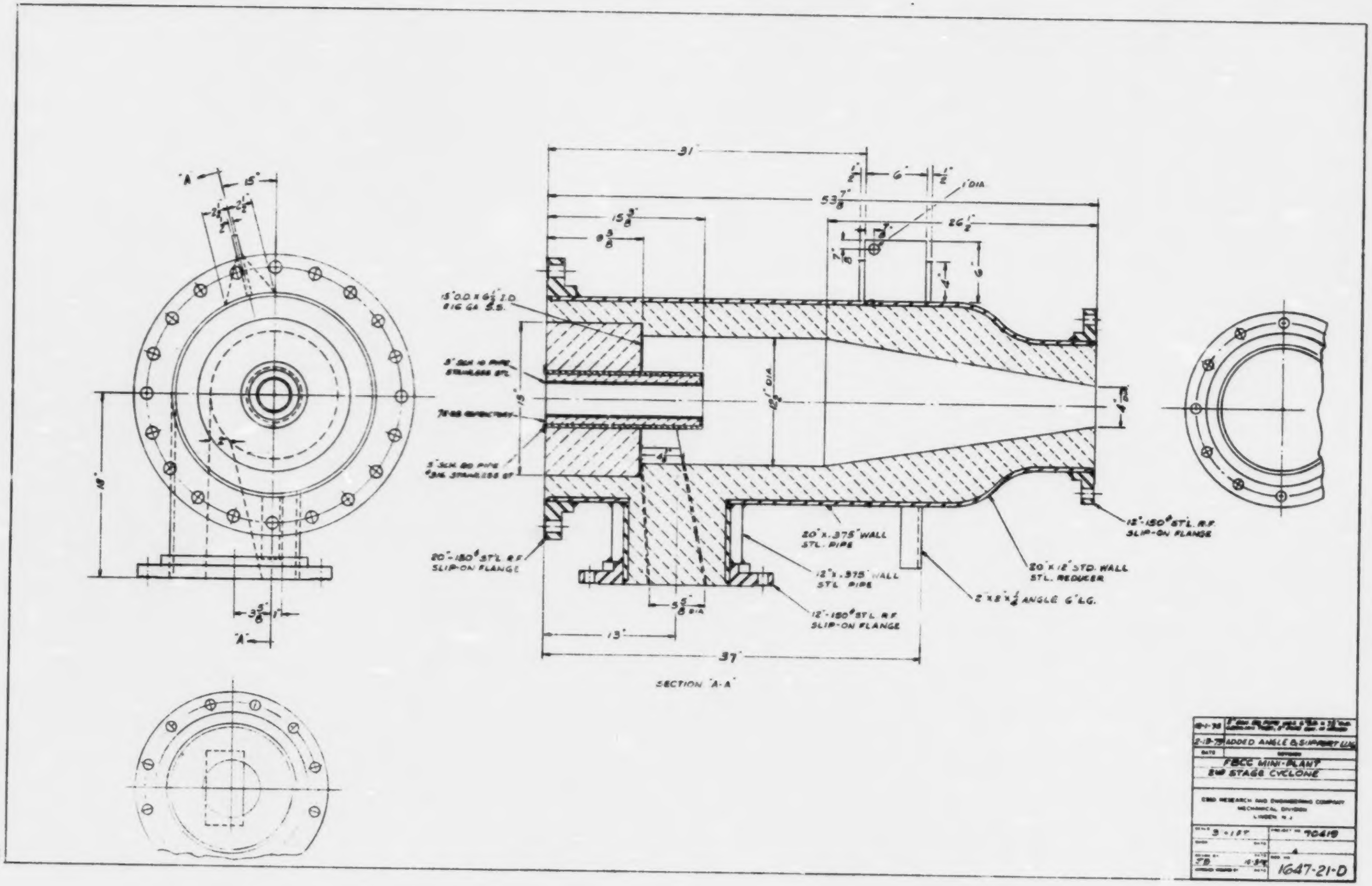
31"
53 7/8"
26 1/2"
15 3/8"
9 3/8"
6"
1/2"
1" DIA
4"
15"
12 1/2" DIA
4 1/4"
5 5/8 DIA
13"
37"
18"
3 5/8"
'A'
15" O.D. x 6 1/2" I.D.
#16 GA S.S.
5" SCH 10 PIPE
STAINLESS STL
5" SCH 80 PIPE
#316 STAINLESS ST
20"-150# ST'L R.F.
SLIP-ON FLANGE
20" x .375" WALL
STL. PIPE
12" x .375" WALL
STL PIPE
12"-150# STL R.F.
SLIP-ON FLANGE
2" x 2" x 1/4" ANGLE 6" LG.
20" x 12" STD. WALL
STL. REDUCER
12"-150# ST'L R.F.
SLIP-ON FLANGE
SECTION 'A-A'
2-13-75 ADDED ANGLE & SUPPORT LUG
DATE
FBCC MINI-PLANT
2ND STAGE CYCLONE
3" = 1 FT
70419
JB
1647-21-D

a penumatic actuator and positioner. By superimposing a secondary flow of air onto the primary flow of flue gas through the nozzle, control of combustor pressure is maintained at the desired level which has been typically 910 kPa.

Downstream of the nozzle, flue gas passes through a 2.5 m 316 stainless steel schedule 40 pipe, water-jacketed by a 4 in, schedule 40-carbon steel pipe, and enters a scrubber for final cleanup before venting to the atmosphere. During transit from the upstream side of the nozzle to the scrubber entrance, flue gas temperature is reduced from approximately 820°C to 260°C, with 35-50% of the reduction due to expansion through the orifice and injection of the low temperature secondary air stream.

## Flue Gas Sampling and Analytical System

Various problems have occurred in previous systems designed to sample exiting flue gas. These are discussed in a subsequent section of the report. Accordingly, discussion here will focus on the flue gas sampling system currently installed.

Flue gas is sampled at a point about 7 metres downstream of the second-stage cyclone exit (ca. 4.5 m upstream of the pressure control nozzle). A schematic of the sampling system is shown in Figure IV-13. The system is designed to produce a solids-free, dry stream of flue gas at approximately ambient temperature and atmospheric pressure whose gas composition is unaltered, except for water content, from that of the original flue gas. In order to allow for cross-checking and backup of the miniplant's main analytical instrument train, the system includes provisions for removing samples for wet chemistry determinations and also direct routing of a stream to the batch fluidized bed combustion unit analytical instruments.

The instrument package for analyzing combustor flue gas composition consists of the following:

| Gas | Instrument | Ranges |
|---|---|---|
| $SO_2$ | Beckman 315A(Infrared) | 0-3000 ppm |
| NO | Beckman 315B (Infrared) | 0-2500 ppm<br>0-1000 ppm<br>0-500 ppm |
| CO | Beckman 315A (Infrared) | 0-6250 ppm<br>0-1250 ppm |
| $CO_2$ | MSA Lira M300 (Infrared) | 0-25 % |
| $O_2$ | Beckman 715 (Pt Electrode) | 0-25 %<br>0-5 % |

Figure IV-13

FLUE GAS SAMPLING SYSTEM

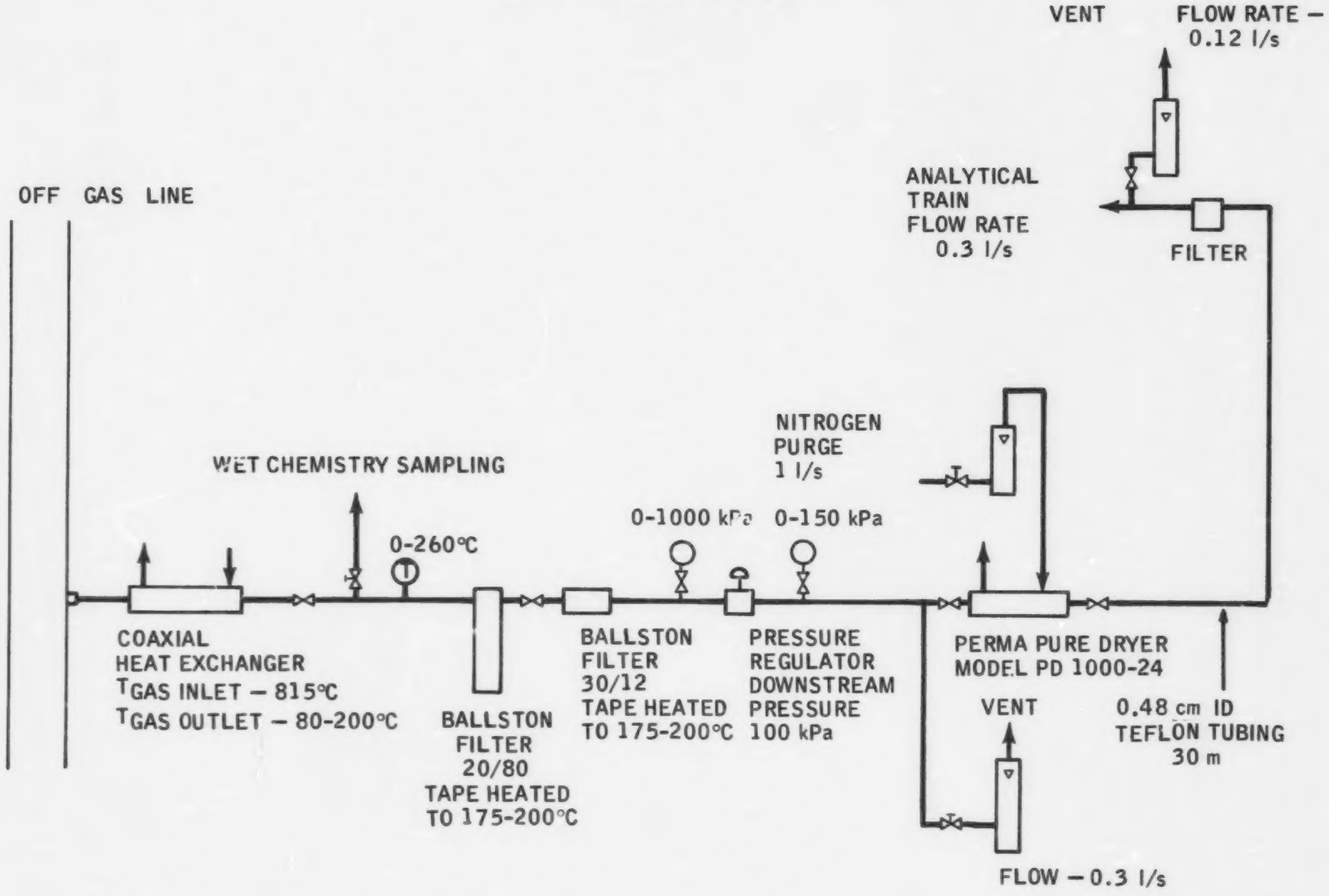
VENT
FLOW RATE – 0.12 l/s
ANALYTICAL TRAIN FLOW RATE 0.3 l/s
FILTER
OFF GAS LINE
NITROGEN PURGE 1 l/s
WET CHEMISTRY SAMPLING
0-1000 kPa
0-150 kPa
0-260°C
COAXIAL HEAT EXCHANGER
TGAS INLET – 815°C
TGAS OUTLET – 80-200°C
BALLSTON FILTER 20/80 TAPE HEATED TO 175-200°C
BALLSTON FILTER 30/12 TAPE HEATED TO 175-200°C
PRESSURE REGULATOR DOWNSTREAM PRESSURE 100 kPa
PERMA PURE DRYER MODEL PD 1000-24
VENT
0.48 cm ID TEFLON TUBING 30 m
FLOW – 0.3 l/s

Output from the instruments is recorded on strip charts every 15 seconds with the exception of $O_2$ data which are recorded continuously.

### Process Monitoring and Data Generation System

With the exception of the output from the analytical system described above, the remaining data characterizing total system operation are handled in a common manner. Three multichannel recorders (24-channel Honeywell Electronik 112) record output from various measuring instruments. In addition, at one minute intervals, the same output is recorded by a data logger system consisting of a Digitrend 210 data logger with printer and a Kennedy 1701 magnetic tape recorder with the electronic interface between the two designed by Automated Technology Corp. Output from the analyzers will also be recorded by the data logger in the future. Approximately 60 pieces of data are logged with three-quarters involving temperature measurement while the rest deal with pressure and material flow rate. The points logged are given in Appendix E.

Signals from the data logger appear as digital output on printed paper tape and are also stored on magnetic tape. The magnetic tape, containing about 3600 items of data per hour of run time, is fed to a computer which converts the logger output to flow rates, pressures, etc with the proper dimensions. The data are then averaged and standard deviations calculated over preselected time intervals (usually 10 min). Other quantities are also calculated. This includes average bed temperature, based on four thermocouple readings covering the 15-114 cm interval above the fluidizing grid, superficial gas velocity, and excess air.

### Combustor Safety and Alarm System

A process alarm system was designed to warn of impeding operational problems. Two general alarm categories exist. The first, dealing with less critical situations, alerts the operator of the problem so that appropriate corrective action can be taken. The second class of more critical alarms results in the immediate or time delayed shutdown of the complete system or specific subsystems. A brief description of the alarms is presented in Appendix D.

### Fluidized Bed Regenerator System

Since shakedown of the regenerator system has not been completed, discussion of the regenerator will be abbreviated.

The regenerator reactor, designed for operation at 1100°C and pressures up to 1010 kPa, consists of a 45.7 cm I.D. steel shell refractory-lined with 75-28 Grefco Litecast to an internal diameter of 21.6 cm (see Figure IV-14). Numerous taps are provided along its 6.66 m overall height to monitor both temperature and pressure, while appropriately located ports allow for material entry and exit.

## FIGURE IV-14

## REGENERATOR VESSEL

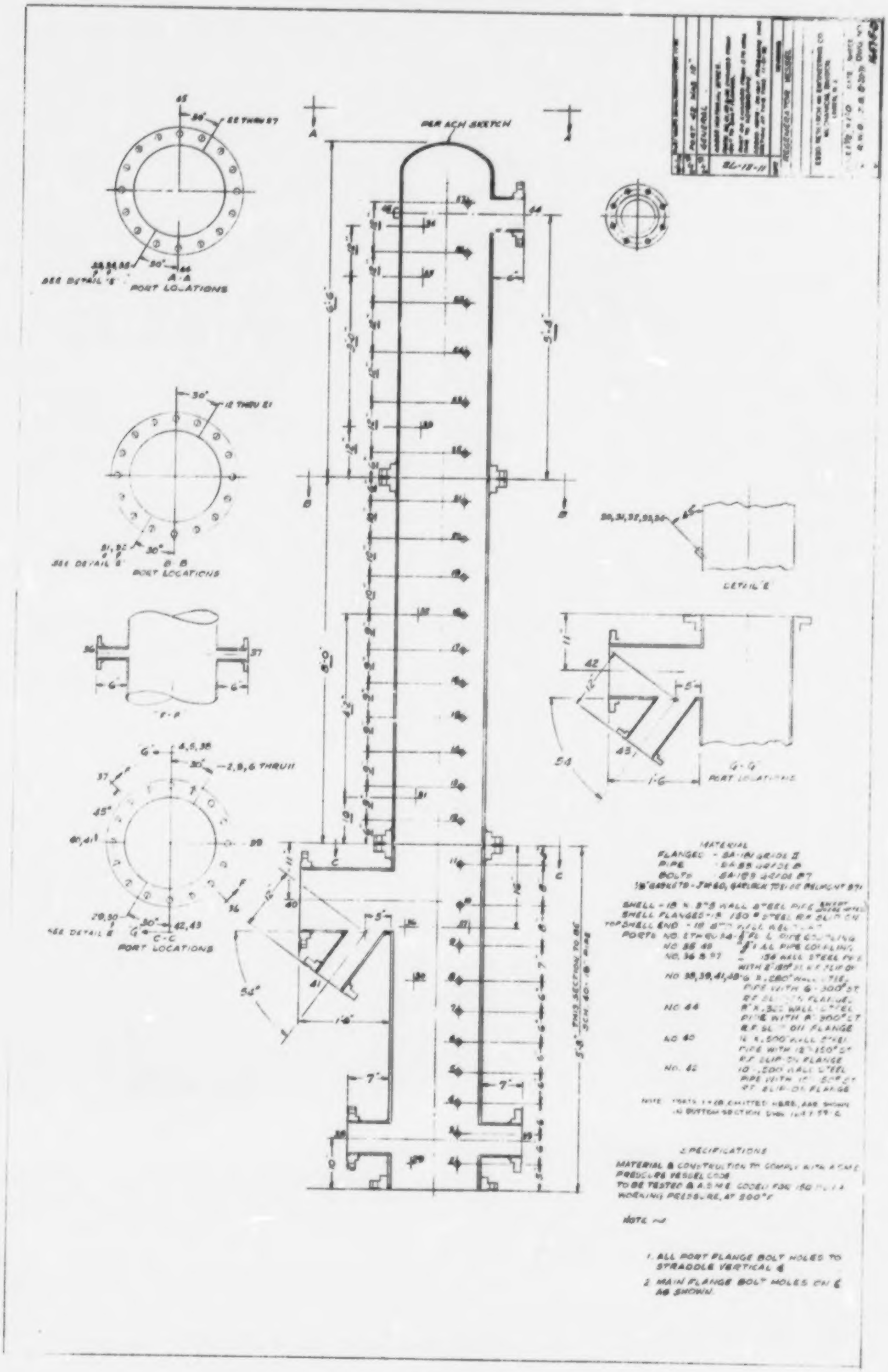
PER ACH SKETCH
A-A
PORT LOCATIONS
SEE DETAIL 'E'
B-B
PORT LOCATIONS
F-F
C-C
PORT LOCATIONS
DETAIL 'E'
G-G
PORT LOCATIONS
MATERIAL
FLANGES - SA-181 GRADE II
PIPE - SA 53 GRADE B
BOLTS - SA-193 GRADE B7
1/8" GASKETS - JM 60, GARLOCK 7021 OR BELMONT 871
SHELL - 18" x .375 WALL STEEL PIPE
SHELL FLANGES - 18" 150# STEEL RF SLIP ON
TOP SHELL END - 18" STD WALL WELD CAP
PORTS NO. 27 THRU 34 - 3/4" FULL PIPE COUPLING
NO 35 43 - 3/4" HALF PIPE COUPLING
NO. 36 & 37 - .154 WALL STEEL PIPE WITH 2" 150# RF SLIP ON
NO 38,39,41,43 - 6" x .280" WALL STEEL PIPE WITH 6" 300# ST RF SLIP ON FLANGE
NO 44 - 8" x .322 WALL STEEL PIPE WITH 8" 300# ST RF SLIP ON FLANGE
NO 40 - 12" x .500 WALL STEEL PIPE WITH 12" 150# ST RF SLIP ON FLANGE
NO. 42 - 10" x .500 WALL STEEL PIPE WITH 10" 150# ST RF SLIP ON FLANGE
NOTE: PORTS 1 THRU 26 OMITTED HERE, ARE SHOWN IN BOTTOM SECTION
SPECIFICATIONS
MATERIAL & CONSTRUCTION TO COMPLY WITH A.S.M.E. PRESSURE VESSEL CODE
TO BE TESTED & A.S.M.E. CODED FOR 150 PSIG WORKING PRESSURE, AT 300°F
NOTE
1. ALL PORT FLANGE BOLT HOLES TO STRADDLE VERTICAL ℄
2. MAIN FLANGE BOLT HOLES ON ℄ AS SHOWN.
REGENERATOR VESSEL

Reducing gas for the regeneration step is produced just above the fluidizing grid by the partial combustion of fuel (natural gas) which is injected directly into the bed. The natural gas is provided by the same compressor (20 SCFM capacity at 200 psig) which services the combustor. Plans are underway to install an independent large capacity compressor (43 SCFM at 200 psig) to allow simultaneous operation of both units at typical miniplant operational loadings. A burner located in the regenerator plenum provides additional heat for the regeneration reaction. The burner is identical to that installed in the combustor.

The water-cooled fluidized grid, located 50.8 cm above the regenerator bottom separates the plenum from the main regenerator chamber. Its design, similar to that used in the combustor consists of a 1.3 cm thick X 53.3 cm diameter stainless steel plate containing 392 equally-spaced holes of 0.20 cm diameter within a 21.6 cm circle.

Ports located 25 cm and 145 cm above the fluidizing grid will serve to receive and discharge solids, when transport between combustor and regenerator becomes operational. Desired bed levels in both units will be achieved through a process control package involving differential pressure transmitter circuits to monitor bed level coupled with appropriate regulation of the two pulse pot feeders operating between the combustor and regenerator.

Provision is also made to inject a secondary source of air (or oxygen) near the top of the bed to create an oxidizing zone. Past experience with the batch unit has indicated that this may be required to minimize the formation of CaS byproduct.

Gases exiting from the regenerator pass through a 20.3 cm I.D. steel pipe, refractory lined to 5.7 cm I.D., and enter a single-stage refractory lined cyclone (Figure IV-15). Collected solids drop through a 15.4 cm I.D. steel dipleg, refractory lined to 5.1 cm I.D. and enter a pressurized lock hopper from which they are periodically discharged to metal drums. Cyclone effluent gas is cooled by a heat exchanger and sent to a scrubber for final cleanup before atmospheric discharge.

Regenerator off-gas is to be sampled after the pressure reducing valve, will be filtered, dried and sent to analyzers at approximately ambient temperature and pressure. Provision for cross-checking and backup of the main instrument package will also be included. Analysis of off-gas composition will be made by the following instruments:

## FIGURE IV-15

## REGENERATOR CYCLONE

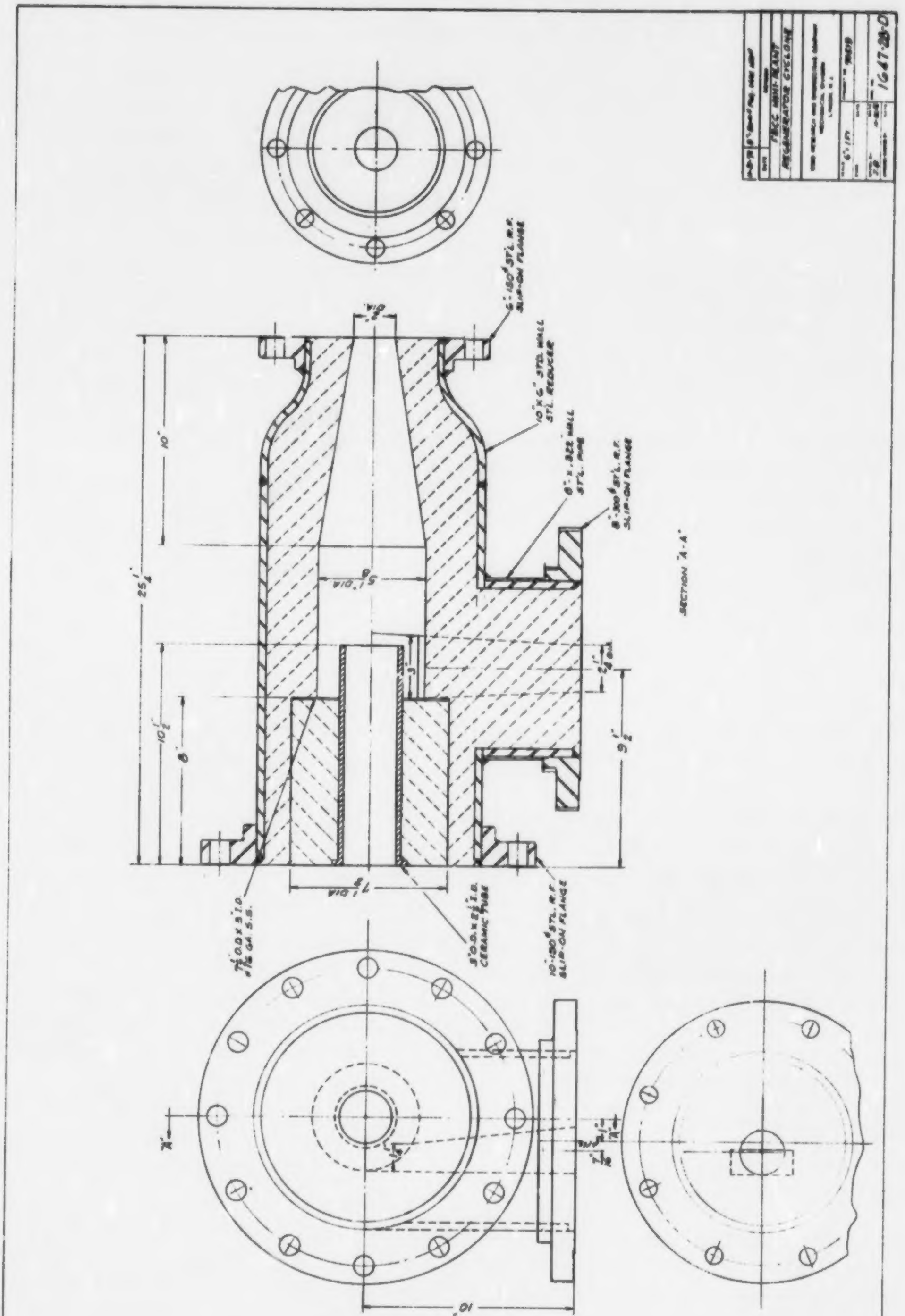
FBCC MINIPLANT
REGENERATOR CYCLONE
1647-28-D
6"·150# STL. R.F. SLIP-ON FLANGE
10"x6" STD. WALL STL. REDUCER
8" x .322 WALL STL. PIPE
8"·300# STL. R.F. SLIP-ON FLANGE
SECTION 'A-A'
10"·150# STL. R.F. SLIP-ON FLANGE
3" O.D. x 2 1/4" I.D. CERAMIC TUBE
7 1/2" O.D. x 3" I.D. 3/16 GA. S.S.
10"
25 1/2"
10 1/2"
8"
9 1/2"
5 1/2" DIA.
7 1/2" DIA.
'A'

| Gas | Instrument | Ranges |
|---|---|---|
| $SO_2$ | Beckman 315A (Infrared) | 0-15 % |
| CO | Beckman 315B (Infrared) | 0-30 %<br>0-10 %<br>0-2.5 % |
| CO | Beckman 315B (Infrared) | 0-1.0 %<br>0-0.5 % |
| $CO_2$ | Beckman 337B (Infrared) | 0-20 %<br>0-5 % |
| $O_2$ | Beckman 715 (Pt Electrode) | 0-25 %<br>0-5 % |

Temperature, pressure, and material flow rate data characterizing regenerator operation will be handled in the same manner as previously discussed for the combustor using multichannel recorders and the data logger system. The points logged are listed in Appendix E. Final processing of data via computer will parallel the scheme previously discussed for the combustor.

Various safety alarm systems have been incorporated into the design of the regenerator control system as was done for the combustor. Depending on the particular problem, these either trigger an automatic system response (immediate or time-delayed) or simply alert the operator so that corrective measures can be initiated. Those conditions which actuate alarms are given in Appendix D.

### Miniplant Support Structure

The flanged steel beam support structure for the miniplant is 12.9 m high, 9.0 m wide, and 3.9 m deep. Three platforms at 2.4 m, 5.7 m, and 9.0 m, with connecting stairways, are provided for servicing the miniplant. The structure rests 18.4 cm off the ground on concrete support pillars. The reactors are supported by the structure at the first platform. Thermal expansion joints are provided at various locations to accomodate thermal expansion of the reactors in the vertical direction. A five-ton bridge hoist, mounted on top of the support structure, is used for assembly and disassembly operations.

## MATERIALS

### Coal

Coal used during the miniplant combustor shakedown was a high volatile bituminous coal obtained from Consolidation Coal Company. In Runs 2-12.2, the coal was obtained from the Arkwright Mine in West Virginia.

In subsequent runs, the coal was obtained from the Champion preparation plant in Pennsylvania. Both coals are Pittsburgh No. 8 seam coals and have similar analyses. Grinding and sizing was done by Penn-Rillton Company. Essentially all of the coal was less than 2380 µm (No. 8 U.S. Mesh) in size. Actual size distributions used during the course of the program are given in Figure IV-16. Two size distributions were used during shakedown. The original batch used in runs 2 to 12.2 contained all the fines. Batches prepared for subsequent runs had most of the fines smaller than 40 mesh removed. This gave a distribution more closely resembling that expected to be used in commercial FBC units. Composition analyses are shown in Table IV-1.

Limestone

The only sorbent used for the miniplant runs was uncalcined limestone obtained from Grove Lime Company (Stephen City, Va) designated as Grove No. 1359. This material, in its calcined form, contained 97.0 wt. % CaO, 1.2 % MgO; 1.1 % $SiO_2$, 0.3% $Al_2O_3$, and 0.2% $Fe_2O_3$. The uncalcined limestone feed was screened to give a distribution with a minimum of 90% between 2380 µm (No. 8 U.S. Mesh) and 841 µm (No. 20 U.S. Mesh). Actual particle size distribution of the limestone bed during the course of a run would be shifted into the smaller particle size range due to attrition.

TABLE IV-1. MINIPLANT COAL ANALYSES

| Component | | Weight Percent | | |
|---|---|---|---|---|
| | Coal | Arkwright | Arkwright | Champion |
| | Run No. | 1-12.2 | 13.1-15.4 | 16.1-19.3 |
| Moisture | | 1.0 | 0.9 | 2.2 |
| Ash | | 8.1 | 7.4 | 8.8 |
| Total Carbon | | 76.5 | 77.1 | 78.1 |
| Hydrogen | | 5.3 | 5.1 | 5.1 |
| Sulfur | | 2.6 | 2.5 | 2.2 |
| Nitrogen | | 1.5 | 1.1 | 1.6 |
| Oxygen (by difference) | | 5.0 | 6.0 | 4.1 |
| Chlorine | | 0.1 | 0.1 | 0.1 |
| Higher Heat Value (BTU/lb) | | 14100 | 13700 | 13600 |

Figure IV-16

COAL PARTICLE SIZE DISTRIBUTION

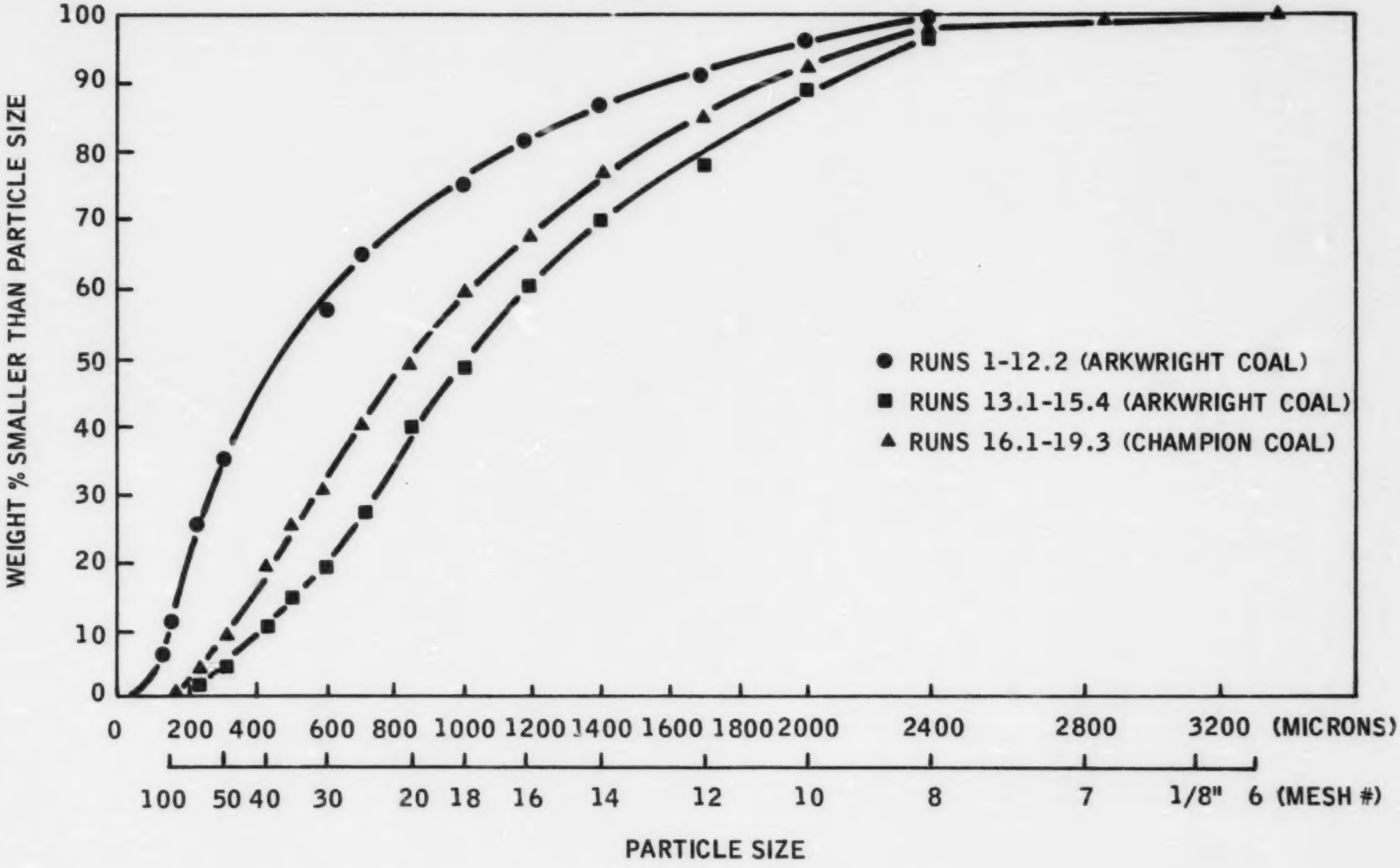

## PROCEDURES

### Combustor Startup

Prior to initiating a run, a detailed checkout procedure is followed to insure that the system is ready for operation. These include such things as various equipment checks, calibration of flue gas analyzers, activation of process monitoring and control systems, and turning on all cooling water systems. All runs were begun with an initial bed of limestone in the combustor. This consisted of either a fresh charge of uncalcined stone or the bed from the previous run.

The first operation of startup involves preheating the limestone bed using natural gas and then by kerosene. Prior to ignition of natural gas, an air flow of about 350 SCFM (9.9 standard $m^3$/min), or about half that used at normal operating conditions, is fed through the burner while combustor pressure is raised to 280 kPa gauge. Once ignition of the natural gas occurs, this procedure maximizes incoming gas temperature under conditions which allow good natural gas combustion and adequate bed fluidization. Ignition begins by simultaneously feeding 20 SCFM (0.57 standard $m^3$/min) of natural gas through the burner while activating an ignition electrode.

Because of the limited capacity of the gas compressor, natural gas is used only to heat the bed to a temperature of about 430°C, sufficient to insure self-ignition of kerosene. This generally requires 20-30 minutes. At this point, kerosene is injected into the lower portion of the bed.

When rising temperatures indicate ignition of liquid fuel, natural gas feed is discontinued to insure sufficient air for complete combustion of kerosene. Approximately 10-15 minutes are required to raise the bed temperature to 650°C which is sufficient to achieve self-ignition of coal.

Coal, usually mixed with limestone, is then fed to the combustor from the primary injector. A steady stream of 60 SCFM (1.7 standard $m^3$/min) of transport air is used to convey coal into the combustor. Actual rate of coal injection is determined by the pressure differential between the injector and combustor. The rate is initially set at an appropriate value based on past experience under similar operating conditions. Once ignition of coal is verified by rapidly rising temperatures, kerosene flow is stopped. At this time, the main combustion air feed line to the plenum is opened allowing most of the air to bypass the burner, and both combustion air flow rate and combustor pressure are rapidly increased to their designated operating values. Flow of water to each cooling coil is adjusted to maintain steam/water exiting temperatures of 138-150°C.

Once the desired bed temperature has been reached, it is held approximately constant by the automatic coal feed rate control system.

## Combustor Shutdown

A run is terminated by first discontinuing coal feed which results in a rapid decrease in bed temperature. As temperature falls, fluidizing air flow rate and combustor pressure are decreased stepwise. When temperature falls below 90°C, which generally requires 10-15 minutes, air flow is halted and the combustor is depressurized. At this time, remaining systems, including cooling water flows, are shut down and a nitrogen purge is introduced into the combustor to prevent condensation of moisture.

## UNIT PERFORMANCE

### Length of Operation and Conditions Tested

During the shakedown phase a total operating time of 500 hours was accumulated and 37 runs conducted. Many of the initial runs were limited to 10 hours or less duration, but as the systems were improved the run durations increased. Included among the longer runs were four of 24 hours duration, one 50 hours in duration and a 100 hour continuous run which culminated shakedown.

The miniplant was demonstrated to be capable of meeting its basic peak design conditions. As indicated in Table IV-2, operating levels such as pressures of 1020 kPa (10 atm.), superficial velocities of 3.2 m/sec (10.5 ft/sec) and temperatures of 980°C (1800°F) were achieved. The coal feed rate and combustion heat release rates reached to date are somewhat lower than designed due to the reduced heat transfer surface area presently installed in the combustor (62% less than the maximum).

High combustion intensities (approx. 5 $MW/m^3$ exp. bed) were achieved while maintaining excellent temperature profiles and without significant agglomeration problems in the combustion zone. Operation at full design conditions and peak coal feed rates will be accomplished at a future date.

Under typical test conditions the superficial gas velocity and bed temperature were maintained at values somewhat lower than the maximum levels. The superficial velocity was normally in the vicinity of 1.8-2.1 m/s. Temperatures were typically in the 870-950°C range.

The expanded bed depths were usually maintained at approximately 3 m which was sufficient to immerse the entire heat transfer surface in the expanded fluidized bed. In some runs lower bed levels were maintained to reduce the immersed cooling surface, thereby, reducing the coal feed rate and enabling operation at higher excess air levels. In this manner an excess air level as high as 130% was achieved. In all runs an Eastern Pittsburgh Seam Coal was burned in the presence of Grove No. 1359 limestone. Alternate coals and sorbents will be tested in future runs. The test conditions for each of the runs is given in Appendix G.

## TABLE IV-2. MINIPLANT FLUIDIZED BED COMBUSTION CONDITIONS

| | Design | Test Range | Typical |
|---|---|---|---|
| Pressure (kPa) | 1010 | 405-1020 | 930 |
| Temperature-lower zone (°C) | 950 | 815-980 | 870-950 |
| Superficial gas velocity (m/s) | 3.0 | 1.5-3.2 | 1.8-2.1 |
| Excess air (%) | 15 | 10-130 | 10-30 |
| Bed depth - static (m) | 1.2 | 0.8-2.0 | 1.4-1.6 |
| Bed depth - expanded (m) | 4.6 | 1.3-3.7 | ∿3 |
| Coal feed rate (kg/hr) | 218 | 90-155 | 120-140 |
| Combustion heat release (MW) | 1.8 | 0.8-1.3 | 1-1.2 |
| Combustion intensity $\left(\frac{\text{MW}}{\text{m}^3 \text{ expanded bed}}\right)$ | 5.2 | ∿5 | ∿5 |
| Coal | Pittsburgh seam<br>-7 +40 mesh | | |
| Sorbent | Grove No. 1359 limestone<br>-8 +20 mesh | | |

## Summary of Operating Results

Details of the equipment performance and combustion results from the miniplant shakedown are reported in other sections of this report. This section briefly summarizes these results.

Good control of each of the operating variables was demonstrated for sustained periods. Standard deviations typical during such times are given in Table IV-3.

TABLE IV-3. CONTROL OF OPERATING VARIABLES

| Variable | Typical Value | Stand. Dev. |
|---|---|---|
| Bed temperature | 900 | ± 10°C |
| Coal feed rate | 130 | ± 9 kg/hr |
| Combustor pressure | 930 | ± 10 kPa |
| Gas superficial velocity | 2.0 | ± .05 m/s |
| Bed height (as determined by the pressure drop across the bed) | | ± 5% of total ΔP |

Bed temperatures were well controlled using the cascade control system described on page 43. In this system, coal feed rates are adjusted to maintain constant combustor bed temperatures. Earlier attempts to maintain a constant coal feed rate resulted in temperature variations in the combustor and this approach was abandoned.

The combustor pressure was well controlled using the fixed converging nozzle with supplementary air addition as described on page 24. This system replaced an earlier system which used a pressure control valve in the flue gas line. The pressure control valve was susceptible to damage by erosion and that approach was dropped. Steady gas velocities were maintained by achieving good control of the air flow rate, pressure and bed temperature.

The combustor bed level was well controlled by continuously removing solids from the combustor through a "pulse pot" as described on page 20. The pulsing rate was adjusted to maintain a constant bed level by maintaining a constant pressure drop across the bed.

Very good temperature profiles were established after the installation of vertical cooling coils. The temperature variation across the bed was almost entirely due to a hot spot caused by the large volumetric heat release in the lower zone of the combustor near the point of coal injection. However, the hot spot temperature was generally less than 30°C higher then the average temperature across the remaining bed. Flue gas exit temperatures were typically close to the temperatures at the top of the expanded bed.

Combustion efficiencies with flyash recycle from the first cyclone ranged from 93 to 97% over a range of excess air levels from 20 to 110%.

A limited amount of $SO_2$ emission data were obtained through the shakedown period due to problems in developing a reliable $SO_2$ sampling system. The data do, however, suggest that the EPA $SO_2$ emission standard of 1.2 lb $SO_2$/M BTU can be readily met with limestone bed material. Prior to run No. 19.3, a reliable $SO_2$ sampling system was installed. The $SO_2$ emission in run 19.3 for a Ca/S molar ratio of only 1.45 was 720-780 ppm or 1.3 lb $SO_2$/M BTU, (60% removal) just slightly over the allowable emission limit.

$NO_x$ emission levels were measured and correlated as an increasing function of the excess air level. Emissions ranged from 50-250 ppm over excess air levels from 10-110%. The maximum $NO_x$ level corresponds to an emission of, 0.4 lb $NO_2$/M BTU, well below the EPA standard of 0.7 lb $NO_2$/M BTU.

CO emissions were typically below 100 ppm, indicative of good combustion.

## Performance Characteristics of the Miniplant

A fluidized bed combustor such as the miniplant, which relies on immersed cooling surface cooled by water to remove heat and thereby control the combustor temperature, has certain operating restrictions. To begin with, the amount of heat removed by the cooling coil is determined solely by the surface area of the immersed coils, the bed temperature and the heat transfer coefficient on the outside of the coils. A change in the flow of cooling water has very little effect on heat removal. This is due first, to the fact that the resistance to heat transfer inside the tubes is very low and does not influence heat transfer rates significantly. Secondly, the temperature difference between the combustor bed and the interior of the cooling coils is relatively insensitive to changes in the flow of cooling water entering the coils. As a result, at a given set of operating conditions i.e., temperature, pressure, fluidization velocity, particle size, etc., the only parameter which affects heat removal rates is the surface area of the cooling coils immersed in the fluidized bed. Once the surface area is fixed, the heat removal rate is also fixed and the only parameter which can be varied to control bed temperature is the coal feed rate.

If saturated or superheated steam is used as the cooling medium, the situation is different. In that case, increasing the flow of steam can increase the temperature difference between the bed and the cooling medium. Therefore, varying the flow rate of the steam will exert some measure of bed temperature control. Since saturated or superheated steam was not used as the cooling medium in the miniplant, this means of temperature control was not available and changing the coal feed rate was the method used to control the bed temperature.

It can also be seen that fluidization velocity and excess air are not independent variables. Once the coal feed rate has been adjusted to give the desired bed temperature, the air feed rate can be adjusted either to the desired excess air level or the desired fluidization velocity. Fixing one sets the other. If it is desired to study the effects of fluidization velocity and excess air independently, this can only be done by changing the heat transfer area immersed in the fluidized bed. This is best done by removing (or adding) cooling coils. It can also be done by dropping the expanded bed level so only a portion of the cooling coils are covered by the expanded bed. This is a less desirable method since it results in a change in bed depth. It also results in a lower flue gas outlet temperature which, in some cases, may not be desirable. Once the heat transfer surface area has been changed, fluidization velocity and excess air level will still be dependent, one on the other, but at different values than before.

## EQUIPMENT PERFORMANCE

### Coal Feeding

The performance of the pneumatic transport coal injection system was originally unsatisfactory and had to be improved considerably (see Figure IV-3 (Equipment Section)). The system was sensitive to plugs, particularly at the orifice of the primary injector. The orifice assembly was redesigned to have no internal discontinuities such as sudden decreases in diameter. Coal had to be dry and be free of any foreign material which might plug the orifice. There was also difficulty in controlling ΔP between the primary injector and combustor during refilling of the primary injector. This problem was alleviated by modifications in design and attentive monitoring of the unit during the primary injector filling operation.

The original orifice assembly contained a 3/4 inch (nominal) ball valve, a 0.95 cm diameter orifice, and a tee for mixing coal with transport air. A number of different sized pipe fittings were used in the assembly, which resulted in a momuniform internal diameter. Performance was erratic and unsteady coal flow and plugging occured frequently. The entire orifice assembly was therefore redesigned, using a larger valve and piping. A sketch of the new assembly is given in Figure IV-17.

Care was taken to be sure that the diameter of the orifice assembly was uniform from the bottom of the hopper to the orifice. This diameter was the inside diameter of the one inch ball valve (2.1 cm). At the orifice, the diameter decreased to 1.3 cm. Although this orifice was larger than the original 1.0 cm orifice, coal feed rates could be kept

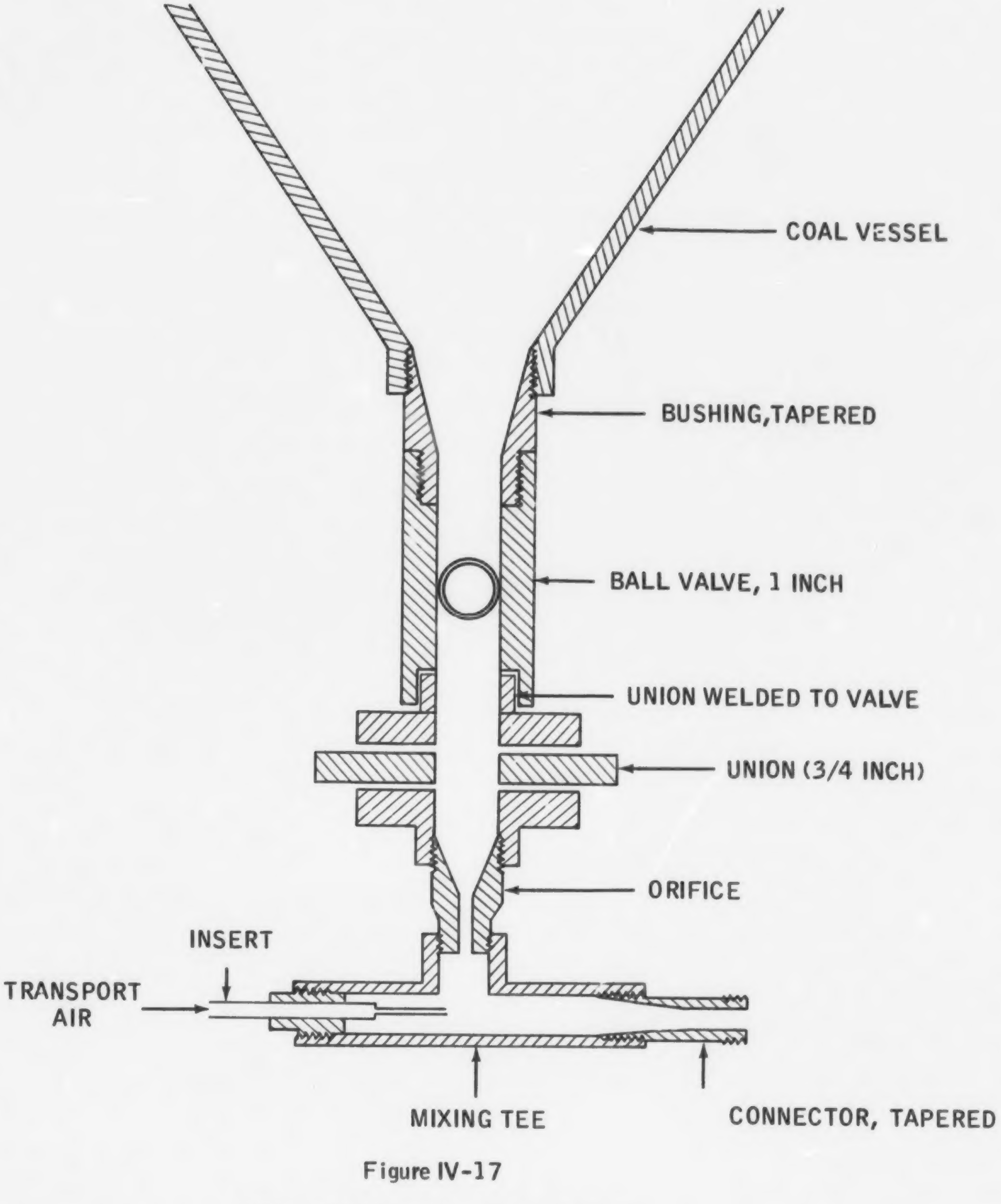
COAL VESSEL
BUSHING,TAPERED
BALL VALVE, 1 INCH
UNION WELDED TO VALVE
UNION (3/4 INCH)
ORIFICE
INSERT
TRANSPORT AIR
MIXING TEE
CONNECTOR, TAPERED

Figure IV-17

COAL FEEDER ORIFICE ASSEMBLY

the same by increasing slightly the flow of transport air and/or decreasing the ΔP from the primary injector to combustor. The larger orifice was much less susceptible to plugging. In fact, performance of the new orifice assembly was significantly improved over the original assembly; coal feeding was steady and plugging became very infrequent. When plugging did occur, it was usually caused by foreign material, such as a piece of scale from the coal hopper, which had become lodged in the orifice.

After flowing through the orifice, coal dropped into the mixing tee, where it was picked up by a stream of transport air and conveyed through the injection line into the combustor. Again, it was of the utmost importance that the change in diameter from the mixing tee to the injection line occurred gradually. It was found best to avoid sharp turns in the transport line because doing so both decreased the chance of plugging and minimized erosion in the line itself. A tee was used to prevent erosion where a sudden turn was necessary (Figure IV-18); however, tees were eventually replaced with gradual bends in the transport line (1/2 inch pipe).

During most of the work, the orifice assembly was vibrated fairly intensely to minimize plugging, however this caused sections of the orifice assembly and transport piping to eventually come loose or sometimes even fracture from fatigue. After several runs were made with the larger orifice, the vibrator was turned off, causing no apparent deleterious effect on coal feeding. As a result, vibration of the orifice assembly is no longer being used.

When the primary coal injector was nearly empty, coal was transferred to it from the feed injector. Since coal feed rate to the combustor was very sensitive to changes in ΔP between the primary injector and combustor, ΔP had to be carefully controlled and monitored during transfers. ΔP is normally controlled by venting air from the primary injector at a constant rate and adding air through a control valve. However, coal entering the primary injector during transfers carried with it transport air, so that there was a tendency for overpressuring the injector. Therefore, in order to relieve some of this pressure, additional air was vented during transfers through a second valve. The system worked satisfactorily if this second valve was sized properly and did not plug. With regard to plugging, a ball valve was found to be much better than the globe valve which was originally used. However, attention by an operator was usually necessary to make sure that the ΔP stayed within the desired range. Some changes to the transfer system are planned in order to reduce the degree of attention required by the operator.

## Temperature Control

The miniplant combustor is operated at bed temperatures from 815 to 955°C (1500 to 1750°F), with temperatures monitored at many elevations within the combustor. The combustor temperature is primarily controlled by adjustment of the rate of coal injected into the fluidized bed.

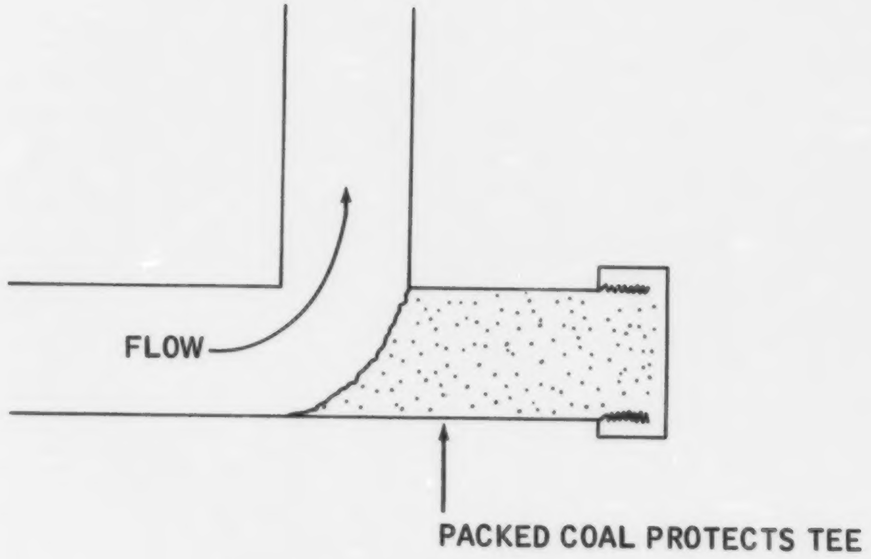
FLOW
PACKED COAL PROTECTS TEE

Figure IV-18

COAL FLOW THROUGH A TEE

A thermocouple in the lower zone of the combustor (at port No. 7) 47 cm (18 inches) above the fluidizing grid is used as the sensor to control temperature of the combustor, and the set point temperature at this location regulates the coal feed rate to the combustor.

As explained on page 10, the coal feed rate to the combustor is regulated by the pressure differential between the primary coal vessel and the combustor - the greater the pressure difference, the greater the feed rate. A sketch of the arrangement is presented in Figure IV-19.

Temperature control is accomplished by a cascade type control loop using two controllers, one for temperature set point and another for ΔP set point. A deviation of the desired (set point) temperature from the actual combustor temperature (at port No. 7) causes a signal to be transmitted by the temperature controller to the ΔP coal feed rate controller. This error signal actually resets the set point of the ΔP controller so that a different ΔP will be established between the coal vessel and the combustor.

This change in the pressure difference between the coal vessel and combustor causes a change in the coal feed rate which will tend to return the bed temperature to the desired (set point) value.

Proper tuning of the controllers was necessary for optimum reaction to system perturbations and anticipation of changes in bed conditions. This control system has performed very satisfactorily and provides excellent temperature control and response.

## Cooling Coils

The miniplant was operated with cooling coils of two different designs during shakedown and a third design is currently being used.

Each of the original coils had a horizontal serpentine configuration with a 5.7 cm horizontal pitch (Figures IV-20 and IV-21). The materials of construction were 3/4 inch type 316 seamless tubing (0.049 inch wall) for the straight sections and 3/4 inch type 316L stainless steel tubing for the 180° U-bends. Ten coils, each covering 0.45 m in the vertical dimension were originally installed. They extended from a height of 0.45 m above the fluidizing grid to an elevation of 5m. The surface area of a coil was 0.58 $m^2$.

These coils were susceptible to fatigue at the inlet and outlet piping and were readily deformed when bed agglomeration occurred. Modifications in the number of coils, their size, and orientation were made after a number of instances of cooling coil damage. Because of their configuration the coils had a high packing density in the cross sectional area of the combustor, limiting the vertical movement of solids and resulting in poor temperature profiles.

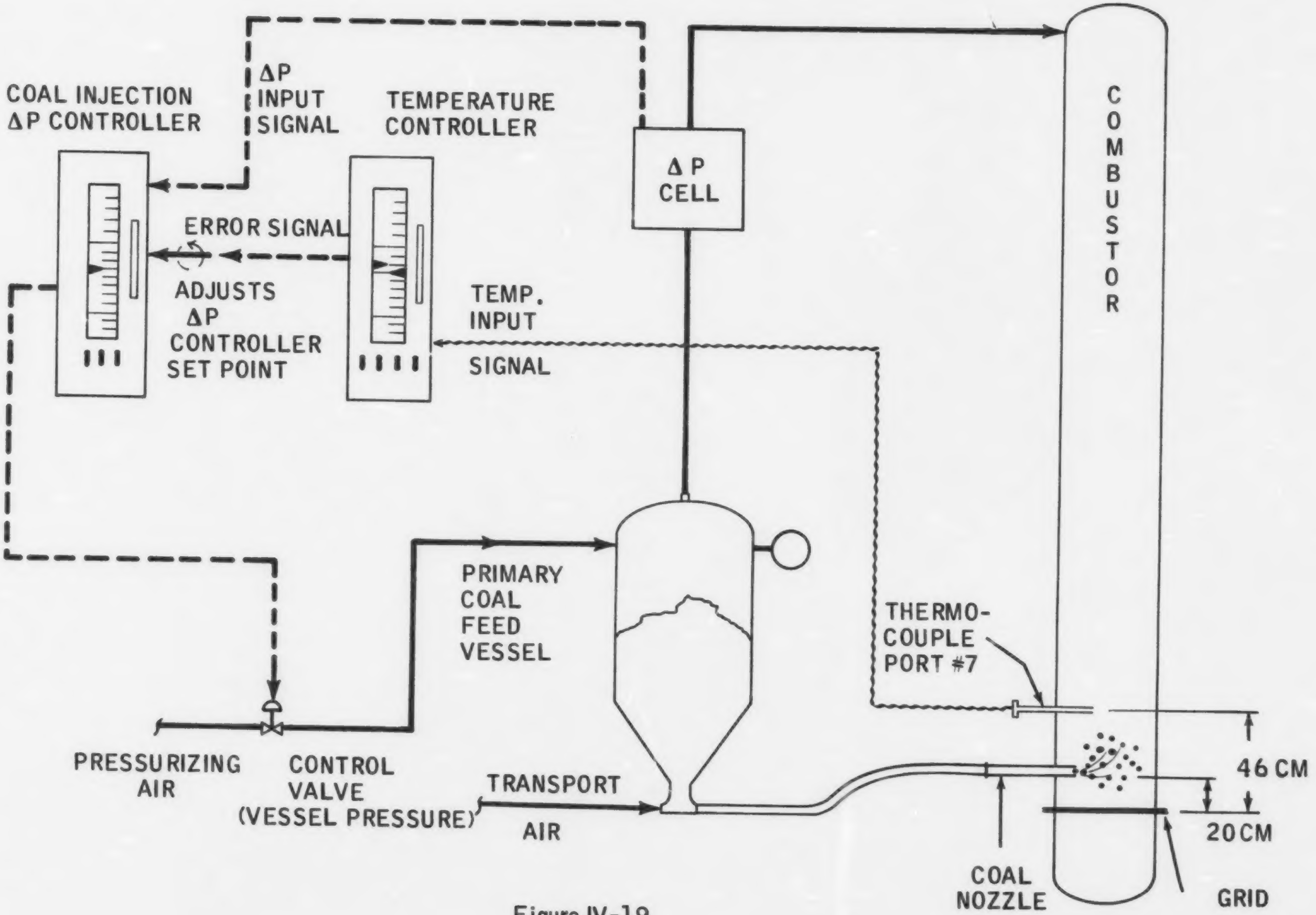
COAL INJECTION
ΔP CONTROLLER
ΔP
INPUT
SIGNAL
TEMPERATURE
CONTROLLER
ΔP
CELL
COMBUSTOR
ERROR SIGNAL
ADJUSTS
ΔP
CONTROLLER
SET POINT
TEMP.
INPUT
SIGNAL
PRIMARY
COAL
FEED
VESSEL
THERMO-
COUPLE
PORT #7
46 CM
20 CM
PRESSURIZING
AIR
CONTROL
VALVE
(VESSEL PRESSURE)
TRANSPORT
AIR
COAL
NOZZLE
GRID

Figure IV-19

COMBUSTOR TEMPERATURE CONTROL SCHEMATIC

## FIGURE IV-20

## HORIZONTAL COOLING COILS

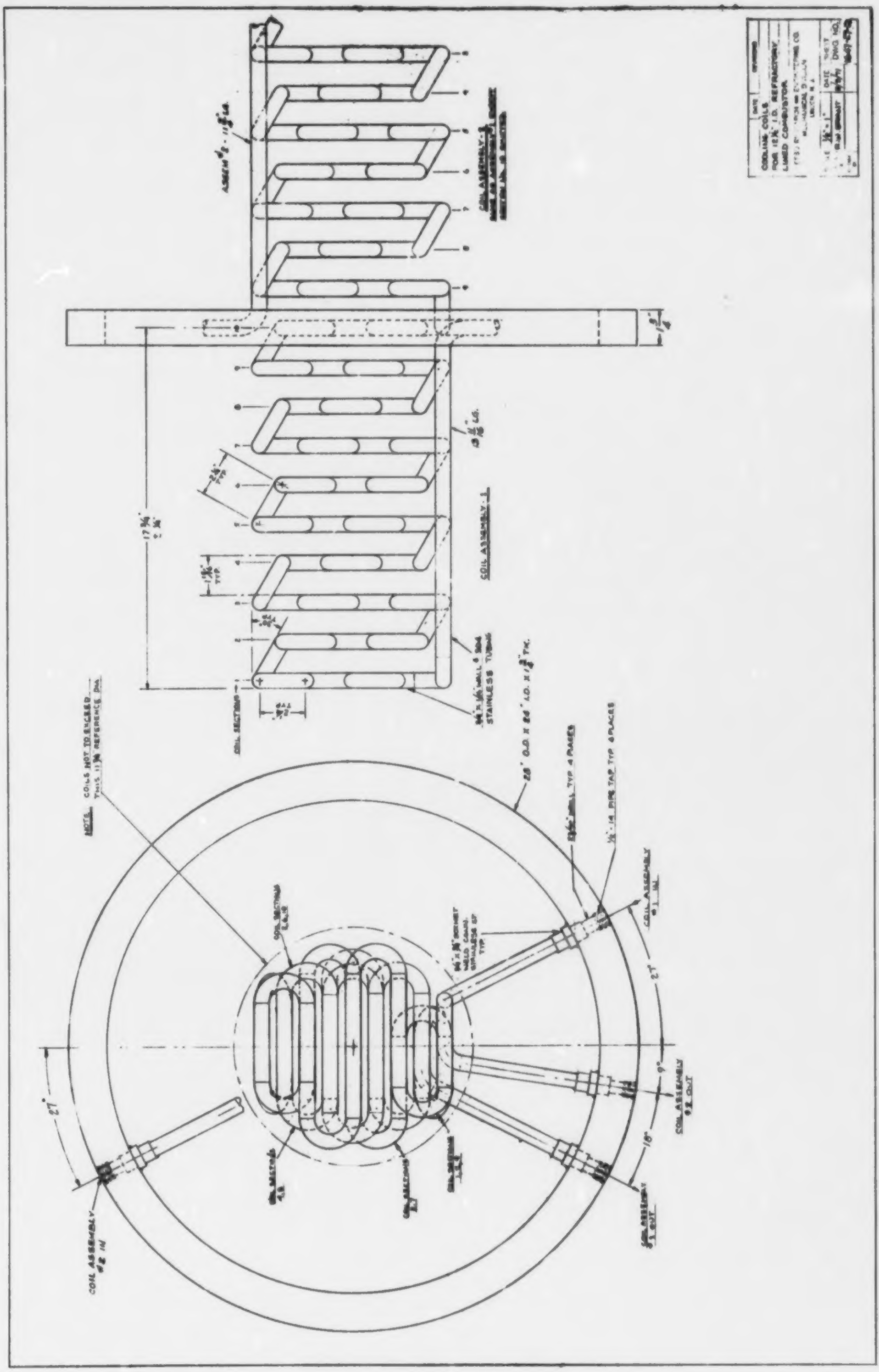
COIL ASSEMBLY 1
COIL SECTION
STAINLESS TUBING
17 3/4"
27°
9°
18°
COIL ASSEMBLY #1 IN
COIL ASSEMBLY #2 IN
COIL ASSEMBLY #1 OUT
COIL ASSEMBLY #2 OUT
COOLING COILS

FIGURE IV-21

HORIZONTAL COOLING COILS

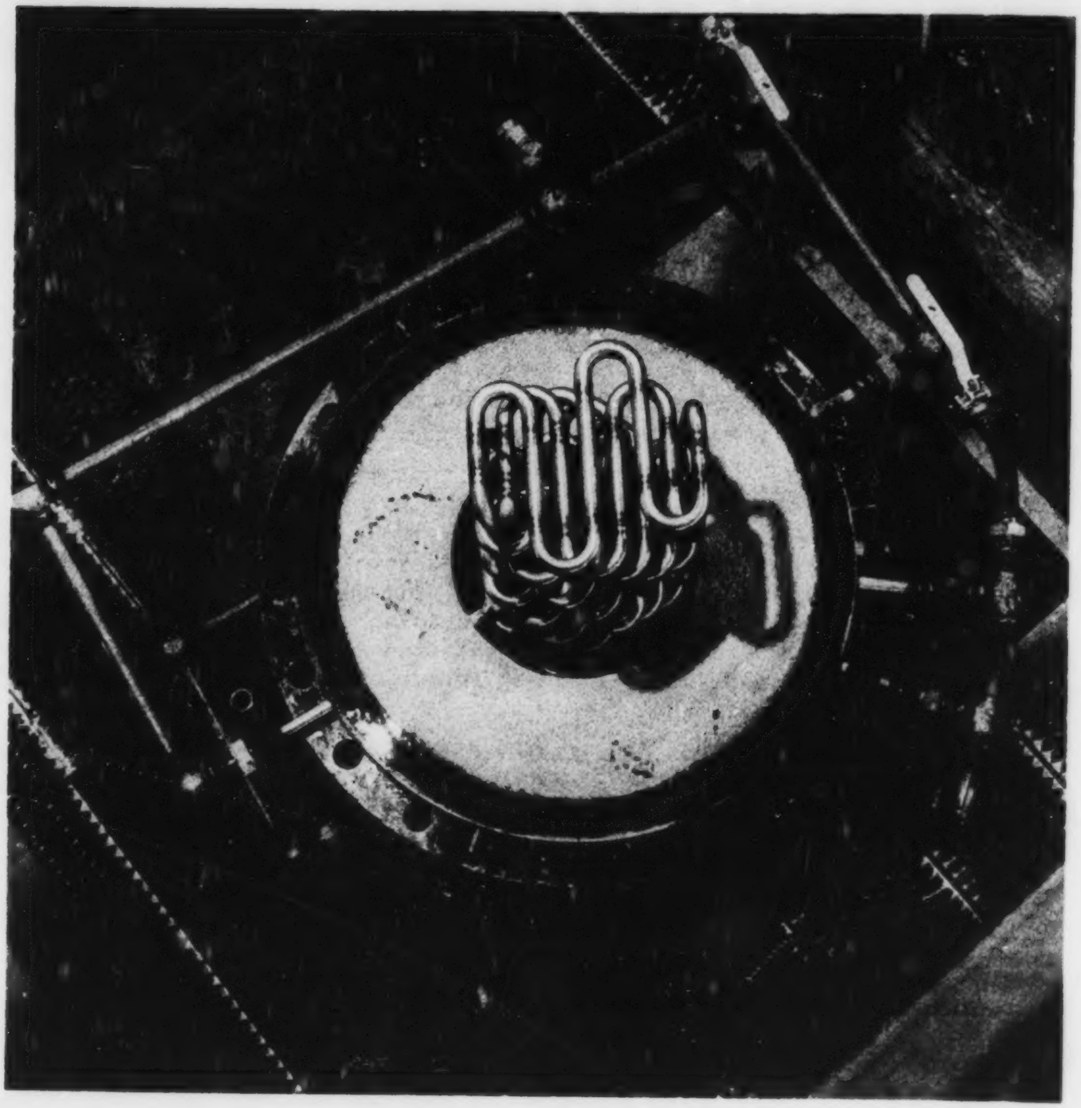

The second generation coils were constructed with a vertical configuration to achieve better top to bottom mixing (see Figures IV-22 and IV-23). These coils were installed after Run 15.4. The loops of the 0.45 m high coil were distributed as uniformly throughout the cross section of the combustor as possible to promote uniform fluidization patterns. The area of one of these coils was 0.55 $m^2$. The materials of construction were 3/4 inch 316 tubing for the straight sections and 3/4 inch 316L tubing for the U-bends. Schedule 40 stainless steel pipe used for the inlets and outlets gave increased support. In addition, reinforcing braces and bands were used to hold the coil rigid. Because of the desire to operate at moderate conditions with all coils immersed in the fluidized bed only the four lowest coils were installed.

The use of these coils did result in significant improvements in the temperature profile, however, the coils were still susceptible to damage. Third generation coils of a vertical configuration were constructed from heavy wall pipe for added sturdiness and installed after Run 18.3. The design is discussed on page 20.

The configuration, number and orientation of the coils used in the various miniplant runs is documented in Table IV-4.

## Temperature Distribution

A representative coal feed rate for the miniplant has been 145 kg/hr (320 lbs/hr), which implies a combustion heat release level of 1.2 MW (4,200,000 BTU/hr). The major portion of the heat liberated occurs in a combustion zone near the coal inlet port and this heat must be immediately transferred to the internal heat transfer surfaces by the rapidly circulating fluidized solids in order to achieve a uniform bed temperature.

In freely fluidized beds, the recirculation rates are generally rapid enough to achieve minimal temperature gradients, even with highly exothermic reactions. However, it was found that the miniplant horizontal coil configuration constrained the solids mixing and recirculation to a degree that adversely affected the temperature profile. Localized high temperatures and large temperature gradients were experienced with the original serpentine horizontal coils (Figure IV-24). This non-uniform temperature distribution limited coal feed rates, caused low flue gas temperatures, created temperature control difficulties and tended to promote bed agglomeration in the high temperature zone.

The coils when viewed from the top were optically dense which suggested they were severely hindering the movement of solids and bubbles in the vertical direction. Therefore some of the coils were shortened and orientated on their side to act as vertical coils and to open the cross sectional area. A dramatic improvement in the profile was observed and subsequently the vertical coils shown in Figure IV-22 were installed. The temperature gradient decreased to 14°C/m or less as illustrated in Figure IV-25. The increasing temperature profile in the freeboard volume shown in Figure IV-25 occurred because the high circulation rates in the

## FIGURE IV-22

VERTICAL COOLING COILS

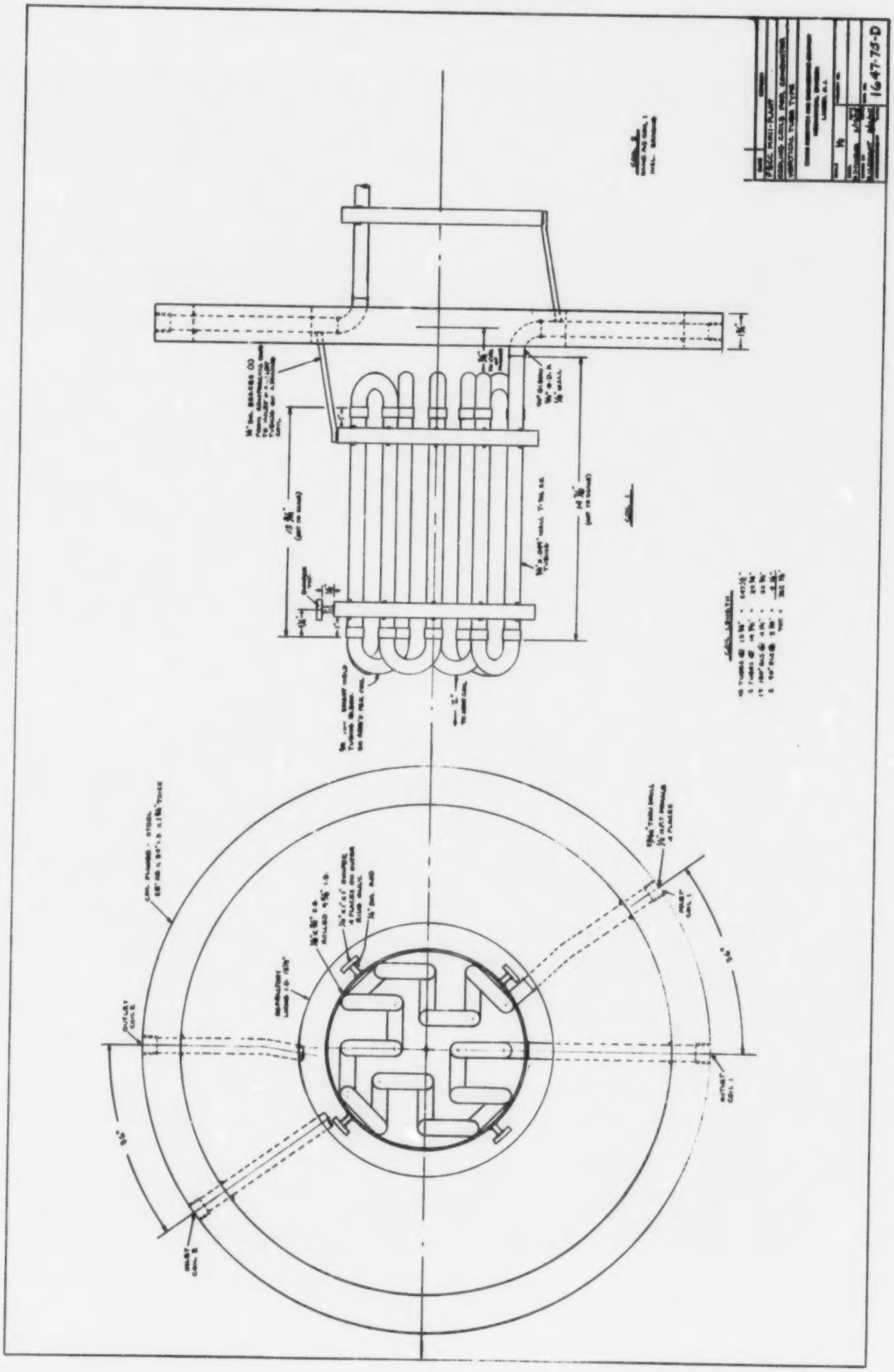
PERC MINI-PLANT
VERTICAL TUBE TYPE
1647-75-D

FIGURE IV-23

VERTICAL COOLING COILS

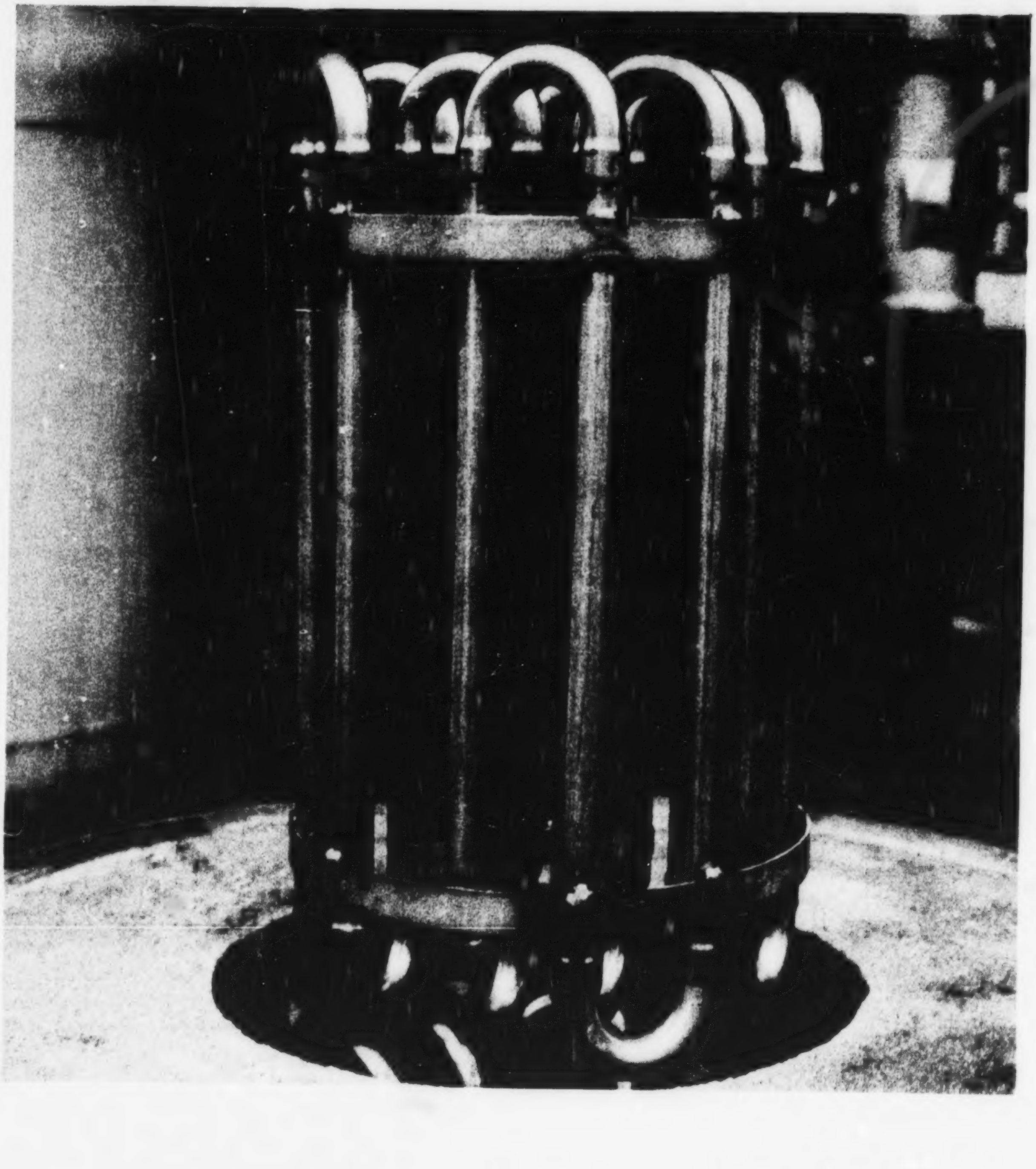

TABLE IV-4. MINIPLANT COOLING COIL MODIFICATIONS

| Runs In Use | Configuration | Size, Orientation and Number |
|---|---|---|
| 1 - 4.3 | Horizontal Serpentine | 10 coils, each with an area of 0.58 $m^2$ |
| 5.1 - 5.4 | Horizontal Serpentine | Coils 1A-4B, 5B, each with an area of 0.58 $m^2$. Coil 5A removed |
| 6.1 - 9.1 | Horizontal Serpentine | Coil 1A - 0.29 $m^2$, Coil 1B - 0.27 $m^2$<br>Coils 2A-4B, 5B - 0.58 $m^2$ each<br>Coil 5A removed |
| 10.1 - 13.3 | Horizontal Serpentine | Coil 1A - 0.29 $m^2$, Coil 1B - 0.27 $m^2$<br>Coil 2A - 0.47 $m^2$, Coil 2B - 0.56 $m^2$<br>Coils 3A, 3B - 0.58 $m^2$ each<br>Coils 4A, 4B, 5A removed<br>Coil 5B - no water flow<br>Coil 1B was orientated with the straight tubes in a vertical direction to act as a vertical coil |
| 14.1 - 15.4 | Horizontal Serpentine | Coil 1A - 0.29 $m^2$, Coil 1B - 0.27 $m^2$<br>Coil 2A - 0.30 $m^2$, Coil 2B - 0.31 $m^2$<br>Coil 3A - 0.23 $m^2$, Coil 3B - 0.58 $m^2$<br>Coils 4A, 4B, 5A removed<br>Coil 5B - no water flow<br>All coils except 3B & 4A were orientated with the straight tubes in a vertical direction to act as vertical coils |

TABLE IV-4. (Continued) MINIPLANT COOLING COIL MODIFICATIONS

| Runs In Use | Configuration | Size, Orientation and Number |
|---|---|---|
| 16.1 - 17.1 | Vertical (second generation) | Coils 1A, 1B, 2A, 2B - 0.55 $m^2$/coil |
| 18.1 - 18.3 | Vertical (second generation) | Coils 1A, 1B - 0.55 $m^2$/coil |
| 19.1 - 19.3 | Vertical (third generation) | Coils 1A, 1B, 2A, 2B - 0.55 $m^2$/coil |

---

Note: The coil number indicates the flange the coil was mounted on. Flanges 1,2,3,4,5 are located at heights above the fluidizing grid of 0.915 m, 1.83 m, 2.74 m, 3.66 m and 4.57 m, respectively. Coils A extend below the flange, coils B extend above the flange.

Figure IV-24

BED TEMPERATURE PROFILE
HORIZONTAL COILS

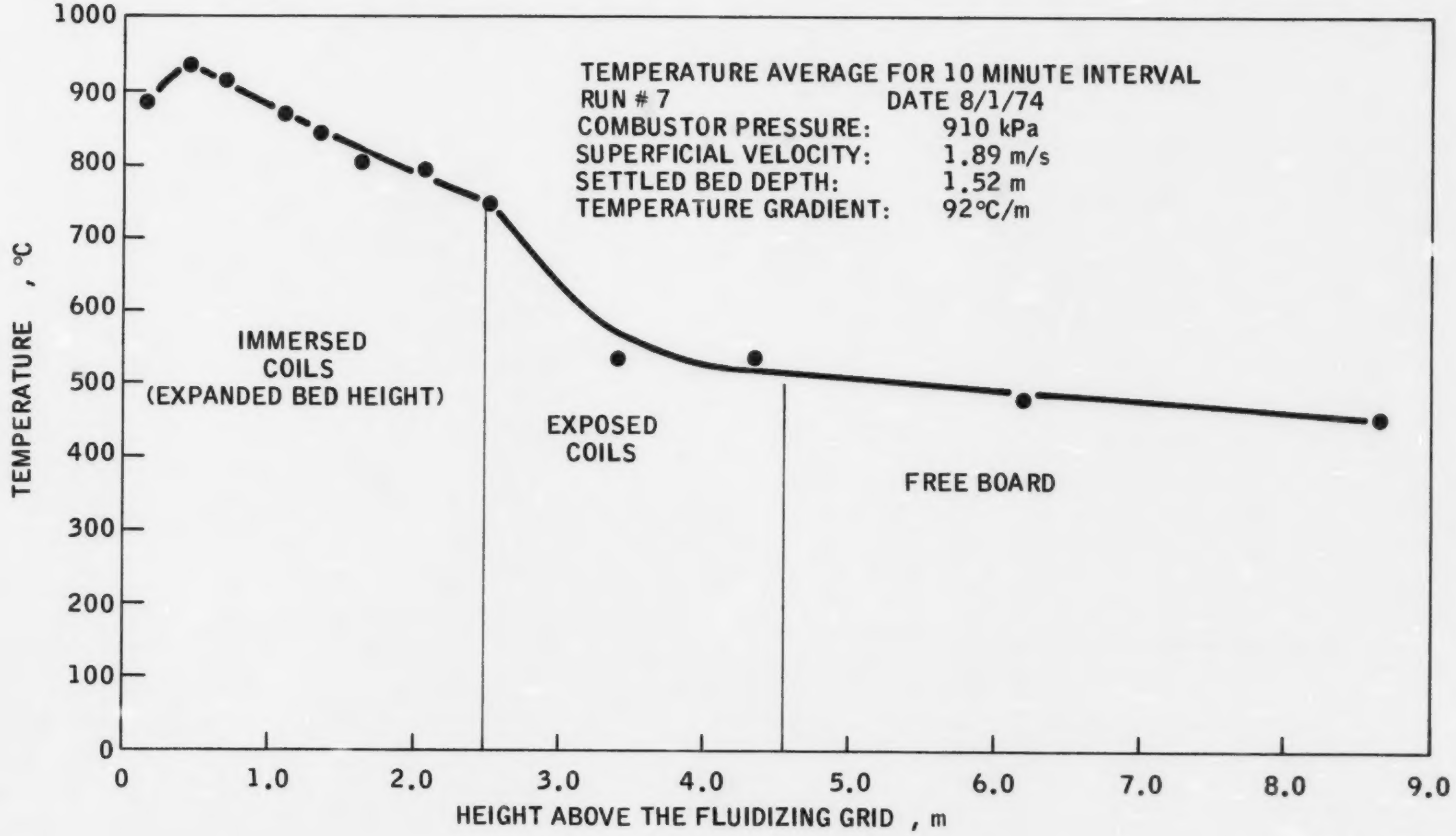

Figure IV-25

BED TEMPERATURE PROFILE
VERTICAL COILS

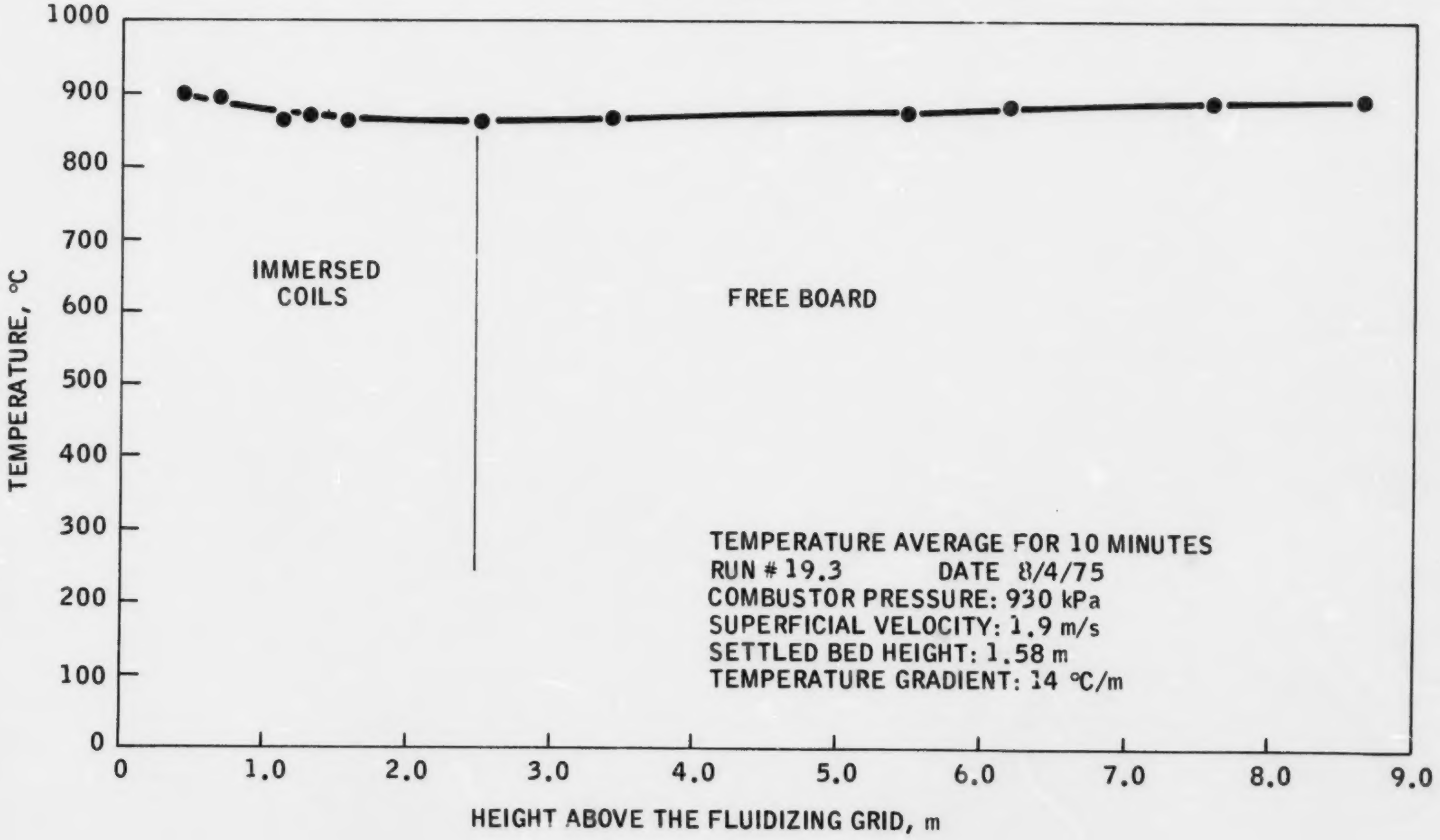

bed caused the elutriation of some partially combusted coal. Flue gas temperatures comparable to the combustion zone temperature were thus achieved. In addition the circulation rates in the combustion zone were high enough to avoid a hot spot problem.

A transparent cold model unit with a diameter of 15.2 cm was used to investigate qualitatively the effect of the baffle configuration on solids mixing. Motion pictures were taken of the mixing in the presence of simulated horizontal and vertical coils.

In the cold model, the top to bottom mixing in a bed with horizontal baffles (simulated coils) was found to be relatively poor. Because of the small diameter of the unit, the bubbles which formed filled much of the cross-section and a dampened slugging action ensued. Much of the vertical movement proceeded in small steps corresponding to the periodic passing of a bubble. Eddies of solids near the wall and on the baffles were relatively motionless between slugs. The transport of solids from the well fluidized section of the bed below the coils to the upper bed was poor. This was due to the slugs which impacted on the bottom of the lower baffle impeding the solids movement to the upper bed. This boundary may in part explain the hot spots observed in the combustion zone of the miniplant when horizontal coils were used.

The slugging action and top to bottom mixing was far more vigorous with vertical baffles. At velocities lower than 1.5 m/sec entire portions of the bed were carried up the column before the slug disintegrated. At higher velocities the slugging became much more frequent and the slugs were smaller and disintegrated faster. The mixing behavior approached that anticipated in the turbulent regime where the movement is very swift and random and the slugging action dissipates.

The cross-sectional area of the miniplant is greater than the area of the cold model unit by a factor of 4.3. In the miniplant, mixing will be influenced to a lesser degree by slugging action. The size of the cold model is closer to that of the batch unit and the mixing patterns may be more representative of what is occuring in the batch unit.

A model was developed to predict temperature profiles in fluidized beds with internal baffles (2). Estimates of the solid recirculation rates and of the cross flow rates between the bubble wake and emulsion phase were obtained using the concepts of the bubbling bed theory. One conclusion was that the length of the free path of bubbles traveling through a baffled volume is of critical importance. The solids transport in the vertical direction is carried in the wake of bubbles. A bubble which impacts on a baffle undergoes destruction and rebirth, and in the process the wake is also disrupted. With a coil configuration which has a small vertical spacing between tubes, the wake is frequently disrupted, creating high solids cross flow rates, short mixing lengths and poor top to bottom solids recirculation rates. The model was able to reproduce fairly well the temperature profile obtained in the miniplant with horizontal serpentine coils using a mixing length of 7-8 cm, the tube spacing in the vertical direction. Reasonable agreement also was obtained for a vertical coil configuration when the mixing length was made equal to the vertical distance between coil bends, i.e., the vertical coil length.

## Cooling Coil Damage

The cooling coils used to extract the heat of combustion were damaged in a number of instances as listed in Table IV-5. The causes were varied, but include fatigue, deformation, erosion and erosion/corrosion.

The original horizontal coils were susceptible to fatigue. These coils were constructed of 3/4 inch O.D. 316 stainless steel tubing and were of a 0.46 m high horizontal serpentine configuration (see Figure IV-26). They were supported solely by the inlet and outlet tubing extending through the refractory lined flanges. The strength of the tubing was not sufficient to hold the coil rigid. The forces exerted by the weight of the coil and the slugging bed were thus able to fatigue the inlet and outlet lines and resulted in the failures during Runs 9.1 and 13.3.

In a number of instances the water entering the bed after a coil failure caused agglomeration of a portion of the bed. The agglomerates would impact with considerable force onto the coils causing severe deformation. Figure IV-26 shows the damage which coils 3A and 3B sustained during Run 13.3. The impact of the agglomerated bed forced the coils to deform in a direction perpendicular to the support rods. The buckled inlet where the failure occurred is to the left of center in the picture.

Samples from the damaged coil removed after Run 4 were sent to Exxon Engineering Technology Department, Materials Engineering Division for metallurgical examination. The coils had been in service for a total of 60 hours. No evidence of corrosion or deterioration of the coil was detected. The circulating cooling water maintained the metal temperature of the coil at an adequately low temperature to prevent sensitization and corrosion attack from the flue gas.

Instances of coil damage due to a high temperature erosion/corrosion attack were observed after the bed heat up procedure was modified. In Runs prior to No. 15.2 cooling water flow was always maintained to the coils, even while heating up the bed with a natural gas burner located in the plenum. In Runs 15.2-17.1 the cooling water flow was turned off during startup because the natural gas supply was found to be inadequate for heating up a deep bed while the coils were extracting heat. The bed was typically heated to 620-650°C before coal feeding was started and the water flow was initiated. In some circumstances, however, the coils experienced even higher temperatures.

TABLE IV-5. MINIPLANT COOLING COIL DAMAGE

| Run No. | Coal Configuration | Damage |
|---|---|---|
| 4.3 | Horizontal | Coil 1A was compressed and pushed to one side, some bed agglomeration occurred. |
| 5.4 | Horizontal | High velocity impingement of particles from the first stage cyclone pulsed return eroded a hole in coil 1A. |
| 9.1 | Horizontal | Coil 2A fatigued at the inlet. |
| 13.3 | Horizontal | The inlet of coil 3A buckled. Bed agglomeration and deformation of other coils resulted. |
| 15.4 | Horizontal | The U-bends of coil 1B were thinned and contained several dimples and holes. Bed agglomeration and deformation of other coils resulted. Cause was diagnosed as high temperature erosion/corrosion. |
| 17.1 | Vertical | The U-bends of coils 2A & 2B were thinned and contained dimples and holes. Much of the bed was agglomerated and deformation of the coils resulted. Cause was again diagnosed as high temperature erosion/corrosion. |
| 18.3 | Vertical | Erosion of the sockets connecting the U-bends to the straight sections of tubing. |

FIGURE IV-26

DAMAGED HORIZONTAL COOLING COILS

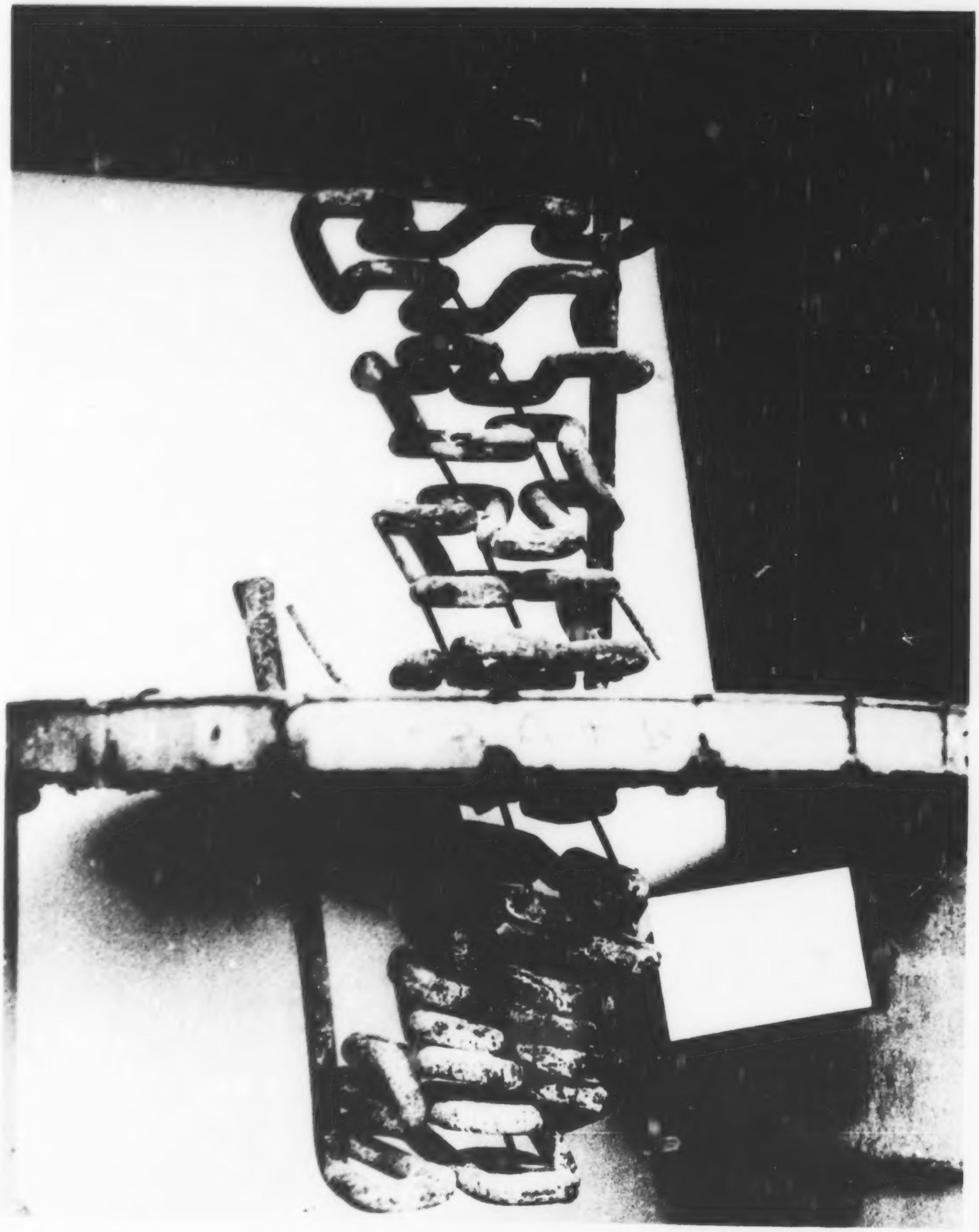

Inspection of the coils after Run 15.4 revealed that coil 1B had a number of dimples, 1 to 3 cm long in the upper bends and that two of the dimples contained holes 0.3 to 0.6 cm in diameter. Many of the U-bends were thinned and some had a shiny polished appearance. A portion of the bed had agglomerated and deformed several of the other coils.

The coils of a vertical configuration which replaced the damaged coils (see Figure IV-22) were subject to damage of a similar nature in Run 17.1. Figure IV-27 shows a photograph of coil 2A, one of the coils damaged during the run. Note the puncture on the top wall of two of the U-bends and the warping in several of the straight sections of tubing.

A metallurgical examination was performed on samples from the damaged coils. The presence of a scale was detected on the outside surface of all of the tubes and the microstructure of the tubes indicated that the coils had experienced temperatures above 870°C. The high temperature resulted in oxidation/sulfidation attack which was aggravated by erosion of the corrosion scale. The attack was for the most part selective to the U-bends.

After the second occurrence of high temperature coil damage, the heat up procedure was again modified. The natural gas supply was supplemented with liquid fuel so that the cooling water flow to the coils could be maintained at all times. This has prevented further high temperature damage during startup.

Two vertical coils were constructed to replace those damaged in Run 17.1. These were used in Runs 18.1, 18.2, and 18.3. One of these coils developed a leak during Run 18.3 and was badly damaged by the high temperatures which occurred after the cooling water flow was stopped. The one remaining coil, while intact, was severely eroded at the sockets connecting the U-bends to the straight sections of tubing. It is probable that the first coil failed due to erosion of the sockets. The erosion may have occurred because the sockets of the U-bends projected from the perimeter of the tube into the path of the vertically directed fluidized particles.

The third generation cooling coils, were built from heavy wall pipe (1/2 inch, Sch. 40, 316 stainless steel) to protect against fatigue and deformation. For additional support the adjacent coils are reinforced by support rods. In addition, precautions will be taken to ensure that these coils are never without a flow of cooling water. The new coil design is shown in Figure IV-8.

## Flue Gas Discharge System

Up to about 470 sdm$^3$/s (1000 SCFM) of flue gases were discharged from the combustor under maximum operating conditions and piped to a scrubber where residual $SO_2$ and particulates were removed before the gas was discharged to the atmosphere. Gas leaving the combustor was hot (about

FIGURE IV-27

DAMAGED VERTICAL COOLING COILS

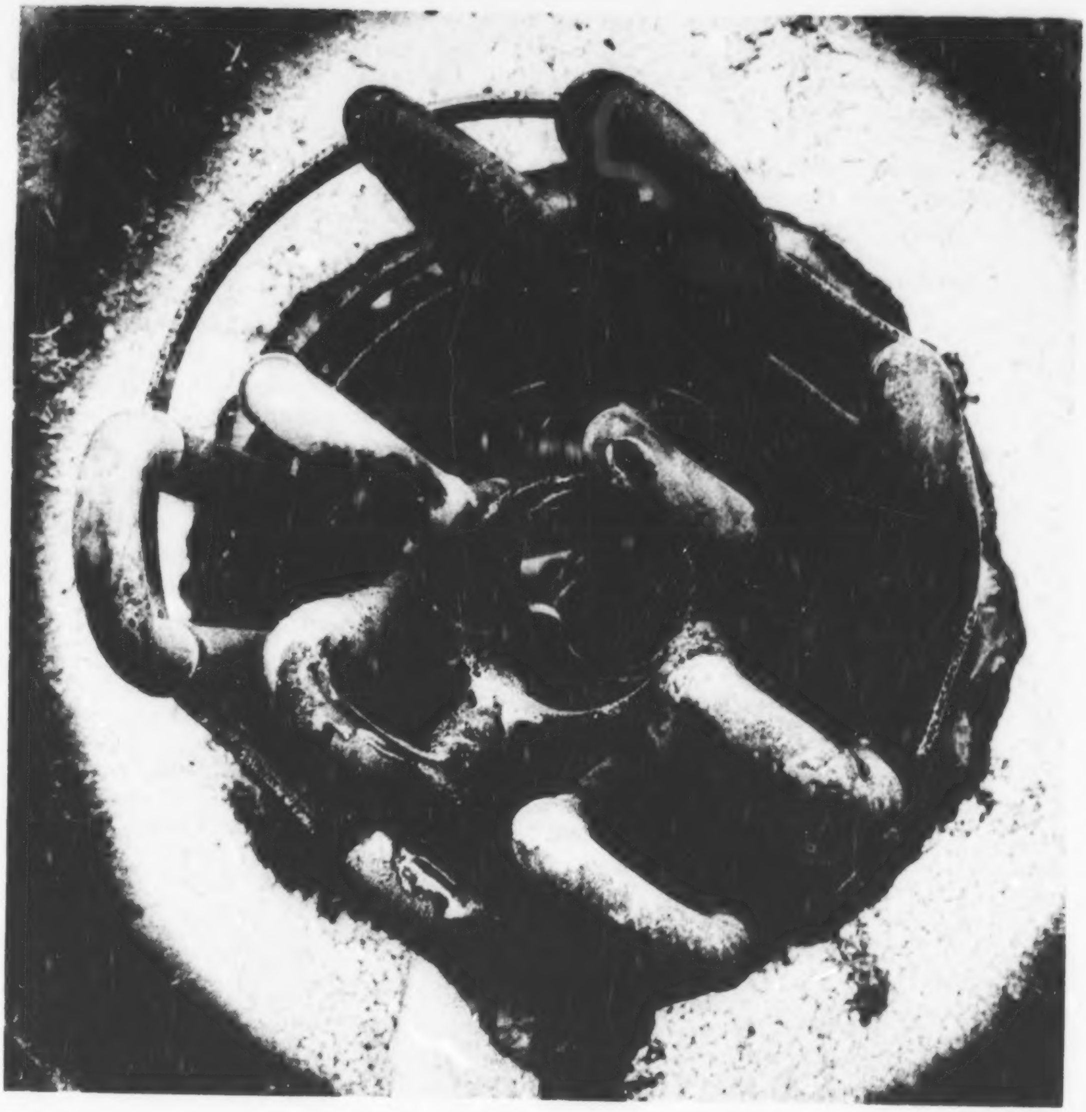

800-900°C) and at elevated pressure (800-1000 kPa) so that it had to be cooled and reduced in pressure before entering the scrubber. Because of poor operation of the secondary cyclone prior to its modification, the discharge gas had high loadings of solids (flyash and sorbent). This caused serious erosion problems in the discharge line and pressure control valve, and also made cooling the gases difficult.

Operation of the shell and tube off-gas cooler was often unsatisfactory. A cooler was needed because a control valve, good for temperatures only up to 250°C, was used to regulate back pressure in the combustor. The tubes of the cooler would plug with solids and gas flow would be restricted. Leaks in the heat exchanger tubes also occurred and once a tube separated from the tube sheet.

Erosion of the pressure control valve was a recurring problem because of the high solids loading in the off-gas. Erosion was so severe that the valve usually failed completely after only 24 hours of operation. Attempts were made to increase the valve's resistance to erosion by flame spraying a coating of aluminum oxide or tungsten carbide. The aluminum oxide coating was eroded away at the point of greatest impact after less than one day's operation. Tungsten carbide showed somewhat better resistance to erosion.

The off-gas piping was also eroded at elbows in the line. However, this problem was solved by replacing elbows with tees. Solids quickly filled the "dead" leg of the tees and provided barrier to erosion of the pipe.

Because of valve erosion and cooling problems, it was decided to control pressure by an alternate technique. Instead of using a control valve, pressure was reduced by expanding the gas across a ceramic-lined sonic nozzle. Pressure was controlled by adding secondary air to the nozzle inlet. This system had the advantages that the nozzle could be flame sprayed for erosion protection much more easily than a valve and that the nozzle could be designed for high temperatures. This meant that the troublesome heat exchanger could be eliminated. Thus, the exhaust gas heat exchanger was replaced with a 20 cm (8 inch) refractory lined pipe with a 10.2 cm (4 inch) diameter bore and the pressure control valve was replaced with a converging nozzle with a source of high pressure air. This secondary air was metered through a 5.1 cm (2 inch) ball valve equipped with a pneumatic actuator and positioner. The nozzle was flame sprayed with nickel aluminide and tungsten carbide. The nickel aluminide provided a sound substrate for the tungsten carbide to adhere to. The inside surfaces of the pipe downstream of the nozzle were also flame sprayed with the same materials. The thickness of the coatings were about 0.20-0.28 mm.

The combustor pressure was well controlled once the correct size nozzle was found, by the sonic nozzle and air supply. However, the tungsten carbide coating on the nozzle peeled off, probably because of high temperatures. Chromium carbide was substituted for the tungsten carbide and showed much better resistance to wear.

High gas temperatures downstream of the nozzle caused flange gaskets to fail and flanges to leak. The non-refractory lined pipe also warped due to thermal expansion. Also, the flue gas had to be cooled before reaching the scrubber. Because of the problems encountered in using a shell and tube heat exchanger to cool flue gas which was heavily loaded with solids, it was decided to use a different method of cooling. A water cooling jacket of 10 cm (4 inch) pipe was installed around the 6.4 cm (2-1/2 inch) off-gas piping from the discharge side of the sonic nozzle to the scrubber, a total run of about 15 m. The flue gases were cooled from about 700°C, as they exited the nozzle, to about 250°C before they entered the scrubber. No plugging problems have occurred with this system, which is effectively a simple double-pipe heat exchanger.

Prior to the use of the double-pipe heat exchanger, another cooling system was tried but eventually abandoned. This consisted in the direct spray of water into the flue gas lines between the secondary cyclone and the pressure control nozzle. Although this technique effectively cooled the flue gas, the flue gas line became plugged with flyash that was deposited near the water spray nozzles. The plugs could be cleared by turning off the water spray nozzles for a time, allowing the flyash deposits to dry and then blow away. However, this caused sudden pressure changes in the combustor which, in turn, caused erratic coal feeding.

### Cyclone Operation

Problems with the miniplant's two cyclones can be divided into three categories: poor collection efficiency, plugging of solids in the diplegs, and combustion in the cyclones themselves. The last problem was not caused by the cyclones per se, but rather by upsets in the combustor which caused large amounts of carbon to be entrained from the bed. However, changes in cyclone design were made to minimize the damage resulting from such upsets. These three problem categories are discussed below, beginning with the problem of cyclone damage and concluding with the problem of low efficiency.

During some upsets in the combustor, especially when superficial velocity reached excessive levels, unburned carbon was blown from the bed into the cyclones. For example, in one run bed velocity increased to 3.2 m/sec during an upset and unburned carbon reached the first and second cyclones and ignited. Temperatures in the cyclones of 1100-1300°C resulted. When the cyclones were inspected it was found that the ceramic gas outlet tubes had broken. Pieces retrieved from the cyclones and diplegs indicated that the tubes had probably been broken for some time, although several fractures were new. The alumina gas outlet tubes in both cyclones were replaced with new sections of heavy wall stainless steel pipe. While the pipes were not susceptible to cracking, they did melt when fires again occurred. However, it was soon appreciated that such fires were the result of abnormal operating conditions, and that they could be avoided by more careful attention to operation of the combustor, particularly when changes in operating conditions were made. Changes in operating procedures were then made which have prevented fires in the cyclones. Under these conditions, the stainless steel gas outlet tubes have given satisfactory service.

Plugging of both the first and second stage cyclone diplegs occurred frequently during early stages of the combustor shakedown. These problems were virtually eliminated by enlarging the diameter of the diplegs, removing sudden reductions in diameter, and keeping the dipleg piping as nearly vertical as possible. It will be recalled that the dipleg from the first cyclone returned solids to the combustor, at a rate controlled by a "pulse-pot" located at the bottom of the dipleg, and that the dipleg of the second cyclone discharged solids into a lock hopper.

Use of a gas purge flow (combustor off-gas) in the second stage cyclone dipleg was tried for awhile as a means of preventing plugging. Both upward and downward flows were tried. At first it seemed that plugging was reduced and cyclone collection efficiency improved, particularly with the downward purge. However, further operating experience indicated that the use of a purge flow may have actually aggravated plugging by causing water condensation in the dipleg. The problem was alleviated by modification of the dipleg geometry to facilitate flow of the solids. By eliminating the purge flow, condensation was avoided and solids that were removed from the second cyclone dipleg were invariably dry.

Poor cyclone collection efficiencies were caused largely by low cyclone inlet velocities. This was partly the result of the cyclones having been designed before any operating data from the miniplant were available, i.e., entrainment rates, particle sizes and size distribution, and particle densities. However, the situation was made worse because the miniplant was being run with lower air flow rates than were originally planned. Hence, at the usual combustor operating condition of 870°C, 2.1 m/sec, and 900 kPa, the inlet velocity was only 6.2 m/sec to the first cyclone and only 10.4 m/sec to the second.

Poor cyclone collection efficiency caused high solids' loading of the combustor off-gas and serious erosion problems in the off-gas piping. To correct this situation in the simplest and least costly manner, the secondary cyclone was modified in order to improve its efficiency. The area of the gas inlet was decreased by three in order to increase the inlet velocity to about 33 m/sec. Figure IV-28 gives the original dimensions of the secondary cyclone and indicates the changes that were made. Only the size of the inlet and outlet pipes were changed, not the

Figure IV-28

CHANGES IN SECONDARY CYCLONE DIMENSIONS

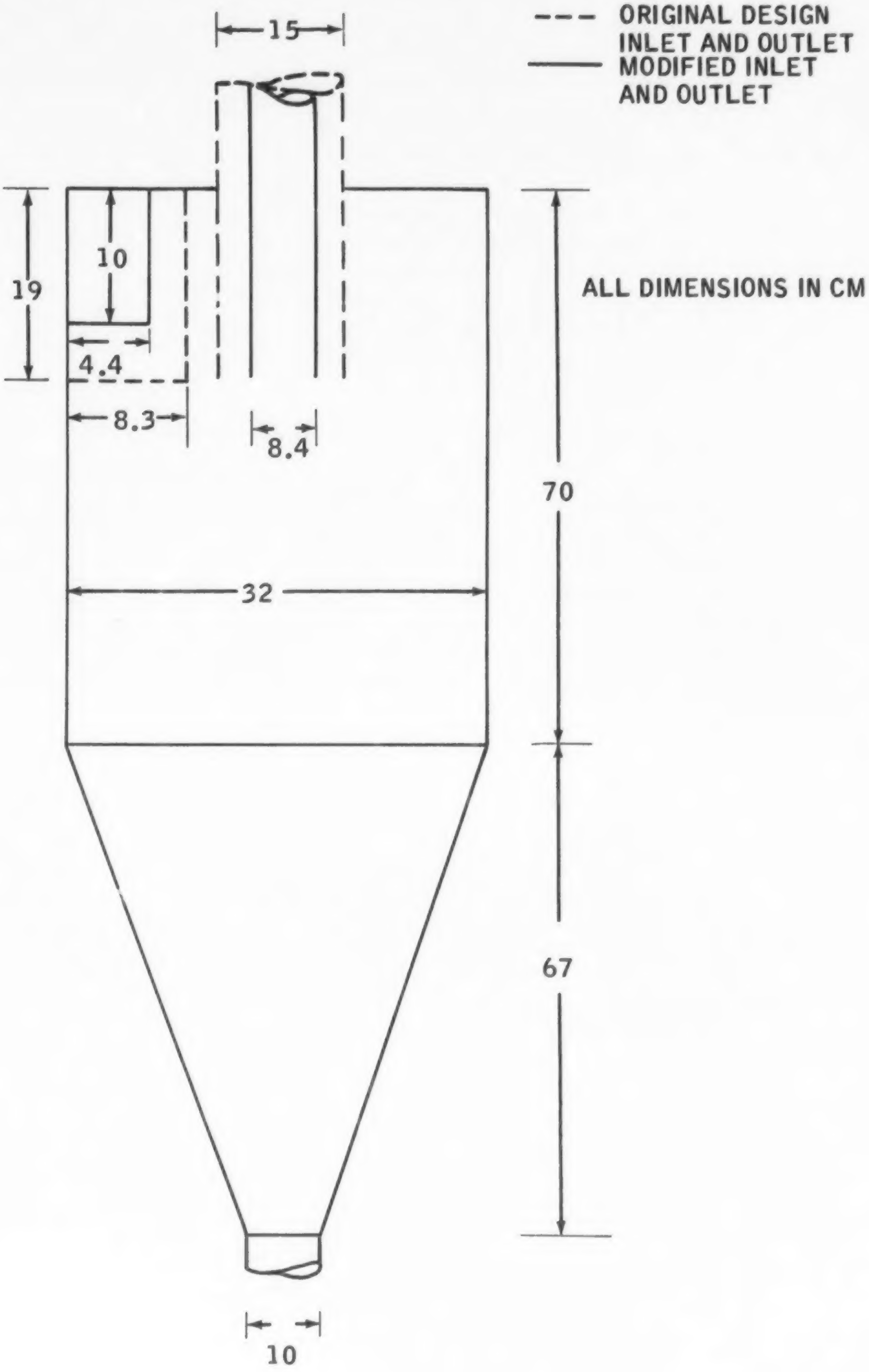

--- ORIGINAL DESIGN INLET AND OUTLET
— MODIFIED INLET AND OUTLET
15
10
19
4.4
8.3
8.4
ALL DIMENSIONS IN CM
70
32
67
10

size of the barrel or cone. This resulted in a cyclone of unconventional geometry but produced a substantial improvement in collection efficiency with a minimum of changes to the cyclone. Also, the walls of the cyclone were found to be rough and were reworked to a smooth surface.

Figure IV-29 is a typical particle size distribution for material collected by the primary cyclone. The particle size cut-off was about 70μ, i.e., 90 percent of the collected particles were larger than 70μ.

Figure IV-30 shows the particle size distribution for solids collected by the secondary cyclone during the last run before the cyclone was modified. Also shown is the size distribution for the first run made after the modification. Comparison of the two distributions shows that a substantial improvement in collection efficiency was made. Before the change, the 50 percent point in the distribution was about 70 microns, i.e., 50 weight percent was smaller than 70 microns. For the modified cyclone the midpoint in the distribution was about 30 microns.

## Bed Solids Removal

Solids can be continuously removed from the combustor to maintain a steady state bed height when a mixture of limestone and coal is continuously fed to the combustor. The solids are removed through a port located at a height of 2.3 m above the grid. Solids flow from the port to a refractory lined pulsing chamber ("pulse pot") through a 5.1 cm I.D. refractory lined pipe. The solids are ejected from the pulse pot into a pressurized lockhopper. The pulse pot and lockhopper are connected by a 0.5 m long horizontal run of 2 inch sched. 40 stainless steel pipe.

The solids withdrawal rate is controlled to equal the rate of limestone feed by adjusting the pulsing rate of the pulse pot. This is done with a 2 second on, 2 second off pulsing cycle and a 240 kPa pressure difference between the pulsing gas and combustor. With this system, a maximum solids rejection rate of 204 kg/hr was measured. The required rejection rate for a coal feed rate of 218 kg/hr and a high Ca/S molar ratio of 5 would be 52.4 kg/hr, well within the capabilities of the solids rejection system.

Bed solids were successfully rejected during a number of runs, beginning with No. 15.1. In several runs, attempts to reject solids failed because agglomerated solids had plugged the withdrawal line. Agglomeration was caused by condensation of water vapor, which developed whenever the withdrawal line was too cool. Condensation occurred when the unit was first heated up or when the solids rejection was stopped for an extended period of time. The reliability of the system was improved by using a plunger type device to seal off the withdrawal line whenever solids are not being removed. This prevents solids from sitting in the line when moisture is

## Figure IV-29

## PARTICLE SIZE DISTRIBUTION
## PRIMARY CYCLONE COLLECTION

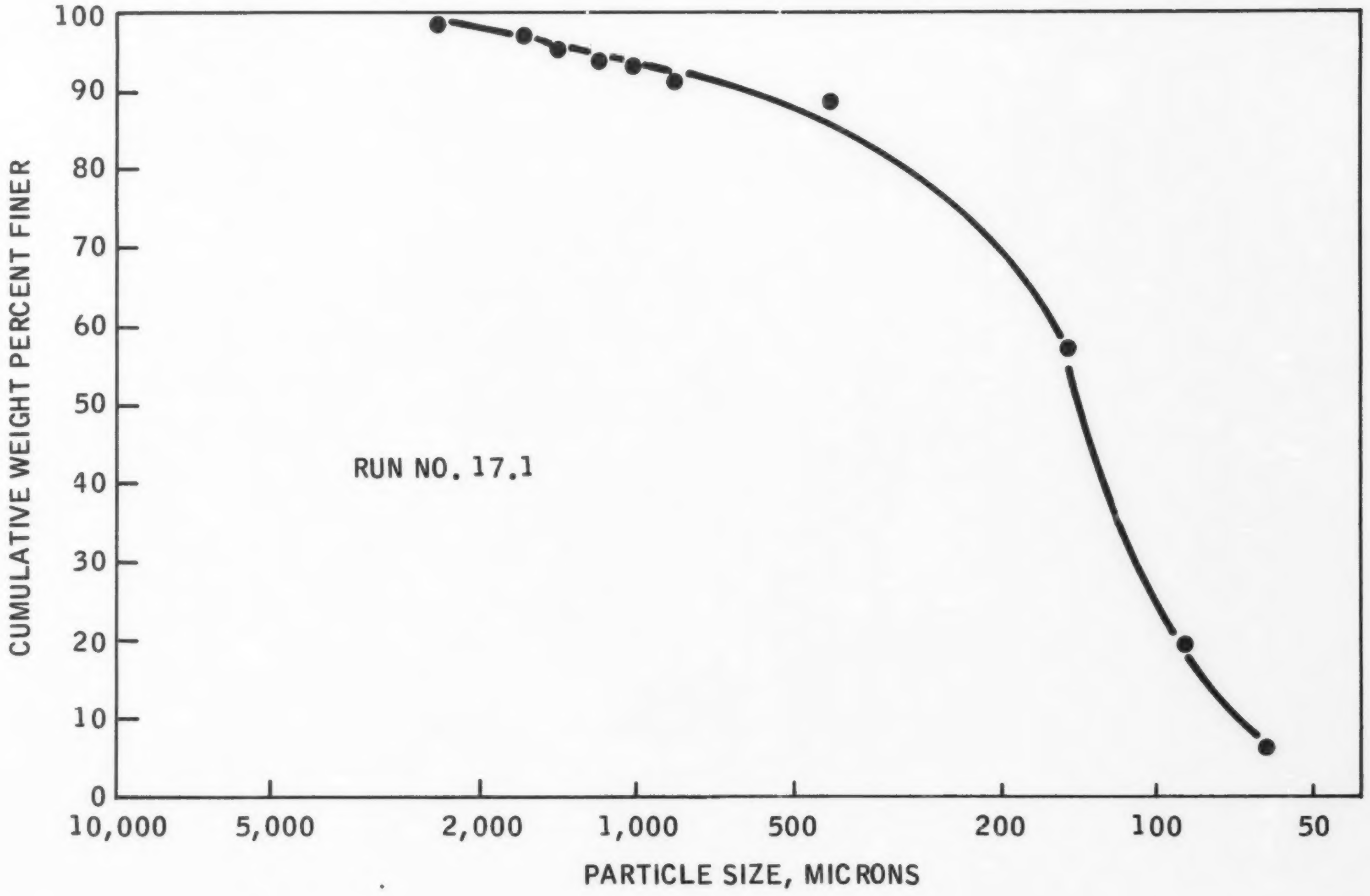

Figure IV-30

COMPARISON OF PARTICLE SIZE DISTRIBUTION FOR
SOLIDS COLLECTED BY SECONDARY CYCLONE
BEFORE AND AFTER MODIFICATION

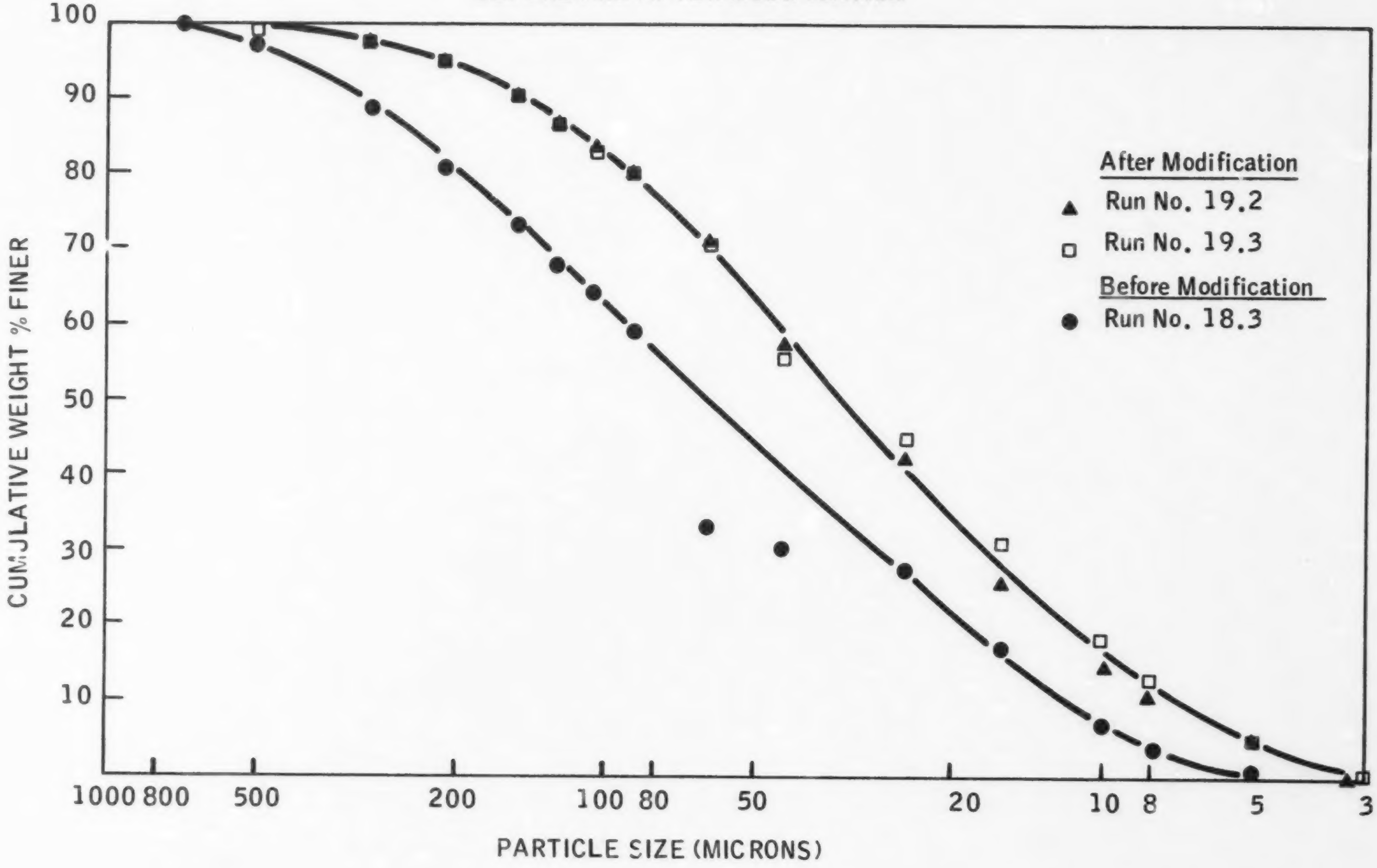

present. In addition, a 2 in. stainless steel pipe was inserted in the line to prevent agglomerated solids from clinging to the refractory.

## Fluidizing Grid

The fluidizing grid first used in the combustor was a water-cooled stainless steel plate continaing 128 caps which extended above the grid, each with eight holes of 0.20 cm diameter. Service life of these caps was short because they were not cooled sufficiently. The holes would gradually enlarge and the top of the cap would eventually fracture at the holes.

Because of these problems, a new fluidizing grid was designed which was similar to the type that had been successfully used in the batch combustor. The new grid (Figure IV-7) was also a water-cooled stainless steel plate but it did not contain any caps. Instead of caps, the grid had 776 holes of 0.16 cm diameter. This number and size of holes was such that the grid pressure drop was equal to about 30% of the typical pressure drop across the fluidized bed. This is the design criterion for which uniform distribution of air flow across the grid is expected. Also, the holes were too small for bed material (limestone) to fall through them into the plenum. A small fraction of the holes plugged occasionally, but this was not a problem. In fact, no problems have been experienced in over 200 hours of operation since the grid was installed.

## Bed Agglomeration

Although the bed material remained freely fluidized in most runs, there were occasional episodes of agglomeration. Operational difficulties which resulted in a portion of the bed seeing temperatures greater than 1150°C would cause agglomerates to form. In some instances an agglomerate would develop on the refractory wall opposite of the coal feeding port due to localized hot spots. Much of the agglomerated material was loosely packed and would disintegrate with time when exposed to ambient conditions. At times a portion of the agglomerates would be composed of fused bed material and flyash. This indicated that temperatures had been well above 1150°C at some points in the combustor, as calcium carbonate and calcium oxide melt at temperatures of 1340°C and 2570°C, respectively, calcium sulfate melts at about 1350°C and flyash softens at temperatures of 1260-1370°C.

Bed agglomeration also occurred when a break developed in a cooling coil allowing water to enter the combustor. The bed in the vicinity of the break apparently absorbed some water before it vaporized. The wet clinging solids probably formed permanent agglomerates once they were dried in other portions of the combustor. In several instances a large portion of the bed was agglomerated in this manner. The agglomerates usually became enmeshed in the cooling coils and caused severe deformation. Agglomerates formed in this fashion also had a different appearance and structure compared to agglomerates formed at high temperatures. The latter were hard, fused solids obviously formed by a high temperature melting process. The former were softer, could be easily broken by hand, were not fused but maintained the appearance of a cluster of particles, each particle maintaining its original shape.

## Burner

The burner shown in Figure IV-6, was used to preheat the bed above the self-ignition temperature of coal. No problems have been encountered with the burner itself; however, because of an insufficient fuel supply (natural gas), there was difficulty in heating the bed to the proper temperature when water flowed through the cooling coils. This necessitated the use of supplemental fuel addition as discussed previously. Also, the ignitor had to be correctly aligned in order to light the pilot. The ignitor and pilot tube were eventually combined into one unit which required no alignment. The combined ignitor-pilot is shown in Figure IV-31.

## Flue Gas Sampling

There have been problems in developing a satisfactory flue gas sampling system. The function of this system is to deliver to the instruments a clean, dry, low pressure, ambient temperature sample. This is a demanding task because the flue gas leaving the combustor is heavily loaded with particulates, contains water vapor, is at high pressure and is hot. Moreover, because the combustor is at a considerable distance from the analytical instruments, the residence time of gas in the sample lines is too long to preclude the possibility of changes in composition of the gas. However, an acceptable system was developed and is now in use on the miniplant based on the system used in the batch combustor unit (see page 27).

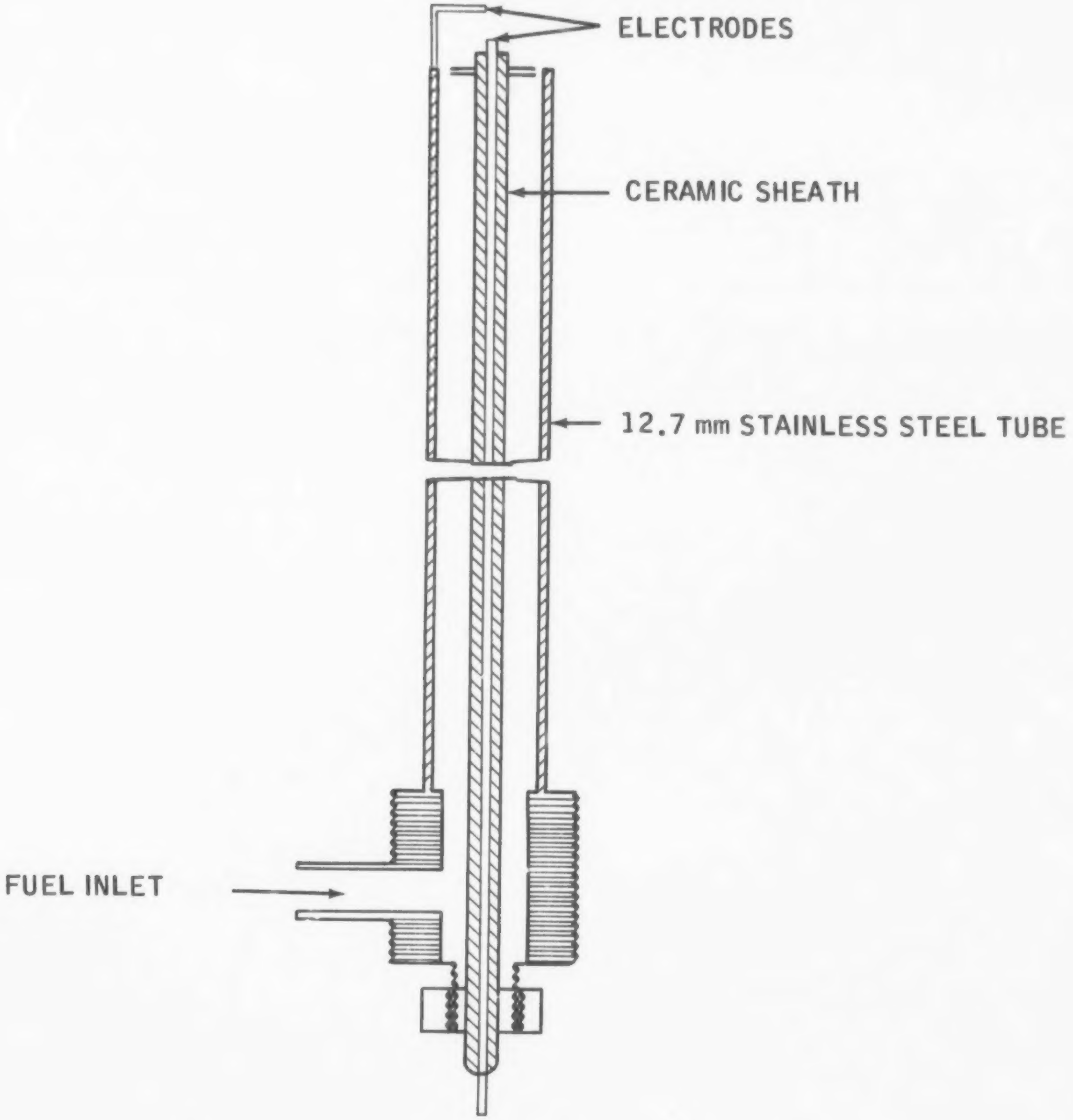
ELECTRODES
CERAMIC SHEATH
12.7 mm STAINLESS STEEL TUBE
FUEL INLET

Figure IV-31

IGNITOR—PILOT

The original sampling system used on the miniplant consisted of a water knockout, stainless steel filter, refrigeration dryer, and glass microfiber filter. The sample was taken downstream of the second stage cyclone. No pressure reducing device was included; sample pressure was dropped across a manual flow control valve just before each analyzer. This system did not work well for several reasons. The stainless steel filter rapidly became clogged with wet solids, reducing the sample flow. $SO_2$ was lost in the knockout and filter, and also in the sample lines. Residence time in the sampling system exceeded two minutes. Changes in concentration of the sample ($SO_2$ and $NO_x$) probably occurred.

In order to reduce the residence time of the sample, the flowrate was increased and a portion of the total flow was vented before the analyzers. However, this caused the filter to plug even more rapidly. The sample line connecting the filter with the combustor off-gas pipe also plugged. Residence time can also be reduced by lowering the pressure in the sample line. This can be done by using a corrosion resistant pressure regulator which is heated above the dew point of the sample to prevent condensation. Removing a sample directly from the low pressure section of the combustor off-gas piping was not considered to be practical because of the method used to control combustor pressure. Pressure is reduced by expanding the off-gas through a sonic orifice and control is obtained by adding varying amounts of air just upstream of the orifice. Hence, the low pressure off-gas has been diluted with a varying amount of air and its concentrations have been changed.

The new sampling system was described in a previous section (see page 27). The flue gas sample is taken downstream of the secondary cyclone and enters a cooler designed to cool the stream to 200°C or less. A sample of gas can be withdrawn after the cooler for analysis by wet chemical techniques. The balance of the gas stream passes through glass microfiber type filters. After the filters, a pressure regulator reduces pressure to slightly above atmospheric, in order to minimize the residence time of the sample in the lines. Following the pressure regulator, a dryer of the permeation distillation type removes water from the flue gas. This type of drier uses a membrane permeable only to water. This reduces the losses of $SO_2$ than would occur if a refrigerated drier were used. The temperature of the sample is maintained above its dew point upstream of the drier. The dried gas is then sent to the analyzers through teflon lines. A portion of the flow is vented before the analyzers, to reduce residence time further.

This system has given acceptable performance on the miniplant. It can deliver sample gas for extended periods, but is still subject to occasional plugs and must be cleaned periodically. Analysis of the flue gas for $SO_2$ by the IR analyzers agrees reasonably well with analysis by the wet chemical method. Since the sample for wet chemical analysis is taken close to the combustor before the sample has been filtered, pressure reduced, dried and passed through long lines to the IR analyzer, it appears that the flue gas sample preparation system does deliver a representative sample to the IR analyzers. However, additional changes are expected to be made to the system to improve operation even more. Included in the improvements will be the installation of a ultraviolet adsorption analyzer to be used along with the infrared analyzer for $SO_2$ measurement.

## COMBUSTION RESULTS

### $SO_2$ Emissions

The measurement of $SO_2$ emissions during most of the shakedown period was hampered by $SO_2$ sampling problems. A reliable sampling system was only developed at the end of the shakedown period. In addition, a number of the runs were made before the bed solids rejection system was operable, and either a captive bed was used with no limestone addition or limestone was added and the bed level was allowed to increase during the run. In either case, interpretation of the $SO_2$ emission data was made more difficult. However, the concluding run in the shakedown phase was made under steady state conditions with continuous addition and rejection of limestone and a functioning flue gas sampling system. This run was made at a Ca/S ratio of 1.45, a temperature of 870°C, a pressure of 930 kpa and a superficial velocity of 1.9 m/s. The $SO_2$ emissions averaged 750 ppm. This is in line with results from the batch combustion unit obtained at comparable operating conditions. In general, $SO_2$ emissions during the shakedown ranged from 150 to 800 ppm, usually in the 300 to 500 ppm range.

### $NO_x$ Emissions

The $NO_x$ emissions measured during the shakedown runs were less susceptible to sampling problems than $SO_2$ emissions and a number of runs yielded data of acceptable quality.

$NO_x$ emissions were largely NO. Only 10 to 15% of the $NO_x$ emissions were present as $NO_2$ and this was quite possibly formed in the sample lines. $NO_x$ emissions were found to correlate with per cent excess air as shown in Figure IV-32. In Figure IV-32, $NO_x$ emissions are expressed as lb (as $NO_2$)/M BTU coal fired. Data were obtained at pressures of 900 kPa, temperatures in the range of 900 to 950°C and at excess air levels from 0 to 140%. As seen, the data generally group well around a single correlating line. The emissions also fell well below the current EPA emission standard of 0.7 lbs $NO_2$/M BTU even at the highest excess air levels standard.

Figure IV-32

NO$_x$ EMISSIONS

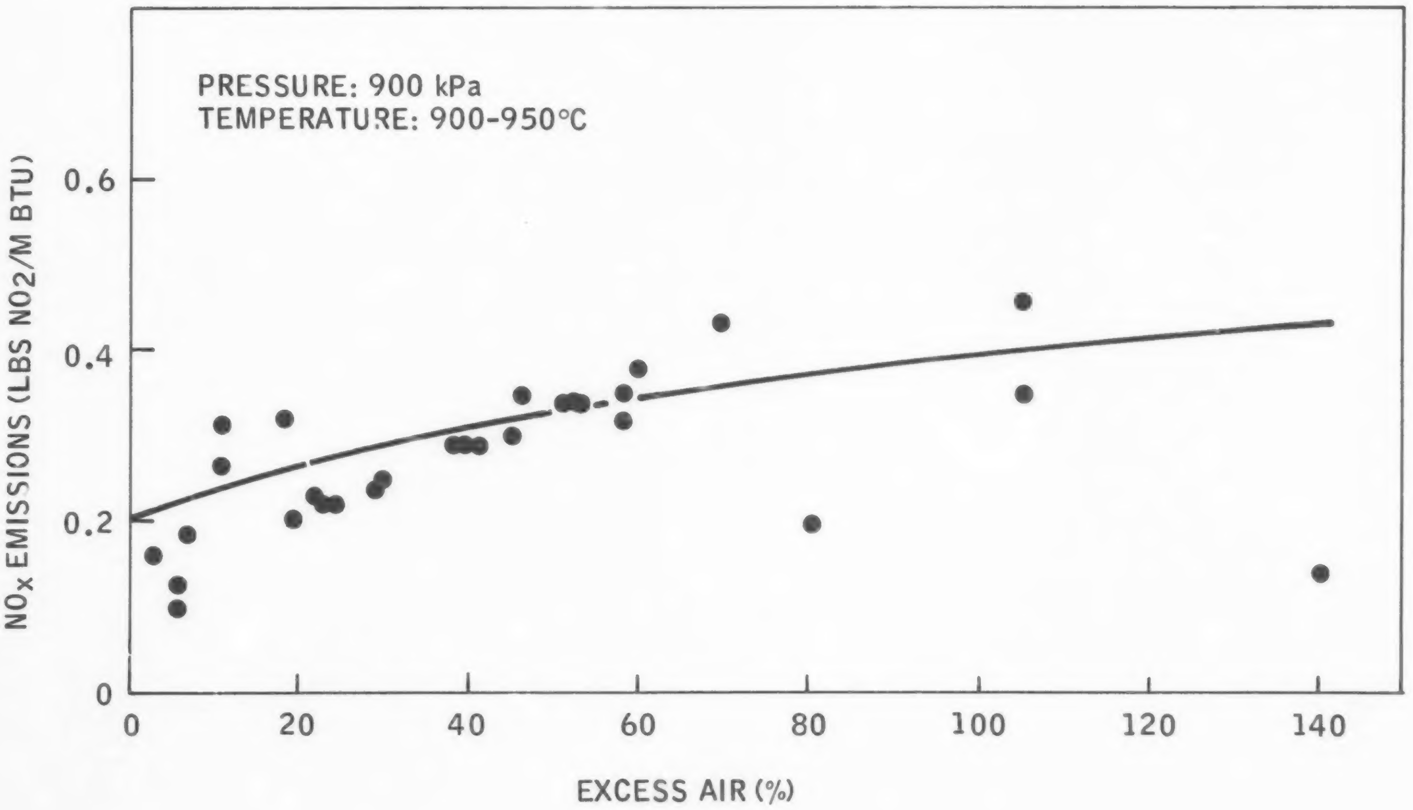

## Combustion Efficiency

Carbon combustion efficiency measured in the miniplant were in the range of 92 to 98%. Combustion efficiency is a function of excess stoichiometric air as shown in Figure IV-33. The miniplant was operated at superficial velocities of 1.8 to 2.2 m/s at temperatures of 800 to 950°C and at a pressure of 900 kPa. Two other factors may influence combustion tion efficiency: bed temperature and the efficiency of the carbon particulate recycle system. In these tests, the effect of these variables could not be determined. However, there were some indications that increasing temperatures would increase combustion efficiency as expected. The efficiency of the carbon particulate recycle system was a variable during a number of the runs due to plugging of the first stage cyclone dipleg or problems with the system which injected the solids from the first stage cyclone back into the combustor. The effect of these variables may be responsible for the data scatter seen in Figure IV- 33. at low excess air levels.

The target combustion efficiency of 99% could not be attained even at high excess air levels in the shakedown runs. Therefore, a more efficient first stage cyclone recycling the unburned carbon fines to the combustor, operation of the combustor at higher temperature or possibly a separate carbon burn-up cell may be required to reach 99% combustion efficiency. Additional work will be done to improve combustion efficiency and attain the target level of 99%.

The loss of combustion efficiency is due chiefly to unburned carbon particles entrained from the bed. This accounts for about 98% of the loss. The balance is due to CO formation.

## CO Emissions

Carbon monoxide emissions were generally quite low as long as conditions conducive to high combustion efficiency were maintained. Typically, levels of less than 500 ppm were observed at excess air levels exceeding 15% and average bed temperatures of ca. 900°C. A sufficient amount of data at widely varying operating conditions was not obtained during miniplant shakedown to allow development of meaningful correlations. However, in addition to the importance of excess air level and average bed temperature, preliminary results indicate that steady coal feeding and high combustor freeboard temperatures favor maintenance of low CO levels. For example, during runs 17.1 and 18.1, under relatively steady conditions of coal feeding, with temperatures throughout the combustor in the 850-920°C range and excess air ranging from 15-60%, measured CO levels were 150-250 ppm.

## Heat Transfer Coefficients

Heat transfer coefficients were measured during selected runs by maintaining the cooling water flow through the coils in the liquid state. The flow rate to each coil was measured with an orifice meter. The

Figure IV-33

COMBUSTION EFFICIENCY

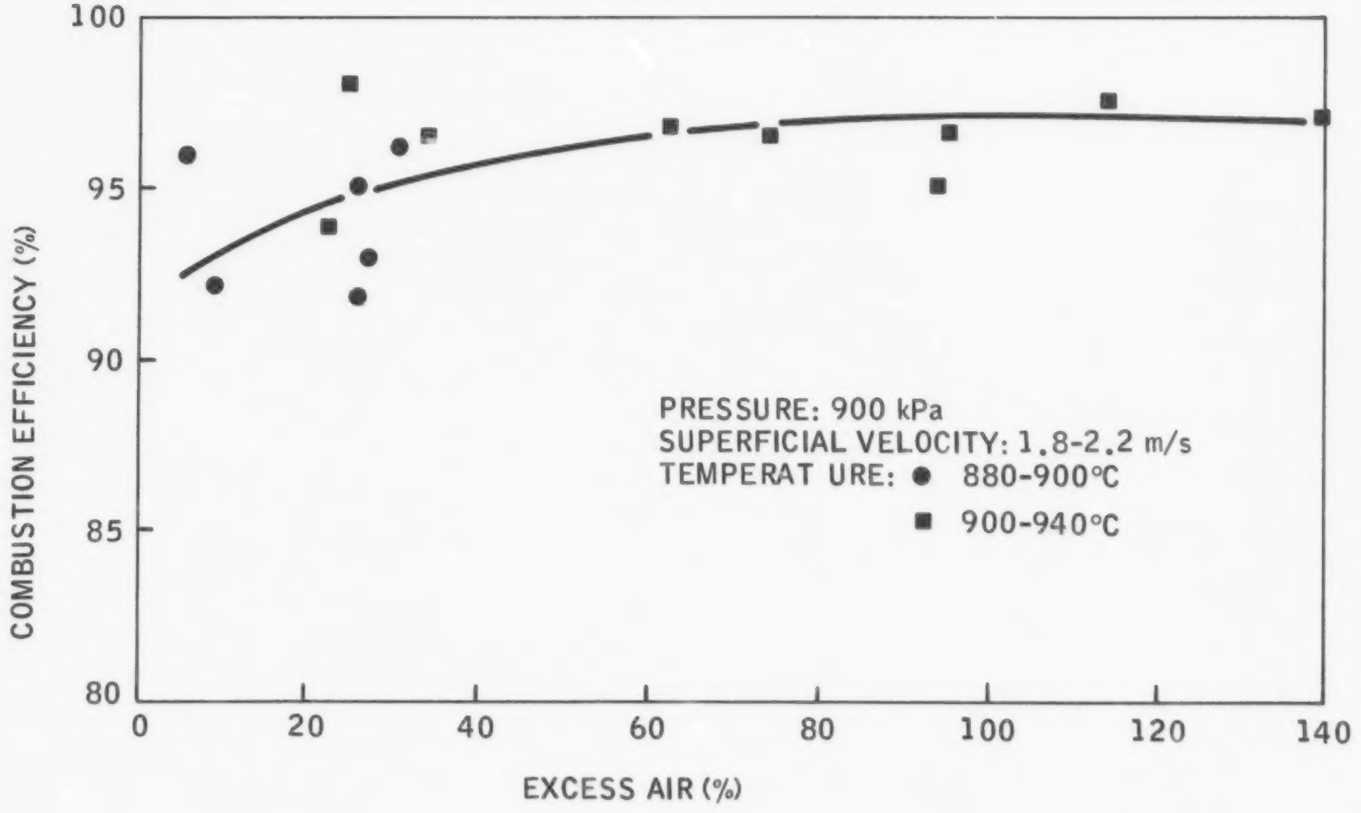

inlet and outlet temperature of the cooling water were measured with thermocouples inserted within the 3/4 in. O.D. tubing. The flows and temperatures were recorded on magnetic tape at one minute intervals. These data were used to calculate the average coefficient and standard deviation for a 10 minute interval. The results are given in Tables IV-6 and IV-7.

The coefficients measured for the vertical coils during Run 19.2 compare closely with those measured in runs 14.1, 14.2 and 15.1 for horizontal serpentine coils oriented vertically. This result implies that as long as the configuration and/or orientation of the heat transfer surface allows good mixing, the coefficients will be similar. Unfortunately coefficients are not available for the horizontal serpentine coils oriented in a horizontal direction. However, it is likely the coefficients would have been somewhat lower due to poorer mixing. The coefficients measured for the lower-most coil, 1A, are consistently slightly lower than those measured for coil 1B. The cause may be poor fluidization at the boundary between the lower-most coil and the combustion zone. Insufficient data are available to determine if there are other variations in the coefficient as a function of axial position.

## Component Balances

Complete material balances were routinely made only for sulfur and calcium. Even for these particular components, various problems were encountered which led to questionable data reliability. For example, flue gas sampling problems introduced some error in $SO_2$ determinations. In addition, $SO_3$ levels in flue gas were not determined. Problems associated with collection, sampling, and analysis of solids were of even more importance. These included such things as poor cyclone efficiency, some inaccuracy in determining the weight of the final bed solids, difficulty in obtaining representative samples of collected and bed solids, and, most importantly, large sensitivity in the overall sulfur balance to relatively small errors in solids analysis. The net result was that sulfur balances fluctuated from 50-120%. Calcium balances were better, but were still subject to similar sources of error with regard to collected and bed solids. Typical balances were in the range of 85-115%. Appendix Tables G3 and G4 give more details. Work is continuing to improve these balances, tentatively to 90% or higher with a higher degree of precision. Preliminary indications are that these levels have been reached in the most recent runs.

## TABLE IV-6. MINIPLANT OVERALL HEAT TRANSFER COEFFICIENT MEASUREMENTS - RUN 19.2

| Coil No. | Average Coeff. $W/m^2K$ | Standard Deviations of 10 Measurements Obtained At One Minute Intervals $W/m^2K$ |
|---|---|---|
| 1A | 319 | 7.7 |
| 1B | 353 | 7.2 |
| 2A | 330 | 11.3 |

| | |
|---|---|
| Surface Area of a Coil, $m^2$ | 0.551 |
| Coil Heat Flux, $W/m^2$ | 280,000 |
| Combustion Intensity, $W/m^3$ Bed | 5,250,000 |
| Heat Removed by Cooling Coils in Bed, % of Coal Heat Input | 57 |
| Calculated Overall Heat Transfer Coeff., from Heat Balance, $W/m^2$ K | 358 |
| Coil Configuration | Vertical |

## TABLE IV-7. MINIPLANT OVERALL HEAT TRANSFER COEFFICIENT MEASUREMENTS - RUNS 14.1, 14.2, 15.1

| Run No. | Coil No. | Average Coeff. $W/m^2K$ | Standard Deviations of 10 Measurements Obtained At One Minute Intervals $W/m^2K$ |
|---|---|---|---|
| 14.1 | 1A | 316 | 8.3 |
| 14.1 | 1B | 327 | 7.4 |
| 14.2 | 1A | 321 | 3.1 |
| 14.2 | 1B | 336 | 6.6 |
| 14.2 | 1B | 348 | 3.9 |
| 15.1 | 1A | 317 | 3.8 |
| 15.1 | 1B | 338 | 5.7 |

Coil Configuration - Horizontal Serpentine Half Coils Oriented in the Vertical Direction

# SECTION V

# BATCH COMBUSTOR STUDIES

## EQUIPMENT, MATERIALS, PROCEDURES

### Fluidized Bed Coal Combustion Unit

A schematic diagram of the Exxon batch fluidized bed combustion unit is shown in Figure V-1. Figure V-2 is a photograph of the unit. The combustor is equipped with a continuous coal feeding system. The sorbent is added batch-wise. The primary components of the unit are (1) the coal feeding system, (2) the fluidized bed combustor, and (3) the gas handling and analytical equipment.

Coal Feeding System - Figure V-3 shows the Petrocarb Model 16-1 ABC injector. The main features are a conical-bottom tank that holds solids to be fed and an orifice and mixing tee assembly that mixes solids with carrier gas. Solids in the tank are aerated by a controlled stream of air at a selected pressure. Aerated solids flow through the orifice at the bottom of the tank into the mixing tee assembly and are picked up by a controlled stream of carrier gas (air). Solids are pneumatically conveyed through a transport line into the combustor. The feed rate of solids is controlled by pressure in the feed tank, carrier or injection air flow rate, and pressure differential between the feed tank and combustor.

The Petrocarb solids feeder was modified to feed ground coal (-16 mesh) at rates of 3-13 kg/hr into the combustor against pressure of up to approximately 1000 kPa. The feeder, as it is supplied by Petrocarb, can handle only much higher feed rates. The diameter of the orifice was reduced to 0.71 cm and the Petrocarb injection hose was replaced with a 0.58 cm diameter (I.D.) X 6.10m long stainless steel tube. In order to make the feeder work satisfactorily with the batch combustor, the feeder to combustor pressure differential had to be held constant. This was accomplished with automatic controls which maintained the pressure in the feed tank above the pressure in the combustor by the desired amount. The entire feeding assembly was mounted on a platform scale which measured the coal feed rates.

Fluidized Bed Combustor - A schematic diagram of the batch fluidized bed coal combustor is given in Figure V-4. The vessel was constructed from four sections of 25 cm (10 inch) diameter standard wall carbon steel pipe and refractory lined with Grefco Litecast No. 7528 to an inside diameter of 11.4 cm. The height of the vessel, above the fluidizing grid, was about 4.9m. Below the grid was a 61 cm long burner section

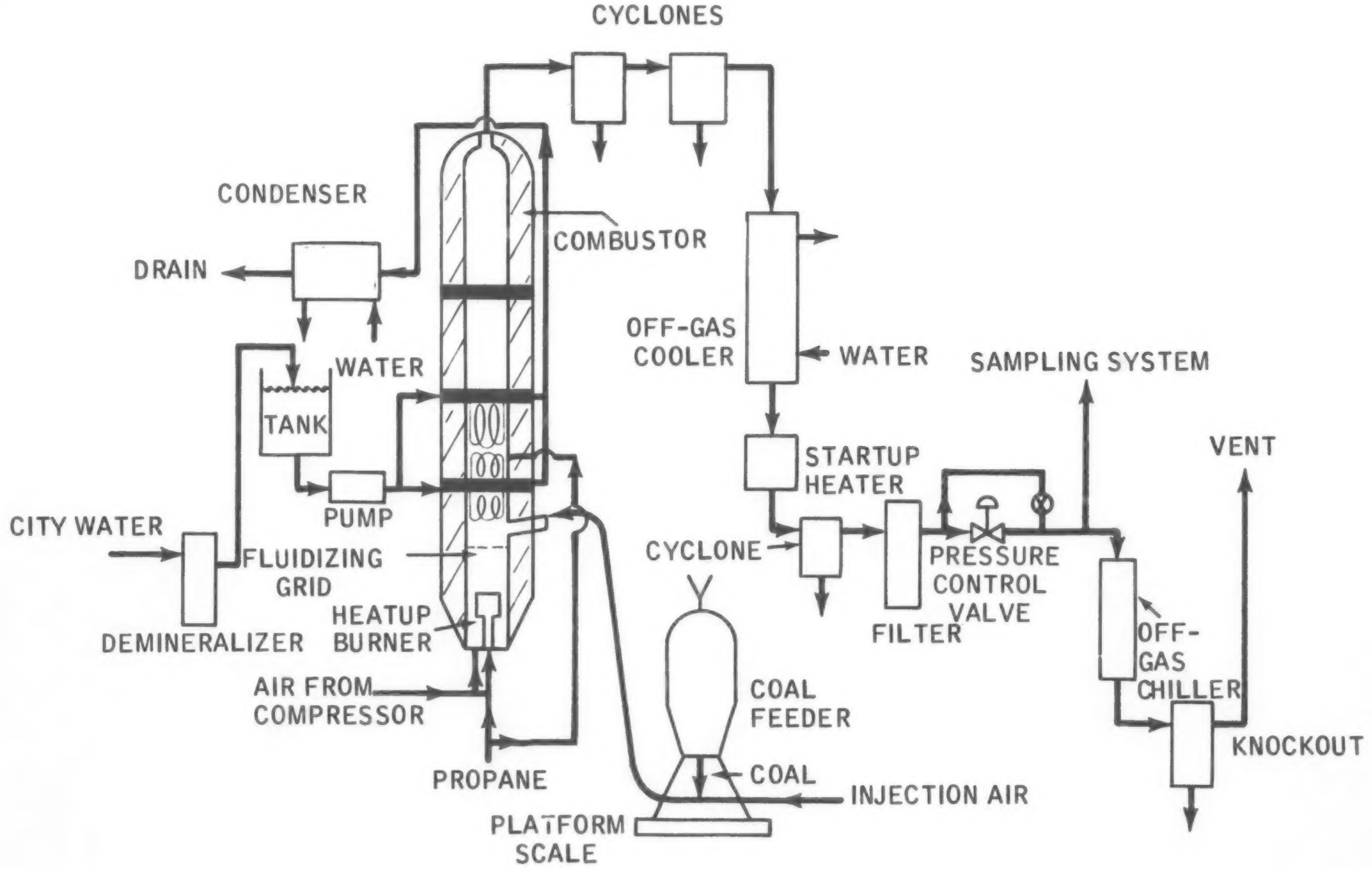
CYCLONES
CONDENSER
DRAIN
COMBUSTOR
WATER
TANK
PUMP
CITY WATER
FLUIDIZING GRID
DEMINERALIZER
HEATUP BURNER
AIR FROM COMPRESSOR
PROPANE
PLATFORM SCALE
COAL FEEDER
COAL
INJECTION AIR
OFF-GAS COOLER
WATER
STARTUP HEATER
CYCLONE
FILTER
PRESSURE CONTROL VALVE
SAMPLING SYSTEM
VENT
OFF-GAS CHILLER
KNOCKOUT

Figure V-1

BATCH FLUIDIZED BED COAL COMBUSTION UNIT

FIGURE V-2

BATCH FLUIDIZED BED COAL COMBUSTION UNIT

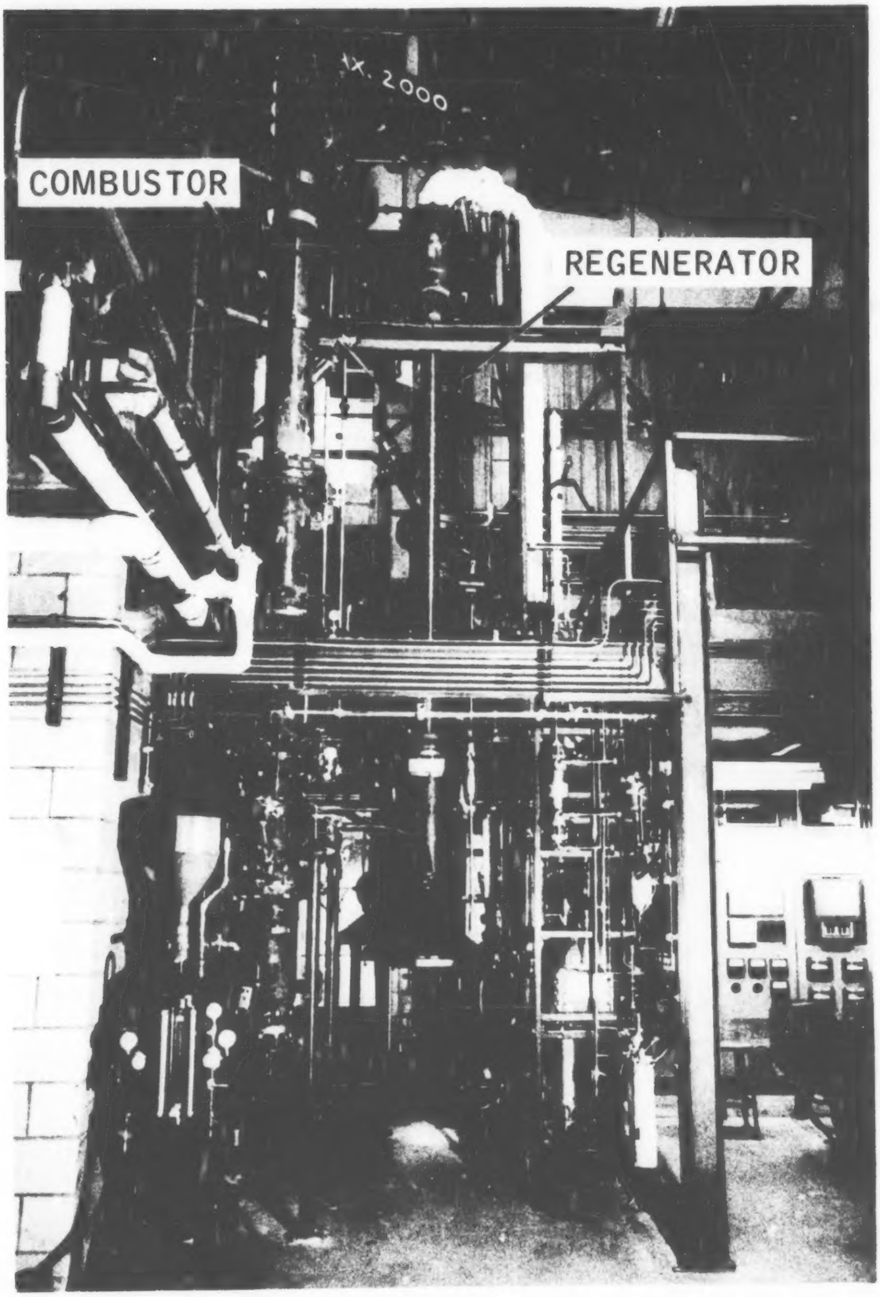
1X. 2000
COMBUSTOR
REGENERATOR

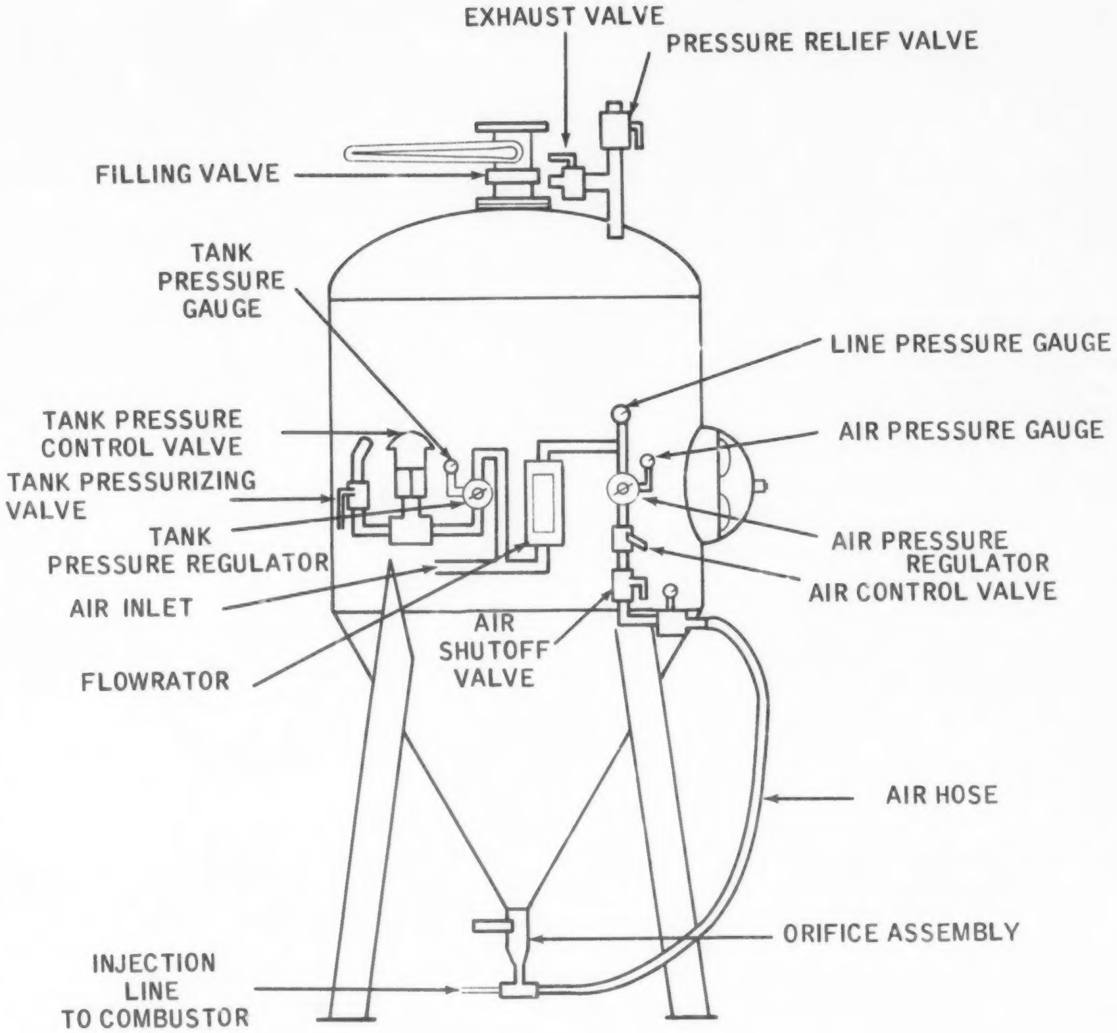
EXHAUST VALVE
PRESSURE RELIEF VALVE
FILLING VALVE
TANK PRESSURE GAUGE
LINE PRESSURE GAUGE
TANK PRESSURE CONTROL VALVE
AIR PRESSURE GAUGE
TANK PRESSURIZING VALVE
TANK PRESSURE REGULATOR
AIR PRESSURE REGULATOR
AIR CONTROL VALVE
AIR INLET
AIR SHUTOFF VALVE
FLOWRATOR
AIR HOSE
ORIFICE ASSEMBLY
INJECTION LINE TO COMBUSTOR

Figure V-3

PETROCARB COAL INJECTOR

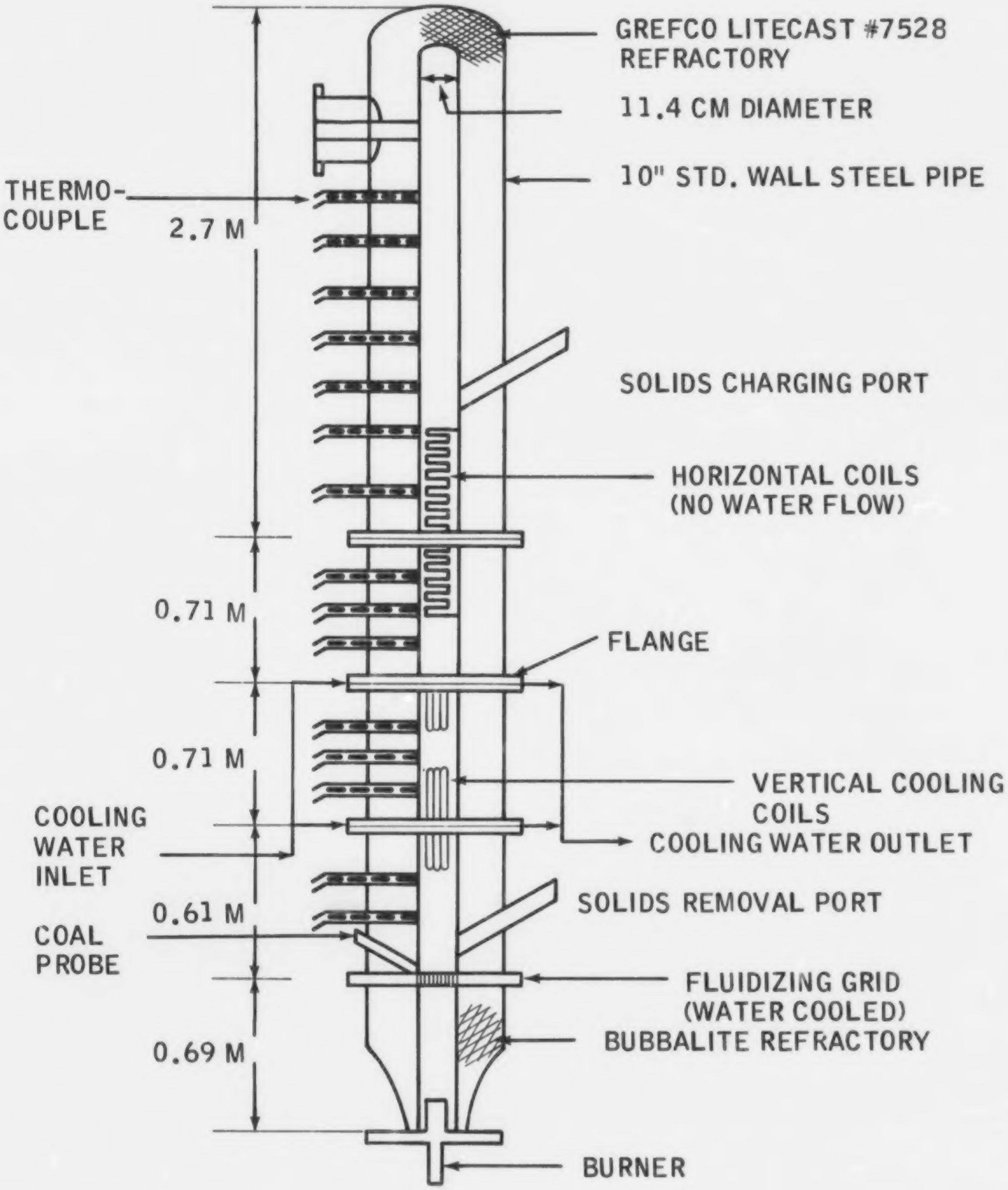
GREFCO LITECAST #7528 REFRACTORY
11.4 CM DIAMETER
10" STD. WALL STEEL PIPE
THERMO-COUPLE
2.7 M
SOLIDS CHARGING PORT
HORIZONTAL COILS (NO WATER FLOW)
0.71 M
FLANGE
0.71 M
VERTICAL COOLING COILS
COOLING WATER INLET
COOLING WATER OUTLET
SOLIDS REMOVAL PORT
0.61 M
COAL PROBE
FLUIDIZING GRID (WATER COOLED)
BUBBALITE REFRACTORY
0.69 M
BURNER

Figure V-4

COMBUSTOR VESSEL

lined with Grefco Bubbalite. The fluidizing grid, which was made of stainless steel, had 80-0.16 cm diameter holes to distribute the fluidiz-air and was water cooled. It is described in Figure V-5. A propane burner, located at the bottom of the burner section, was used to preheat the unit to above the self-ignition temperature of propane (505°C). At this point propane was added directly into the bed just above the fluidizing grid to raise the temperature of the bed above the self-ignition temperature of coal. A schematic diagram of the burner is shown in Figure V-6. The maximum operating temperature and pressure of the batch combustor were approximately 1000°C and 1000 kPa respectively.

The combustor had three vertical cooling coils made of 0.95 cm diameter (O.D.) stainless steel tubing. The locations of the coils within the combustor are shown schematically in Figure V-7. They extended from 27 to 141 cm above the fluidizing grid and each had a surface area of 0.060 $m^2$. Each coil had its own rotameter and control valve and the water flow into each coil and the temperature of the steam issuing from the coils was easily controlled. Initially, the combustor contained six horizontal serpentine cooling coils of 0.093 $m^2$ surface area each. The bottom four coils were removed and replaced by three vertical coils as detailed on page 98. Two horizontal coils, 180-249 cm above the fluidizing grid were left in place but were not cooled. Thermocouples were located 15 cm apart in the lower section of the combustor and 30 cm apart in the upper section.

Sorbent was loaded into the combustor through a charging port located in the upper section. Solids could be removed through a port in the lower section or, alternatively, transferred directly to the adjacent batch regenerator by blowing them through a 5 cm diameter pipe supplied for this purpose.

Coal entered through a "sonic" coal injection probe which was connected to the end of the 6.10m X 0.58 cm diameter (I.D.) coal injection tube. Figure V-8 gives a schematic of the "sonic" probe. The inside diameter of the probe was 0.77 cm. The stream of flowing coal was surrounded by seven sonic air jets. The primary intent of the high velocity air jets was to improve coal feeding by clearing a path through the bed of fluidized solids in the combustor. Air flow through the annulus of the probe helped to cool the probe. This flow was about 1.89 $dm^3/s$ and compares to an air flow of about 3.30-3.78 $dm^3/s$ used to transport the coal.

Gas Handling and Analytical Equipment - Flow of air and fuel into the combustor, and system pressure, were under automatic control. Gases leaving the combustor first passed through two cyclones, which removed

Figure V-5

BATCH COMBUSTOR
FLUIDIZING GRID

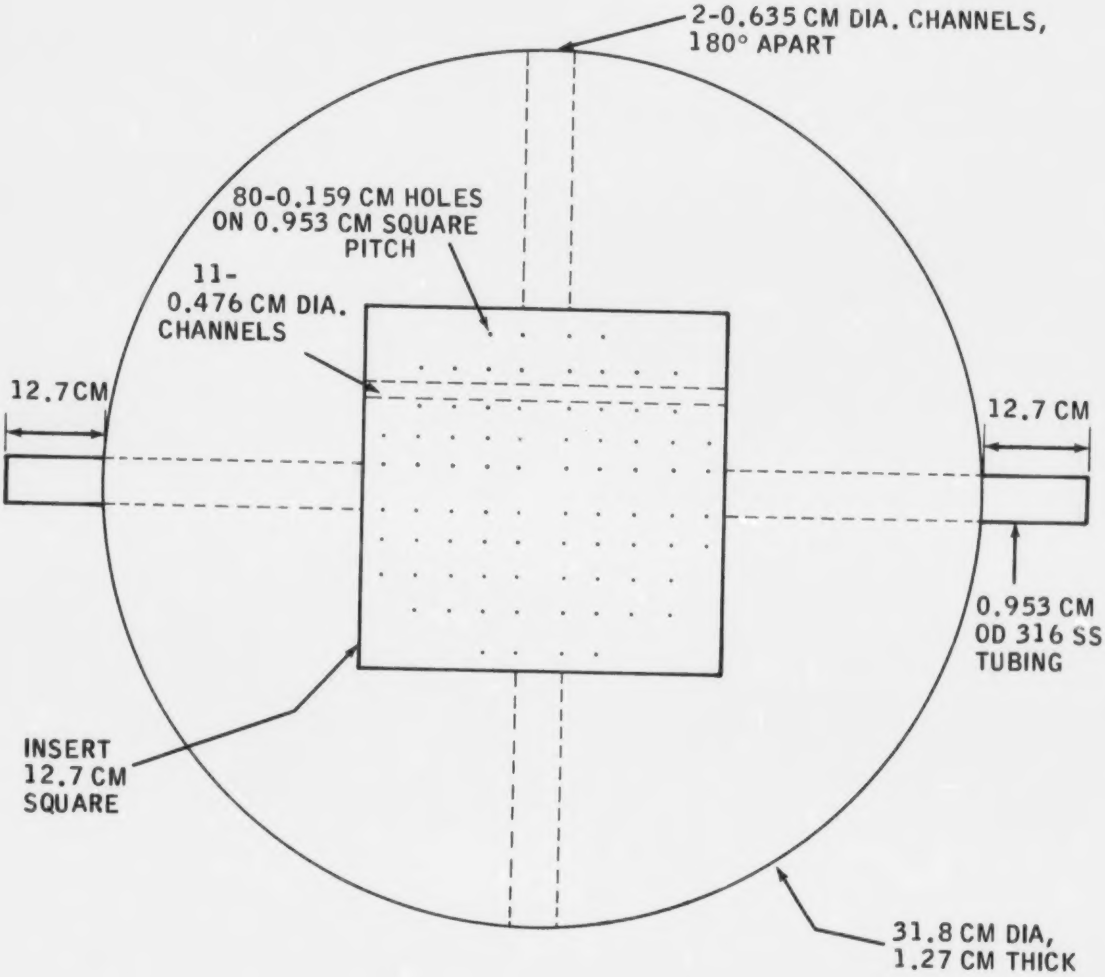
2-0.635 CM DIA. CHANNELS,
180° APART
80-0.159 CM HOLES
ON 0.953 CM SQUARE
PITCH
11-
0.476 CM DIA.
CHANNELS
12.7 CM
12.7 CM
0.953 CM
OD 316 SS
TUBING
INSERT
12.7 CM
SQUARE
31.8 CM DIA,
1.27 CM THICK

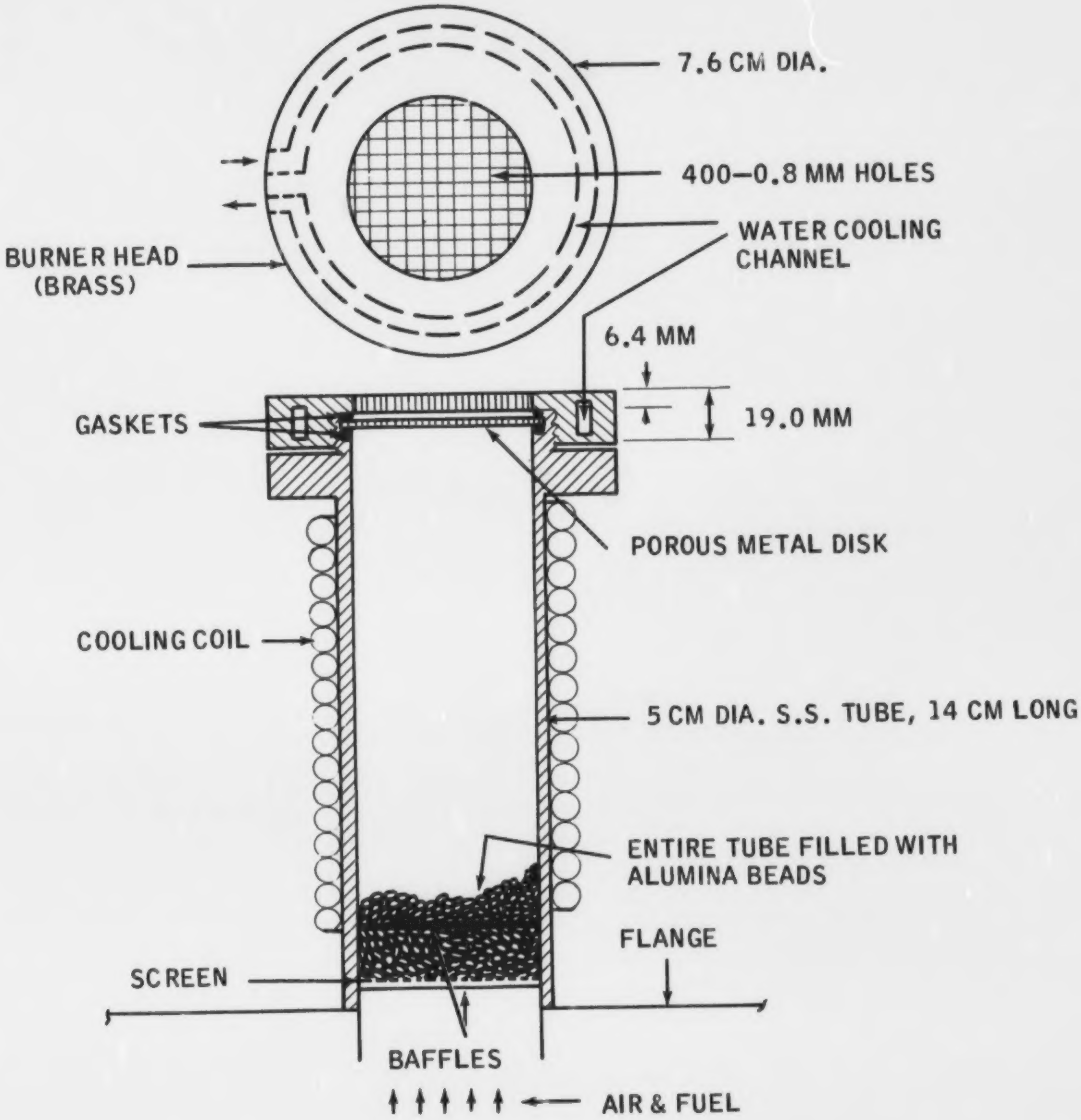
7.6 CM DIA.
400–0.8 MM HOLES
WATER COOLING CHANNEL
BURNER HEAD (BRASS)
6.4 MM
19.0 MM
GASKETS
POROUS METAL DISK
COOLING COIL
5 CM DIA. S.S. TUBE, 14 CM LONG
ENTIRE TUBE FILLED WITH ALUMINA BEADS
FLANGE
SCREEN
BAFFLES
AIR & FUEL

Figure V-6

PREHEATER BURNER

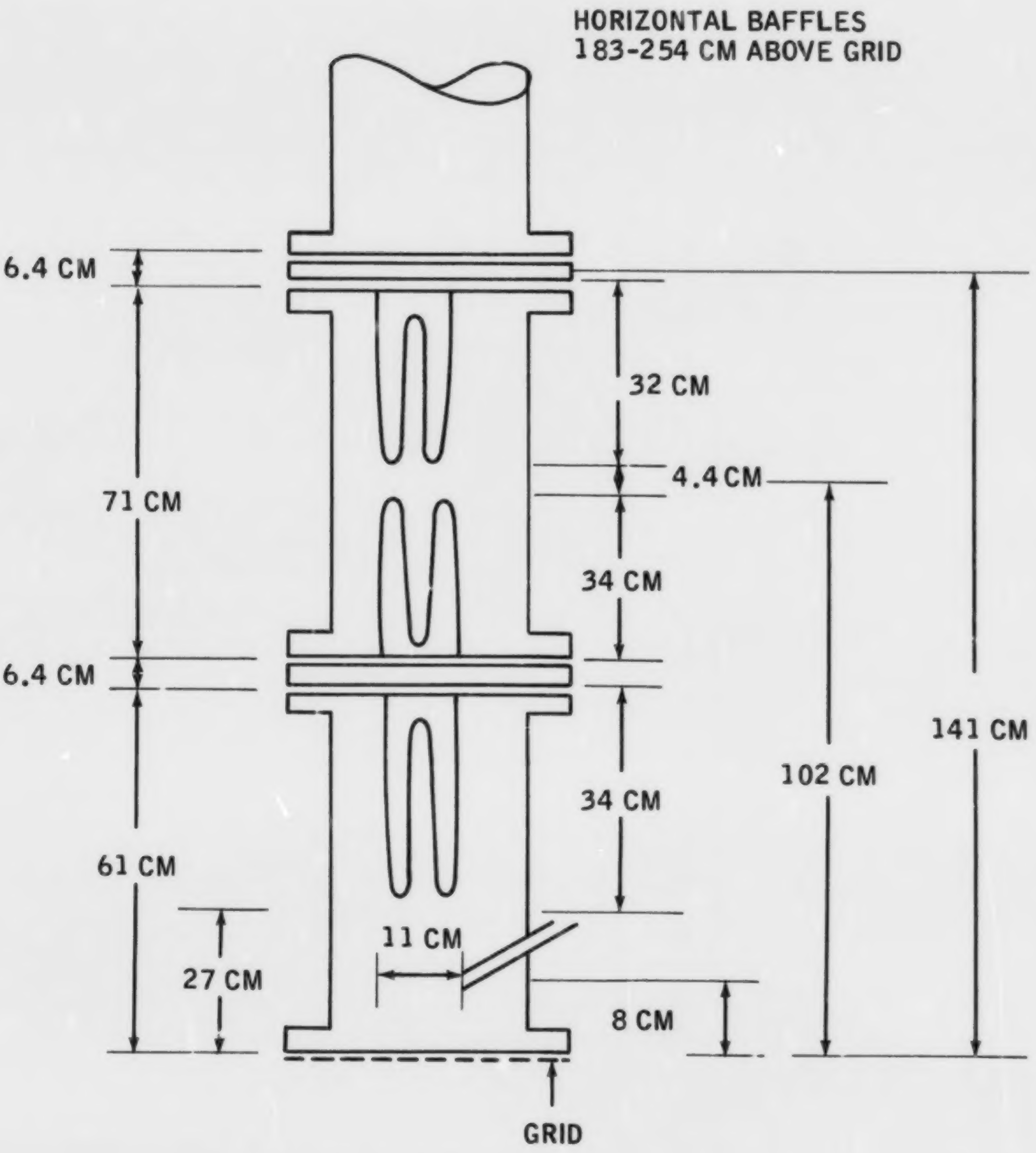
HORIZONTAL BAFFLES
183-254 CM ABOVE GRID
6.4 CM
32 CM
4.4 CM
71 CM
34 CM
6.4 CM
141 CM
102 CM
34 CM
61 CM
11 CM
27 CM
8 CM
GRID

VERTICAL COILS—316 SS TUBING, 6.4 MM O.D., 0.89 MM WALL
EACH COIL = 0.060 $M^2$ SURFACE AREA

Figure V-7

LOCATION OF COOLING COILS

Figure V-8

COAL INJECTOR

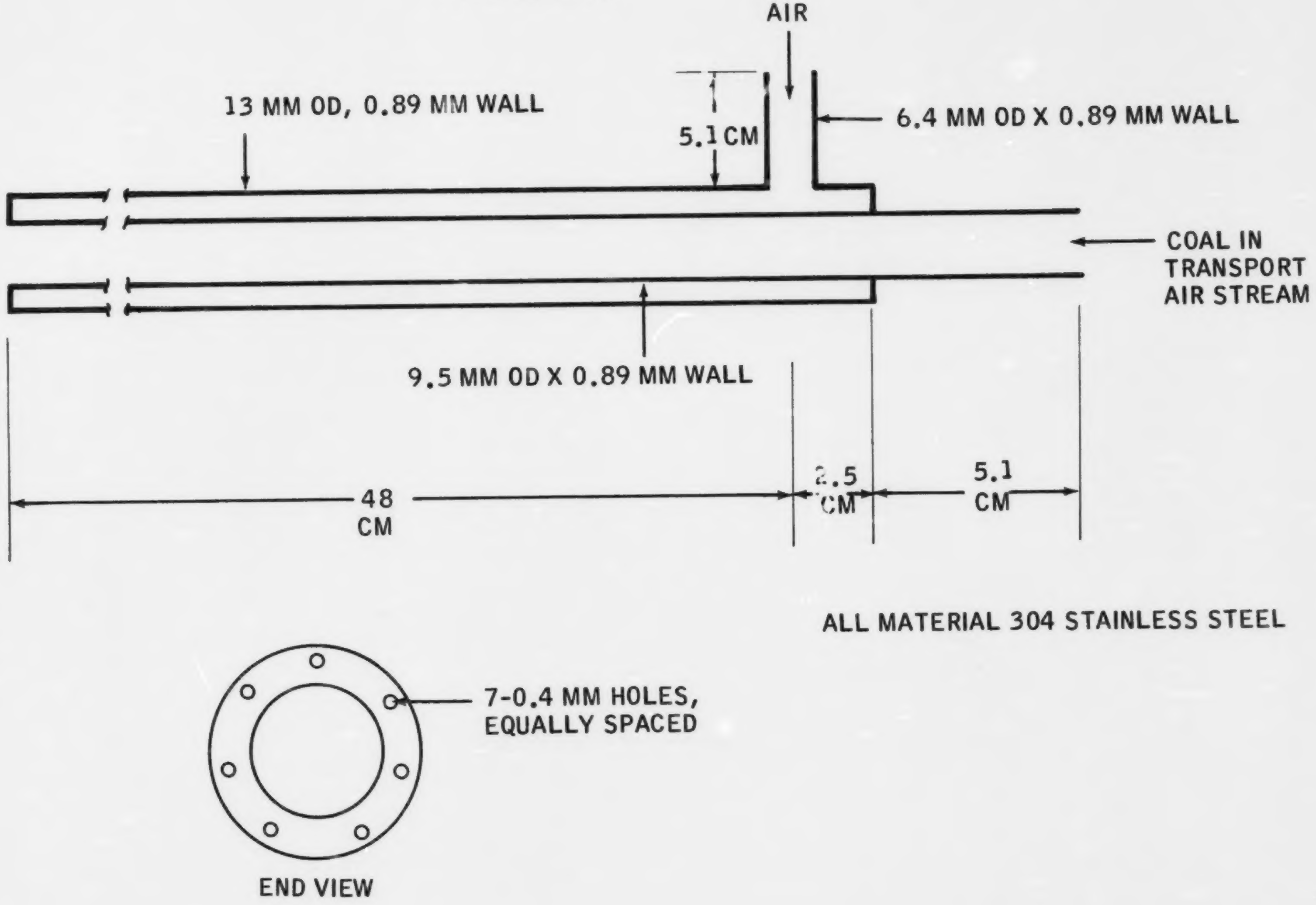
AIR
13 MM OD, 0.89 MM WALL
5.1 CM
6.4 MM OD X 0.89 MM WALL
COAL IN TRANSPORT AIR STREAM
9.5 MM OD X 0.89 MM WALL
48 CM
2.5 CM
5.1 CM
ALL MATERIAL 304 STAINLESS STEEL
7-0.4 MM HOLES, EQUALLY SPACED
END VIEW

entrained sorbent and fly ash. An off-gas cooler, which followed the cyclones, reduced the temperature of the off-gas to the desired level. The off-gas then entered a coil of 2.5 cm diameter stainless tubing which was electrically heated during startup to raise the temperature of the gases above the dew point. A 3.81 cm diameter Aerotec cyclone, following the heater, was used to remove particulates during startup of the combustor, when water vapor condensation in the first two cyclones caused them to operate at reduced efficiency. Fine particulates were removed with a Pall Model MEC-800-18-C filter, located upstream of the back-pressure control valve. This filter had a mean pore size of 165 microns and an area of 0.37 $m^2$. Before being vented, the off-gas entered a chiller and knockout to remove moisture so that the water content of the gas could be determined. A small portion of the off-gas was diverted after the back-pressure control valve and sent to the gas sampling system. A schematic of the sampling system is shown in Figure V-9. The sample gas passed through a small length of heated stainless tubing before entering a Balston Model 33 filter for final particulate cleanup. The gas then went through a 1.8 m section of heated Teflon line before passing through a permeation drying tube (Perma Pure Dryer Model PD-1000-24S) for moisture removal. Downstream of the dryer the line was unheated Teflon tubing to the analytical instruments. The analytical instruments used in the system were:

| | | |
|---|---|---|
| 1. | Beckman 865 $SO_2$ Analyzer (Infrared) | 0-2000 ppm<br>0-3000 ppm<br>0-10,000 ppm |
| 2. | Beckman 864 CO Analyzer (Infrared) | 0-1000 ppm<br>0-2500 ppm<br>0-5000 ppm |
| 3. | Beckman 864 $CO_2$ Analyzer (Infrared) | 0-5 %<br>0-10 %<br>0-20 % |
| 4. | Beckman 715 Oxygen Analyzer (Polarographic) | 0-5 %<br>0-25% |
| 5. | Thermo-Electron 10B NO/$NO_x$ Analyzer (Chemiluminescence) | 8 ranges from 0.01-10,000 ppm |

Coal - Three different coals were used in the batch fluidized bed coal combustion program. The majority of the runs were made using a high volatile (A) bituminous coal from Consolidation Coal Company's Arkwright mine in West Virginia. It was ground to -16 mesh by Penn-Rillton Co. The specified particle size distribution is given in Table V-1. A measured particle size distribution is presented in Figure V-10 and corresponds very closely to the specified distribution. Runs were also

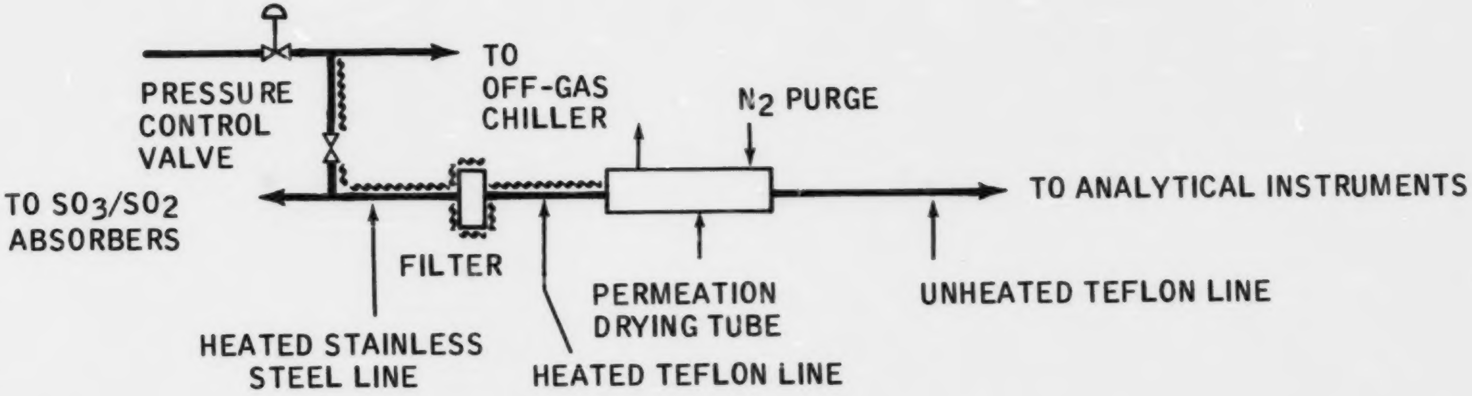
PRESSURE CONTROL VALVE
TO OFF-GAS CHILLER
$N_2$ PURGE
TO $SO_3/SO_2$ ABSORBERS
TO ANALYTICAL INSTRUMENTS
FILTER
PERMEATION DRYING TUBE
UNHEATED TEFLON LINE
HEATED STAINLESS STEEL LINE
HEATED TEFLON LINE

Figure V-9

FLUE GAS SAMPLING SYSTEM

Figure V-10

PARTICLE SIZE DISTRIBUTION OF ARKWRIGHT COAL

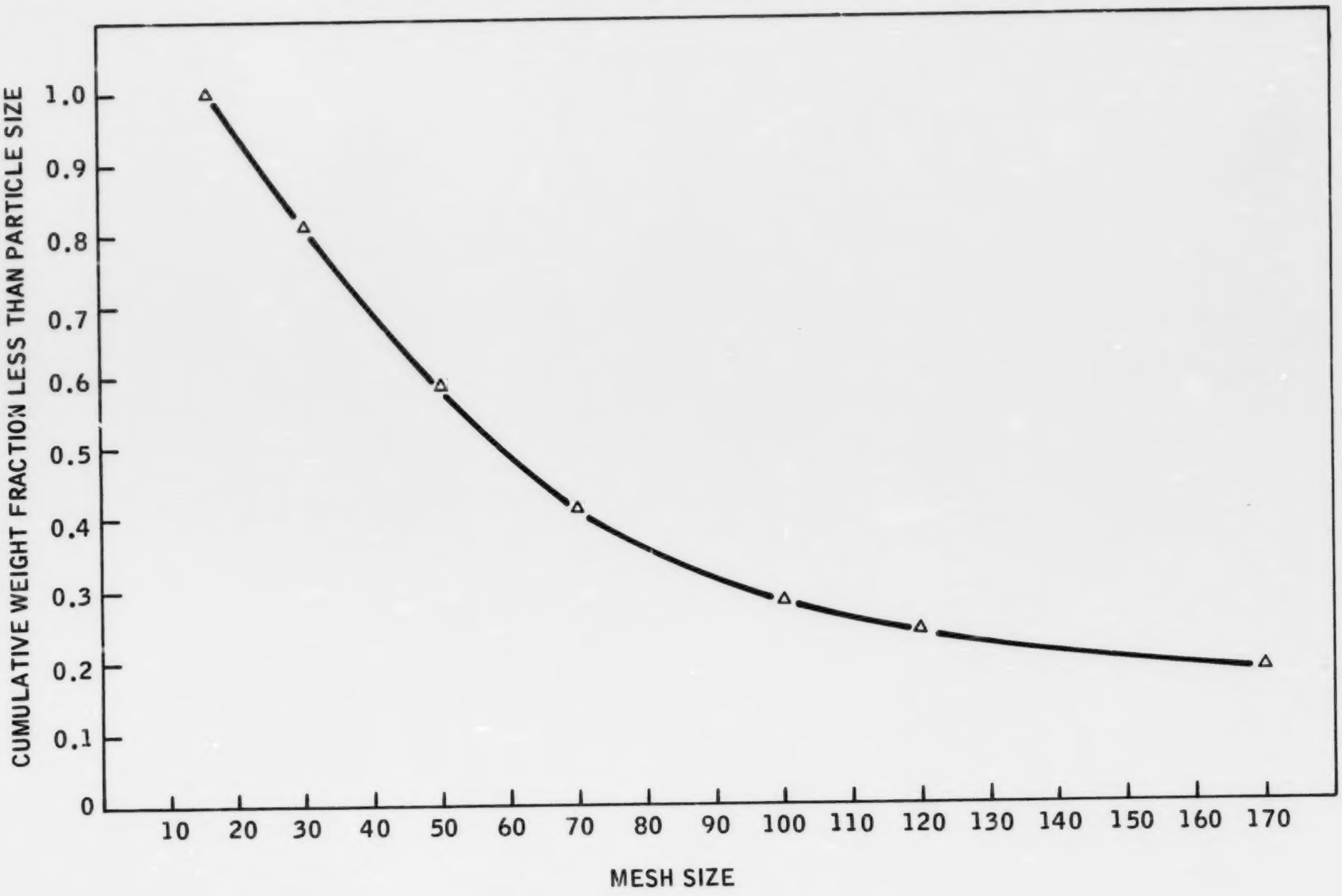

made with a low sulfur Western sub-bituminous coal and a high sulfur Illinois bituminous coal. The Illinois coal was provided by Argonne National Laboratory. A proximate and ultimate analysis was made on each of the coals and the results are presented in Table V-2.

TABLE V-1. COAL PARTICLE SIZE DISTRIBUTION
PENN-RILLTON CO. GRIND B-2 SPECIFICATION

| U.S. Mesh Size | 10 | 20 | 30 | 40 | 100 | 200 | pan |
|---|---|---|---|---|---|---|---|
| Wt. Fraction on Screen | 0 | 4.5 | 15.5 | 14 | 35.5 | 12.5 | 18 |

TABLE V-2. COMPOSITION OF COALS USED IN BATCH
FLUIDIZED BED COAL COMBUSTION PROGRAM

Source - Consolidation Coal Co. (Arkwright Mine - West Virginia)

| Proximate | | Ultimate | |
|---|---|---|---|
| Moisture | 1.00 wt. % | Moisture | 1.00 wt. % |
| Ash | 8.11 | Ash | 8.11 |
| Volatiles | 36.86 | Total Carbon | 76.26 |
| Fixed Carbon | 54.03 | Hydrogen | 5.30 |
| | | Sulfur | 2.66 |
| | | Nitrogen | 1.49 |
| | | Chlorine | 0.07 |
| | | Oxygen(1) | 5.11 |

Higher Heat Value = 14,045 Btu/lb

Source - Peabody Coal Co. (Mine 10, Seam 6 - Illinois)

| Proximate | | Ultimate | |
|---|---|---|---|
| Moisture | 6.0 wt. % | Moisture | 6.0 wt. % |
| Ash | 12.7 | Ash | 12.7 |
| Volatiles | 40.5 | Total Carbon | 62.9 |
| Fixed Carbon | 40.8 | Hydrogen | 4.5 |
| | | Sulfur | 4.1 |
| | | Nitrogen | 1.2 |
| | | Chlorine | 0.0 |
| | | Oxygen(1) | 8.5 |

Higher Heat Value = 11,300 Btu/lb

Source - Carter Oil Co. (Wyoming)

| Proximate | |
|---|---|
| Moisture | 2.2 wt. % |
| Ash | 7.9 |
| Volatiles | 44.0 |
| Fixed Carbon | 45.9 |

| Ultimate | |
|---|---|
| Ash | 7.9 wt. % (Dry) |
| Total Carbon | 68.0 |
| Hydrogen | 5.0 |
| Sulfur | 0.7 |
| Nitrogen | 0.9 |
| Chlorine | 0.0 |
| Oxygen(1) | 17.9 |

Higher Heating Value = 11,850 Btu/lb (Dry)

(1) By difference

Sorbents - Grove limestone (BCR No. 1359) and Tymochtee dolomite were the primary sorbents used in the experimental studies. The stones and their properties are given in Table V-3. The particle size of these materials was generally in the 8 X 25 mesh range. Typical particle size distribution curves for the limestone and dolomite are shown in Figure V-11. Baker dolomite and Pfizer dolomite (BCR No. 1337) were also tried but, because of their high attrition rates, their use was discontinued.

TABLE V-3. PROPERTIES OF SORBENTS USED IN BATCH FLUIDIZED BED COAL COMBUSTION PROGRAM

| Designation | Quarry Source | Stone Type | Chemical Analysis, wt. % CaO | MgO | $SiO_2$ | $Al_2O_3$ | $Fe_2O_3$ |
|---|---|---|---|---|---|---|---|
| 1359 | Grove Lime Co. (Stephen City, Va.) | Limestone | 97.0 | 1.2 | 1.1 | 0.3 | 0.2 |
| Tymochtee | C. F. Duff & Sons (Huntsville, O.) | Dolomite | 53.8 | 38.7 | 5.3 | 0.9 | 1.2 |

Experimental Procedures - Operation of the batch fluidized bed combustor can be divided into four phases: startup, ignition and pre-heating, coal feeding, and shutdown. Startup consisted of those activities preliminary to ignition of the propane burner. These activities included checking equipment to make sure it was ready for a run, checkout of the analyzer calibration, charging sorbent, turning on electrical circuits and the air compressor, turning on all cooling water systems (fluidizing grid, burner, steam coils, condenser) and purge air systems (pressure taps, sight-glasses, ΔP cells).

Figure V-11

PARTICLE SIZE DISTRIBUTION OF SORBENTS

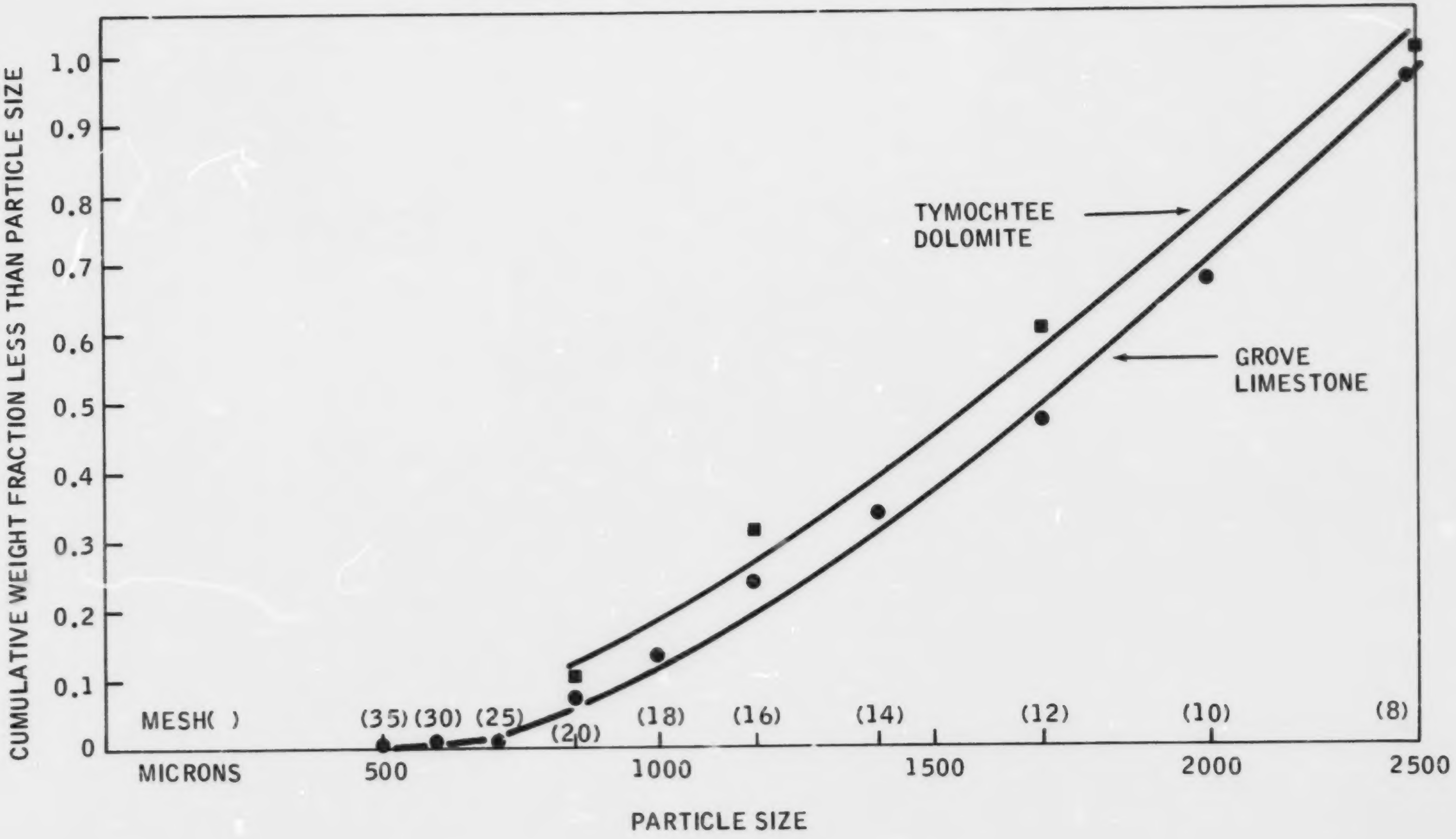

To ignite the propane burner, air and fuel flows were set and the ignition electrode was activated. Safety devices shut down all flows if ignition was not obtained within ten seconds or if a flame-out occurred afterwards. A safety interlock prevented startup for 3 minutes after an automatic shutdown to assure adequate purging of the combustor. Subsequent to ignition, combustor air flow and pressure were adjusted to the values desired for making the run. All gas flows and pressure were controlled automatically. After the bed temperature reached the ignition temperature of propane, propane flow to the bed was initiated to heat the bed up to the coal ignition temperature.

Preparation of the coal feed system for a run consisted of setting the flow of injection air and activating and adjusting the coal feeder-to-combustor ΔP control system. Coal injection could be started only after the temperature in the combustor was high enough for self-ignition of the coal to occur. Propane flow was stopped automatically at the same time that feeding of coal was started. An automatic safety circuit would shut down coal injection if the combustor temperature dropped too low to ensure combustion of the coal or if the feeder to combustor ΔP dropped below a pre-set minimum (about one psi).

Data on the weight of the coal feeder vs. time was taken so that the feed rate of coal could be determined. Another method of estimating the feed rate was to observe the oxygen concentration in the off-gas from the combustor. A rapid rise in oxygen concentration was usually the quickest way of determining that a problem was developing with the coal feeding system.

Temperatures in the combustor could be controlled by regulating the amount of coal burned. The feed rate of coal could be adjusted by changing the flow of injection air or coal feeder to combustor ΔP.

To shut down the combustor routinely, the coal feed valve was shut, fluidizing air was stopped, and nitrogen purge was started to preserve the solids. Flow of injection air was kept on for several minutes so that the coal feed line could be cleared of coal. All water flows were reduced. Solids could be discharged from the reactor (by blowing them out of a port located just above the fluidizing grid) after the bed cooled overnight.

## EQUIPMENT AND TECHNIQUE DEVELOPMENT

### Coal Feeding

A detailed discussion of the early phases in the development of the modified Petrocarb coal feed system used on the batch unit was discussed in a previous report (3). In the earlier study an extensive program was undertaken to test the suitability of the Petrocarb feeder for supplying coal to the batch combustor. The effect of feed tank pressure, feed tank-combustor pressure differential, injection line diameter, and injection air flow rate on the coal feed rate were thoroughly investigated.

As a result of numerous coal combustion runs since then, additional insight into the nature of the coal feeding system has been gained. Other factors such as coal probe design, orifice assembly design, and moisture content of the coal have been shown to have a pronounced effect on the ability of the Petrocarb system to deliver a steady and dependable coal flow.

Observations of the mixing of solids in Exxon's cold model test unit were also made. The depth of the injection air jet penetration into the fluidized bed was also observed in this unit to obtain qualitative information about coal feeding by pneumatic transport into fluidized beds. The solids mixing in the vicinity of the coal injection point was observed to be poor, especially with deep beds. The poor mixing was due to the horizontal orientation of the coils. Only when the settled bed depth was 0.30 m or less and the superficial velocity was 1.83 m/sec or more did the solids mix well. Slugging occurred in the space between the fluidizing grid and the bottom of the simulated cooling coils. Also, the downward moving solids tended to be densely packed at the reactor walls. Penetration of air jets into the bed from a simulated coal injection probe was very low. These observations suggested that the bed solids were impeding the flow of coal into the bed. At this point a significant improvement was made to the batch unit coal feeding system by modifying the coal injection probe. The water-cooled probe which had been used up to this point was replaced with a new air-cooled probe which had sonic flow air jets surrounding the central air/coal stream. The primary intent of the high velocity air jets was to improve coal feeding by clearing a path through the bed of fluidized solids.

The sonic jet probe was then tested in the cold model unit. It was observed that the bed was penetrated to a much greater depth by the jets issuing both from the sonic flow holes and the central coal transport air stream. The system was then installed on the combustor and the coal feed rate became much steadier with significantly fewer stoppages due to plugs in the coal feeding line.

The coal feeding system was improved further by redesigning the orifice assembly at the bottom of the injector vessel. The dependability of the coal feeding system had often been poor due to the numerous instances in which the coal had plugged the orifice of the feed vessel. Some of the plugs appeared to be due to the bridging of fine coal at the orifice or by a caking of moist coal on the orifice walls. To alleviate these problems an orifice assembly was designed in which the inside bore was perfectly smooth with no sudden changes in diameter. Thus, no shoulders would exist where coal would tend to accumulate. Figure V-12 shows a schematic of the orifice assembly presently used. Also, to insure that dry coal was used, it became a routine practice to store the coal in a "hot" room for several days prior to its use. The coal had apparently become wet during extended storage. After installation of the sonic jet probe and the improved orifice assembly, and the use of the additional drying step, coal feeding became very steady and dependable.

## Bed Temperature Distribution - Cooling Coils

A serious problem which occurred during the early testing of the combustor was a poor temperature profile in the bed, characterized by severe hot spots at the coal feed point. Temperature drops of over 330°C were measured across expanded beds 0.9 m high. The cause of this problem was believed to be combustion of the powdered coal occurring at a much faster rate than solids could mix and distribute heat throughout the bed. In the 11.4 cm diameter reactor, bed heights of 60-180 cm were used, corresponding to length-to-diameter ratios of 5-16. Top-to-bottom mixing of solids was poor because of the high L/D ratio of the bed and also because the tightly wound horizontal serpentine cooling coils hindered movement of solids. The intent of this coil design was to break up slugs of solids and promote better mixing between gas and solid phases. Visual observation in the cold model unit confirmed that slugging was absent in the coil section but that top-to-bottom mixing was very poor.

In order to improve mixing, the coils were changed from the horizontal serpentine design to vertical loops. Four of the six horizontal coils (0.093 $m^2$ area each) were replaced by three vertical coils of the same surface area per coil. The top two horizontal coils remained in place. Figure V-13 is a photo of a vertical coil. Figure V-14 is a comparison of temperature profiles obtained with horizontal and vertical coils. It is clear that vertical coils produced a dramatic improvement; hot spots were nearly eliminated and the temperature drops across the bed were reduced to about 50°C.

Vertical coils had another effect on the operation of the combustor. The first set of vertical coils had the same surface area as the horizontal coils which they replaced. However, in the first run made with vertical coils, there was some difficulty in maintaining bed temperatures even though the coal input was higher than normally used with horizontal coils. It was quickly apparent that vertical coils produced higher heat transfer coefficients than horizontal coils, and an explanation was that solids were moving more freely with vertical coils. Indeed, measurements of heat transfer coefficients indicated that vertical tube coefficients were significantly higher (see page 123). Eventually, the first set of vertical coils had to be replaced with coils with less surface area (0.060 $m^2$ per coil). The coil tubing O.D. was also increased from 0.64 to 0.95 cm.

Figure V-12

COAL FEEDER ORIFICE ASSEMBLY

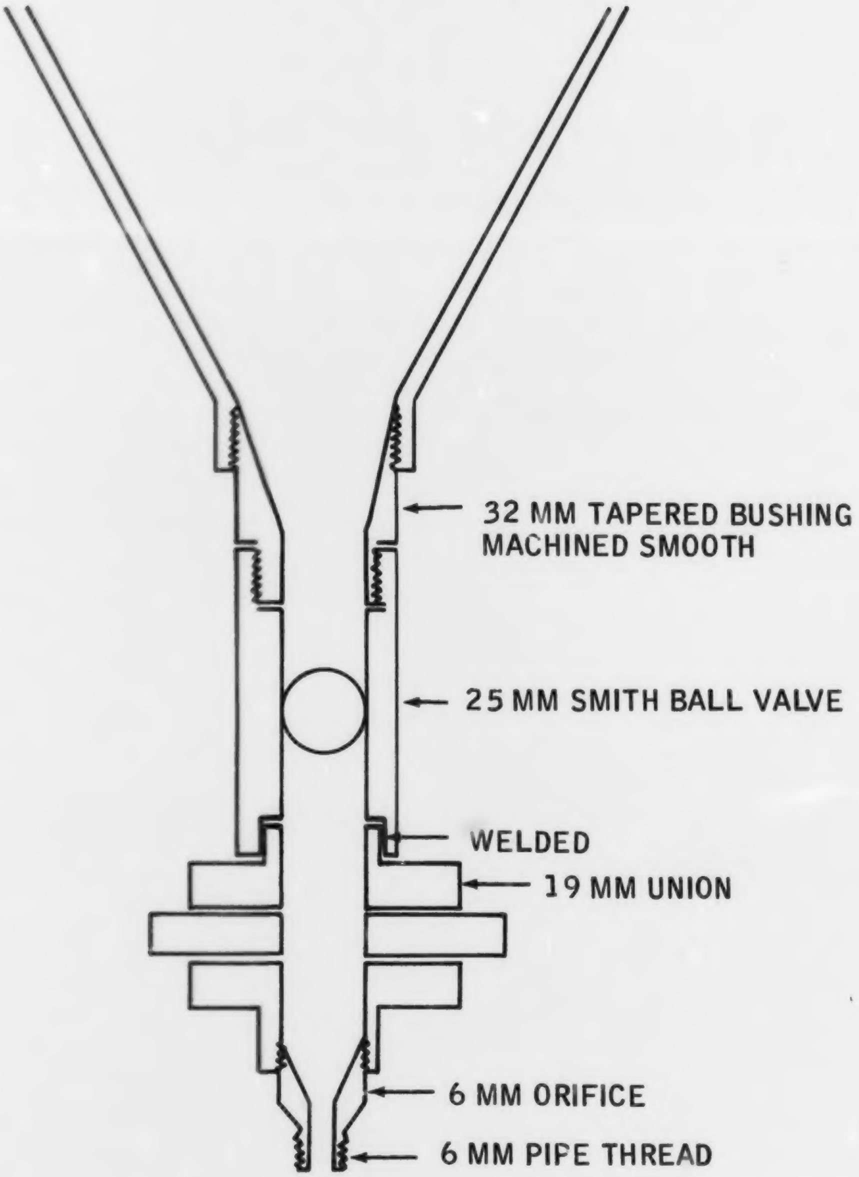
32 MM TAPERED BUSHING
MACHINED SMOOTH
25 MM SMITH BALL VALVE
WELDED
19 MM UNION
6 MM ORIFICE
6 MM PIPE THREAD

MATERIAL: ALL STAINLESS STEEL

FIGURE V-13

VERTICAL COOLING COIL

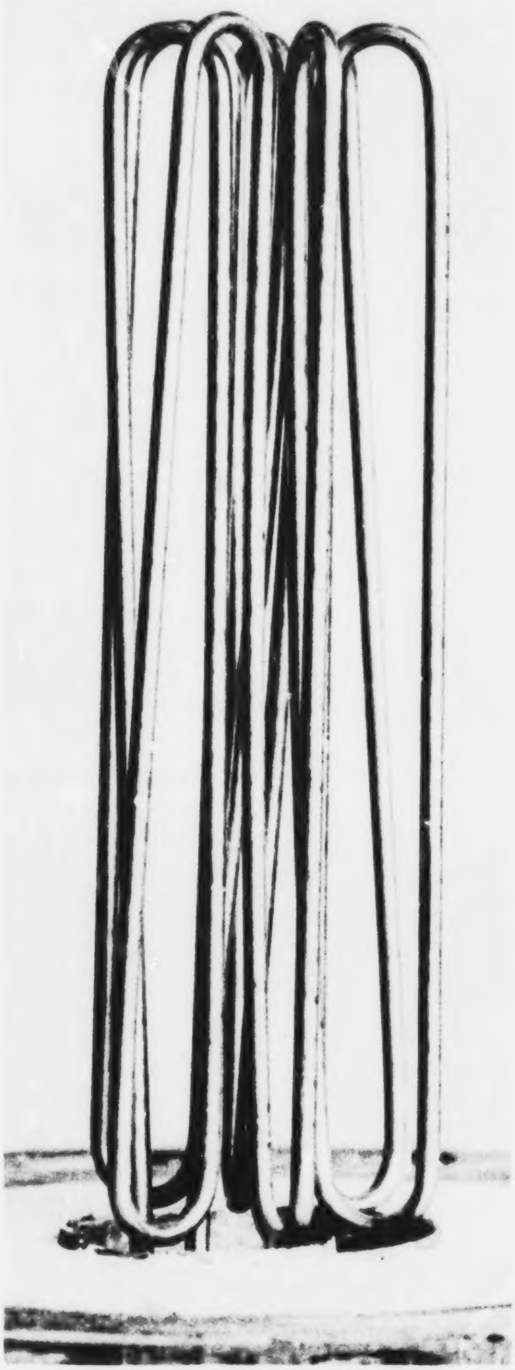

Figure V-14

COMPARISON OF BED TEMPERATURE PROFILES FOR HORIZONTAL AND VERTICAL COOLING COILS

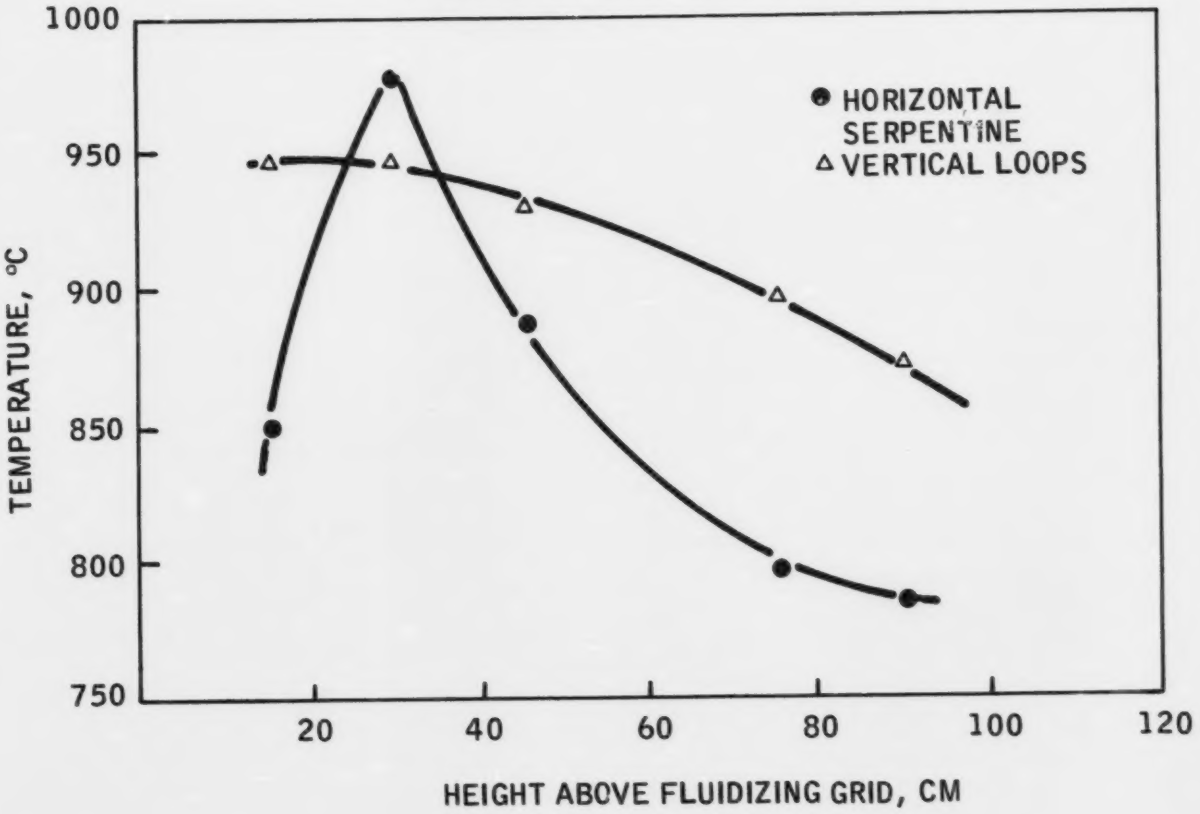

## Sampling System

To assure reliable, accurate flue gas analyses the sampling system used on the batch fluidized bed combustion unit was continually modified and improved. The system has undergone three distinct phases and each will be discussed below.

1. Phase I - This system was the initial one used on the batch unit. A small portion of the off-gas was drawn off from the gas handling system and diverted to a refrigerator which lowered the dew point of the gas to about 2°C before it was sent to the gas analysis equipment. This system had several drawbacks which may have prevented an accurate analysis of the flue gas. With this system the possibility of $SO_2$ dissolving and being removed by liquid water existed and the analyzer response times to changes in concentration of the off-gas were slower than desired.

2. Phase II - This system consisted of a steam-heated pressure regulator, a glass microfiber filter (Balston Type 33) and a self regenerative permeation drier. The sampling line was stainless steel and was heated up to the drier. The sampling port on the combustor was located downstream of the second cyclone and before the off-gas cooler. Another major difference between the Phase I and II sampling systems was the sampling pressure. The Phase I sampling was done at atmospheric pressure and the Phase II sampling was done at 800 kPa.

The sampling system was tested by burning coal in an inert bed and then comparing the measured and calculated (by material balance) $SO_2$ concentrations. The inert material used was alundum (38X, Size 20, supplied by Norton Company). On the first test, an O-ring in the drier failed at about 700 kPa, even though the unit was rated for 800 kPa. For this test only, the drier was replaced with a refrigerator. The average measured $SO_2$ concentration was only about one-third of the calculated concentration. Also, the $SO_2$ concentration increased when the sample flow rate was increased; the maximum concentration was about two-thirds of that calculated.

In the second test, the self-regenerative drier was used and the sample gas flow was increased. The residence time in the sample line was about 45 seconds. The measured $SO_2$ concentration averaged about one-half of the calculated concentration. Increasing the sample flow further caused only a slight increase in the indicated concentration.

In the third and fourth tests, the flue gas was analyzed for $SO_2$ by absorption in a 3% hydrogen peroxide solution. This is a modification of the EPA test method (titrimetric). In both cases, the measured $SO_2$ was less than half of the calculated values. The sampling points were different for each test. In test no. 3, the sample to the peroxide bubbler was removed downstream of the drier, after passing through the heated stainless steel sample line and filter. In test no. 4, the sample was removed from the combustor and connected with polyethylene tubing to a heated glass wool filter and the bubbler. Hence, the sample did not contact any metallic surfaces after leaving the combustor.

As a result of these tests, it was determined that this sampling system was inadequate for reliable $SO_2$ measurements. A possible reason for the $SO_2$ loss might have been the condensation of $H_2SO_4$ in the sampling line. There were some signs of corrosion in the sampling system which supports the possibility of condensation and $SO_3$ formation. Another drawback of this system was the high residence time of the gas in the lines.

3. Phase III - This system is the one presently used on the batch unit. The location of the sampling port was changed to a position downstream of the combustor pressure control valve. The major advantage of sampling at low pressure is that the residence time in the lines is substantially reduced. The gas sample passed through a small length of stainless steel line, electrically heated to about 200°C to prevent condensation of $H_2SO_4$, a heated glass microfiber filter, and a permeation drying tube. A 1.83 m length of heated Teflon tubing connected the filter and dryer. Unheated Teflon line was used downstream of the dryer.

Checks were made on the sampling system and the results indicated that the system worked well. A series of tests were made in which a $SO_2/N_2$ gas mixture was metered into the combustor along with air and the $SO_2$ was analyzed in the off-gas. The results showed that the actual vs. expected measurements were within the expected range of error. Several tests were also conducted in which the $SO_2/N_2$ gas mixture was injected into the combustor while the preheat burner was operating. The infrared analyzer read 25 to 38% lower than the calculated concentration. Measurement by the wet chemical method was 10-12% higher than calculated. Additional testing will be continued to aid in the development of an even more reliable sampling system.

### Cooling Coil Damage

Damage to the 316 SS cooling coils has occurred several times. It is difficult to attribute failures to one cause; however, it was probable that tube failures occurred because of one or more of the following conditions: excessively high tube metal temperatures, corrosion, and mechanical causes.

The first failure of a horizontal serpentine coil occurred after about 50 hours of operation. This coil had been subjected to conditions that were much more severe than would be encountered in normal operation. Because of hot spots in the fluidized bed, temperatures external to the coil frequently exceeded 1100°C. A lack of water pumping capacity caused steam temperatures inside the coil to be about 500-600°C. These conditions may have caused tube temperatures to be higher than the metal could withstand, particularly with regard to corrosion.

A specimen from this coil was analyzed by optical and electron microprobe techniques. The conclusion was that the coil was in a "sensitized" condition and had suffered severe sulfur attack on its outer surface. "Sensitized" means that chromium carbides had precipitated at the grain boundaries, leaving regions close to the grain boundaries low in chromium and thus less resistant to intergranular corrosion. This would have been particularly detrimental during "downtime" when sulfur acids and chlorides present in condensed water could produce intergranular cracking. Type 316 SS is susceptible to sensitization when it is heated to temperatures of 450-650°C. The external surface of the tube showed sulfur attack down to a depth of about 25 $\mu m$ (wall thickness = 890 $\mu m$). Corrosion took the form of a surface scale of Cr-Fe oxide and an area beneath the scale rich in Fe, Ni, and S, but low in Cr. The internal surface contained deposits of Mg, Ca, and Si and showed slight erosion. No erosion was noted on the outside of the coils.

A second horizontal coil which failed showed similar damage. A section of coil located near the steam outlet had heavy sensitization and intergranular attack; but, a section near the water inlet had negligible damage. All the coils had a scale deposited on the outer surface which consisted primarily of carbon and sulfur. Beneath this scale was the metal surface and intergranular scale.

Failure of a vertical coil has also occurred; in this case a 20 cm length of tubing near the water inlet had melted. Surprisingly, the remainder of the coil appeared to be in good shape.

Cooling coil failures appeared to be related to excessive metal temperatures. However, analysis showed that tube metal temepratures should be quite low, under normal operating conditions. The tube wall temperature, Tw, is given by the following expression:

$$T_w = \frac{To + r\,Ti}{1 + r}$$

where To = temperature outside coil
Ti = temperature inside coil
$r = \frac{hi}{ho}$ = ratio of inside to outside heat transfer coefficients

Since hi is at least 5500 $W/m^2$ °C and ho is about 425 $W/m^2$ °C, r is at least about 13. For a fluidized bed temperature of 870°C and a steam temperature of 120°C, Tw = 174°C. This seems too low a temperature to cause damage to the coil except, perhaps, by corrosion. For example, at some regions of the tube, especially near the water inlet, metal temperatures could be low enough to permit condensation of $H_2SO_4$ on the outside wall. Corrosion could result, particularly if the metal had previously been sensitized. This might be the mechanism by which cooling coils were damaged so that they eventually failed.

Another explanation for coil damage that was considered was that the critical or "burnout" heat flux was exceeded. Above this flux, the metal temperature rises sharply as a consequence of a drop in the inside film coefficient. Under normal conditions, the actual heat flux should be safely below burnout. However, it is possible that on occasion the burnout flux was exceeded at certain regions of the coils.

There has been no evidence of erosion to the cooling coils. Slight mechanical damage (bending) did occur on one occasion when the bed had agglomerated because of high temperatures.

### Bed Agglomeration

A problem which periodically occurred in the batch combustor was bed agglomeration. This was a problem not only because of the high temperature situation which it creates, but also because agglomerated solids can cause a deformation of the cooling coils. Bed agglomeration normally occurs when the ash in the coal begins to soften. This happens at temperatures in excess of 1150°C. As the stone begins to agglomerate, the solids mixing becomes poorer resulting in poorer heat transfer to the cooling coils, and an uncontrolled temperature condition. However in runs where bed agglomeration occurred, temperatures in excess of 1150°C were usually not observed. This implies that localized hot spots which are not picked up by the thermocouples may develop and cause the agglomeration process to begin. These high temperatures could be caused by a sudden surge of coal into the combustor. A sudden surge in the coal feed to the combustor could be caused by an upset in the system which controls the pressure differential between the coal injector and the combustor or by an upset in the injection air rate. Upsets of these types have been observed at times.

## COMBUSTION RESULTS

### $SO_2$ Emissions

$SO_2$ emissions measured during batch runs varied with time during the run as the bed of sorbent became more highly sulfated. At the beginning of a run, the $SO_2$ emissions were low. After a period of time, $SO_2$ levels increased and then, if the run lasted long enough, reached a maximum determined by the sulfur content of the coal. Runs were made at various $SO_2$ concentrations in the flue gas, the bed analyzed for $SO_4^{=}$, and the equivalent calcium to sulfur molar ratio calculated as

$$Ca/S = \text{fraction } SO_2 \text{ removed/fraction of calcium sulfated}$$

The emissions at the end of the run were then plotted against the equivalent calcium to sulfur ratio calculated for conditions at the end of the run. It had been planned to calculate equivalent calcium to sulfur ratios for periods before the end of a run by calculating a sulfur mass balance and using the final sulfation level as an anchor point.

Figure V-15

SO$_2$ EMISSIONS—LIMESTONE SORBENT

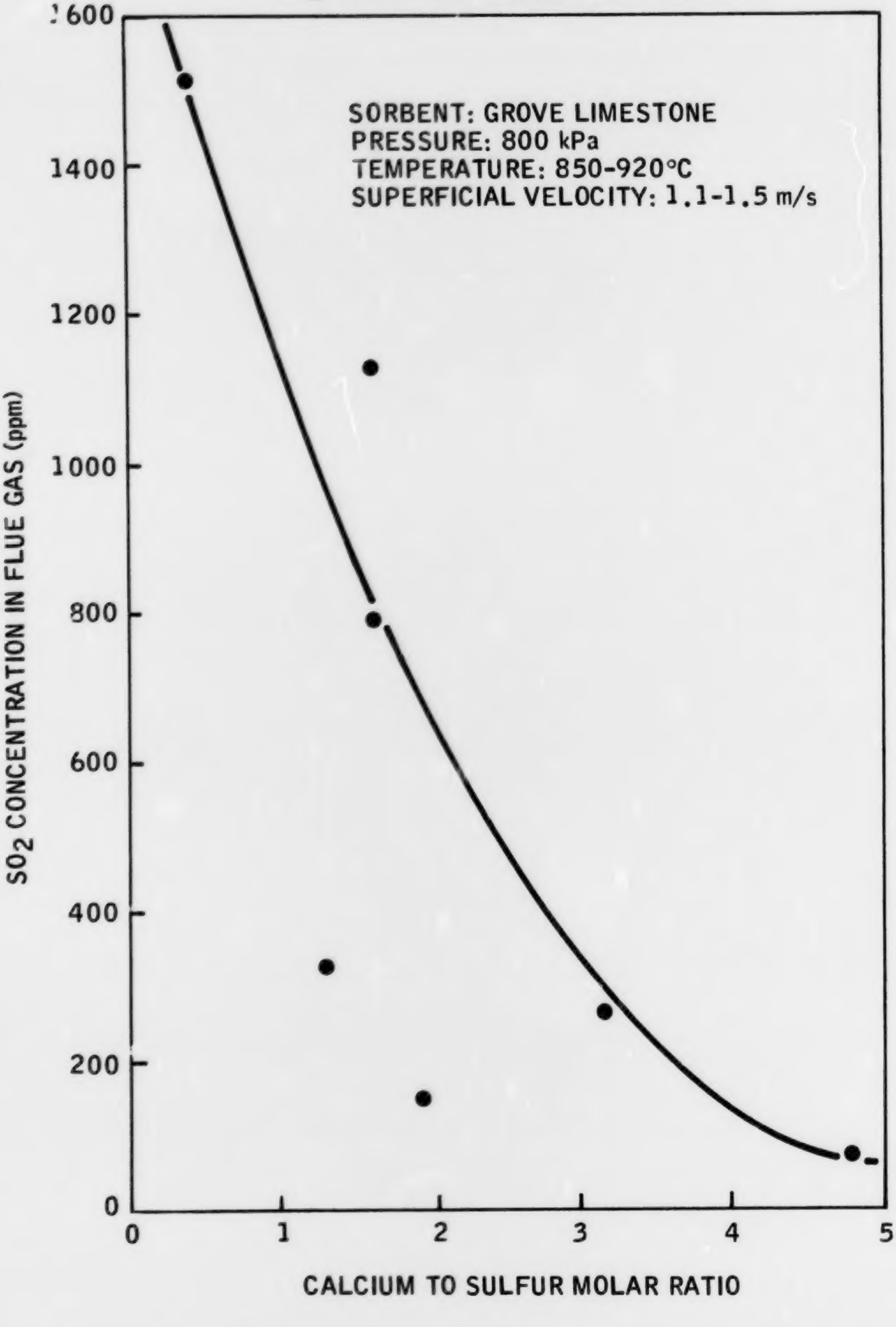

Figure V-16

$SO_2$ EMISSIONS—DOLOMITE SORBENT

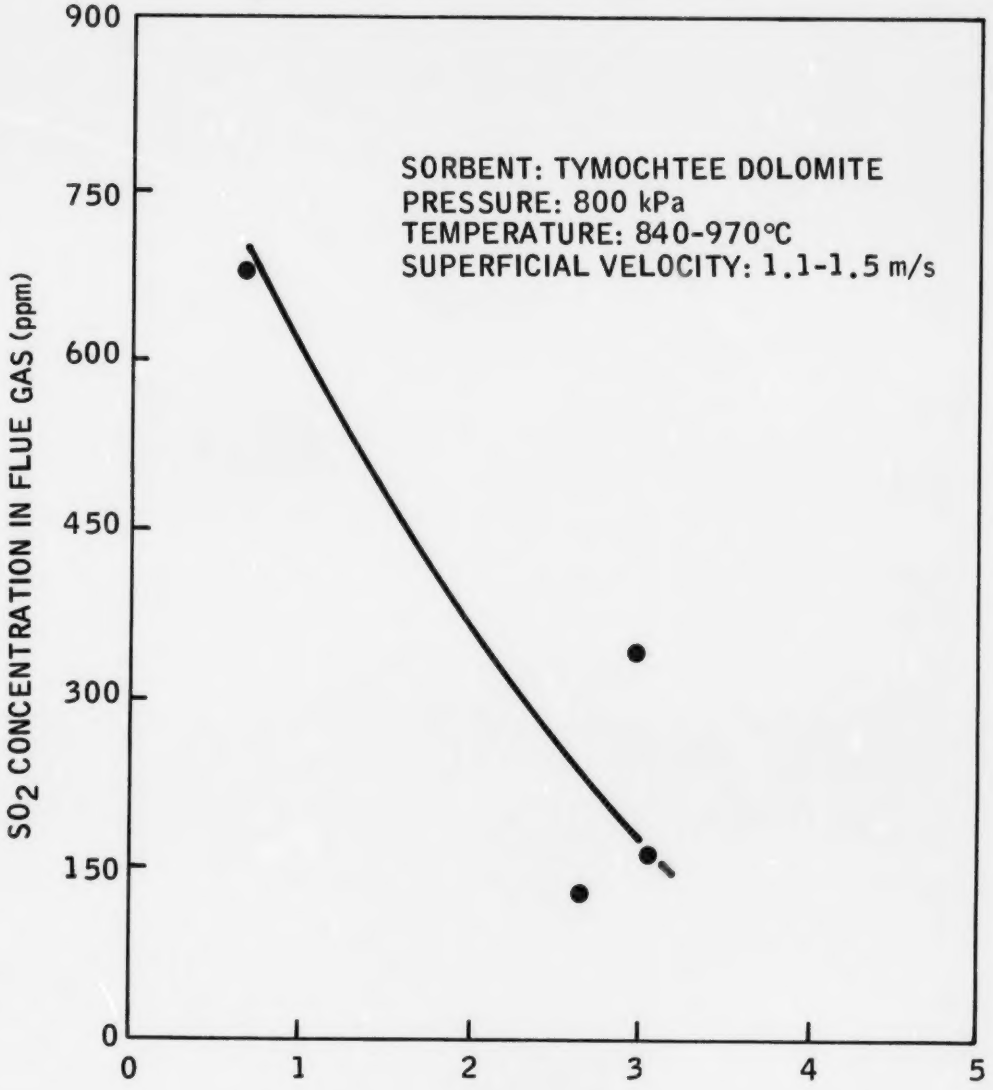

However, this approach was not workable since a portion of the bed was lost by attrition and entrainment during the run and corrections for bed loss could not be made accurately.

$SO_2$ emissions for runs using Grove limestone are shown in Figure V-15 as a function of the equivalent calcium to sulfur ratio. Data are also tabulated in Appendix H. Data were obtained at a pressure of 800 kPa, at superficial velocities of 1.1 to 1.5 m/s over a temperature range of 850 to 920°C. Figure V-16 shows $SO_2$ emissions for runs using Tymochtee dolomite made over the same range of conditions. As expected, emissions were lower when dolomite was used.

## $SO_3$ Emissions

$SO_3/SO_2$ levels were determined during several runs using a modified version of the EPA test method. A flue gas sample was extracted from the ducting just downstream of the combustor pressure control valve. The $SO_3$ levels were much higher than expected and additional measurements will be made to determine the source of the $SO_3$ formation, the combustor itself, the flue gas outlet piping or the sample system. Possible errors in the sampling and analytical techniques will also be investigated.

## $NO_x$ Emissions

$NO_x$ emissions measured during batch unit runs are shown in Figure V-17 as a function of percent excess air. The data were obtained at pressures of 800 kPa, and at temperatures generally in the range of 820 to 975°C. The data were fairly represented by a single correlating line as seen in Figure V-17 despite some variation in temperature. There were some indications of a temperature effect, but additional data must be obtained to determine the magnitude of the effect. Data are also shown in Figure V-17 for three runs made with inert alundum beds. As seen, the $NO_x$ emissions were very similar to, if not a little lower than emissions measured from runs with limestone or dolomite beds. A similar results was reported by Argonne National Laboratory at 800 kPa pressure (4).

As in the case of the miniplant data, the $NO_x$ levels were well below the EPA emission standard of 0.7 lb $NO_2$/M BTU. At excess air levels of 15 to 20%, the range anticipated for commercial FBC units, the emissions were in the range of 0.2 to 0.3 lb $NO_2$/M BTU.

The data shown in Figure V-17 were measured using vertical cooling coils. Earlier runs made with horizontal cooling coils showed higher NO levels, although the levels were still well below 0.7 lb $NO_2$/M BTU at excess air levels in the range of 15 to 20%. It is believed the higher NO levels measured with the horizontal coils were caused by the higher bed temperatures and combustion intensities (heat release rate per unit volume) occuring near the coal feed point when the horizontal coils were used. The $NO_x$ produced by the batch unit combustor was predominately NO. Less than 5% was present as $NO_2$ and this was probably formed in the sampling system, since the equilibrium concentration for $NO_2$ formation is very low at the high temperatures occurring in the combustors.

Figure V-17

$NO_x$ EMISSIONS

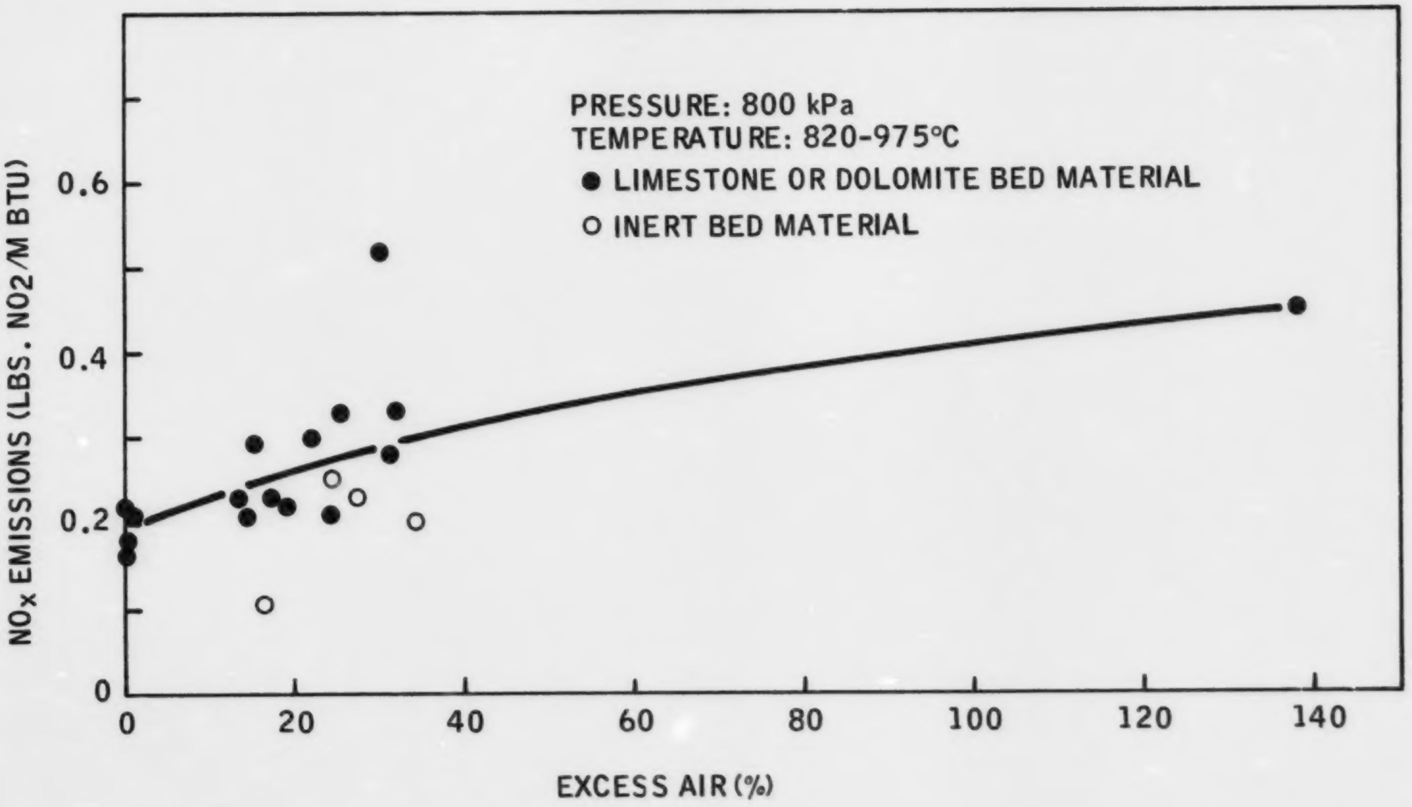

## Trace Metal Emissions

One of the advantages claimed for fluidized bed combustion, compared with conventional combustion techniques, is that a larger fraction of trace elements present in the coal remain in the solid constituents leaving the boiler. In other words, due to the flower combustion temperature, smaller amounts of trace elements are vaporized and emitted with the flue gas as a vapor. Elements which are of particular environmental interest include antimony, arsenic, cadmium, chromium, cobalt, manganese, mercury, nickel, selenium, tellurium, vanadium, beryllium and lead.

In order to determine the capabilities of the fluidized bed combustion system for retaining trace elements, several samples of solids were submitted to General Activation Analysis (San Diego, California) for neutron activation analysis. The samples analyzed were W. Virginia coal (Arkwright), Tymochtee dolomite, and specimens of bed and overhead solids from run no. 3675-2C. The overhead solids consisted of a composite of the material collected in the off-gas cyclones and filter.

The temperatures in the first two cyclones were relatively low, around 300-400°C, and the third cyclone and filter were at even lower temperatures, around 150°C. Therefore, no conclusions could be drawn about the physical state of the trace elements leaving the combustor since collection was at temperatures much lower than combustor temperature.

Table V-4 gives operating conditions for run no. 3675-2C and the results of chemical analysis of the bed and overhead solids. Results of the neutron activation analysis are given in Table V-5. In general, the highest concentrations were found in the overhead solids which contains flyash and some entrained stone and unburned carbon. For many elements, actual concentrations could not be determined; instead, upper limits, or the maximum amounts of elements that could be present in the sample, were given. These are listed in Table V-6.

The analytical procedure used in the neutron activation analysis was as follows: The samples were irradiated for 30 minutes in the TRIGA Mark I Nuclear Reactor at a flux of $1.8 \times 10^{12}$ n/cm$^2$ sec. After a decay of one hour, one day, eight days, and twenty days they were counted on a Ge(Li) detector coupled to a multi-channel gamma-ray spectrometer. A second portion of the samples were irradiated for 15 seconds in the TRIGA Mark I Nuclear Reactor and counted in a Na(Tl) detector coupled to a 400 channel gamma-ray spectrometer for short-lived isotopes. The data thus acquired was examined and the detected elements identified. The data was then processed in a UNIVAC 1108 computer.

Material balances were calculated for each of the elements for which concentrations were determined in the coal, dolomite, bed, and overhead. The balances accounted for elements present in these solid phases only. Material which had vaporized and left the filter in the gaseous state

## TABLE V-4. DATA FOR RUN NO. 3675-2C FROM WHICH SAMPLES WERE ANALYZED FOR TRACE ELEMENTS

**Charge:** Tymochtee dolomite, 7.6 kg (0.6 m settled bed) pre-calcined prior to introduction of coal.

**Coal:** W. Virigina (Arkwright), 6 kg/hr fed for about 3 hours.

**Average Run Conditions:**
T = 940 ± 60°C
Sup. Vel. = 1.9 m/s
Pressure = 640 kPa
Excess Air = 61%

**Analytical Results:**

|  | Bed |  |  | Overhead |  |
|---|---|---|---|---|---|
|  | Weight % | Mole %* |  | Weight % | Mole %* |
| $CaSO_4$ | 37.7 | 18.0 | $CaSO_4$ | 15.8 | 4.4 |
| $CaCO_3$ | 2.6 | 1.7 | $CaCO_3$ | 4.2 | 1.6 |
| CaO | 18.8 | 21.9 | CaO | 5.2 | 3.5 |
| MgO | 28.2 | 45.6 | MgO | 18.4 | 17.4 |
| $Al_2O_3$ | 4.4 | 2.8 | $Al_2O_3$ | 7.0 | 2.6 |
| $SiO_2$ | 7.7 | 8.3 | $SiO_2$ | 14.1 | 8.9 |
| $Fe_2O_3$ | 4.0 | 1.6 | $Fe_2O_3$ | 4.9 | 1.2 |
| Other (+ Error) | -3.4 | -- | C | 19.0 | 60.2 |
|  |  |  | Other (+ Error) | 11.4 | -- |

---

* "other-free" basis

TABLE V-5. ELEMENTS DETECTED BY NEUTRON ACTIVATION ANALYSIS

(All concentrations in ppm)

| Element | Arkwright Coal | Tymochtee Dolomite | Bed | Overhead |
|---|---|---|---|---|
| Al | 27000 ± 5400 | 10900 ± 2200 | 27000 ± 5400 | 71300 ± 14000 |
| *Sb | .253 ± .063 | .0527 ± .015 | .501 ± .11 | .606 ± .13 |
| Ar | 29.1 ± 6.1 | 13.2 ± 2.9 | 18.9 ± 4.2 | 55 ± 12 |
| *As | 3.7 ± .78 | .566 ± .17 | 8.02 ± 1.6 | 9.4 ± 2.0 |
| Ba | | | 107 ± 24 | |
| Br | 12.4 ± 2.6 | 6.75 ± 1.4 | 2.75 ± .75 | |
| *Cd | 2.03 ± .41 | | | |
| Cs | .349 ± .091 | .439 ± .091 | .403 ± .094 | 2.04 ± .42 |
| Cl | 1050 ± 220 | 447 ± 96 | 787 ± 170 | 627 ± 170 |
| *Cr | 17 ± 3.4 | 4.23 ± .85 | 52.9 ± 11 | 133 ± 27 |
| *Co | | 1.03 ± .21 | 3.05 ± .61 | 6.81 ± .14 |
| Dy | 2.74 ± .57 | | | |
| Eu | .171 ± .036 | .0598 ± .013 | .135 ± .028 | .459 ± .098 |
| Fe | 13800 ± 2800 | 3240 ± 650 | 19600 ± 3900 | 39900 ± 8000 |
| La | 2.74 ± 1.1 | | | |
| *Mn | 20 ± 4 | 42 ± 8.4 | 102 ± 20 | 105 ± 21 |
| K | 599 ± 120 | 2180 ± 440 | 1280 ± 260 | 4040 ± 820 |
| Rb | 3.74 ± 1.3 | 12.2 ± 2.5 | 9.17 ± 2.1 | 31.1 ± 6.5 |
| Sm | | .658 ± .13 | | |
| Sc | 2.09 ± .42 | .952 ± .19 | 2.29 ± .46 | 7.63 ± 1.50 |
| Na | 784 ± 160 | 303 ± 61 | 364 ± 73 | 3200 ± 640 |
| Sr | 205 ± 44 | 130 ± 29 | 278 ± 60 | 690 ± 150 |
| *Te | | 2.81 ± .63 | 3.6 ± .91 | |
| Th | 1.75 ± .35 | .58 ± .12 | 1.58 ± .32 | 6.71 ± 1.3 |
| U | .652 ± .30 | 2.23 ± .45 | 3.13 ± .67 | 4.41 ± .94 |

---

* Of particular environmental interest

## TABLE V-6. NEUTRON ACTIVATION ANALYSIS - UPPER LIMITS
(All concentrations in ppm)

| Element | Arkwright Coal | Tymochtee Dolomite | Bed | Overhead |
|---|---|---|---|---|
| Ca | <12000 | <56000 | <68000 | <17000 |
| Ce | 33 | 12 | 34 | 130 |
| *Cu | 100 | 46 | 60 | 380 |
| Er | 14 | 5.8 | 6.2 | 26 |
| *F | 9500 | 5300 | 9400 | 27000 |
| Gd | | | | |
| Ga | 16 | 6.2 | 12 | 30 |
| Ge | 130 | 46 | 72 | 340 |
| Au | .034 | .011 | .028 | 4 |
| Hf | .35 | .38 | .29 | .98 |
| Ho | .49 | .21 | .35 | 1.8 |
| I | 3.1 | 1.6 | 4.2 | 5.9 |
| In | 2.1 | 1.5 | 3.6 | 4.5 |
| Ir | .075 | .0093 | .10 | .28 |
| Kr | 47 | 23 | 31 | 130 |
| *Pb | -- | -- | -- | -- |
| Lu | .095 | .038 | .1 | .4 |
| Mg | 18000 | 81000 | 61000 | 59000 |
| *Hg | .82 | .27 | .7 | 2.7 |
| Mo | 35 | 12 | 31 | 120 |
| Nd | 6.8 | 2.9 | 6.2 | 23 |
| Ne | 72000 | 220000 | 45000 | 140000 |
| *Ni | 140 | 160 | 220 | 590 |
| Nb | 1700 | 610 | 1000 | 5400 |
| N | -- | -- | -- | -- |
| Os | <.77 | <.15 | <.40 | <1.6 |
| O | -- | -- | -- | -- |
| Pd | 6.0 | 3.3 | 5.4 | 16 |
| *P | -- | -- | -- | -- |
| Pt | 12 | 30 | 43 | 93 |
| Pr | 76 | 33 | 44 | 300 |
| Re | .35 | .039 | .15 | .95 |
| Rh | 290 | 1000 | 250 | 810 |
| Ru | -- | -- | -- | -- |
| Sm | 1.2 | .52 | 1.1 | 4.2 |
| *Se | 2.8 | .33 | 1.7 | 8.3 |
| Si | -- | -- | -- | -- |
| Ag | 2.4 | 1.1 | 1.7 | 4.0 |
| S | 320000 | -- | 610000 | 440000 |
| Tg | .34 | .086 | .28 | 1.0 |
| Tb | .29 | .095 | .35 | 1.2 |
| Tm | .39 | .11 | .18 | .94 |
| Ti | 4300 | 11000 | 4100 | 8300 |

TABLE V-6. (Continued) NEUTRON ACTIVATION ANALYSIS - UPPER LIMITS

(All Concentrations in ppm)

| Element | Arkwright Coal | Tymochtee Dolomite | Bed | Overhead |
|---|---|---|---|---|
| W | 3.3 | 1.7 | 2.1 | 13.0 |
| *V | 140 | 120 | 160 | 420 |
| Xe | 110 | 51 | 130 | 400 |
| Yb | .26 | .068 | .21 | .90 |
| Y | 4800 | 3700 | 6400 | 9300 |
| *Zn | 180 | 82 | 130 | 790 |
| Zr | 1300 | 530 | 1400 | 7100 |

---

* Of particular environmental interest

## TABLE V-7. MATERIAL BALANCES FOR TYPICAL COMPONENTS

| Element | In | | Out | | % |
|---|---|---|---|---|---|
| | Coal | Dolomite | Bed | Overhead | Recovery |
| Al | $4.85 \times 10^{-1}$kg | $8.16 \times 10^{-2}$kg | $7.08 \times 10^{-2}$kg | $2.99 \times 10^{-1}$kg | 65.3 |
| Sb | $4.54 \times 10^{-6}$ | $3.97 \times 10^{-7}$ | $1.32 \times 10^{-6}$ | $2.54 \times 10^{-6}$ | 78.2 |
| Ar | $5.22 \times 10^{-4}$ | $9.93 \times 10^{-5}$ | $4.99 \times 10^{-5}$ | $2.31 \times 10^{-4}$ | 45.2 |
| As | $6.67 \times 10^{-5}$ | $4.26 \times 10^{-6}$ | $2.11 \times 10^{-5}$ | $3.95 \times 10^{-5}$ | 85.9 |
| Cs | $6.26 \times 10^{-6}$ | $3.31 \times 10^{-6}$ | $1.06 \times 10^{-6}$ | $8.57 \times 10^{-6}$ | 100.0 |
| Cl | $1.89 \times 10^{-2}$ | $3.37 \times 10^{-3}$ | $2.07 \times 10^{-3}$ | $2.63 \times 10^{-3}$ | 21.2 |
| Cr | $3.05 \times 10^{-4}$ | $3.18 \times 10^{-5}$ | $1.39 \times 10^{-4}$ | $5.58 \times 10^{-4}$ | 207.0 |
| Eu | $3.07 \times 10^{-6}$ | $4.50 \times 10^{-7}$ | $3.55 \times 10^{-7}$ | $1.93 \times 10^{-6}$ | 64.8 |
| Fe | $2.48 \times 10^{-1}$ | $2.44 \times 10^{-2}$ | $5.17 \times 10^{-2}$ | $1.67 \times 10^{-1}$ | 80.5 |
| Mn | $3.59 \times 10^{-4}$ | $3.16 \times 10^{-4}$ | $2.69 \times 10^{-4}$ | $4.40 \times 10^{-4}$ | 95.5 |
| K | $1.08 \times 10^{-2}$ | $1.64 \times 10^{-2}$ | $3.37 \times 10^{-3}$ | $1.70 \times 10^{-2}$ | 74.8 |
| Rb | $6.71 \times 10^{-5}$ | $9.21 \times 10^{-5}$ | $2.41 \times 10^{-5}$ | $1.31 \times 10^{-4}$ | 97.2 |
| Sc | $3.76 \times 10^{-5}$ | $7.17 \times 10^{-6}$ | $6.03 \times 10^{-6}$ | $3.20 \times 10^{-5}$ | 85.1 |
| Na | $1.41 \times 10^{-2}$ | $2.28 \times 10^{-3}$ | $9.57 \times 10^{-4}$ | $1.34 \times 10^{-2}$ | 88.1 |
| Sr | $3.68 \times 10^{-3}$ | $9.80 \times 10^{-4}$ | $7.30 \times 10^{-4}$ | $2.89 \times 10^{-3}$ | 77.6 |
| Th | $3.14 \times 10^{-5}$ | $4.37 \times 10^{-6}$ | $4.15 \times 10^{-6}$ | $2.82 \times 10^{-5}$ | 90.4 |
| U | $1.17 \times 10^{-5}$ | $1.68 \times 10^{-5}$ | $8.26 \times 10^{-6}$ | $1.85 \times 10^{-5}$ | 93.9 |

Ca recovery (based on analysis by atomic absorption) = 69.5%

S recovery (based on wet chemical analysis, includes sulfur in flue gas) = 94%

was not included. Table V-7 gives the results. Recoveries are quite high, particularly when two factors are taken into account. First, it is estimated that 10-15% of the solids (bed and overhead) were lost either because they remained in the combustor or were spilled prior to weighing. This would, of course, reduce the recoveries. Secondly, as can be noted in Table V-7, the concentrations reported are accurate only to about ± 20 percent.

The important conclusion to be drawn from Table V-7 is that the fraction of trace elements retained by solid constituents was generally high. There are several exceptions, particularly chlorine; however, chlorine might be expected to volatilize at lower temperatures than the other elements. The recovery of chromium, 207 percent, was probably caused by addition of this element from chromium alloys used in the materials of construction of the combustor (e.g., cooling coils).

In addition to the recovery, or the fraction of elements retained in solid phases (stone + flyash), it is also of interest to know the fraction of each element fed with the coal that was retained by the dolomite only (not flyash). This term was called the "retention." Retention could not be determined precisely because assumptions had to be made. One assumption was that the dolomite which was found in the overhead had the same concentration of a particular element as did the bed. Also, it was estimated that 1.82 kg out of 4.20 kg total overhead collected was entrained stone.

Table V-8 gives the retentions as the percentage of element fed with the coal that was retained by the dolomite. The retentions are quite variable with the highest (not counting chromium) being 47 percent for arsenic. Retentions for the alkali metals were negative. This means that there was a net loss of these elements from the dolomite during the run. In general, retention by the bed was low, indicating that most of the trace elements were lost from the bed as flyash particulates (or possibly as a vapor in the case of some elements.)

This study did not indicate the point where the trace elements present in coal and limestone will be removed from the combustion system, since that determination must be made by sampling at more representative cyclone temperatures. However, it does indicate that the trace elements at some point, will be largely in the form of particulates, and particulate removal from the flue gas must be sufficient to prevent environmental problems. The fate of the more volatile elements such as mercury or alkali metals must be studied separately since different sampling and analytical techniques are required.

Argonne National Laboratory reported mass balances and recoveries for trace elements calculated from neutron activation analysis (5). Table V-9 compares these results with those reported above. The agreement is quite good.

## TABLE V-8. RETENTION BY STONE OF ELEMENTS PRESENT IN COAL

| Element | Retention, %* |
|---|---|
| Al | 7.9 |
| Sb | 40.3 |
| Ar | -2.9 |
| As | 47.1 |
| Br | -17.2 |
| Cs | -24.3 |
| Cl | 0.7 |
| Cr | 66.6(1) |
| Eu | 4.9 |
| Fe | 25.3 |
| Mn | 38.4 |
| K | -99.1 |
| Rb | -76.5 |
| Sc | 8.1 |
| Na | -4.1 |
| Sr | 7.1 |
| Th | 8.5 |
| U | -24.8 |

---

$$* \text{ Retention} = \frac{\text{Weight of element present in coal picked up by stone (bed + entrained stone)}}{\text{Wt. of element fed with coal}} \times 100$$

(based on assumption that entrained stone has same concentration of elements as bed).

(1) May be high due to high material balance. See Table V-7

TABLE V-9. COMPARISON OF EXXON AND ARGONNE N.L.
DATA ON TRACE ELEMENT RECOVERIES (a)

| Element | Recovery, % | |
|---|---|---|
| | Exxon | ANL |
| As | 86 | 85 |
| Br | 21 (Cl) | 18 |
| Fe | 80 | 100 |
| K | 75 | 90 |
| Mn | 96 | 130 |
| Na | 88 | 96 |
| Sc | 85 | 97 |

---

(a) Recovery = percentage of element entering combustor that can be accounted for in solids leaving combustor.

## CO Emissions

CO emission levels were measured during the batch unit coal combustion runs. Although the data are not conclusive, it appears that the CO level is a function of the steadiness of the coal feed rate, the average bed temperature, and the excess air level. The average CO level for all the runs was 946 ppm. However, in some cases, it was obvious that the feed rate was not steady or the CO levels were inordinately high for other reasons. The data were then treated statistically, and data were rejected which were greater than the mean by more than twice the error limit. This treatment gave an average CO level of 409 ± 276 ppm (1s limit) for all runs. For the most recent runs made, this treatment indicated the average CO concentration was approximately 220 ppm. As further tests are performed, correlations will be developed to relate the CO level to the bed temperature and excess air level under more closely controlled conditions of coal feeding.

## Particulate Emissions

Particulate Loadings - The average bed outlet particulate loading obtained by summing the particulates captured in the cyclones and filter was 8.5 gr/scf. The average outlet loading from cyclone #1 was 2.0 gr/scf and from cyclone #2 was 0.9 gr/scf. However, in some cases, it was obvious that the cyclones were not operating properly or loadings were inordinately high for other reasons. The data were than treated statistically, and data were rejected which were greater than the mean by more than twice the error limit. This treatment gave the following results:

Bed outlet loading - 6.9 ± 1.4 gr/scf (1s limit)
Cyclone #1 outlet loading - 0.70 ± 0.35 gr/scf (1s limit)
Cyclone #2 outlet loading - 0.33 ± 0.26 gr/scf (1s limit)

Cyclone Efficiency - Overall collection efficiencies for the two stage cyclone system have generally been over 90%. Low efficiencies for a given run could usually be traced to a plugged cyclone dipleg. The average collection efficiency based on the average grain loadings calculated in the previous section was 90% for cyclone #1 and 53% for cyclone #2, giving an overall combined efficiency of 95%.

## Particle Size Distribution

A sieve analysis was used to determine the particle size distribution of samples collected from the overhead from run no. 3675-46C. This run was made with Grove limestone. The samples studied were collected in the first stage cyclone and on the off-gas filter. Chemical analysis indicated that the amount of carbon present was 51.4% for the material collected by the first stage cyclone and 30.8% for the filter solids. Figure V-18 shows the results of the sieve analysis for the first stage

Figure V-18

PARTICLE SIZE DISTRIBUTION
OVERHEAD SAMPLES

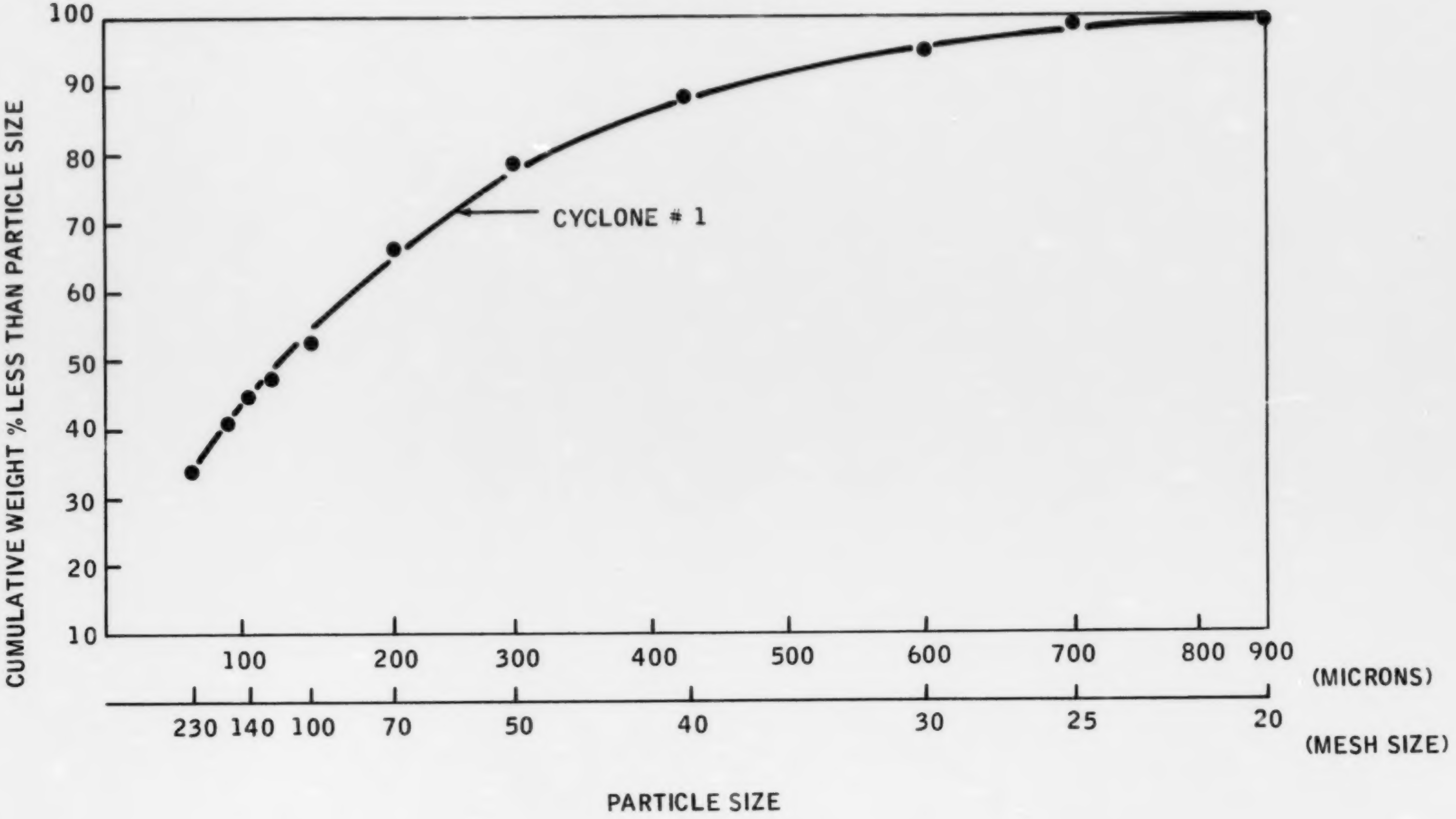

cyclone sample. The particle size for the 50% point was about 130 microns. The size distribution measured for the filter sample was distorted by prilling of the fine particulates during sieving.

A particle size distribution for particulates collected in the overhead during run no. 3675-23C using optical microscopy was also determined. Microphotographs of the solids collected showed that two classes of solids were distinguishable, a white "popcorn" solid and a black solid. The black solids were more prevalent in the filter sample and are probably carbon and ash, while the white material is stone, possibly sulfated. The measurements indicated that the particulates ranged from 1 to 30 microns in the cyclone samples and 1 to 20 microns in the filter sample.

A problem in determining the size distribution using this technique is that the particles are skeletal in nature and not easily defined. Agglomerates may be present and the range of sizes present is very large. The particles also appear to be fragile and break into very small pieces upon handling. These factors may have caused a smaller average particulate size for the first stage cyclone sample compared to that measured by sieving.

### Combustion Efficiency

Carbon combustion efficiencies measured in the batch unit varied from 87 to 98%. Combustion efficiency is a function of excess stoichiometric air and temperature as shown in Figure V-19. The batch unit was operated at superficial velocities of 1.1 to 1.5 m/s, at temperatures of 750 to 970°C, and at pressures of about 800 kPa.

Another condition which affected combustion efficiency was the steadiness of coal feeding. When coal feeding was unsteady, combustion efficiencies were consistently lower. For the runs shown in Figure V-19, coal feeding was fairly steady, but variations in coal feeding were probably responsible for some of the data scatter apparent in Figure V-19.

Low bed temperatures were also found to cause low combustion efficiencies. At temperatures lower than 840°C, combustion efficiency decreased significantly as seen in Figure V-19. At the lower temperatures a sharp increase in CO emissions occurred. At temperatures below 600-650°C, it was difficult to maintain coal combustion.

Changing the coil design from horizontal to vertical orientation did not appear to have any significant effect on combustion efficiency.

The results shown in Figure V-19 are consistent with those reported previously from miniplant runs. A more detailed comparison of results from the two units is made in Section VI.

Figure V-19

COMBUSTION EFFICIENCY

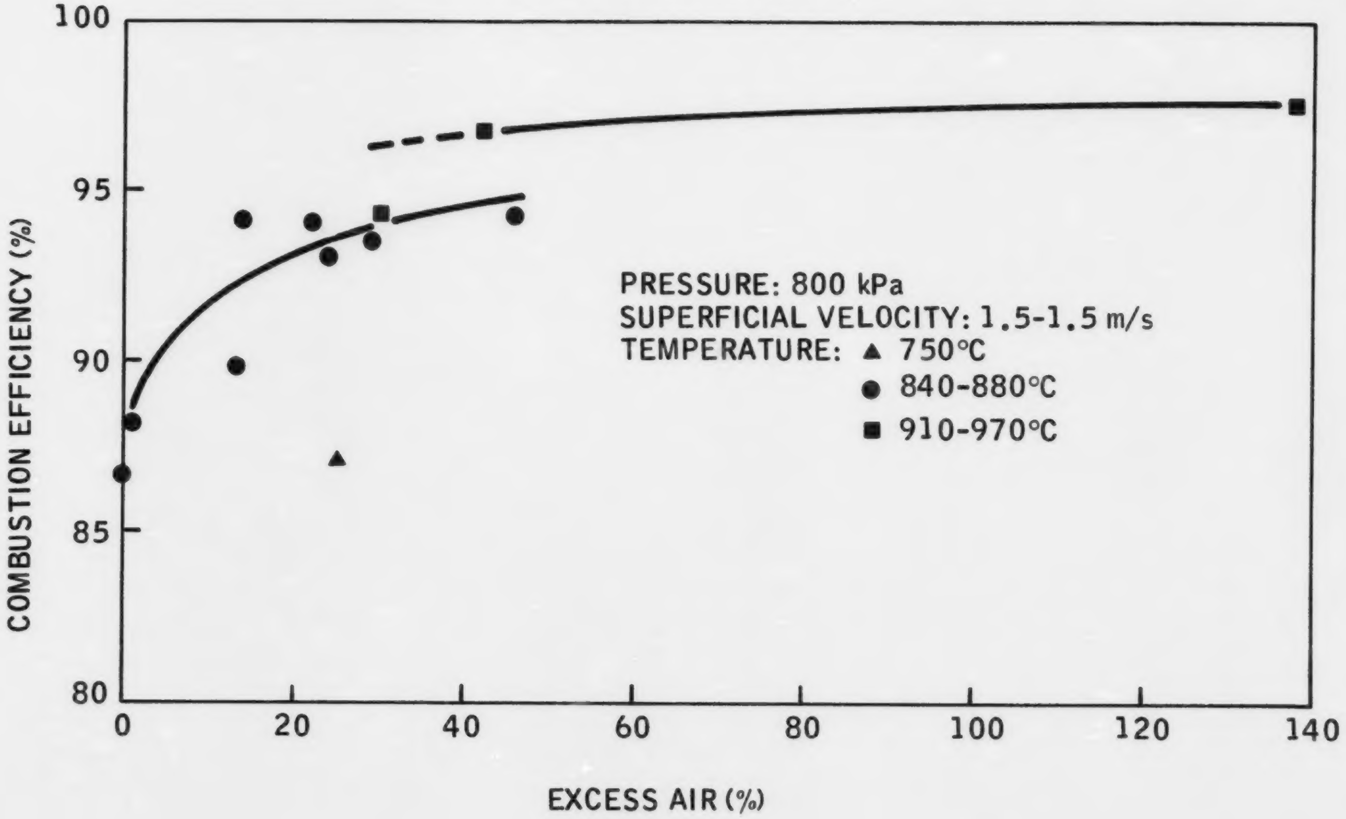

As in the case of the miniplant, the loss of combustion efficiency was due largely to unburned carbon particles entrained from the combustor. CO loss accounted for only 2% of the carbon losses.

## Heat Transfer Coefficients

Overall heat transfer coefficients were measured during coal combustion for vertical coils no. 1 and no. 2 (27-62 cm and 67-102 cm above the fluidizing grid, respectively). Tubing O.D. for these tests was 0.64 cm. Results of measurements made during three runs are given in Table V-10. During the time data were taken, a sufficient flow of water was pumped into each coil to prevent any phase change. Temperature rise of the water and flowrate were carefully measured to determine the heat absorbed by each coil. Measurements were repeated several times to achieve good accuracy and to determine variability. Overall coefficients averaged 395 $W/m^2{}^\circ C$ for coil 1 (lower coil) and 452 $W/m^2{}^\circ C$ for coil 2 (upper coil). The reason for the higher coefficient for coil 2 is not certain but may be due to slightly more vigorous mixing of solids higher in the combustor.

Heat transfer coefficients were also measured while the bed was heated using the pre-heat (propane) burner. Table V-11 gives these coefficients for four vertical and two horizontal serpentine coils. Three of the vertical coils were always immersed in the bed whereas both horizontal coils were always in the freeboard. Operating conditions for the combustor are also given. Bed-to-tube coefficients during preheating were somewhat lower than those given in Table V-10 for coal combustion because bed temperatures, and hence the radiation component of heat transfer, were lower. Coefficients for coils in the freeboard averaged 106 $W/m^2{}^\circ C$. This is large enough for the coils located in the freeboard to remove enough heat to cause a sharp drop in the flue gas temperatures.

The overall coefficients for the original horizontal serpentine coils (located in the bed) were estimated to be 230-310 $W/m^2{}^\circ C$ under coal combustion conditions at temperatures of 850 to 900°C. This was lower than the coefficients for vertical coils and is probably due to the much slower motion of bed solids with horizontal coils.

It should be appreciated that the overall coefficients reported in this section are nearly the same as the film coefficients outside of the tubes, a consequence of the fact that the inside film coefficients are very high. The outside coefficients are probably not more than 10 per cent higher, at most, than the overall coefficients.

## Coal and Sorbent Effects

Three types of coal have been burned in the batch combustor. Most work has been with West Virginia Coal (Arkwright), which is highly caking; the other coals tested were slightly caking Wyoming coal and moderately caking Illinois No. 6 coal. The foremost reason for using these coals was to determine if the temperature profile in the bed was affected by

## TABLE V-10. HEAT TRANSFER COEFFICIENTS (BED TO TUBE) MEASURED DURING COAL COMBUSTION

### Vertical Coils
### 0.64 cm O.D.

| | Overall Coefficients | | | |
|---|---|---|---|---|
| Run No. | Coil 1 ($W/m^2°C$) | Coil 2 ($W/m^2°C$) | Average Bed Temperature (°C) | Superficial Bed Velocity (m/s) |
| 3675-28C | 395 ± 23 | -- | 840 | 1.1 |
| -31C | 392 ± 12 | 432 ± 5 | 895 | 1.6 |
| -32C | 399 ± 3 | 472 ± 11 | 885 | 1.6 |

Coil Positions in Combustor

| | |
|---|---|
| Coil 1 | 27-62 cm above fluidizing grid |
| Coil 2 | 67-102 cm above fluidizing grid |

TABLE V-11. HEAT TRANSFER COEFFICIENTS MEASURED DURING BED PRE-HEATING

| Coil No. | Coil Orientation | Overall Coefficients ($W/m^2°C$) Run No. 1 | Run No. 2 | Run No. 3 | Run No. 4 |
|---|---|---|---|---|---|
| 1 | Vertical | 340 | 300 | 330 | 350 |
| 2 | Vertical | 320 | 330 | 280 | 350 |
| 3 | Vertical | 300 | 280 | 280 | 300 |
| 4 | Vertical | 300 | 200 | 280 | --- |
| 5 | Horizontal Serpentine | 120 | 100 | 100 | 110 |
| 6 | Horizontal Serpentine | --- | 100 | 110 | 100 |

Operating Conditions

| Run No. | Inside Coil | Superficial Velocity m/sec. | Average Bed Temperature °C | Expanded Bed Height, m | Pressure kPa | Coils Immersed In Bed |
|---|---|---|---|---|---|---|
| 1 | Water-steam | 1.16 | 600 | 1.65 | 810 | 1,2,3,4 |
| 2 | Water-steam | 1.06 | 530 | 1.30 | 490 | 1,2,3 |
| 3 | Water-steam | 1.62 | 550 | 1.75 | 500 | 1,2,3,4 |
| 4 | Water only | 1.15 | 455 | 1.27 | 500 | 1,2,3 |

Coil O.D. = 0.64 cm

coal type, in particular by the tendency of the coal to cake when heated. The coal comparison study was made early in our work when the combustor was fitted with tightly packed horizontal serpentine coils. There was a severe longitudinal temperature gradient across the bed at the time.

There was a slight improvement in temperature profile, i.e., a reduction in the gradient, when Wyoming coal was substituted for West Virginia coal. Figure V-20 shows the profile for the run made with Wyoming coal and an average profile for two runs made with W. Virginia coal. A 0.6 m (settled) bed of half-calcined Tymochtee dolomite was used for all three runs. The energy input was slightly higher in the run with Wyoming coal, which could indicate that the improvement shown in Figure V-20 might have been even better with equivalent feed rates. It should be noted, however, that even though the use of low caking coal improved the temperature profile somewhat, there was still a temperature drop of about 280°C over the expanded bed. The effect of coal type on temperature profile was very small when compared to the effect of changing the cooling coils from a horizontal serpentine to a vertical configuration.

The run made with Illinois coal resulted in a highly non-typical temperature profile because much of the coal burned above the bed. A number of factors could have caused this but a characteristic of the coal is not believed to have been one of them.

The effect on temperature profile of varying particle size of the coal was also investigated. Since larger particles burn slower, a run was made in which fines smaller than 70 mesh (about 40% of the coal) were removed from Arkwright coal. The result was a slightly flatter profile with the screened coal. This run was also made with horizontal coils. Again, the effect was small when compared to the effect of cooling coil configuration.

In addition to different coals, several sorbents were also tested, including Grove limestone (BCR No. 1359), Tymochtee dolomite, and Pfizer dolomite (BCR No. 1337). Stones varied with respect to sulfur removal abilities (discussed on page 135) and resistance to attrition. The resistance to attrition was indicated indirectly by the amount of sorbent entrained from the bed during a combustion run. Entrainment rates are inversely proportional to particle size, and since the sorbents were all screened initially to the same size distribution, the entrainment rates are a relative measure of the degree of attrition. For the stones tested, the average entrainment rates were:

| | |
|---|---|
| Grove limestone (BCR 1359) | 15 wt. percent/hour |
| Tymochtee dolomite | 20-25 wt. percent/hour |
| Pfizer dolomite (BCR 1337) | 50 wt. percent/hour |

Rates are given as the weight percentage lost per hour of material remaining in the fluidized bed. For example, if $\alpha$ = fractional loss per hour ($\alpha$ = 0.15 for Grove limestone), then $W = Woe^{-\alpha t}$, where W =

Figure V-20

COMPARISON OF TEMPERATURE PROFILES—WYOMING AND VIRGINIA COAL

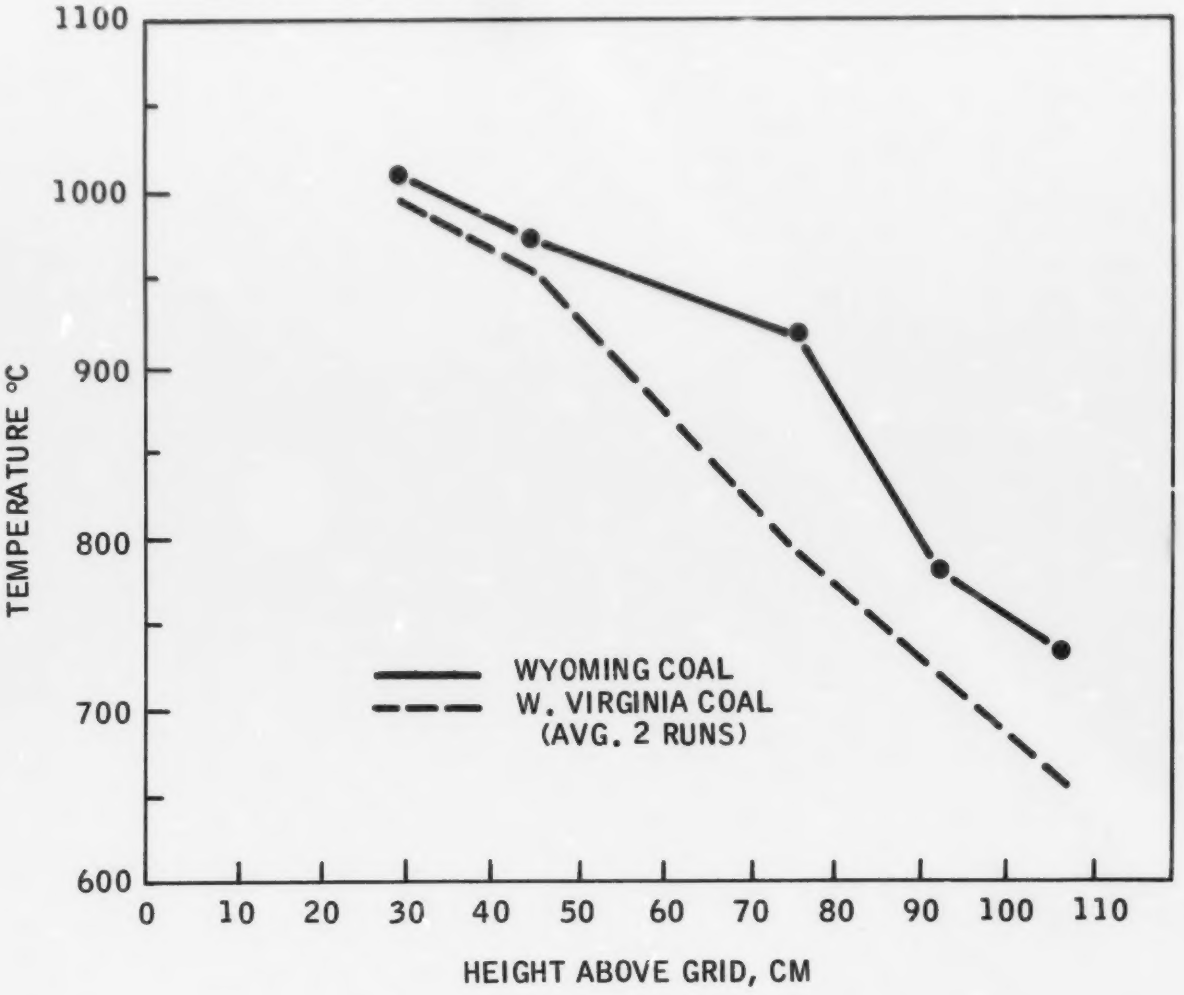

weight of bed remaining in batch reactor after time t (hours), and Wo = initial bed weight. These rates are fairly high, especially for the dolomites. However, lower rates are expected for continuous operation. This will be studied in future runs in the miniplant.

Samples of sulfated bed material were also screened after runs and the particle size distribution compared to that for the starting materials. Table V-12 shows results for runs made with Grove limestone and Tymochtee dolomite.

TABLE V-12. PARTICLE SIZE DISTRIBUTION OF SULFATED SORBENTS

| | PER CENT LESS THAN SCREEN SIZE | | | | | | | | |
|---|---|---|---|---|---|---|---|---|---|
| US Screen Size | 6 | 8 | 12 | 16 | 20 | 25 | 30 | 40 | 50 |
| Grove Limestone | | | | | | | | | |
| New | -- | 98 | 48 | 24 | 10 | -- | -- | -- | -- |
| Sulfated[1] | -- | 100 | 92 | 67 | 35 | 17 | 7 | 4 | -- |
| Tymochtee Dolomite | | | | | | | | | |
| New | -- | 100 | 60 | 31 | 10 | -- | -- | -- | -- |
| Sulfated[2] | 97 | 93 | 84 | 67 | 50 | 39 | 24 | 9 | 3 |

---

[1] Run 675-11C

[2] Run 675-8C

The particle size whose terminal velocity corresponded to the fluidization velocity of the runs was 25 to 30 mesh. Therefore, a good part of the particulates below that mesh size were entrained from the bed. However, the data in Table V-12 still show that significant attrition did occur and the dolomite was more suceptible to attrition than the limestone.

It was observed that even stone from the same quarry can display variable attrition resistance. Tymochtee dolomite had always been a satisfactory stone with regard to attrition resistance but a recently arrived shipment showed very high entrainment rates. It was assumed that a change in properties of the stone since the prior shipment was responsible; perhaps the stone was being mined from a different portion of the quarry.

## Component Balances

Sulfur and calcium balances were made for a number of batch unit runs. The results are presented in Tables V-13 and V-14. The weight of sulfur into the combustor was determined from the coal feed rate, the run length, and the sulfur content of the coal. The calcium input was determined from an initial bed analysis. For the solids output streams (material collected in the cyclone diplegs, off-gas filter, and the final bed), the quantity accumulated was weighed and then analyzed for

## TABLE V-13. SULFUR BALANCES FOR BATCH COMBUSTOR

(All weights in kg)

| | | Sulfur Out | | | | |
|---|---|---|---|---|---|---|
| Run No. | Sulfur In Coal | Flue Gas (1) | Overhead Solids | Final Bed | Total | % Sulfur Balance |
| 145C | 0.631 | 0.177 | 0.091 | 0.254 | 0.522 | 83 |
| 2C | 0.468 | 0.050 | 0.154 | 0.232 | 0.436 | 93 |
| 3C | 0.527 | 0.159 | 0.095 | 0.100 | 0.354 | 67 |
| 4C | 0.159 | 0.014 | 0.132 | 0.023 | 0.169 | 106 |
| 5C | 0.331 | 0.204 | 0.036 | 0.027 | 0.267 | 81 |
| 17C | 0.536 | 0.007 | 0.058 | 0.375 | 0.440 | 82 |
| 18C | 0.633 | 0.144 | 0.086 | 0.530 | 0.760 | 120 |
| 23C | 0.513 | 0.014 | 0.081 | 0.269 | 0.364 | 71 |
| 25C | 1.027 | 0.003 | 0.128 | 0.311 | 0.442 | 43 |
| 28C | 0.880 | 0.051 | 0.183 | 0.523 | 0.757 | 86 |
| 29C | 0.884 | 0.132 | 0.123 | 0.829 | 1.084 | 123 |
| 31C | 0.717 | 0.019 | 0.271 | 0.384 | 0.674 | 94 |
| 32C | 1.003 | 0.031 | 0.226 | 1.328 | 1.585 | 158 |
| 46C | 0.386 | 0.120 | 0.178 | 0.235 | 0.533 | 138 |
| 56C | 0.719 | 0.101 | 0.057 | 0.437 | 0.595 | 83 |
| | | | | | | Avg. 91<br>± 25%<br>(excluding run 32C) |

---

(1) Based on average $SO_2$ concentration

### TABLE V-14. CALCIUM BALANCES FOR BATCH COMBUSTOR

| Run No. | Charge (stone, kg) | Input (kgCa) | Wt. Bed Recovered, kg | Wt. fr. Ca in Bed | Wt. Ca in Bed kg | Wt. Overhead Solids Recovered, kg | Wt. fr. Ca in Overhead | Wt. Ca in Overhead kg | Total Output (kgCa) | % Calcium Balance |
|---|---|---|---|---|---|---|---|---|---|---|
| 145 | TD, 7.54 | 1.58 | 2.63 | 0.220 | 0.58 | 5.04 | 0.170 | 0.86 | 1.44 | 91 |
| 2C | TD, 7.54 | 1.58 | 2.63 | 0.256 | 0.67 | 4.20 | 0.101 | 0.42 | 1.09 | 69 |
| 3C | G, 7.72 | 3.02 | 4.72 | 0.433 | 2.05 | 4.23 | 0.090 | 0.38 | 2.43 | 80 |
| 4C | TD, 7.54 | 1.58 | 0.82 | 0.285 | 0.23 | 4.72 | 0.218 | 1.03 | 1.26 | 80 |
| 5C | TD, 7.54 | 1.58 | 4.65 | 0.265 | 1.23 | 1.81 | 0.081 | 0.15 | 1.38 | 87 |
| | | | | | | | | | | Avg. 81<br>± 8% |

---

TD - Tymochtee dolomite, 20.9 wt. % Ca

G - Grove limestone, 39.1 wt. % Ca

sulfur, sulfate, and calcium. The quantity of sulfur in the flue gas was determined from data obtained by continuously monitoring the off-gas for $SO_2$ using a Beckman infrared analyzer.

After neglecting data outside the ±2s limits, the sulfur balances averaged 91 ± 25% (1s limit) and the calcium balances averaged 81 ± 8% (1s limit). Possible causes of the low balances are uncertainties in the analysis of the solids and loss of solids during removal of the bed and flyash. In the case of the sulfur balances, loss of $SO_2$ through $SO_3$ formation is not likely to have a major effect on the sulfur balances because the fraction of total sulfur entering the system that exits in the flue gas is normally small.

## SECTION VI

## DISCUSSION OF RESULTS

### $SO_2$ EMISSIONS

$SO_2$ emission data measured in the batch unit using limestone sorbent were compared to data reported by the National Coal Board (NCB) (6) and Argonne National Laboratory (ANL) (7). The data previously shown in Figure V-15 were replotted in Figure VI-1 as percent reduction in $SO_2$ along with the NCB and ANL results. NCB measured emissions at a lower velocity, 0.6 m/s, compared to 1.1 to 1.5 m/s used in the batch combustor program. The pressure was also lower in the NCB study, 600 kPa vs. 800 kPa and the limestone particle size was smaller, 350 µm median diameter vs. 1400 µm. These factors should have made desulfurization more effective in the NCB study, but as seen in Figure VI-1, the emissions reported by NCB were equivalent to those measured from the batch combustor. The two studies were made with different coals and limestones and this factor may be partly responsible for the anomaly.

Results reported by ANL were measured at a velocity of 1.1 m/s, and at a pressure of 800 kPa using limestone with a median particle size of about 700 µm. The coal and limestone were from the same sources as those used in the batch unit studies. Again, the results of the ANL study and the batch unit results compare very well. However, in this case, the data were obtained under more comparable conditions and good agreement would be expected.

The emissions measured from the miniplant after the sample system was operating properly as mentioned previously corresponded very well with data from the batch unit. This is also shown in Figure VI-1.

From the results shown in Figure VI-1, a calcium to sulfur molar ratio of 2.0 appears to be sufficient with limestone to meet the EPA emission standard of 1.2 lbs $SO_2$/M BTU for the 2.6% sulfur coal used in this study. A comparison was also made between $SO_2$ emission data reported by ANL (4) and data obtained from the batch combustor using Tymochtee dolomite sorbent. The comparison is shown in Figure VI-2. In this case the same coal and sorbent were used in both studies and the operating conditions were comparable except for sorbent particle size. Both studies were carried out at pressures of 800 kPa and at superficial velocities of 1.1 to 1.6 m/s. However, the ANL study used a dolomite with a median particle diameter of 750 µm compared to 1400 µm used in the batch unit. The curve in Figure VI-2 represents the best line through the batch combustor results. As seen, the data from the two combustors compare very well. The NCB study reported much lower emissions using dolomite sorbent, but this is not surprising considering the difference in operating conditions. From the results shown in Figure VI-2, a calcium to sulfur molar ratio of 1.5 appears to be

Figure VI-1

COMPARISON OF $SO_2$ REMOVAL RESULTS - LIMESTONE SORBENT

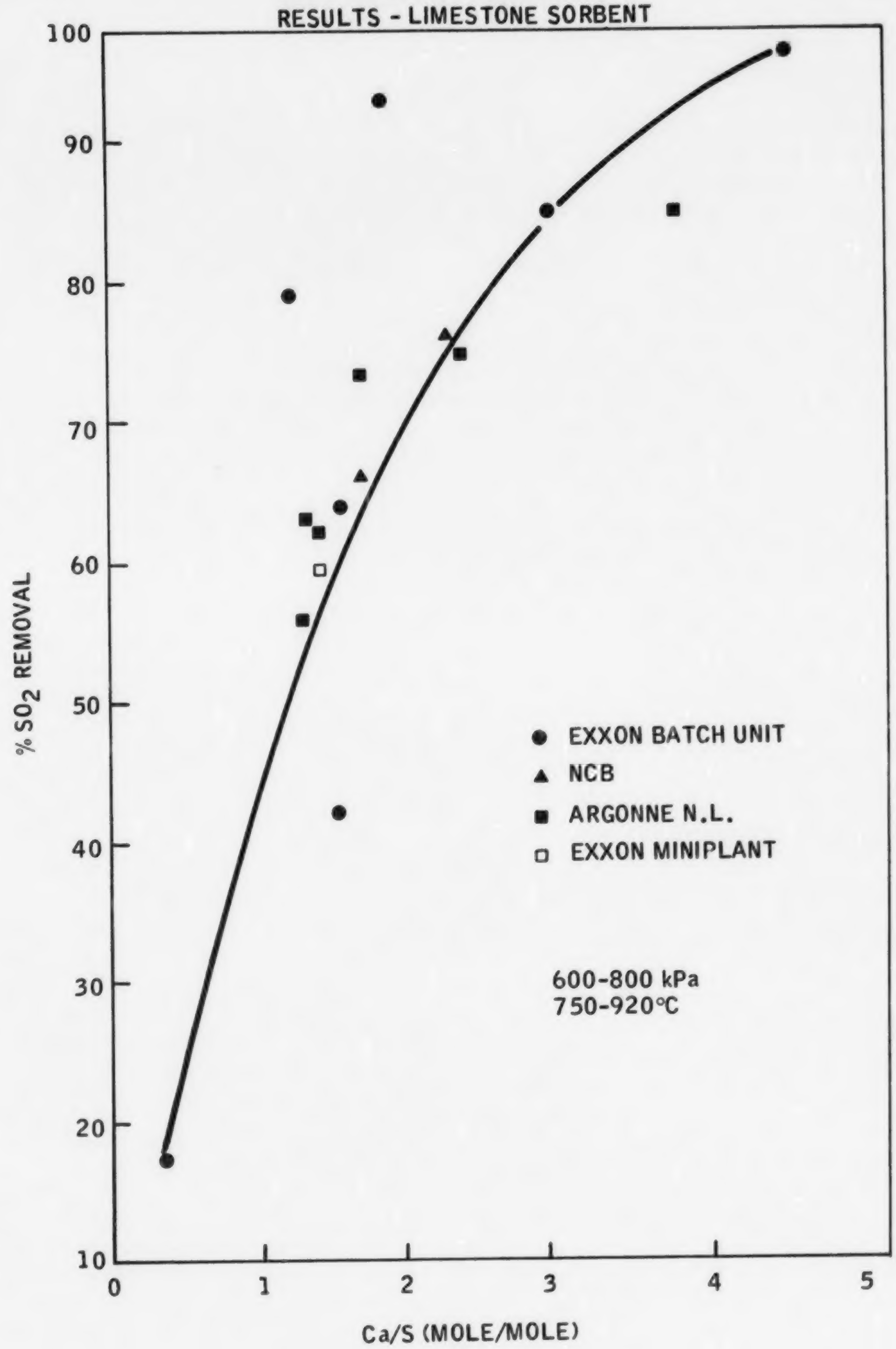

Figure VI-2

COMPARISON OF $SO_2$ EMISSIONS
FROM BATCH UNIT AND ARGONNE N.L. STUDY
DOLOMITE SORBENT

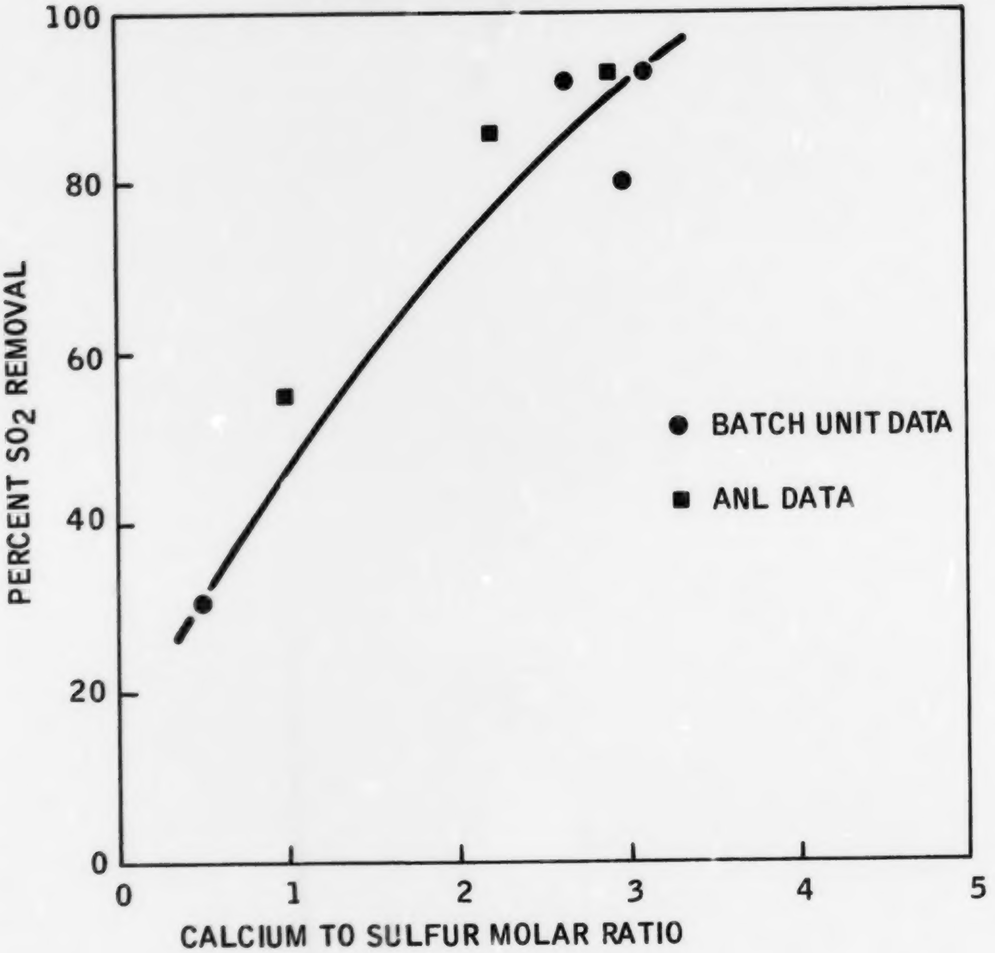

sufficient with dolomite to meet the EPA $SO_2$ emission standard for the 2.6% sulfur coal used in this study. This corresponds to an $SO_2$ concentration in the flue gas of 550 to 600 ppm and a percent $SO_2$ retention of 68%.

Emissions resulting from the use of limestone and dolomite in the batch unit were compared and the results are shown in Figure VI-3. As expected, emissions resulting from the use of dolomite were lower than those obtained with limestone. However, the emissions differ by only about 300 ppm at a Ca/S ratio of 2. NCB and ANL reported a much larger difference, on the order of 500 to 600 ppm. The reason for this difference requires further investigation.

## $NO_x$ EMISSIONS

$NO_x$ emissions measured in the miniplant and batch combustors are compared in Figure VI-4. These data were shown previously in Figures IV-32 and V-17. As seen, the comparison is very good and the data from both units can be correlated by a single curve. In addition, the range of $NO_x$ data reported by NCB (8) is also shown and also agrees well with miniplant and batch unit results. The $NO_x$ levels measured in this study are well below the current EPA emission standard of 0.7 lb $NO_2$/M BTU even at excess air levels as high as 140%. The range of excess air levels anticipated for commercial FBC units is 15 to 20%. In this range, it is expected the $NO_x$ emission levels will be on the order of 0.2 to 0.3 lb $NO_2$/M BTU. These levels are significantly lower than those reported previously for atmospheric pressure fluidized bed combustion (9). In this case, $NO_x$ emissions on the order of 0.4 to 0.5 lb $NO_2$/M BTU were reported.

## COMBUSTION EFFICIENCY

A comparison of combustion efficiencies measured in the batch unit and the miniplant is given in Figure VI-5. The data agree well although the miniplant results do not show a temperature effect as do those from the batch unit. However, as shown in Figure IV-33 the miniplant results at excess air levels less than 40% exhibit a fair degree of data scatter. The data obtained in this range also were obtained at a lower temperature, so a true measure of the effect of temperature has not as yet been established in the miniplant. Also, these early miniplant results were affected by operating problems with the cyclones. Further operation of the miniplant under more closely controlled conditions is necessary before a true measure of combustion efficiency can be established in this unit.

Some difficulties also occurred in the miniplant carbon recycle system. This system recycles fines collected in the first stage cyclone back to the combustor to improve combustion efficiency. Since this recycle system was not always operating properly during early runs, the results shown in Figure VI-5 are probably more indicative of a once through system than a carbon recycle system.

Figure VI-3

COMPARISON OF $SO_2$ EMISSIONS FROM LIMESTONE AND DOLOMITE SORBENTS. BATCH UNIT DATA

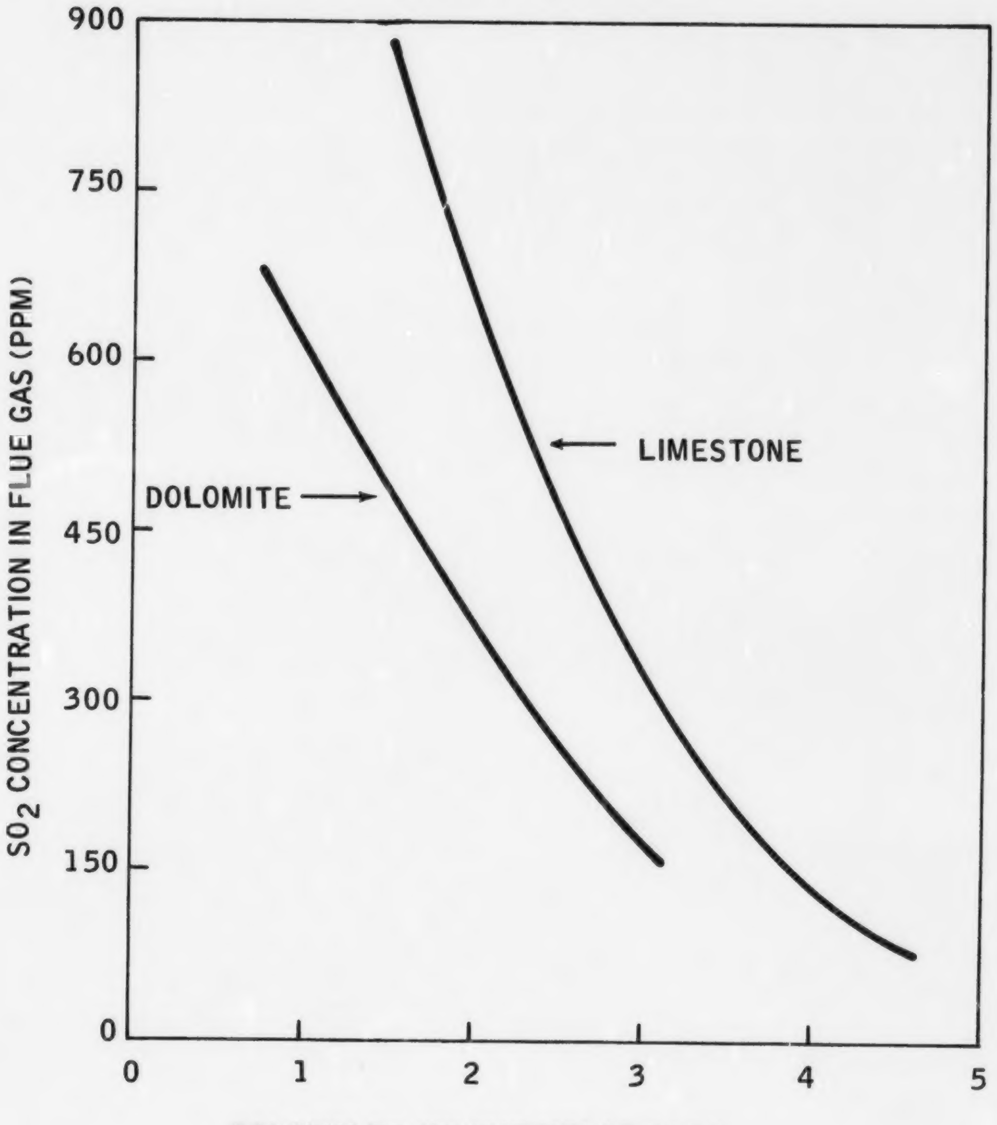

Figure VI-4

COMPARISON OF $NO_x$ EMISSIONS

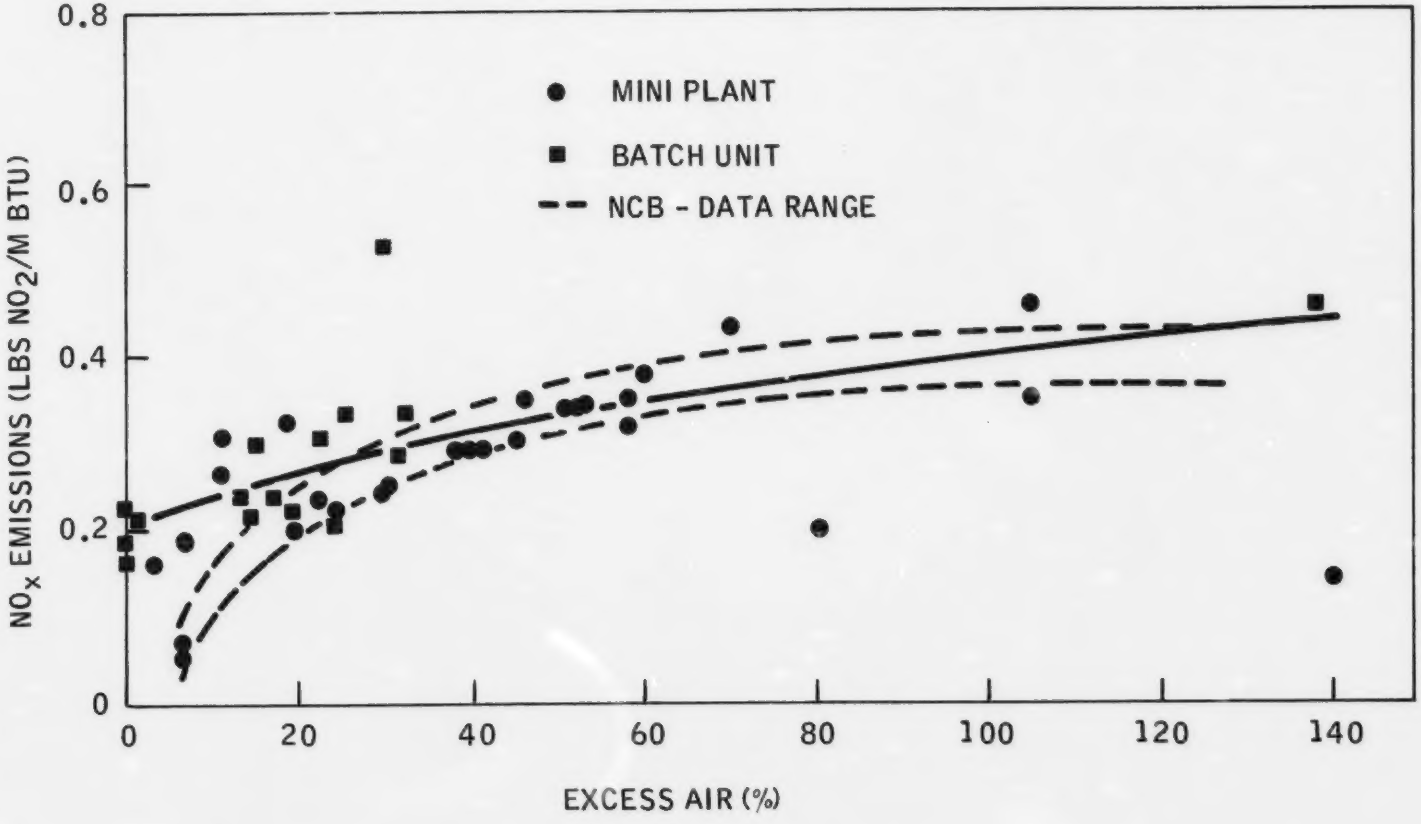

## Figure VI-5

## COMPARISON OF COMBUSTION EFFICIENCIES

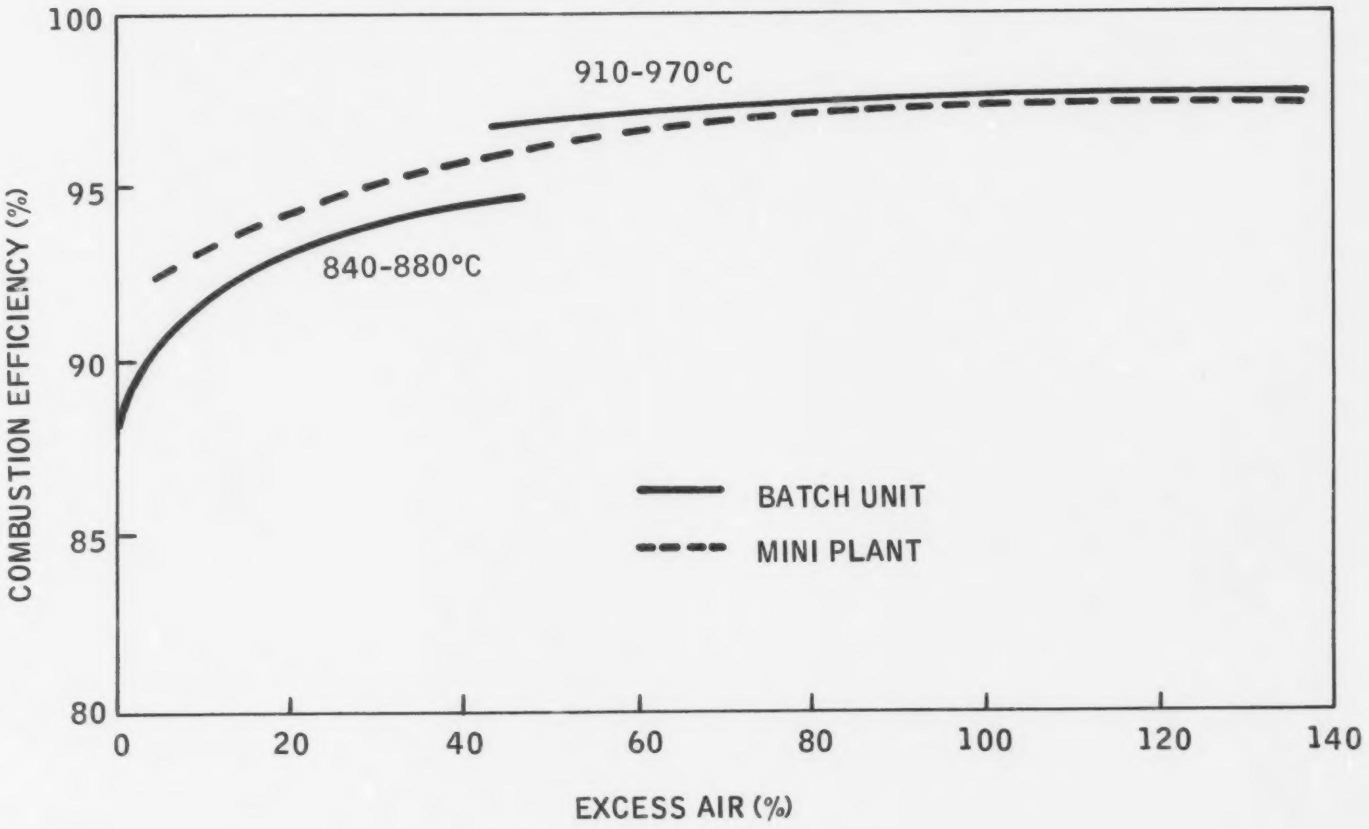

Results reported by ANL (4) show combustion efficiencies generally in the same range as those given in Figure VI-5. However, the NCB (8) reports much higher combustion efficiencies, usually in the range of 98.5 to 99.5%. These higher combustion efficiencies may be caused by longer residence time in the NCB combustor.

A target combustion efficiency of 98.5 to 99% has been suggested by Westinghouse Research Laboratory (10). The results obtained in the Exxon units to date have not reached that level. A more effective carbon recycle system, operation at higher temperatures, or use of a carbon burn up cell, may be necessary to reach this target.

## HEAT TRANSFER COEFFICIENTS

Heat transfer coefficients measured in the batch combustor were about 30% higher than those measured in the miniplant. This is shown in Table VI-1.

TABLE VI-1. COMPARISON OF HEAT TRANSFER COEFFICIENTS

| Unit | Coil Diam. (cm) | Coil Position(1) | Bed Temp. (°C) | Superficial Vel. (m/s) | Heat Transfer Coefficient ($W/m^2K$) |
|---|---|---|---|---|---|
| Batch | 0.64 | 1A | 840-895 | 1.1-1.6 | 395 |
| | | 1B | 840-895 | 1.1-1.6 | 452 |
| Miniplant | 1.91 | 1A | 870-950 | 1.8-2.1 | 318 |
| | | 1B | 870-950 | 1.8-2.1 | 340 |
| | | 2A | 870-950 | 1.8-2.1 | 330 |

(1) Coil positions are in ascending order from the bottom

The reason for the higher coefficients measured in the batch unit is probably due to the smaller diameter of batch unit coils, partly offset by a lower superficial velocity (11).

NCB also reports heat transfer coefficiencts of about 400 $W/m^2K$ (8). However, the particle size used in the NCB study was much less and the superficial velocity was also much lower than used in the present work.

# SECTION VII

## REFERENCES

1. Skopp, A., Nutkis, M. S., Hammons, G. A., and Bertrand, R. R., "Studies of the Fluidized Lime-Bed Coal Combustion Desulfurization System." Report to U.S. Environmental Protection Agency, Exxon (Esso) Research and Engineering Company. December 31, 1971.

2. Hodges, J. L., "Predicting Temperature Profiles in Fluidized Bed with Internal Baffling," worked performed under NSF Grant HES75-05125, Exxon Research and Engineering Company, August 1975.

3. Hoke, R. C., Nutkis, M. S., Ruth, L. A., and Shaw, H., "A Regenerative Limestone Process for Fluidized-Bed Coal Combustion and Desulfurization." EPA Report No. EPA-650/2-74-001, Exxon Research and Engineering Company, January, 1974.

4. Jonke, A. A., et al., "Reduction of Atmospheric Pollution by the Application of Fluidized-Bed Combustion," EPA Report No. EPA-650/2-74-104, Argonne National Laboratory, September, 1974.

5. Vogel, G. J., et al., "A Development Program on Pressurized Fluidized-Bed Combustion." Annual Report to ERDA Office of Fossil Energy. Argonne National Laboratory. July, 1975.

6. Roberts, A. G., et al., "Fluidised Combustion of Coal and Oil Under Pressure," Institute of Fuel Symposium Series No. 1 (1975) Proceedings Vol. 1 p D4-1, D4-11.

7. Vogel, G. J., et al., "Application of Pressurized, Fluidized-Bed Combustion to Reduction of Atmospheric Pollution." Institute of Fuel Symposium Series No. 1 (1975) Proceedings Vol. 1 p D3-1, D3-11.

8. "Pressurized Fluidised Bed Combustion" R&D Report No. 85, Interim No. 1 Report to OCR by National Research and Development Corp. September, 1973.

9. Ehrlich, S., "A Coal Fired Fluidized-Bed Boiler" Institute of Fuel Symposium Series No. 1 (1975) Proceedings Vol. 1 p C4-1, C4-10.

10. Keairns, D. L., et al., "Fluidized Bed Combustion Process Evaluation" Phase II - Pressurized Fluidized Bed Coal Combustion Development. EPA Report No. EPA-650/2-75-027-C, Westinghouse Research Laboratories, September 1975.

11. Kunii, D., and Levenspiel, O., Fluidization Engineering, John Wiley and Sons, Inc., New York (1969).

# SECTION VIII

# LIST OF PUBLICATIONS

1. Hoke, R. C., Ruth, L. A., Shaw, H., "Combustion and Desulfurization of Coal in a Fluidized Bed of Limestone," Presented at the IEEE-ASME Joint Power Generation Conference, Miami Beach, FL, September 15-19, 1974.

2. Hoke, R. C., Ruth, L. A., Shaw, H., Combustion 46, No. 7, pp 6-12, January 1975.

3. Hoke, R. C., Workshop on Regeneration of Sulfated Limestone/Dolomite for Fluidized Bed Combustion, ERDA, Fossil Energy. Washington, D.C., March 3-4, 1975.

4. Nutkis, M. S., "Pressurized Fluidized Bed Coal Combustion," Presented at the International Fluidization Conference, Pacific Grove, CA, June 15-20, 1975.

5. Ruth, L. A., "Combustion and Desulfurization of Coal in a Fluidized Bed of Limestone," Presented at the International Fluidization Conference, Pacific Grove, CA, June 15-20, 1975.

6. Hoke, R. C., Bertrand, R. R., "Pressurized Fluidized Bed Combustion of Coal," Institute of Fuel Symposium Series No. 1 (1975) Proceedings Vol. 1. September, 1975.

7. Hoke, R. C., Bertrand, R. R., "Combustione Di Carbone Su Letto Fluido Sotto Pressione," Associazone Termotecniea Italiana, Fluidized Bed Combustion Symposium, Cagliari, Sardinia September 27, 1975.

8. Nutkis, M. S., Bertrand, R. R., "Operation and Performance of the Pressurized FBC Miniplant," Presented at the Fourth International Conference on Fluidized Bed Combustion, McLean, VA, December 9-11, 1975.

9. Ruth, L. A., "Regeneration of $CaSO_4$ in FBC," Presented at the Fourth International Conference on Fluidized Bed Combustion, McLean, VA, December 9-11, 1975.

10. Hoke, R. C., "Emissions from Pressurized Fluidized Bed Coal Combustion," Presented at the Fourth International Conference on Fluidized Bed Combustion, McLean, VA, December 9-11, 1975.

# PATENT MEMORANDA SUBMITTED

1. Ruth, L. A., Hoke, R. C., A Calcining Zone to Permit Use of Limestone in Pressurized Fluidized Bed Combustion.

2. Ruth, L. A., Hoke, R. C., Steam Coils for a Fluidized Bed Coal Combustor.

3. Siminski, V. J., Positive Blow-Back Granular Bed Filter.

## SECTION IX

## APPENDICES

Page

A. MATERIALS OF CONSTRUCTION 144

B. REPORTS OF METALLURGICAL EXAMINATIONS 152

C. SAFETY CONSEQUENCES OF A STEAM-COIL BREAK. STEAM-CARBON EQUILIBRIUM 162

D. MINIPLANT ALARM ANNUNCIATORS 164

E. MINIPLANT DATA LOGGER POINTS 166

F. ANALYTICAL TECHNIQUES 169

G. MINIPLANT RUN SUMMARIES 170

H. BATCH UNIT RUN SUMMARIES 198

# APPENDIX A

## MATERIALS OF CONSTRUCTION

Presented here is a brief review of materials which are candidates for use in future generations of high-temperature, fluidized bed, coal combustion-limestone regeneration units. Two classes of materials are discussed: refractories (ceramics) and metals. The approach will be to outline selection criteria while emphasizing underlying basic principles. Some examples of specific materials will be given but there has been no attempt to present a broad review of the published literature or manufacturers' brochures. Results will be given of our experience with several materials.

### A. Refractories

#### 1. Function of Refractories

A fluidized bed combustor or regenerator would normally be constructed with a steel outer shell, lined with a refractory material. The refractory limits heat losses and also protects the steel shell from excessive temperatures and corrosive materials. Temperatures inside the combustor are typically about 1600°F, and in the regenerator, 2000°F. The refractory should limit the temperature at the steel shell to 240-400°F. At this temperature the shell retains most of its room temperature strength and is still hot enough to prevent condensation of water vapor on its surface, thereby reducing corrosive attack. The shell is protected against hot corrosive gases because gas is cooled as it migrates through the refractory.

#### 2. Classes of Refractories

The primary components of most refractories are aluminum oxide (alumina) and silicon dioxide (silica). The physical forms most commonly encountered are brick, castables, plastic refractories, and ceramic fiber materials. Castable refractories are mixtures of raw and calcined clays of carefully chosen size and particle size distribution. They also contain compounds which hydrate on addition of water, usualy calcium aluminate. Plastic refractories are mixtures of ground fireclays with chemical binding agents and are similar to castables except that they are shipped wet from the manufacturer and are usually applied by ramming with pneumatic hammers. They can be formulated to harden on exposure to air or when heated. Refractory brick consists of a mixture of clays which have been fired to a high temperature to drive off volatiles and form strong ceramic bonds between component particles.

Bricks, castables, and plastics of similar composition have almost identical properties after firing at high temperatures. Castable refractories, as a class, are particularly well suited to fluidized bed reactors because they may be used for any shape where installation of forms is possible. Monolithic materials also tend to be slightly less permeable than their brick analogs. The fourth class of refractories, ceramic fiber board, have temperature limits which are too low (<1800°F), limited strength, and relatively poor erosion resistance, and will not be considered further.

## 3. Selection Criteria

### Use Temperature

Use temperature is probably the single most important consideration in selecting a refractory. Castables and plastic refractories can be obtained with ratings as high as 3300°F for continuous service. High alumina brick is available with ratings up to about 3500°F. In general, maximum use temperature increases with alumina content.

It is not desirable to specify refractories, especially castables and plastics, with maximum use temperatures far above anticipated operating conditions. In the case of monolithic linings, ceramic bonds do not form until the lining is thoroughly cured near maximum use temperature. At low temperatures, which occur near the cool face of the lining, strength is usually provided by hydraulic bonds. If a section of monolithic material is heated sufficiently to destroy hydraulic bonds but not enough to form ceramic bonds, the material is relatively weak. This condition is often found near the center of a monolithic lining. The presence of a relatively weak center makes the structure somewhat more flexible than brick construction, and may allow it to better resist thermal shock. However, if the hot face of the lining is never thoroughly cured by soaking at near maximum temperatures, the entire structure will be weak, and likely to spall. Even in brick, ceramic bonds have not been completely formed during manufacture. Use of brick at temperatures well below the rated temperature will minimize formation of additional bonds and leave the brick relatively weak.

### Resistance to Chemical Attack

Alumina-silica refractories are relatively inert although problems can occur in some cases. Chemical attack usually results in refractory failure of three kinds. In one kind, the presence of fluxing agents can cause melting of the refractory surface. The rate of attack will depend on how fast the melted material is removed and fresh refractory surface exposed. Another kind of failure involves formation of solid reaction products. This can occur if corrosive species diffuse to cooler parts of the refractory and condense. Because the solid reaction product will usually have a thermal expansion coefficient markedly different from the bulk refractory, spalling can occur on start-up or shut-down. A third kind of attack involves condensation of water in the refractory during shut-down. Rapid heating on startup can cause steam evolution and even explosion of the refractory.

Accumulation of water in the refractory is accelerated by the presence of hygroscopic products of high temperature attack.

### Thermal Conductivity and Density

Thermal conductivities and density of brick and castable refractories vary over a wide range. Generally, denser materials have higher thermal conductivities. For example, a lightweight insulating castable could have a density of 50-55 $lb/ft^3$ and a thermal conductivity of about 0.16 Btu/hr ft°F at 1000°F. A dense castable (60% $Al_2O_3$) with a density of about 140 $lb/ft^3$ could have a thermal conductivity of about 0.43 at 1000°F. Similarly, densities and thermal conductivities of brick vary from about 45 $lb/ft^3$ for insulating firebrick ($K = 0.2$ at 1000°F) to about 145 $lb/ft^3$ ($K = 0.78$ at 1000°F) for super-duty brick.

Dense refractories do have a decided advantage, however, over lightweight materials: they have much better resistance to chemical attack and usually more mechanical strenght.

### Thermal Shock Resistance

Refractories are brittle and can crack when subjected to sharp temperature fluctuations; hence, care is necessary when heating and cooling refractory-lined vessels. Thermal shock resistance increases with increasing thermal conductivity and decreasing density. Mullite ($3Al_2O_3 \cdot 2SiO_2$) is the best alumina-silica material for applications requiring good thermal shock resistance.

### Cost

The total cost of refractory includes the cost of materials, installation, and maintenance. Monolithic materials may cost more than the equivalent brick for the same degree of insulation but this may not be so for brick shapes other than simple configurations. Brick linings are almost always installed in the field and skilled workmen are required. Castable linings are much simpler to install and withstand shipment rather well. Maintenance costs of various lining types depend strongly on the type of operation, amount of supervision and accessibility for repair.

## 4. Experience With Fluidized Bed Combustion - Regeneration

Refractory materials which have been used in the batch and miniplant fluidized bed combustor and regenerators are listed with their application below:

- Grefco Litecast 75-28: refractory lining for combustor and regenerator vessels.
- Grefco Bubbalite: refractory lining for pre-heat burner sections.

- Aremco Ceramacast 511: supports for combustor cooling coils.
- Cast alumina and zirconia: batch unit regenerator fluidizing grids.
- Alumina and mullite tubes: liner in batch regenerator.

Performance of the cast ceramic fluidizing grids and the mullite and alumina liners have already been discussed in a recent report (EPA-650/2-74-001) and will not be repeated here.

Grefco Litecast 75-28 is the refractory lining for the batch equipment and miniplant (excluding pre-heat burner sections). This material has a service limit of 2800°F, a bulk density of 75 $lb/ft^3$, and a thermal conductivity of 0.32 Btu/hr ft °F at 1000°F. The manufacturer claims that Litecast has excellent strength and good resistance to thermal shock. This material has held up very well with use.

Grefco Bubbalite is a high temperature lightweight castable with a fused bubble alumina aggregate and high-purity low-iron calcium aluminate binder. It has a service limit of 3300°F and a thermal conductivity at 1000°F of 0.5 Btu/hr ft °F. It was selected for use in the burner sections of the combustors and regenerators because of its high temperature rating. It has held up very well considering the high probability of flame impingement and rapid heating and cooling.

The combustor cooling coils were supported at flanges with Aremco Ceramacast 511. This is a magnesium oxide/zircon refractory with a temperature limit of 2800°F. No problems have occurred with this material in this application.

### 5. Manufacturers of Refractories

In addition to General Refractories-Grefco and Aremco Products (specialties)(Briarcliff Manor, New York) other manufacturers of castable and brick refractories include Babcock and Wilcox Company, Refractories Division (Augusta, Georgia), J. H. France Refractories Company (Snow Shoe, Pennsylvania), and Harbison-Walker Refractories Co. (Pittsburgh, Pennsylvania). Each produces a large line of competitive refractories.

## B. Metals

Successful application of metals in high-temperature process service requires consideration of mechanical and metallurgical properties and corrosion and oxidation resistance. These factors will be discussed and specific references to high temperature alloys and corrosive atmospheres will be included. Experience with materials used in the fluidized bed combustors and regenerators will also be given.

### 1. Mechanical and Metallurgical Considerations at High Temperatures

At moderate temperatures, below about 700°F for steels, ordinary yield strength is the mechanical property that limits the application of engineering alloys. However, at very high temperatures, creep, rupture, and short-time strengths are important. Creep is the gradual straining that metals experience under relatively low stresses at high temperatures. It is usually expressed as the stress required to produce a given creep rate, e.g., 1% in 10,000 hrs. Rupture strength is the stress required to produce rupture in a definite time at a given temperature. Short-time strength is simply the ordinary tensile strength at a high temperature. Among alloys, as a rule, ferritic materials are weaker than austenitic compositions, and molybdenum increases strength in both groups.

In addition to changes in mechanical properties, many alloys are subject to changes in metallurgical properties at elevated temperature. Specific comments on various materials are given below:

#### Carbon Steel and 1/2% Mo Steel

Spheroidization of carbides and graphitization generally occur in carbon steel and 1/2% Mo steel after prolonged exposure to temperatures in the 800-1300°F range. Significant reduction in strength accompanies both spheroidization and graphitization.

#### Low Alloy Steels (1% Cr, 1/2% Mo to 5% Cr, 1/2% Mo)

If heated above the transformation temperature ( 1300°F) and subsequently cooled rapidly, these steels will have reduced ductility at lower temperatures.

#### High Chromium Stainless Steels

Steels containing 17% or more Cr are susceptible to "885°F embrittlement." This aging phenomena produces extensive decreases in toughness and ductility after long term exposure in the 700-900°F range.

#### Chromium-Nickel Stainless Steel (Types 304, 321, 347, 316, 309, 310, 330)

When chromium-nickel stainless steel are subjected to temperatures of 850-1200°F, "sensitization" can occur, which involves carbide precipitation at the grain boundaries. Chromium carbides will be precipitated leaving areas close to the grain boundaries low in chromium and thus less resistant to intergranular corrosion. This would be particularly detrimental under conditions where water is also present, such as during "downtime." Sensitization can be prevented by using very low carbon contents (about 0.03%), but generally the customary 0.08 percent carbon is stabilized by the addition of titanium or columbium.

Exposure of these steels to temperatures of 1000 to 1600°F can result in formation of "sigma phase." Above 1000°F, this may increase tensile strength without much effect on ductility; however, room temperature ductility can be markedly reduced.

## 2. Oxidation and Corrosion Resistance

In many process applications, strength and mechanical properties become of secondary importance compared with resistance to oxidation and corrosion. All common alloys form oxides when exposed to hot oxidizing environments. Whether or not the alloy is resistant depends upon whether the oxide is stable and forms a protective film. Mild steel is seldom used above 950°F because of excessive scaling rates. Adding chromium to steel improves oxidation resistance; thus 4-6% Cr steel is acceptable to 1150°F, 9-12% Cr steel to 1300-1400°F, 14-18% Cr steel to 1500°F, and 27% Cr to 2000°F. Silicon (0.75-2%) also improves oxidation resistance when added to low chromium steels.

There is a multitude of possible corrosion reactions and it is sometimes advantageous to classify them into a few broad types, including direct corrosion and electrochemical corrosion. Although practically all corrosion is electrochemical (anodic and cathodic regions on the metal surface are involved), electrochemical corrosion usually refers to the type of corrosion that takes place at or near room temperature as a result of reaction of metals with water or with aqueous solutions of salts, acids, or bases. Direct corrosion is essentially ordinary chemical attack. The corrosive agent usually attacks the surface uniformly and at an almost constant rate that can be conveniently measured, e.g., in inches penetration per year. Of course, more specific descriptions are widely used for certain types of industrially important corrosion. Some examples of non-uniform attack are pitting and intergranular corrosion. Other specific types of corrosion include stress-corrosion, corrosion fatigue, and erosion corrosion.

Problems of special chemical environments that can be encountered in fluidized bed combustion are briefly discussed below.

### Sulfur Dioxide and Hydrogen Sulfide

The relative effect of $SO_2$ in air plus water vapor on corrosion of steel at 1650°F is given in Table A-1.

TABLE A-1. EFFECT OF $SO_2$ AND $H_2O$ ON CORROSION OF CARBON STEEL AT 1650°F

| Atmosphere | Relative Corrosion |
|---|---|
| Pure Air | 100 |
| Air + 2% $SO_2$ | 118 |
| Air + 5% $H_2O$ | 135 |
| Air + 5% $SO_2$ + 5% $H_2O$ | 276 |

Data from Tomashov, N. D., Theory of Corrosion and Protection of Metals, The MacMillan Company, New York, 1966, p. 114.

Sulfides usually form when an alloy contacts S or $H_2S$ at high tem -tures. Attack is generally more severe than during oxidation because sulfides have higher molar volumes than oxides. High volume ratios can lead to the build-up of stresses resulting in the cracking of scale and exposure of fresh surface to further attack. Metal sulfides usually melt at lower temperatures than do oxides and metal-metal sulfide eutectics frequently have low melting points. The melting point of the Ni-$Ni_3S_2$ eutectic is particularly low, and this seems to account for the fact that alloys containing more than 15-30% Ni are exceptionally sensitive to sulfur-containing gases under non-oxidizing conditions. The liquid sulfide destroys the scale locally and opens up new centers for attack by the corroding gas.

Alloys rich in nickel should not be used in contact with sulfur containing gases, particularly in the absence of oxygen, and often even in the presence of oxygen. Even when excess oxygen is present, as in the combustion of fuel, local reducing conditions can exist in regions where combustion is incomplete.

Chromium is the most important material in imparting resistance against sulfide scales. For this reason, straight chromium stainless steels are recommended in high $H_2S$ atmospheres. High chromium steels (>20%) are also quite resistant to $SO_2$ atmospheres. Corrosion in moist $SO_2$ is stronger than in the dry gas at both high and low temperatures (See Table A-1). It is interesting and important that alloys rich in nickel are relatively resistant only to dry $SO_2$ while they are heavily attacked in moist $SO_2$ at low and high temperatures. It is also interesting that moist $H_2S$ attacks the various steels at about the same rate as dry $H_2S$.

### Sulfur Trioxide

Small amounts of $SO_3$ normally present in flue gas are strongly absorbed in water droplets so that the corresponding acid condensates are quite concentrated. With $SO_3$ present, the dewpoint may be as high as 340°F, and possibly higher. Severe corrosion can result to steels, stainless steels, and many nickel-base alloys. Hence, serious problems can occur when metal temperatures are below the dewpoint.

### Compounds Containing Vanadium, Sodium, Potassium, Sulfur, Molybdenum, or Lead

Compounds containing the above elements can accelerate the corrosion of steels, stainless steels, and other alloys at elevated temperature. While the concentration of these elements in coal may be low, deposits on metal surfaces within a fluidized bed boiler may not be. Vanadium and sodium, in particular, react to form a corrosive liquid (m.p. 980°F). However, calcium oxide and some other compounds can combine with vanadium oxides and minimize corrosion.

### Carbon Dioxide and Carbon Monoxide

Carbon dioxide and monoxide in flue gas probably does not accelerate corrosion with iron based alloys in most cases. However, high $CO_2$ concentrations or sufficiently high temperatures can decarburize or carburize steels and other alloys, depending on the temperature and $CO/CO_2$ ratio.

# APPENDIX B

# REPORTS OF METALLURGICAL EXAMINATIONS

**EXXON RESEARCH AND ENGINEERING COMPANY**
P O BOX 101 FLORHAM PARK NEW JERSEY 07932

EXXON ENGINEERING TECHNOLOGY DEPARTMENT
Mechanical and Materials Engineering Division

K. G. FEEHAN
Manager
R. D. MERRICK
Senior Engineering Associate

Cable ENGREXXON N Y

59983 July 23, 1974

Linden Fluidized Bed Coal
Combustion Miniplant Analysis of
Cooling Coil Samples

Mr. Melvyn S. Nutkis
Government Research Laboratory
Exxon Research and Engineering Co.
P.O. Box 8
Linden, N.J. 07036

Dear Mr. Nutkis:

We have completed our examination of the cooling coil samples from your Fluidized Bed Coal Combustion Miniplant. The samples accompanied your letter of June 17, 1974. We found no evidence of corrosion or deterioration of the coil. Apparently the cooling water maintained the coil at a sufficiently low temperature so that neither sensitization nor attack from flue gas occurred. However, the rod, which was not cooled, suffered both sensitization and corrosive attack. We recommend that a thicker 316 stainless steel rod or a rod made of 310 stainless steel be used in this application in the future.

The samples are from a damaged cooling coil removed from the combustor after approximately 60 hours of exposure. Three samples were received for metallurgical examination; sample #1 was a tube section near the water inlet, sample #2 was a tube section near the water outlet, and sample #3 was a length of stiffening rod which was tack welded to the coil. The coil was fabricated from 3/4" OD type 316 and 316L stainless steel tubing. The stiffening rod is 3/16" type 316 stainless steel rod.

In operation, the tubing was water cooled and did not experience the reaction temperature of 1500-1850°F. The rod, however, was not cooled and was exposed to the high temperature.

The microstructure of the rod (Figure 1) shows carbide precipitation in the grain boundaries, which is typical of sensitized stainless steel. Type 316 stainless steel is susceptible to sensitization in the temperature range of 950 to 1450°F. Above 1450°F sensitization is not a problem. However, stainless steels operated above this temperature may become sensitized when cooled through the range. Thus, the rod apparently became sensitized during cooling and not during the operation of the vessel. Figure 1 also shows a layer of corroded metal at the outer surface of the rod. The layer is approximately one mil thick and is probably due to high temperature attack from flue gases containing $SO_2$ and $SO_3$.

The coil (Figure 2) appears to be less affected than the rod. There is no heavy carbide precipitation at the grain boundaries. We feel that the cooling water maintained the coil at a temperature below the sensitization range, and that the microstructure of the coil is "normal". In addition, there is no evidence of metal depletion on either the outside or inside surfaces of the coil.

There was a layer of residue on both the outside and inside surfaces of the coil. A qualitative analysis of the outside layer indicated that the major constituents were calcium, sulfur, and silicon. Small atomic weight atoms such as oxygen cannot be determined by this method. The outside layer is probably a residue of the combustor reaction. The inside layer analysis showed copper, sulfur and small amounts of aluminum present. This residue was probably formed from particles in the cooling water. We do not feel that this residue has had a detrimental effect on the tubing.

In general, the coil was unaffected by the service; however, since the system operated for only 60 hours it is possible that a significant corrosion rate could go undetected. We know that oxidizing agents such as $SO_2$ will corrode type 316 stainless steel above 1600°F. It appears, however, that the cooling water has maintained the coils at a safe temperature. We feel that type 316 stainless steel can provide good service in this application.

The rods, where not cooled, were subjected to the operating temperatures of 1500-1850°F. Type 316 stainless steel is not recommended for use above 1500°F. We feel, however, that 316 stainless steel can be used in this application since the rods are not a critical component of the system and are not subjected to large stresses. However, if 316 stainless steel is specified, we would recommend that a thicker rod (at least 1/4" in diameter) be used. Alternatively, a more corrosion resistant material such as 310 stainless steel could be used.

Very truly yours,

J.W. Slusser
J.W. SLUSSER

JWS:km
Attach.

cc: K. Macnamara ( 000 )

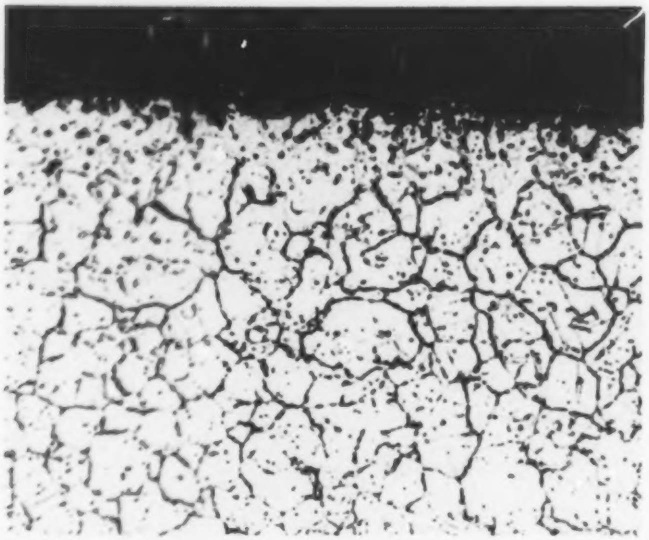

Figure 1

Micrograph of the rod (sample #3) near the outer surface.
Mt #7903 Etch: oxalic acid 500X

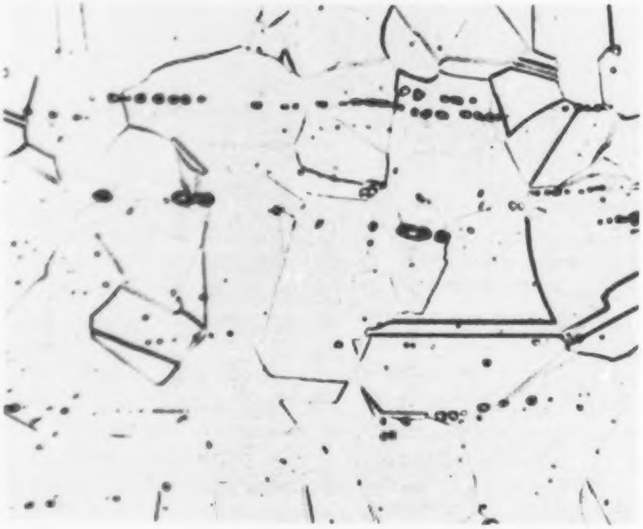

Figure 2

Micrograph of the coil (sample #1) from the Fluidized Bed Coal Combustion Miniplant - Linden
Mt #7901 Etch: oxalic acid 500X

**EXXON RESEARCH AND ENGINEERING COMPANY**
P.O. BOX 101, FLORHAM PARK, NEW JERSEY 07932

Cable: ENGREXXON, N.Y.

**EXXON ENGINEERING TECHNOLOGY DEPARTMENT**
Mechanical and Materials Engineering Division

**K. G. FEEHAN**
Manager

54882 June 30, 1975

J.E. Guthrie
Section Head

Analysis of Cooling Coil Samples
- Linden Coal Combustion Miniplant

Mr. D.D. Kinzler
Government Research Laboratory
Exxon Research & Engineering Company
P.O. Box 8
Linden, N.J. 07036

Dear Mr. Kinzler:

Our analysis of the tubing from your coal combustion miniplant indicates high temperature gas attack (probably oxidation/sulfidation) has caused most of the corrosion. We also found some evidence of high temperature slag attack most likely caused by the combination of Na, V, and S in the coal combustion products. The worst corrosion and metal loss occurred on the tube elbows with only minor pitting occurring on the straight sections. This was due to continuous erosion of the corrosion product formed at the elbows and the constant exposure of fresh surface. We believe the corrosion can be reduced by insuring cooling water flow during operation and, thus, lower tube metal temperature (TMT). If this is not practical, Type 310SS should be used instead of Type 316SS. Type 310SS has better high temperature corrosion resistance than Type 316SS.

Samples from cooling coils 2A, 4A, 1B, and 2B were received for examination. The tubes are 3/4" OD, 0.048" thick Type 316SS (straight sections) and Type 316L SS (elbows) and were removed after 60 hours of exposure in the combustor. The environment inthe combustor contains $CO_2$, $SO_2$, and $O_2$ gases at 1500 to 1850°F. Type 316 and 316L SS have similar high temperature corrosion resistance in this type of environment and are usually acceptable to about 1600°F TMT. Tubeside environment is cooling water which is converted to saturated steam during operation.

We previously examined tubing from this plant (July 23, 1974, letter No. 59938) and found it unattacked. One of the changes made since then was to start the reaction without cooling water in the coils. Previously, cooling water was turned on at the startup of the reaction; now it is turned on after the reaction has started, and as a consequence, it is believed that the TMT has exceeded 1600°F.

Table 1 gives wall thickness measurements taken randomly on the tube samples and shows the attack was localized with considerable metal loss occurring on the outside of the elbows. The inside of the elbows and the straight sections suffered little attack. We also found that there was no scale on the OD surface where the highest metal loss had occurred. This localized metal loss indicates erosive removal of scale.

Coil 2A in particular showed this localized metal loss at elbows. Figure 1 is a micrograph of an elbow at a section in which the wall thickness has been reduced to 16 mils. Notice the uniform metal loss at the OD surface. A combination of high temperature gas corrosion and erosion of the resulting scale by the bed particles would produce this type of metal removal. The bed particles are quite hard, but the low velocity of the particles (6 fps) discounts the possibility of erosion of the stainless steel. The particles, though, may abrade the scale which forms during corrosion. When this scale is removed, it exposes fresh metal to the environment and results in uniform metal loss.

Examination of the coil 4A elbows again showed high metal loss at the outside of the elbows; however, in this case, pitting attack was present. Microprobe analysis showed sulfur was present in the pits. Figure 2, a micrograph of a straight section adjacent to an elbow, shows the undercutting type of pitting typical of sulfidation/oxidation gas attack. The attack in this case is similar but less severe than that found on coil 2A. The difference may be due to an oxide scale on the surface of 4A which hindered attack. However, this scale was permeable, and extensive pitting occurred beneath the scale.

Pitting attack, although less severe than on the 4A elbows, also occurred on a straight section of coil 2B as shown in Figure 3. This pitting does not have the undercut appearance shown in Figure 2, and we believe it was due to slag attack. At high temperatures, elements in the coal such as Na, V, and S can combine on the tube surface to form liquid slags which are corrosive.

The scale on the coils indicates the coils experienced temperatures above 1600°F. Little or no scaling would be expected in only 60 hours of exposure if the TMT had been maintained below 1600°F; however, above this temperature, Type 316 and 316L SS scale rapidly. The microstructure of the coils, especially the large grains and rounded grain intersections of Figure 2, also reflect high temperature service.

The structure shown in Figure 1, while quite different from that in Figure 2, is also typical of high temperature service. The difference is that the structure shown in Figure 2 is an annealed Type 316 SS while that shown in Figure 1 is a recrystallized Type 316L SS, typical of a metal which is cold worked and then heated. The temperature required for recrystallization is a function of the metal, the amount of cold work, and the time at temperature. Type 316L SS will not recrystallize below 1600°F. In this case, the cold work resulted from the bending of the elbow, and the recrystallization occurred during operation. We cannot determine the exact temperature reached, but, regardless of the degree of cold work, recrystallization would not occur below 1600°F. Also, the thin grain boundaries show this structure is not sensitized because the metal is Type 316L SS which, unlike Type 316 SS, will not sensitize at any temperature in only 60 hours.

The structure shown in Figure 3 is that of a lightly cold worked structure which has not recrystallized. The cold work is indicated by the twinning shown in Figure 3 (note the absence of twinning in Figure 1). Since the metal is only lightly cold worked, the recrystallization temperature would be well above 1600°F.

The scale found on the OD surface of all the tubes and the microstructure of the tubes indicate the coils have experienced temperatures above 1600°F. This high temperature has resulted in oxidation/sulfidation attack which has been aggravated by erosion of the corrosion scale. We also found indications of a slag attack. Lowering the TMT by insuring cooling water flow will result in reduced attack. If continuous cooling water flow is impractical, Type 310 SS should be used instead of Type 316 and 316L SS. Type 310 SS has better high temperature corrosion resistance and is acceptable to 1900°F.

Very truly yours,

JOSEPH W. SLUSSER

JWS:km
Attach.

cc: K. Macnamara (5150)

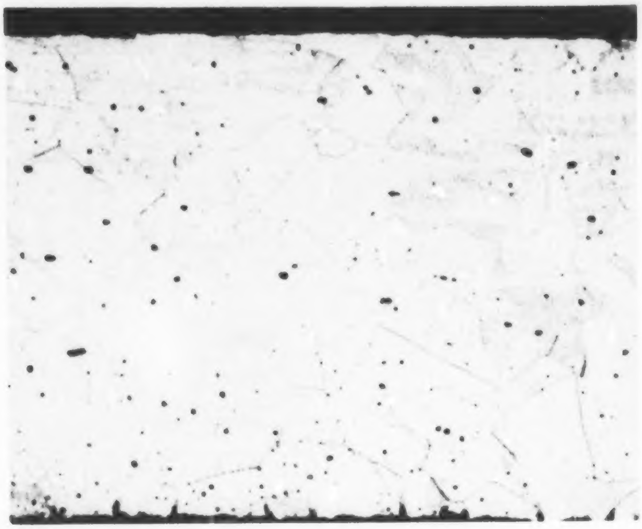

Figure 1

Micrograph of Coil 2A elbow (Type 316L SS) showing uniform metal loss. Sample was over etched to show recrystallized structure. Note large grains indicative of high temperature service.

Mt. 8412 200X

OD
Grain Size
ID

Figure 2

Micrograph of Coil 4A straight section adjacent to elbow (Type 316 SS) showing pitting on OD surface. Note large grains and rounded grain intersections typical of high temperature service.

Mt. 8379 100X

OD
Twin
Twin

Figure 3

Micrograph of Coil 2B straight section (Type 316 SS) showing pitting from slag attack. Structure has twins indicating light amount of cold work.

Mt. 8413 200X

## TABLE I

### Thickness Measurements (inches) of Samples from Coils 2A, 4A, 2B, and 1B (Randomly taken)

### Elbows

| Sample | Coil | Thickness Outside of Bend | Loss | Thickness Inside of Bend* | Loss |
|---|---|---|---|---|---|
| 1 | 2A | 0 (failure) | .048 | .050 | - |
|  |  | .017 | .031 | .047 | .001 |
|  |  |  |  | .039 | .009 |
| 2 | 2A | .020 | .028 | .048 | - |
|  |  | .021 | .027 | .053 | - |
|  |  | .019 | .029 |  |  |
| 3 | 2A | .022 | .026 | .048 | - |
|  |  | .025 | .023 | .052 | - |
|  |  | .016 | .032 | .054 | - |
| 4 | 4A | .023 | .025 | .040 | .008 |
|  |  | .025 | .023 | .037 | .011 |
|  |  | .027 | .021 | .050 | - |
| 5 | 1B | .032 | .016 | .037 | .011 |
|  |  | .030 | .018 | .045 | .003 |
|  |  | .031 | .017 | .035 | .013 |

### Straight Sections

| Sample | Coil | Thickness |  | Loss |
|---|---|---|---|---|
| 3 | 2A | .048 |  | - |
|  |  | .045 |  | .003 |
|  |  | .046 |  | .002 |
| 6 | 2B | .046 | scale on ID removed for measurement | .002 |

---

* The tube scale has resulted in some wall thicknesses greater than the original thickness.

JWS:km

# APPENDIX C

## SAFETY CONSEQUENCES OF A STEAM-COIL BREAK
## STEAM-CARBON EQUILIBRIUM

The consequences of a rupture in an internal heat transfer coil in a fluidized bed coal combustor were examined because of the possibility of hydrogen formation via the carbon-steam reaction should such an event occur.

The equilibrium constants for the reactions of carbon with oxygen ($10^{10}$-$10^{20}$ at 1000K) are much higher than those for the reactions of carbon with steam (about 1-4 at 1000 K). Therefore, in the presence of oxygen and at the temperatures involved in fluid bed combustion, the amount of steam decomposition will be insignificant. The steam-carbon reactions can only occur where the oxygen partial pressure is very small as, for example, might occur if the fluidizing air were shut down after steam was introduced. Hence, the system is fail-safe and potentially dangerous hydrogen-oxygen mixtures cannot form. The recommended action in the event of a break in a steam coil is to (1) shut down coal flow, (2) leave fluidizing air ON, (3) shut down water supply to affected coil.

To support these conclusions, a computer program was run to determine both adiabatic reaction temperature and equilibrium composition. It was assumed that the miniplant was operating at maximum conditions when one heat transfer coil ruptured. The material inputs were:

carbon - 480 lb/hr. entering at 125°F (equiv. to about
630 lb/hr of coal)

air - 1200 SCFM entering at 125°F

steam - 353 SCFM entering at 1000°F (equiv. to about
2 gal/min. liquid water)

pressure - 10 atm

These inputs represent nearly stoichiometric proportions and the temperature produced will be a maximum. The computer results are given below:

adiabatic reaction temperature - 3200°F
gas composition -

| | |
|---|---|
| $N_2$ | 61.0 mole percent |
| $H_2O$ | 22.4 |
| $CO_2$ | 16.0 |
| CO | 0.3 |
| $O_2$ | 0.1 |
| $H_2$ | 0.09 |
| NO, DH, H, O | balance |

It should be noted that the maximum temperature reached during a real accident would be considerably lower than the adiabatic reaction temperature. Since equilibrium for hydrogen production is less favorable at lower temperatures, the concentration of hydrogen would also be less.

In the absence of air, steam and carbon could react but the reaction temperature would drop rapidly due to the high endothermicity of the steam-carbon reactions. For the same input of materials as before, but without any air, equilibrium conditions are:

adiabatic reaction temperature - 680°F
gas composition -

| | |
|---|---|
| $H_2O$ | 54.6 mole percent |
| $CO_2$ | 22.1 |
| $CH_4$ | 21.0 |
| $H_2$ | 2.2 |
| CO | <0.1 |

The high methane concentration is the result of favorable equilibrium for methane production at 680°F; however, reaction kinetics are poor at low temperatures so that little methane should actually form. Moreover, for the same reason, only a small amount of steam decomposition would be expected to occur.

## APPENDIX D

## MINIPLANT ALARM ANNUNCIATORS

| Identification | Action | Remarks |
|---|---|---|
| Low U.V. Level Inside Plenum Upon Initiation of Gas Feed for Preheating | Alarm; Gas Feed Stops if No Ignition Occurs in 10 Seconds; Delay of 30 Seconds Before Ignition Can Be Attempted | Prevents Accumulation of Uncombusted Natural Gas in Combustor |
| Low U.V. Level Inside Plenum During Gas Feed for Preheating | Alarm; Gas Feed Stops; Delay of 30 Seconds Before Reignition Can Be Attempted | Prevents Accumulation of Uncombusted Natural Gas in Combustor |
| Low Pressure Difference Between Primary Injector and Combustor | Alarm; Block Valve on Coal Feed Probe Closes | Prevents Entry of Combustion Gases into Primary Injector |
| Low Flow in Primary Injector Feed Line | Alarm | Relative Flow Level Monitored by Measuring Sound Intensity in Feed Line with Scarpa Meter |
| High Coal Feed Line or Feed Nozzle Temperature | Alarm; Block Valve on Coal Feed Nozzle Closes | Prevents Entry of Combustor Gas and Solids into Atmosphere if Feed Line Breaks |
| Low Pressure from Main Air Compressor, Auxiliary Air Compressor, or Site Air | Alarm | |
| Low Combustor Air Flow | Shutdown | Prevents High Bed Temperature Due to Poor Bed Mixing |
| High Exterior Surface Combustor Temperature | Alarm | |
| High Burner Grid or Fluidizing Grid Temperature | Alarm | |
| High Fluidizing Grid Pressure Drop | Alarm | Indicates Blockage of Grid Holes |
| High Combustor Pressure | Shutdown | |
| High Bed Temperature | Alarm @ 980°C;<br>Shutdown @ 1090°C | Prevents Temperatures Causing Bed Agglomeration |
| Low Bed Temperature (for Coal Ignition) | Alarm; Primary Injector Feed Valve Closes | Alarm Setting is 650°C |

MINIPLANT ALARM ANNUNCIATORS (CONTINUED)

| Identification | Action | Remarks |
|---|---|---|
| Low Bed Temperature (for Liquid Fuel Combustion) | Alarm; Solenoid Valve on Fuel Line Will Not Activate | Alarm Setting is 425°C |
| High Water Temperature From Any Cooling Coil | Alarm; Shutdown After 4 Minutes if Uncorrected | Prevents Cooling Coil Damage |
| Low Water Flow From Any Cooling Coil | Alarm; Shutdown After 4 Minutes if Uncorrected | Prevents Cooling Coil Damage |
| Low Pressure in Cooling Water Tower | Alarm | |
| High or Low Level in Cooling Water Tower | Alarm | |
| Low Pressure Drop Across Bed | Alarm | Indicates Bed Level Too Low to Reject Solids |
| Low Temperature in Dipleg of Either Cyclone | Alarm | Indicates Blockage of Solids Flow Down Dipleg |
| High Temperature in Rejected Solids Lock Hopper | Alarm | |
| High Downstream Flue Gas Temperature | Alarm | Prevents Flue Gas Scrubber Damage |
| High or Low Pressure Difference from Expansion Joint Compensation | Shutdown | Prevents System Damage Due to Vertical Thermal Expansion of Combustor |

# APPENDIX E

## MINIPLANT DATA LOGGER POINTS

| Point No. | Function |
|---|---|
| 1 | Constant 40 millivolt standard signal |
|  | COMBUSTOR |
| 2 | Weight of coal in primary injector |
| 3 | Cooling water flow, Coil 1A |
| 4 | 1B |
| 5 | 2A |
| 6 | 2B |
| 7 | 3A |
| 8 | 3B |
| 9 | 4A (future) |
| 10 | 4B (future) |
| 11 | Air flow |
| 12 | Pressure |
| 13 | ΔP, coal feed vessel |
| 14 | ΔP, grid |
| 15 | ΔP, Bed Ports 4 to 31 |
| 16 | ΔP, Bed Ports 4 to 11 or 15 |
| 17 | Cooling water heat transfer loop |
| 18 | Spare |
|  | REGENERATOR |
| 19 | Burner air flow |
| 20 | Burner fuel flow |
| 21 | Supplemental air flow |
| 22 | Supplemental fuel flow |
| 23 | Pressure, ΔP to combustor |
| 24 | ΔP, grid |
| 25 | ΔP, bed Ports 29 to 34 |
| 26 | ΔP, bed Ports 29 to 31 |
|  | COMBUSTOR |
| 27 | Ratio coal to limestone |
| 28 | Air pressure to measuring orifice |
| 29 | Run identification no. |
| 30 | Burner grid metal temp. |
| 31 | Cooling water temp., burner grid |
| 32 | Fluidizing grid metal temp. |
| 33 | Cooling water temp., fluidizing grid |
| 34 | Port #3, burner zone temp. |

| Point No. | Function |
|---|---|
| 35 | Temp. port #5, 6" |
| 36 | 7, 18" |
| 37 | 8, 27" |
| 38 | 9, 45" |
| 39 | 12, 63" |
| 40 | 13, 81" |
| 41 | 14, 87" |
| 42 | 17, 117" |
| 43 | 20, 135" |
| 44 | 22, 162" |
| 45 | 26, 216" |
| 46 | 32, 341" |
| 47 | Coal injection probe temp., (spare) |
| 48 | Coal injection line temp., (spare) |
| 49 | Cooling water temp. to all coils |
| 50 | Cooling water temp. from Coil # 1a |
| 51 | 1B |
| 52 | 2A |
| 53 | 2B |
| 54 | 3A |
| 55 | 3B |
| 56 | 4A |
| 57 | 4B |
| 58 | 5A (spare) |
| 59 | 5B (spare) |
| 60 | Cyclone gas discharge temp., 1st stage |
| 61 | Cyclone gas discharge temp., 2nd stage |
| 62 | Off gas temp. upstream of nozzle |
| 63 | Off gas temp. downstream of nozzle |
| 64 | Cyclone dipleg temp., 1st stage (mid) |
| 65 | 2nd stage (btm) |
| 66 | Solids reject line temp. before pulse pot |
| 67 | Lockhopper temp., solids reject from bed (spare) |
| 68 | Lockhopper temp., flyash from cyclone #2 |
| 69 | Surface temp. "A", lower deck, east side |
| 70 | Surface temp. "B", 1st deck, west side (spare) |
| 71 | Spare |
| 72 | Air temp. to measuring orifice |
| 73 | Ambient air |
| 74 | Fuel temp. to measuring orifice |
|  | REGENERATOR |
| 75 | Spare |
| 76 | Spare |
| 77 | Temp. port #3, 11" |
| 78 | 5, 23" |
| 79 | 7, 35" |

| Point No. | Function |
|---|---|
| 80 | Temp. port #8, 41" |
| 81 | 9, 48" |
| 82 | 10, 56" |
| 83 | 12, 74" |
| 84 | 14, 92" |
| 85 | 21, 158" |
| 86 | 26, 218" |
| 87 | Cyclone gas discharge |
| 88 | Spare |
| 89 | Spare |
| | COMBUSTOR |
| 90 | Analyzer for $SO_2$ |
| 91 | NO |
| 92 | $O_2$ |
| 93 | $CO_2$ |
| 94 | CO |
| | REGENERATOR |
| 95 | Analyzer for $SO_2$ |
| 96 | $O_2$ |
| 97 | $CO_2$ |
| 98 | CO |
| 99 | Clock |

# APPENDIX F

## ANALYTICAL TECHNIQUES

### Analysis of Solids

Solids from combustion runs were analyzed for $SO_4^{-2}$, $CO_3^{-2}$, $Ca^{+2}$, $Mg^{+2}$ carbon and total sulfur. The analytical techniques that were used are described below.

$SO_4^{-2}$ - The sample was treated with acidic $BaCl_2$ solution. The $BaSO_4$ precipitate was weighed.

$CO_3^{-2}$ - HCl was added to an acidified sample. The solution was stripped with $N_2$ and the gas passed through drierite, $CuSO_4$ and ascarite. $CO_3^{-2}$ was determined from the weight gain of the ascarite.

$Ca^{+2}$ $Mg^{+2}$ - The sample was digested by heating vigorously in a medium of perchloric acid/nitric acid. The determination of Ca and Mg was made by atomic absorption.

Total sulfur - The sample was mixed with sodium peroxide and a catalyst. The sulfur was converted to the sodium sulfate. The sample was heated above the melting point and the melt was extracted with water. The sulfur was converted to barium sulfate, precipitated and weighed.

Carbon - Samples were combusted within a packed tube in an oxygen atmosphere. Helium was used to sweep the combustion gases into the analytical system. Carbon dioxide was determined by differences in thermal conductivity.

### Analysis of Flue Gas by Wet Chemical Methods

$SO_3$ - The amount absorbed by an 80% isopropanol solution was determined titrimetrically using 0.01N barium perchlorate as the titrant and thorin as the indicator.

$SO_2$ - The amount absorbed by a 3% hydrogen peroxide solution was determined titrimetrically using 0.01N sodium hydroxide as the titrant and methyl orange as the indicator.

# APPENDIX G

## MINIPLANT RUN SUMMARIES

Page

TABLE G1. SUMMARY OF MINIPLANT RUN CONDITIONS 171

TABLE G2. MINIPLANT $NO_x$ EMISSION DATA 187

TABLE G3. MINIPLANT SOLIDS ANALYSES 189

TABLE G4. MINIPLANT CALCIUM AND SULFUR BALANCES 197

## TABLE G1. SUMMARY OF MINIPLANT RUN CONDITIONS

(See explanation of footnotes on pages 185 and 186)

| | | | |
|---|---|---|---|
| Run No.[a] | 2.1 | 3.1 | |
| Date | 4/11/74 | 5/3/74 | |
| Run Length (hrs)[b] | 3.5 | 5.5 | |
| Cooling Coil Orientation[c] | H | H | |
| Area of Coils, Total ($m^2$) | 5.80 | 5.80 | |
| Limestone Feed | No | No | |
| Bed Rejection[d] | No | No | |
| Bed Depth, Settled (m) | | | |
| Start of Run | 0.76 | 0.92 | |
| End of Run | | | |
| Coal/Limestone Feed Ratio | | | |
| Ca/S Molar Feed Ratio | | | |
| Combustion Efficiency, Entire Run (%)[e] | | | |
| Conditions[f] | | | |
| Time Interval[k] | 9:24-11:34 | 11:30-13:40 | 13:50-16:00 |
| Pressure (kPa)[l] | 395 | 395 | 395 |
| Super. Velocity (m/sec)[m] | | | |
| Average[g] | 2.46 | 2.30 | 2.50 |
| S.D. of 10 Min. Avg's[h] | 0.08 | 0.04 | 0.09 |
| Minimum 10 Min. Avg.[i] | 2.35 | 2.23 | 2.41 |
| Maximum 10 Min. Avg.[i] | 2.56 | 2.35 | 2.59 |
| Temperature, Bed (°C) | | | |
| Average | 861 | 840 | 939 |
| S.D. of 10 Min. Avg's | 31 | 15 | 46 |
| Minimum 10 Min. Avg. | 796 | 827 | 887 |
| Maximum 10 Min. Avg. | 896 | 865 | 989 |
| Temperature, Flue Gas (°C)[n] | | | |
| Average | 295 | 291 | 326 |
| S.D. of 10 Min. Avg's | 7 | 14 | 6 |
| Minimum 10 Min. Avg. | 280 | 268 | 314 |
| Maximum 10 Min. Avg. | 303 | 308 | 333 |
| Coal Feed Rate (kg/hr) | | | |
| Average | 64.3 | 69.5 | 85.3 |
| S.D. of 10 Min. Avg's | 3.6 | 2.7 | 5.6 |
| Initial 30 Min. Avg.[j] | 66.2 | 70.1 | 84.4 |
| Final 30 Min. Avg.[j] | 65.3 | 68.1 | 81.0 |
| Excess Air (%)[o] | | | |
| Average | 27.5 | 11.8 | -8.9 |
| S.D. of 10 Min. Avg's | 8.9 | 4.2 | 5.5 |
| Initial 30 Min. Avg. | 25.0 | 10.7 | -7.8 |
| Final 30 Min. Avg. | 23.0 | 14.1 | -5.4 |

## TABLE G1. SUMMARY OF MINIPLANT RUN CONDITIONS
(See explanation of footnotes on pages 185 and 186)

| Run No.[a] | 4.1 | 4.3 | 5.1 |
|---|---|---|---|
| Date | 5/10/74 | 5/20/74 | 6/20/74 |
| Run Length (hrs)[b] | 3.5 | 4 | 4 |
| Cooling Coil Orientation[c] | H | H | H |
| Area of Coils, Total ($m^2$) | 5.80 | 5.80 | 5.22 |
| Limestone Feed | No | No | No |
| Bed Rejection[d] | No | No | No |
| Bed Depth, Settled (m) | | | |
| Start of Run | 0.92 | | |
| End of Run | | | |
| Coal/Limestone Feed Ratio | | | |
| Ca/S Molar Feed Ratio | | | |
| Combustion Efficiency, Entire Run (%)[e] | | | |
| Conditions[f] | | | |
| Time Interval[k] | 13:50-14:50 | 14:30-15:40 | 14:12-15:22 |
| Pressure (kPa)[l] | 1033 | 922 | 912 |
| Super. Velocity (m/sec)[m] | | | |
| Average[g] | 1.69 | 1.89 | 1.88 |
| S.D. of 10 Min. Avg's[h] | 0.03 | 0.06 | 0.07 |
| Minimum 10 Min. Avg.[i] | 1.65 | 1.80 | 1.80 |
| Maximum 10 Min. Avg.[i] | 1.74 | 1.92 | 1.92 |
| Temperature, Bed (°C) | | | |
| Average | 885 | 919 | 849 |
| S.D. of 10 Min. Avg's | 12 | 42 | 28 |
| Minimum 10 Min. Avg. | 868 | 857 | 802 |
| Maximum 10 Min. Avg. | 902 | 949 | 887 |
| Temperature, Flue Gas (°C)[n] | | | |
| Average | 403 | 350 | 381 |
| S.D. of 10 Min. Avg's | 10 | 11 | 12 |
| Minimum 10 Min. Avg. | 397 | 334 | 361 |
| Maximum 10 Min. Avg. | 411 | 360 | 397 |
| Coal Feed Rate (kg/hr) | | | |
| Average | 80.7 | 64.8 | 72.9 |
| S.D. of 10 Min. Avg's | 3.9 | 5.9 | 3.4 |
| Initial 30 Min. Avg.[j] | 79.5 | 65.2 | 73.8 |
| Final 30 Min. Avg.[j] | 82.0 | 64.4 | 72.4 |
| Excess Air (%)[o] | | | |
| Average | 78.9 | 115 | 98.9 |
| S.D. of 10 Min. Avg's | 8.1 | 19 | 12 |
| Initial 30 Min. Avg. | 80.4 | 116 | 95.9 |
| Final 30 Min. Avg. | 77.4 | 115 | 102 |

## TABLE G1. SUMMARY OF MINIPLANT RUN CONDITIONS
(See explanation of footnotes on pages 185 and 186)

| Run No.[a] | 5.2 | 6.1 | 6.2 |
|---|---|---|---|
| Date | 6/24/74 | 7/17/74 | 7/22/74 |
| Run Length (hrs)[b] | 4.5 | 6 | 4.5 |
| Cooling Coil Orientation[c] | H | H | H |
| Area of Coils, Total ($m^2$) | 5.22 | 4.62 | 4.62 |
| Limestone Feed | No | No | No |
| Bed Rejection[d] | No | No | No |
| Bed Depth, Settled (m) | | | |
| Start of Run | | 0.92 | |
| End of Run | | | |
| Coal/Limestone Feed Ratio | | | |
| Ca/S Molar Feed Ratio | | | |
| Combustion Efficiency, Entire Run (%)[e] | | | |
| Conditions[f] | | | |
| Time Interval[k] | 12:10-12:50 | 11:20-15:40 | 11:52-13:32 |
| Pressure (kPa)[l] | 896 | 902 | 912 |
| Super. Velocity (m/sec)[m] | | | |
| Average[g] | 1.98 | 1.96 | 1.91 |
| S.D. of 10 Min. Avg's[h] | 0.07 | 0.17 | 0.04 |
| Minimum 10 Min. Avg.[i] | 1.89 | 1.77 | 1.86 |
| Maximum 10 Min. Avg.[i] | 2.07 | 2.01 | 1.98 |
| Temperature, Bed (°C) | | | |
| Average | 889 | 949 | 938 |
| S.D. of 10 Min. Avg's | 39 | 29 | 21 |
| Minimum 10 Min. Avg. | 828 | 839 | 912 |
| Maximum 10 Min. Avg. | 944 | 980 | 979 |
| Temperature, Flue Gas (°C)[n] | | | |
| Average | 358 | 377 | 407 |
| S.D. of 10 Min. Avg's | 11 | 10 | 11 |
| Minimum 10 Min. Avg. | 342 | 353 | 396 |
| Maximum 10 Min. Avg. | 375 | 388 | 423 |
| Coal Feed Rate (kg/hr) | | | |
| Average | 74.2 | 73.9 | 68.5 |
| S.D. of 10 Min. Avg's | 4.4 | 6.9 | 4.5 |
| Initial 30 Min. Avg.[j] | 74.3 | 80.8 | 72.5 |
| Final 30 Min. Avg.[j] | 77.6 | 69.9 | 65.1 |
| Excess Air (%)[o] | | | |
| Average | 96.1 | 87.8 | 100 |
| S.D. of 10 Min. Avg's | 10 | 17 | 13 |
| Initial 30 Min. Avg. | 94.9 | 74.1 | 88.6 |
| Final 30 Min. Avg. | 88.2 | 97.1 | 109 |

## TABLE G1. SUMMARY OF MINIPLANT RUN CONDITIONS
(See explanation of footnotes on pages 185 and 186)

| Run No.[a] | 7.1 | 7.2 | 7.3[p] |
|---|---|---|---|
| Date | 7/25/75 | 8/1/74 | 8/20/74 |
| Run Length (hrs)[b] | 4 | 7 | 2 |
| Cooling Coil Orientation[c] | H | H | H |
| Area of Coils, Total ($m^2$) | 4.62 | 4.62 | 4.62 |
| Limestone Feed | No | No | No |
| Bed Rejection[d] | No | No | No |
| Bed Depth, Settled (m) | | | |
| Start of Run | 1.53 | | |
| End of Run | | | |
| Coal/Limestone Feed Ratio | | | |
| Ca/S Molar Feed Ratio | | | |
| Combustion Efficiency, Entire Run (%)[e] | | | |
| Conditions[f] | | | |
| Time Interval[k] | 14:19-15:49 | 11:10-15:00 | |
| Pressure (kPa)[l] | 912 | 912 | 698 |
| Super. Velocity (m/sec)[m] | | | 2.1 |
| Average[g] | 1.84 | 1.89 | |
| S.D. of 10 Min. Avg's[h] | 0.11 | 0.08 | |
| Minimum 10 Min. Avg.[i] | 1.65 | 1.71 | |
| Maximum 10 Min. Avg.[i] | 1.95 | 2.04 | |
| Temperature, Bed (°C) | | | 880 |
| Average | 876 | 884 | |
| S.D. of 10 Min. Avg's | 65 | 35 | |
| Minimum 10 Min. Avg. | 782 | 809 | |
| Maximum 10 Min. Avg. | 953 | 944 | |
| Temperature, Flue Gas (°C)[n] | | | |
| Average | 440 | 444 | |
| S.D. of 10 Min. Avg's | 31 | 15 | |
| Minimum 10 Min. Avg. | 387 | 416 | |
| Maximum 10 Min. Avg. | 476 | 476 | |
| Coal Feed Rate (kg/hr) | | | 106 |
| Average | 114 | 105 | |
| S.D. of 10 Min. Avg's | 9.1 | 11.3 | |
| Initial 30 Min. Avg.[j] | 108 | 107 | |
| Final 30 Min. Avg.[j] | 109 | 112 | |
| Excess Air (%)[o] | | | |
| Average | 23.2 | 36.7 | |
| S.D. of 10 Min. Avg's | 10 | 16 | |
| Initial 30 Min. Avg. | 29.9 | 36.0 | |
| Final 30 Min. Avg. | 27.2 | 26.6 | |

TABLE G1. SUMMARY OF MINIPLANT RUN CONDITIONS
(See explanation of footnotes on pages 185 and 186)

| Run No.[a] | 7.4 | 8.4[p] | | 9.1 |
|---|---|---|---|---|
| Date | 8/27/74 | 10/9/75 | | 10/24/75 |
| Run Length (hrs)[b] | 4.5 | 11 | | 13.5 |
| Cooling Coil Orientation[c] | H | H | | H |
| Area of Coils, Total ($m^2$) | 4.62 | 4.62 | | 4.62 |
| Limestone Feed | Yes | Yes | | Yes |
| Bed Rejection[d] | No | No | | No |
| Bed Depth, Settled (m) | | | | |
| Start of Run | | 0.58 | | 0.61 |
| End of Run | 1.98 | 1.30 | | 1.17 |
| Coal/Limestone Feed Ratio | 3.0 | 7.35 | | 12.0 |
| Ca/S Molar Feed Ratio | 4.0 | 1.67 | | 1.0 |
| Combustion Efficiency, Entire Run (%)[e] | | 96 | | 96.4 |
| Conditions[f] | | | | |
| Time Interval[k] | 12:30-14:10 | 15:00 | 21:00 | 15:33-23:33 |
| Pressure (kPa)[l] | 912 | 907 | 906 | 932 |
| Super. Velocity (m/sec)[m] | | 1.83 | 1.77 | |
| Average[g] | 1.73 | | | 1.76 |
| S.D. of 10 Min. Avg's[h] | 0.06 | | | 0.03 |
| Minimum 10 Min. Avg.[i] | 1.62 | | | 1.71 |
| Maximum 10 Min. Avg.[i] | 1.80 | | | 1.83 |
| Temperature, Bed (°C) | | 908 | 877 | |
| Average | 877 | | | 881 |
| S.D. of 10 Min. Avg's | 38 | | | 20 |
| Minimum 10 Min. Avg. | 807 | | | 846 |
| Maximum 10 Min. Avg. | 927 | | | 933 |
| Temperature, Flue Gas (°C)[n] | | | | |
| Average | 434 | | | 371 |
| S.D. of 10 Min. Avg's | 23 | | | 23 |
| Minimum 10 Min. Avg. | 407 | | | 343 |
| Maximum 10 Min. Avg. | 476 | | | 422 |
| Coal Feed Rate (kg/hr) | | 75 | 112 | |
| Average | 97.2 | | | 75.7 |
| S.D. of 10 Min. Avg's | 5.1 | | | 13.2 |
| Initial 30 Min. Avg.[j] | 93.5 | | | 52.5 |
| Final 30 Min. Avg.[j] | 97.8 | | | 96.9 |
| Excess Air (%)[o] | | 67 | 15 | |
| Average | 34.3 | | | 80.5 |
| S.D. of 10 Min. Avg's | 13 | | | 37 |
| Initial 30 Min. Avg. | 39.9 | | | 150 |
| Final 30 Min. Avg. | 32.2 | | | 35.7 |

### TABLE G1. SUMMARY OF MINIPLANT RUN CONDITIONS
(See explanation of footnotes on pages 185 and 186)

| | | | |
|---|---|---|---|
| Run No.[a] | 10.1 | 10.2 | 10.3 |
| Date | 11/21/74 | 11/26/74 | 12/10/74 |
| Run Length (hrs)[b] | 10 | 10.5 | 6 |
| Cooling Coil Orientation[c] | H/V | H/V | H/V |
| Area of Coils, Total ($m^2$) | 2.75 | 2.75 | 2.75 |
| Limestone Feed | Yes | Yes | Yes |
| Bed Rejection[d] | Yes | No | Yes |
| Bed Depth, Settled (m) | | | |
| Start of Run | 0.61 | 0.58 | 1.12 |
| End of Run | 0.58 | 1.12 | |
| Coal/Limestone Feed Ratio | 10 | 10 | 10 |
| Ca/S Molar Feed Ratio | 1.2 | 1.2 | 1.2 |
| Combustion Efficiency, Entire Run (%)[e] | 97.5 | 87.7 | 95 |
| Conditions[f] | | | |
| Time Interval[k] | 17:18-23.38 | 12:00-14:40 | 13:40-16:20 |
| Pressure (kPa)[l] | 901 | 901 | 912 |
| Super. Velocity (m/sec)[m] | | | |
| Average[g] | 1.96 | 1.84 | 2.04 |
| S.D. of 10 Min. Avg's[h] | 0.03 | 0.05 | |
| Minimum 10 Min. Avg.[i] | 1.89 | 1.74 | 1.89 |
| Maximum 10 Min. Avg.[i] | 2.05 | 1.92 | 2.11 |
| Temperature, Bed (°C) | | | |
| Average | 916 | 891 | 904 |
| S.D. of 10 Min. Avg's | 17 | 22 | 35 |
| Minimum 10 Min. Avg. | 888 | 842 | 821 |
| Maximum 10 Min. Avg. | 972 | 923 | 947 |
| Temperature, Flue Gas (°C)[n] | | | |
| Average | 513 | 523 | 541 |
| S.D. of 10 Min. Avg's | 6 | 9 | 10 |
| Minimum 10 Min. Avg. | 493 | 508 | 527 |
| Maximum 10 Min. Avg. | 530 | 546 | 563 |
| Coal Feed Rate (kg/hr) | | | |
| Average | 65.2 | 71.0 | 77.7 |
| S.D. of 10 Min. Avg's | 5.4 | 6.1 | 4.2 |
| Initial 30 Min. Avg.[j] | 56.3 | 73.7 | 80.2 |
| Final 30 Min. Avg.[j] | 68.2 | 75.0 | 74.5 |
| Excess Air (%)[o] | | | |
| Average | 114 | 87.6 | 93.9 |
| S.D. of 10 Min. Avg's | 18 | 19 | 12.4 |
| Initial 30 Min. Avg. | 146 | 81.7 | 90.6 |
| Final 30 Min. Avg. | 105 | 77.8 | 101 |

TABLE G1. SUMMARY OF MINIPLANT RUN CONDITIONS
(See explanation of footnotes on pages 185 and 186)

| Run No.[a] | 11.1 | 11.2 | 12.1 |
|---|---|---|---|
| Date | 12/17/74 | 12/23/74 | 1/8/75 |
| Run Length (hrs)[b] | 9.5 | 10 | 8.5 |
| Cooling Coil Orientation[c] | H/V | H/V | H/V |
| Area of Coils, Total ($m^2$) | 2.75 | 2.75 | 2.75 |
| Limestone Feed | No | No | Yes |
| Bed Rejection[d] | No | No | No |
| Bed Depth, Settled (m) | | | |
| Start of Run | 0.61 | 0.84[q] | 0.76 |
| End of Run | 0.48 | 0.61 | 1.27 |
| Coal/Limestone Feed Ratio | -- | -- | 10 |
| Ca/S Molar Feed Ratio | -- | -- | 1.2 |
| Combustion Efficiency, Entire Run (%)[e] | 96.9 | 96.6 | 97 |
| Conditions[f] | | | |
| Time Interval[k] | 12:20-17:10 | 12:00-17:30 | 11:29-19:19 |
| Pressure (kPa)[l] | 915 | 912 | 922 |
| Super. Velocity (m/sec)[m] | | | |
| Average[g] | 2.05 | 1.89 | 1.78 |
| S.D. of 10 Min. Avg's[h] | 0.03 | 0.04 | 0.03 |
| Minimum 10 Min. Avg.[i] | 2.01 | 1.74 | 1.71 |
| Maximum 10 Min. Avg.[i] | 2.14 | 1.95 | 1.86 |
| Temperature, Bed (°C) | | | |
| Average | 909 | 915 | 903 |
| S.D. of 10 Min. Avg's | 16 | 28 | 22 |
| Minimum 10 Min. Avg. | 876 | 820 | 849 |
| Maximum 10 Min. Avg. | 954 | 954 | 963 |
| Temperature, Flue Gas (°C)[n] | | | |
| Average | 507 | 514 | 527 |
| S.D. of 10 Min. Avg's | 15 | 12 | 39 |
| Minimum 10 Min. Avg. | 475 | 468 | 482 |
| Maximum 10 Min. Avg. | 537 | 533 | 623 |
| Coal Feed Rate (kg/hr) | | | |
| Average | 61.9 | 69.1 | 80.2 |
| S.D. of 10 Min. Avg's | 1.5 | 2.6 | 14.2 |
| Initial 30 Min. Avg.[j] | 61.8 | 66.7 | 67.1 |
| Final 30 Min. Avg.[j] | 62.0 | 69.1 | 110 |
| Excess Air (%)[o] | | | |
| Average | 139 | 95.8 | 66.5 |
| S.D. of 10 Min. Avg's | 6.0 | 7.8 | 26 |
| Initial 30 Min. Avg. | 141 | 104 | 93.5 |
| Final 30 Min. Avg. | 139 | 95.1 | 18.9 |

## TABLE G1. SUMMARY OF MINIPLANT RUN CONDITIONS

(See explanation of footnotes on pages 185 and 186)

| Run No.[a] | 12.2 | 13.2 |
|---|---|---|
| Date | 1/16/75 | 1/30/75 |
| Run Length (hrs)[b] | 8 | 10 |
| Cooling Coil Orientation[c] | H/V | H/V |
| Area of Coils, Total ($m^2$) | 2.75 | 2.75 |
| Limestone Feed | Yes | Yes |
| Bed Rejection[d] | No | No |
| Bed Depth, Settled (m) | | |
| Start of Run | 1.27 | 0.89 |
| End of Run | 1.80 | 1.60 |
| Coal/Limestone Feed Ratio | 10 | 10 |
| Ca/S Molar Feed Ratio | 1.2 | 1.2 |
| Combustion Efficiency, Entire Run (%)[e] | 93 | 96.7 |
| Conditions[f] | | |
| Time Interval[k] | 14:22-20:22 | 10:20-19:30 |
| Pressure (kPa)[l] | 912 | 912 |
| Super. Velocity (m/sec)[m] | | |
| Average[g] | 1.83 | 1.86 |
| S.D. of 10 Min. Avg's[h] | 0.04 | 0.03 |
| Minimum 10 Min. Avg.[i] | 1.77 | 1.77 |
| Maximum 10 Min. Avg.[i] | 1.92 | 1.92 |
| Temperature, Bed (°C) | | |
| Average | 896 | 910 |
| S.D. of 10 Min. Avg's | 11 | 13 |
| Minimum 10 Min. Avg. | 878 | 874 |
| Maximum 10 Min. Avg. | 923 | 949 |
| Temperature, Flue Gas (°C)[n] | | |
| Average | 647 | 607 |
| S.D. of 10 Min. Avg's | 70 | 51 |
| Minimum 10 Min. Avg. | 549 | 538 |
| Maximum 10 Min. Avg. | 764 | 719 |
| Coal Feed Rate (kg/hr) | | |
| Average | 107 | 91.9 |
| S.D. of 10 Min. Avg's | 16.7 | 12.2 |
| Initial 30 Min. Avg.[j] | 84.5 | 79.8 |
| Final 30 Min. Avg.[j] | 134 | 120 |
| Excess Air (%)[o] | | |
| Average | 27.3 | 48.7 |
| S.D. of 10 Min. Avg's | 18 | 18 |
| Initial 30 Min. Avg. | 54.6 | 69.4 |
| Final 30 Min. Avg. | 0 | 10.5 |

TABLE G1. SUMMARY OF MINIPLANT RUN CONDITIONS
(See explanation of footnotes on pages 185 and 186)

| Run No.[a] | 14.1 | | 14.2 |
|---|---|---|---|
| Date | 2/27/75 | | 3/10/75 |
| Run Length (hrs)[b] | 24 | | 27.5 |
| Cooling Coil Orientation[c] | V/H | | V/H |
| Area of Coils, Total ($m^2$) | 1.98 | | 1.98 |
| Limestone Feed | Yes | | Intermittent |
| Bed Rejection[d] | No | | No |
| Bed Depth, Settled (m) | | | |
| Start of Run | 0.84 | | 1.33 |
| End of Run | 1.33 | | 2.00 |
| Coal/Limestone Feed Ratio | 10 | | 10 |
| Ca/S Molar Feed Ratio | 1.2 | | 1.2 |
| Combustion Efficiency, Entire Run (%)[e] | 96.5 | | 93.7 |
| Conditions[f] | | | |
| Time Interval[k] | 16:40-21:50 | 1:40-8:30 | 18:52-7:12 |
| Pressure (kPa)[l] | 902 | 912 | 912 |
| Super. Velocity (m/sec)[m] | | | |
| Average[g] | 1.84 | 1.83 | 1.91 |
| S.D. of 10 Min. Avg's[h] | 0.02 | 0.02 | 0.03 |
| Minimum 10 Min. Avg.[i] | 1.80 | 1.80 | 1.83 |
| Maximum 10 Min. Avg.[i] | 1.86 | 1.86 | 1.99 |
| Temperature, Bed (°C) | | | |
| Average | 909 | 916 | 934 |
| S.D. of 10 Min. Avg's | 13 | 7 | 7 |
| Minimum 10 Min. Avg. | 882 | 904 | 913 |
| Maximum 10 Min. Avg. | 934 | 947 | 960 |
| Temperature, Flue Gas (°C)[n] | | | |
| Average | 589 | 679 | 796 |
| S.D. of 10 Min. Avg's | 18 | 12 | 54 |
| Minimum 10 Min. Avg. | 556 | 658 | 681 |
| Maximum 10 Min. Avg. | 642 | 714 | 851 |
| Coal Feed Rate (kg/hr) | | | |
| Average | 70.3 | 80.8 | 110 |
| S.D. of 10 Min. Avg's | 2.4 | 2.5 | 4.9 |
| Initial 30 Min. Avg.[j] | 67.9 | 77.7 | 108 |
| Final 30 Min. Avg.[j] | 72.9 | 81.4 | 110 |
| Excess Air (%)[o] | | | |
| Average | 86.8 | 61.0 | 22.5 |
| S.D. of 10 Min. Avg's | 7 | 5 | 6 |
| Initial 30 Min. Avg. | 95.8 | 67.1 | 24.8 |
| Final 30 Min. Avg. | 79.6 | 60.5 | 22.6 |

## TABLE G1. SUMMARY OF MINIPLANT RUN CONDITIONS
(See explanation of footnotes on pages 185 and 186)

| | | | |
|---|---|---|---|
| Run No.[a] | 15.1 | | 15.2 |
| Date | 3/20/75 | | 3/26/75 |
| Run Length (hrs)[b] | 24 | | 11 |
| Cooling Coil Orientation[c] | V/H | | V/H |
| Area of Coils, Total ($m^2$) | 1.98 | | 1.98 |
| Limestone Feed | Yes | | Yes |
| Bed Rejection[d] | Intermittent | | Yes |
| Bed Depth, Settled (m) | | | |
| Start of Run | 1.04 | | 1.92 |
| End of Run | 1.93 | | 1.80 |
| Coal/Limestone Feed Ratio | 10 | | 10 |
| Ca/S Molar Feed Ratio | 1.2 | | 1.2 |
| Combustion Efficiency, Entire Run (%)[e] | 96.5 | | 96.8 |
| Conditions[f] | | | |
| Time Interval[k] | 14:10-19:50 | 4:00-9:40 | 1:10-8:20 |
| Pressure (kPa)[l] | 907 | 902 | 912 |
| Super. Velocity (m/sec)[m] | | | |
| Average[g] | 1.92 | 2.09 | 1.83 |
| S.D. of 10 Min. Avg's[h] | 0.03 | 0.03 | 0.01 |
| Minimum 10 Min. Avg.[i] | 1.86 | 2.04 | 1.80 |
| Maximum 10 Min. Avg.[i] | 1.98 | 2.17 | 1.86 |
| Temperature, Bed (°C) | | | |
| Average | 910 | 902 | 916 |
| S.D. of 10 Min. Avg's | 6 | 7 | 8 |
| Minimum 10 Min. Avg. | 889 | 891 | 902 |
| Maximum 10 Min. Avg. | 924 | 927 | 948 |
| Temperature, Flue Gas (°C)[n] | | | |
| Average | 710 | 857 | 678 |
| S.D. of 10 Min. Avg's | 46 | 13 | 13 |
| Minimum 10 Min. Avg. | 641 | 827 | 653 |
| Maximum 10 Min. Avg. | 794 | 877 | 714 |
| Coal Feed Rate (kg/hr) | | | |
| Average | 96.8 | 121 | 80.3 |
| S.D. of 10 Min. Avg's | 15.4 | 8.7 | 3.1 |
| Initial 30 Min. Avg.[j] | 77.0 | 125 | 74.0 |
| Final 30 Min. Avg.[j] | 119 | 123 | 80.1 |
| Excess Air (%)[o] | | | |
| Average | 44.2 | 24.0 | 62.2 |
| S.D. of 10 Min. Avg's | 20 | 8 | 6 |
| Initial 30 Min. Avg. | 78.9 | 20.4 | 76.2 |
| Final 30 Min. Avg. | 14.2 | 22.5 | 63.3 |

TABLE G1. SUMMARY OF MINIPLANT RUN CONDITIONS
(See explanation of footnotes on pages 185 and 186)

| | | | |
|---|---|---|---|
| Run No.[a] | 15.3 | | 15.4 |
| Date | 3/31/75 | | 4/2/75 |
| Run Length (hrs)[b] | 16 | | 15 |
| Cooling Coil Orientation[c] | V/H | | V/H |
| Area of Coils, Total ($m^2$) | 1.98 | | 1.98 |
| Limestone Feed | Yes | | Yes |
| Bed Rejection[d] | Yes | | Yes |
| Bed Depth, Settled (m) | | | |
| Start of Run | 1.80 | | 2.29 |
| End of Run | 2.29 | | |
| Coal/Limestone Feed Ratio | 10 | | 10 |
| Ca/S Molar Feed Ratio | 1.2 | | 1.2 |
| Combustion Efficiency, Entire Run (%)[e] | 91.9 | | 98.0 |
| Conditions[f] | | | |
| Time Interval[k] | 10:40-16:00 | 4:00-10:00 | 14:20-19:10 |
| Pressure (kPa)[l] | 921 | 902 | 912 |
| Super. Velocity (m/sec)[m] | | | |
| Average[g] | 1.87 | 2.09 | 2.03 |
| S.D. of 10 Min. Avg's[h] | 0.06 | 0.03 | 0.02 |
| Minimum 10 Min. Avg.[i] | 1.76 | 2.04 | 1.99 |
| Maximum 10 Min. Avg.[i] | 2.00 | 2.17 | 2.10 |
| Temperature, Bed (°C) | | | |
| Average | 889 | 901 | 905 |
| S.D. of 10 Min. Avg's | 13 | 8 | 14 |
| Minimum 10 Min. Avg. | 863 | 891 | 880 |
| Maximum 10 Min. Avg. | 914 | 927 | 924 |
| Temperature, Flue Gas (°C)[n] | | | |
| Average | 761 | 858 | 803 |
| S.D. of 10 Min. Avg's | 13 | 13 | 55 |
| Minimum 10 Min. Avg. | 732 | 827 | 736 |
| Maximum 10 Min. Avg. | 786 | 879 | 887 |
| Coal Feed Rate (kg/hr) | | | |
| Average | 108 | 122 | 119 |
| S.D. of 10 Min. Avg's | 4.6 | 5.4 | 11.9 |
| Initial 30 Min. Avg.[j] | 106 | 125 | 105 |
| Final 30 Min. Avg.[j] | 107 | 122 | 134 |
| Excess Air (%)[o] | | | |
| Average | 27.1 | 23.6 | 25.0 |
| S.D. of 10 Min. Avg's | 5 | 6 | 12 |
| Initial 30 Min. Avg. | 31.1 | 20.4 | 39.1 |
| Final 30 Min. Avg. | 28.4 | 23.4 | 11.6 |

TABLE G1. SUMMARY OF MINIPLANT RUN CONDITIONS
(See explanation of footnotes on pages 185 and 186)

| | | | |
|---|---|---|---|
| Run No.[a] | 16.1 | | 16.3 |
| Date | 5/5/75 | | 5/14/75 |
| Run Length (hrs)[b] | 16.5 | | 25 |
| Cooling Coil Orientation[c] | V | | V |
| Area of Coils, Total ($m^2$) | 2.20 | | 2.20 |
| Limestone Feed | Yes | | Yes |
| Bed Rejection[d] | No | | Yes |
| Bed Depth, Settled (m) | | | |
| Start of Run | 0.78 | | 0.84 |
| End of Run | 1.75 | | 1.04 |
| Coal/Limestone Feed Ratio | 10 | | 10 |
| Ca/S Molar Feed Ratio | 1.45 | | 1.45 |
| Combustion Efficiency, Entire Run (%)[e] | 92.4 | | |
| Conditions[f] | | | |
| Time Interval[k] | 18:05-0:45 | 3:05-6:55 | 9:50-13:20 |
| Pressure (kPa)[l] | 821 | 826 | 932 |
| Super. Velocity (m/sec)[m] | | | |
| Average[g] | 1.83 | 1.84 | 2.05 |
| S.D. of 10 Min. Avg's[h] | 0.02 | 0.04 | 0.02 |
| Minimum 10 Min. Avg.[i] | 1.80 | 1.80 | 2.01 |
| Maximum 10 Min. Avg.[i] | 1.89 | 1.92 | 2.10 |
| Temperature, Bed (°C) | | | |
| Average | 882 | 875 | 893 |
| S.D. of 10 Min. Avg's | 5 | 8 | 5 |
| Minimum 10 Min. Avg. | 870 | 865 | 876 |
| Maximum 10 Min. Avg. | 891 | 887 | 898 |
| Temperature, Flue Gas (°C)[n] | | | |
| Average | 859 | 914 | 784 |
| S.D. of 10 Min. Avg's | 74 | 19 | 29 |
| Minimum 10 Min. Avg. | 714 | 866 | 731 |
| Maximum 10 Min. Avg. | 953 | 951 | 829 |
| Coal Feed Rate (kg/hr) | | | |
| Average | 112 | 128 | 117 |
| S.D. of 10 Min. Avg's | 9.6 | 8.9 | 6.2 |
| Initial 30 Min. Avg.[j] | 94.5 | 122 | 112 |
| Final 30 Min. Avg.[j] | 122 | 134 | 126 |
| Excess Air (%)[o] | | | |
| Average | 8.9 | -3.1 | 31.0 |
| S.D. of 10 Min. Avg's | 10.3 | 7.4 | 6.9 |
| Initial 30 Min. Avg. | 29.8 | 3.4 | 37.5 |
| Final 30 Min. Avg. | 0.1 | -9.1 | 22.1 |

TABLE G1. SUMMARY OF MINIPLANT RUN CONDITIONS
(See explanation of footnotes on pages 185 and 186)

| Run No.[a] | 17.1 | | 18.1 |
|---|---|---|---|
| Date | 5/27/75 | | 6/9/75 |
| Run Length (hrs)[b] | 55 | | 23 |
| Cooling Coil Orientation[c] | V | | V |
| Area of Coils, Total ($m^2$) | 2.20 | | 1.10 |
| Limestone Feed | Yes | No | Yes |
| Bed Rejection[d] | Yes | No | Intermittent |
| Bed Depth, Settled (m) | | | |
| Start of Run | 0.74 | | 0.66 |
| End of Run | 1.95 | | |
| Coal/Limestone Feed Ratio | 10 | — | 10 |
| Ca/S Molar Feed Ratio | 1.45 | -- | 1.45 |
| Combustion Efficiency, Entire Run (%)[e] | 95.1 | | |
| Conditions[f] | | | |
| Time Interval[k] | 15:51-1:31 | 23:31-6:11 | 13:50-3:00 |
| Pressure (kPa)[l] | 906 | 913 | 935 |
| Super. Velocity (m/sec)[m] | | | |
| Average[g] | 2.13 | 2.03 | 1.71 |
| S.D. of 10 Min. Avg's[h] | 0.05 | 0.06 | 0.06 |
| Minimum 10 Min. Avg.[i] | 2.04 | 1.86 | 1.59 |
| Maximum 10 Min. Avg.[i] | 2.26 | 2.13 | 1.80 |
| Temperature, Bed (°C) | | | |
| Average | 898 | 863 | 899 |
| S.D. of 10 Min. Avg's | 4 | 7 | 10 |
| Minimum 10 Min. Avg. | 891 | 841 | 877 |
| Maximum 10 Min. Avg. | 912 | 869 | 921 |
| Temperature, Flue Gas (°C)[n] | | | |
| Average | 902 | 894 | 850 |
| S.D. of 10 Min. Avg's | 28 | 10 | 24 |
| Minimum 10 Min. Avg. | 847 | 867 | 791 |
| Maximum 10 Min. Avg. | 934 | 912 | 877 |
| Coal Feed Rate (kg/hr) | | | |
| Average | 133 | 124 | 82.6 |
| S.D. of 10 Min. Avg's | 13.1 | 5.0 | 5.4 |
| Initial 30 Min. Avg.[j] | 118 | 120 | 72.2 |
| Final 30 Min. Avg.[j] | 140 | 130 | 88.3 |
| Excess Air (%)[o] | | | |
| Average | 16.7 | 35.3 | 57.3 |
| S.D. of 10 Min. Avg's | 11.7 | 6.6 | 9.2 |
| Initial 30 Min. Avg. | 28.1 | 39.6 | 84.4 |
| Final 30 Min. Avg. | 15.8 | 29.0 | 46.2 |

## TABLE G1. SUMMARY OF MINIPLANT RUN CONDITIONS

(See explanation of footnotes on pages 185 and 186)

| | | | |
|---|---|---|---|
| Run No.[a] | 18.3[s] | 19.2 | 19.3 |
| Date | 6/23/75 | 7/31/75 | 8/4/75 |
| Run Length (hrs)[b] | 100 | 10.5 | 6 |
| Cooling Coil Orientation[c] | V | V | V |
| Area of Coils, Total ($m^2$) | 1.10 | 2.21 | 2.21 |
| Limestone Feed | Intermittent[t] | Yes | Yes |
| Bed Rejection[d] | Intermittent[t] | No | First 3 hrs |
| Bed Depth, Settled (m) | | | |
| Start of Run | 0.76 | 0.71 | 1.45 |
| End of Run | 0.98 | 1.45 | 1.58 |
| Coal/Limestone Feed Ratio | 10 | 10 | 10 |
| Ca/S Molar Feed Ratio | 1.45 | 1.45 | 1.45 |
| Combustion Efficiency, Entire Run (%)[e] | | 96.2 | 95.8 |
| Conditions[f] | | | |
| Time Interval[k] | 12:56-23:13 (6/25/75)[s] | 11:00-20:10 | 12:00-16:20 |
| Pressure (kPa)[l] | 958 | 922 | 922 |
| Super. Velocity (m/sec)[m] | | | |
| Average[g] | 1.86 | 1.81 | 1.89 |
| S.D. of 10 Min. Avg's[h] | 0.01 | 0.02 | 0.01 |
| Minimum 10 Min. Avg.[i] | 1.83 | 1.77 | 1.86 |
| Maximum 10 Min. Avg.[i] | 1.89 | 1.83 | 1.89 |
| Temperature, Bed (°C) | | | |
| Average | 910 | 874 | 879 |
| S.D. of 10 Min. Avg's | 1 | 4 | 3 |
| Minimum 10 Min. Avg. | 908 | 866 | 873 |
| Maximum 10 Min. Avg. | 912 | 882 | 883 |
| Temperature, Flue Gas (°C)[n] | | | |
| Average | 901 | 785 | 883 |
| S.D. of 10 Min. Avg's | 3 | 74 | 10 |
| Minimum 10 Min. Avg. | 894 | 664 | 855 |
| Maximum 10 Min. Avg. | 904 | 887 | 894 |
| Coal Feed Rate (kg/hr) | | | |
| Average | 89.0 | 110 | 136 |
| S.D. of 10 Min. Avg's | 1.5 | 15.8 | 2.2 |
| Initial 30 Min. Avg.[j] | 90.4 | 82.7 | 136 |
| Final 30 Min. Avg.[j] | 89.5 | 133 | 136 |
| Excess Air (%)[o] | | | |
| Average | 61.5 | 30.4 | 5.7 |
| S.D. of 10 Min. Avg's | 3.0 | 19.5 | 1.6 |
| Initial 30 Min. Avg. | 59.9 | 70.0 | 6.0 |
| Final 30 Min. Avg. | 60.9 | 6.0 | 6.4 |

Notes for Table G1.

Runs summarized represent those which achieved a reasonable period of continuous, well-controlled operation. For runs made early in the shakedown program, this arbitrary period was selected to be at least one hour, while for later runs, a 5-10 hour minimum was chosen. Also see comment h.

[a] Run No. was assigned in a sequential manner with the number preceding the decimal point specifying the run series whose first run was made using an initial bed of fresh limestone. Subsequent runs within a series, specified by the number after the decimal point, used the final bed from the preceding run as the starting bed.

[b] Run Length is defined as the period between the start and end of coal feeding and does not include periods when feeding may have been interrupted.

[c] Cooling Coil Orientation signifies the orientation of the cooling loops with H indicating horizontal, V indicating vertical, while mixed orientation is indicated using both symbols with the dominant orientation listed first.

[d] Bed Rejection indicates whether a portion of the fluidized bed was purposely being removed during a run in order to limit growth of solids inventory within the combustor when limestone was fed with coal.

[e] Combustion Efficiency for a run is based on fraction of feed carbon found in final solids. Since some uncombusted carbon may have escaped with flue gas, initially calculated efficiency was adjusted downward using calculated cyclone efficiency and assuming carbon composition in escaping solids equal to that in solids captured by second stage cyclone.

[f] Conditions listed (pressure, superficial velocity, etc.) apply to time interval indicated. Data characterizing mini-plant operation are automatically recorded at one-minute intervals. Volume of data is reduced by averaging data, generally over consecutive 10-minute periods.

[g] Average is the true average of all one-minute readings over the entire time interval.

[h] S.D. of 10 Min. Avg's is the standard deviation of the 10-minute averages over the interval.

[i] Minimum (Maximum) 10 Min. Avg. represents the minimum (maximum) value of the consecutive 10-minute averages over the time interval. It is presented for those quantities (e.g., superficial velocity, bed temperature) which were purposely controlled at approximately constant values during a run.

j Initial (Final) 30 Min. Avg. is the average of the one-minute readings over the first (last) 30 minutes of the time interval listed. It is presented for those quantities which do not necessarily remain constant during a run but which change continuously in a regular fashion during a run.

k Time Interval represents a period of continuous, well-controlled operation during a specific run. In general, especially for long duration runs, more than one such interval existed. If conditions were essentially equivalent for different intervals, only one is presented. If substantial changes in operating conditions occurred, these are reflected by listing more than one interval.

l Pressure was effectively constant (variation of <2%) and, accordingly, only one value is listed except where noted otherwise. It was measured above the fluidizing bed.

m Superficial Velocity was calculated using the total air flow (combustion plus solids transport) to the combustor with temperature equal to the bed temperature as defined below and pressure as noted in table.

n Bed Temperature is the average of four readings taken over a distance of 1.14 meters above the fluidizing grid.

o Excess Air is a calculated value based on the total air flow to the combustor and the coal feed rate, and assumes complete combustion of coal. Accordingly, values listed are somewhat biased on the high side, especially at excess air levels below 10-15%.

p Conditions shown are typical values. Data logger was inoperable.

q Fresh limestone added to final bed from previous run before starting run.

r Pressure varied from 880 to 970 kPa.

s Data logger was inoperable during much of the run. Data logger was operating properly during time intervals shown. The combustor performed steadily during most of the run.

t No limestone was fed or bed rejected over time intervals selected.

## TABLE G2. MINIPLANT $NO_x$ EMISSION DATA

| Run No.[a] | Time[b] | $NO_x$ (ppm)[c] | lb. $NO_2/10^6$ BTU[d] | % $O_2$ | % Excess Air[e] |
|---|---|---|---|---|---|
| 10.3 | | 90 | 0.19 | ∿9.2 | ∿80 |
| 11.1 | | 45 | 0.13 | ∿12.1 | ∿140 |
| 11.2 | | 140-185 | 0.35-0.46 | ∿10.7 | ∿105 |
| 12.1 | 14:15 | 170 | 0.33 | 6.9 | 50 |
| " | 14:30 | 165 | 0.34 | 7.4 | 55 |
| " | 14:45 | 160 | 0.33 | 7.0 | 51 |
| " | 15:00 | 170 | 0.38 | 7.6 | 58 |
| " | 15:15 | 160 | 0.33 | 6.8 | 49 |
| " | 15:30 | 155 | 0.29 | 6.0 | 40 |
| " | 15:45 | 165 | 0.35 | 6.5 | 46 |
| " | 16:00 | 170 | 0.29 | 5.8 | 39 |
| " | 16:15 | 160 | 0.30 | 6.4 | 44 |
| " | 16:30 | 160 | 0.29 | 5.7 | 38 |
| " | 16:45 | 165 | 0.29 | 5.6 | 37 |
| " | 17:00 | 175 | 0.32 | 7.4 | 55 |
| " | 17:15 | 160 | 0.25 | 4.6 | 28 |
| " | 17:30 | 155 | 0.24 | 4.5 | 28 |
| " | 17:45 | 170 | 0.25 | 4.6 | 28 |
| " | 18:00 | 150 | 0.20 | 3.2 | 18 |
| " | 18:15 | 150 | 0.22 | 3.7 | 22 |
| " | 18:45 | 160 | 0.23 | 3.6 | 21 |
| 13.2 | 13:50-14:00 | 130 | 0.26 | 6.5 | 46 |
| " | 15:20-15:30 | 140 | 0.27 | 5.3 | 34 |
| " | 15:50-16:00 | 135 | 0.25 | 5.0 | 32 |
| " | 16:20-16:30 | 135 | 0.24 | 4.5 | 28 |
| " | 16:50-17:00 | 125 | 0.21 | 3.8 | 22 |
| " | 18:00-18:10 | 115 | 0.19 | 3.0 | 17 |
| " | 19:50-20:00 | 75 | 0.10 | 1.3 | 7 |
| 16.1 | 19:00 | 225 | 0.32 | 3.2 | 18 |
| " | 20:00 | 225 | 0.31 | 2.0 | 10 |
| " | 21:00 | 205 | 0.26 | 2.0 | 10 |
| " | 22:00 | 140 | 0.18 | 1.2 | 6 |
| " | 23:00 | 130 | 0.16 | 0.5 | 3 |
| " | 24:00 | 125 | 0.15 | 0.4 | 2 |
| 18.3 | | 140 | 0.29 | ∿6.7 | ∿48 |
| 19.2 | 11:25-11:35 | 210 | 0.43 | | ∿65 |
| " | 12:25-12:35 | 175 | 0.33 | 6.4 | 44 |
| " | 13:25-13:35 | 170 | 0.32 | 5.2 | 33 |
| " | 14:25-14:35 | 160 | 0.26 | 5.1 | 32 |
| " | 15:25-15:35 | 140 | 0.22 | 3.6 | 21 |
| " | 16:25-16:35 | 120 | 0.18 | 2.8 | 15 |
| " | 17:25-17:35 | 115 | 0.17 | 2.6 | 15 |
| " | 19:25-19:35 | 90 | 0.12 | 1.7 | 9 |

## TABLE G2. (CONTINUED) MINIPLANT $NO_x$ EMISSION DATA

| Run No.[a] | Time[b] | $NO_x$ (ppm)[c] | lb. $NO_2/10^6$ BTU[d] | % $O_2$ | % Excess Air[e] |
|---|---|---|---|---|---|
| 19.3 | 14:25-14:35 | 65 | 0.08 | 1.7 | 9 |
| " | 14:35-14:45 | 80 | 0.10 | 1.0 | 5 |
| " | 15:25-15:35 | 45 | 0.06 | 2.1 | 11 |
| " | 15:35-15:45 | 80 | 0.10 | 1.4 | 7 |

[a] Refer to Table G1, Summary of Miniplant Run Conditions for operating conditions.

[b] When time interval is indicated, data represent averaged values.

[c] Data obtained by infrared (NO measured) or chemiluminescence (NO + $NO_2$ measured) analysis. Actual $NO_2$ content was less than 10-15% of total $NO_x$. In practice, both techniques gave essentially equivalent results.

[d] Equivalent $NO_2$ based on measured concentration of NO or $NO_x$.

[e] Based on flue gas $O_2$ content.

## TABLE G3. MINIPLANT SOLIDS ANALYSES

| Run No. | 11.1 | | | | | |
|---|---|---|---|---|---|---|
| | Wgt (kg) | %Ca | %S | $\%SO_4^{=}$ | %C | $\%CO_3^{=}$ |
| Coal Feed | 540.2 | - | 2.6 | - | 76.5 | - |
| Limestone Feed | 0.0 | - | - | - | - | - |
| Initial Bed (Fresh) | 68.0 | 39.1 | - | - | - | 59.6 |
| Final Bed | 50.8 | 35.1 | - | 26.5 | - | 1.53 |
| Bed Withdrawal | 0.0 | - | - | - | - | - |
| First Stage Cyclone[a] | 12.7 | 17.8 | 2.9 | 7.3 | 16.4 | - |
| Second Stage Cyclone | 40.0 | 7.4 | 1.5 | 4.4 | 23.3 | - |

---

[a] Solids from dipleg in first stage cyclone.

| Run No. | 11.2 | | | | | |
|---|---|---|---|---|---|---|
| | Wgt (kg) | %Ca | %S | $\%SO_4^{=}$ | %C | $\%CO_3^{=}$ |
| Coal Feed | 441.8 | - | 2.6 | - | 76.5 | - |
| Limestone Feed | 0.0 | - | - | - | - | - |
| Initial Bed[b] | 50.8 | 35.1 | - | 26.5 | - | 1.53 |
| Final Bed | 64.4 | 29.2 | - | 35.0 | - | 4.21 |
| Bed Withdrawal | 0.0 | - | - | - | - | - |
| First Stage Cyclone | 27.2 | 15.3 | - | 8.5 | 18.5 | - |
| Second Stage Cyclone | 24.1 | 2.9 | - | 3.5 | 26.6 | - |

---

[b] Does not include 36.3 kg fresh limestone added to bed before start of run.

## TABLE G3. MINIPLANT SOLIDS ANALYSES (CONTINUED)

| Run No. | 12.1 | | | | | |
|---|---|---|---|---|---|---|
| | Wgt (kg) | %Ca | %S | %$SO_4^=$ | %C | %$CO_3^=$ |
| Coal Feed | 619.2 | - | 2.6 | - | 76.5 | - |
| Limestone Feed | 52.6 | - | - | - | - | - |
| Initial Bed (Fresh) | 83.9 | 39.1 | - | - | - | 59.6 |
| Final Bed | 131.1 | 38.0 | 11.7 | 34.2 | 2.4 | 7.7 |
| Bed Withdrawal | 0.0 | - | - | - | - | - |
| First Stage Cyclone | 10.9 | 29.4 | 4.5 | 12.6 | 8.3 | 12.1 |
| Second Stage Cyclone | 51.8 | 11.6 | 3.1 | 8.7 | 17.3 | 2.4 |

| Run No. | 12.2 | | | | | |
|---|---|---|---|---|---|---|
| | Wgt (kg) | %Ca | %S | %$SO_4^=$ | %C | %$CO_3^=$ |
| Coal Feed | 793.4 | - | 2.6 | - | 76.5 | - |
| Limestone Feed | 78.9 | - | - | - | - | - |
| Initial Bed | 131.1 | 38.0 | 11.7 | 34.2 | 2.4 | 7.7 |
| Final Bed | 176.9 | 34.3 | 12.8 | 34.0 | 2.5 | 5.4 |
| Bed Withdrawal | 0.0 | - | - | - | - | - |
| First Stage Cyclone | 19.4 | - | 10.2 | 26.4 | 2.1 | 6.4 |
| Second Stage Cyclone | 120.1 | 11.6 | 5.2 | 10.9 | 30.8 | 1.6 |

TABLE G3. MINIPLANT SOLIDS ANALYSES (CONTINUED)

| Run No. | 13.2 | | | | | |
|---|---|---|---|---|---|---|
| | Wgt (kg) | %Ca | %S | $\%SO_4^=$ | %C | $\%CO_3^=$ |
| Coal Feed | 887.7 | - | 2.4 | - | 76.1 | - |
| Limestone Feed | 88.9 | 39.1 | - | - | - | 59.6 |
| Initial Bed[c] | 102.1 | 39.1 | - | - | - | 59.6 |
| Final Bed | 175.1 | 35.5 | 12.2 | 35.1 | 2.2 | 9.1 |
| Bed Withdrawal | 0.0 | - | - | - | - | - |
| First Stage Cyclone | 20.9 | 27.3 | 4.8 | 13.5 | 4.4 | 6.1 |
| Second Stage Cyclone | 59.0 | 5.5 | 2.7 | 6.2 | 30.7 | 1.0 |

---

[c] Essentially fresh limestone

| Run No. | 14.1 | | | | | |
|---|---|---|---|---|---|---|
| | Wgt (kg) | %Ca | %S | $\%SO_4^=$ | %C | $\%CO_3^=$ |
| Coal Feed | 1548.6 | - | 2.4 | - | 76.1 | - |
| Limestone Feed | 129.7 | 39.1 | - | - | - | 59.6 |
| Initial Bed (Fresh) | 93.6 | 39.1 | - | - | - | 59.6 |
| Final Bed | 141.1 | 39.0 | - | 34.3 | 1.3 | 2.1 |
| Bed Withdrawal | 0.0 | - | - | - | - | - |
| First Stage Cyclone | 34.0 | 23.9 | 5.1 | 13.5 | 2.8 | 4.9 |
| Second Stage Cyclone[d] | 177.8 | 22.4 | 2.6 | 5.8 | 28.5 | 2.0 |

---

[d] Analyses based on material collected between 15 and 18 hour point during run.

## TABLE G3. MINIPLANT SOLIDS ANALYSES (CONTINUED)

| Run No. | 14.2 | | | | | |
|---|---|---|---|---|---|---|
| | Wgt (kg) | %Ca | %S | $\%SO_4^=$ | %C | $\%CO_3^=$ |
| Coal Feed | 2508.9 | - | 2.4 | - | 76.1 | - |
| Limestone Feed | 117.5 | 39.1 | - | - | - | 59.6 |
| Initial Bed | 141.1 | 39.0 | - | 34.3 | 1.3 | 2.1 |
| Final Bed | 229.5 | - | - | 46.9 | 1.3 | 7.0 |
| Bed Withdrawal | 0.0 | - | - | - | - | - |
| First Stage Cyclone | 53.3 | 30.7 | - | - | 3.0 | 2.0 |
| Second Stage Cyclone | 191.9 | 7.7 | 2.4 | 5.6 | 35.7 | 1.5 |

| Run No. | 15.1 | | | | | |
|---|---|---|---|---|---|---|
| | Wgt (kg) | %Ca | %S | $\%SO_4^=$ | %C | $\%CO_3^=$ |
| Coal Feed | 2409.5 | - | 2.4 | - | 76.1 | - |
| Limestone Feed | 240.9 | 39.1 | - | - | - | 59.6 |
| Initial Bed (Fresh) | 116.1 | 39.1 | - | - | - | 59.6 |
| Final Bed | 217.7 | - | - | - | - | - |
| Bed Withdrawal | 220.9 | - | 8.0 | 22.0 | 2.3 | - |
| First Stage Cyclone | - | - | - | - | - | - |
| Second Stage Cyclone | 116.0 | 9.7 | - | 7.0 | 24.4 | 2.3 |

## TABLE G3. MINIPLANT SOLIDS ANALYSES (CONTINUED)

| Run No. | 15.2<br>Wgt (kg) | %Ca | %S | $\%SO_4^=$ | %C | $\%CO_3^=$ |
|---|---|---|---|---|---|---|
| Coal Feed | 985.7 | - | 2.4 | - | 76.1 | - |
| Limestone Feed | 98.4 | 39.1 | - | - | - | 59.6 |
| Initial Bed | 217.7 | - | - | - | - | - |
| Final Bed | 205.9 | 29.8 | 9.0 | 25.6 | 2.5 | - |
| Bed Withdrawal | 108.0 | - | - | - | - | - |
| First Stage Cyclone | 24.0 | 20.5 | 4.0 | 11.6 | 5.0 | 7.6 |
| Second Stage Cyclone | 48.5 | 10.1 | 3.1 | 7.4 | 27.8 | 1.3 |

| Run No. | 15.3<br>Wgt (kg) | %Ca | %S | $\%SO_4^=$ | %C | $\%CO_3^=$ |
|---|---|---|---|---|---|---|
| Coal Feed | 1262.4 | - | 2.4 | - | 76.1 | - |
| Limestone Feed | 126.1 | 39.1 | - | - | - | 59.6 |
| Initial Bed | 205.9 | 29.8 | 9.0 | 25.6 | 2.5 | - |
| Final Bed | - | - | - | - | - | - |
| Bed Withdrawal | 95.7 | 37.2 | 11.3 | 30.9 | 4.1 | - |
| First Stage Cyclone | 19.3 | 26.7 | 7.1 | 19.7 | 12.8 | - |
| Second Stage Cyclone | 67.5 | 19.4 | 3.1 | 7.5 | 32.7 | - |

## TABLE G3. MINIPLANT SOLIDS ANALYSES (CONTINUED)

| Run No. | 15.4<br>Wgt (kg) | %Ca | %S | $\%SO_4^=$ | %C | $\%CO_3^=$ |
|---|---|---|---|---|---|---|
| Coal Feed | 1778.1 | - | 2.4 | - | 76.1 | - |
| Limestone Feed | 177.8 | 39.1 | - | - | - | 59.6 |
| Initial Bed | - | - | - | - | - | - |
| Final Bed | - | - | - | - | - | - |
| Bed Withdrawal | 84.1 | 34.5 | 10.9 | 31.8 | 3.3 | 13.7 |
| First Stage Cyclone | 21.8 | 21.9 | 9.8 | - | 12.2 | - |
| Second Stage Cyclone | 125.7 | 10.2 | 3.4 | 12.5 | 12.1 | 1.0 |

| Run No. | 16.1<br>Wgt (kg) | %Ca | %S | $\%SO_4^=$ | %C | $\%CO_3^=$ |
|---|---|---|---|---|---|---|
| Coal Feed | 1451.5 | - | 2.2 | - | 76.4 | - |
| Limestone Feed | 145.6 | 39.1 | - | - | - | 59.6 |
| Initial Bed (Fresh) | 122.5 | 39.1 | - | - | - | 59.6 |
| Final Bed | 204.1 | 46.2 | 5.3 | 15.7 | - | 37.4 |
| Bed Withdrawal | 11.1 | 17.0 | - | 15.2 | - | 4.8 |
| First Stage Cyclone | 15.6 | 8.2 | 3.0 | 4.4 | 53.1 | 2.0 |
| Second Stage Cyclone | 90.9 | 6.3 | 3.1 | 6.4 | 32.1 | 1.8 |

## TABLE G3. MINIPLANT SOLIDS ANALYSES (CONTINUED)

| Run No. | 17.1 | | | | | |
|---|---|---|---|---|---|---|
| | Wgt (kg) | %Ca | %S | %$SO_4^=$ | %C | %$CO_3^=$ |
| Coal Feed | 6053.7 | - | 2.2 | - | 76.4 | - |
| Limestone Feed | - | 39.1 | - | - | - | 59.6 |
| Initial Bed (Fresh) | 82.1 | 39.1 | - | - | - | 59.6 |
| Final Bed | 196.8 | 29.2 | 9.7 | 28.6 | 5.1 | 24.7 |
| Bed Withdrawal | 95.7 | 33.7 | 5.6 | 17.6 | 7.6 | 32.9 |
| First Stage Cyclone | 17.2 | 20.1 | 5.8 | 11.1 | 0.7 | 2.7 |
| Second Stage Cyclone | 321.1 | 9.5 | 2.7 | 4.0 | 20.6 | 3.0 |

| Run No. | 18.3 | | | | | |
|---|---|---|---|---|---|---|
| | Wgt (kg) | %Ca | %S | %$SO_4^=$ | %C | %$CO_3^=$ |
| Coal Feed | 6481.3 | - | 2.2 | - | 76.4 | - |
| Limestone Feed | 280.8 | 39.1 | - | - | - | 59.6 |
| Initial Bed | 102.1 | - | - | - | - | - |
| Final Bed | 140.6 | 18.8 | 14.2 | 37.7 | 0.4 | 1.0 |
| Bed Withdrawal | 86.4 | 25.5 | 8 | 27.0 | 1.7 | 7.3 |
| First Stage Cyclone | 4.5 | - | - | - | 0.6 | - |
| Second Stage Cyclone | 475.8 | 5.1 | 2.6 | 13.5 | 6.1 | 0.5 |

## TABLE G3. MINIPLANT SOLIDS ANALYSES (CONTINUED)

| Run No. | 19.2<br>Wgt (kg) | %Ca | %S | %$SO_4^=$ | %C | %$CO_3^=$ |
|---|---|---|---|---|---|---|
| Coal Feed | 1072.3 | - | 2.2 | - | 76.4 | - |
| Limestone Feed | 107.0 | 39.1 | - | - | - | 59.6 |
| Initial Bed | 117.9 | - | - | - | - | - |
| Final Bed | 195.0 | 24.0[e] | 4.9[e] | 23.0 | - | 20.9 |
| Bed Withdrawal | 17.7 | 32.2 | 5.9 | 18.2 | - | 6.4 |
| First Stage Cyclone | - | - | - | - | - | - |
| Second Stage Cyclone | 149.5 | 9.6 | 1.4 | 6.0 | 22.5 | 1.7 |

---

e Questionable results.

| Run. No. | 19.3<br>Wgt (kg) | %Ca | %S | %$SO_4^=$ | %C | %$CO_3^=$ |
|---|---|---|---|---|---|---|
| Coal Feed | 714.0 | - | 2.2 | - | 76.5 | - |
| Limestone Feed | 70.8 | 39.1 | - | - | - | 59.6 |
| Initial Bed | 195.0 | 24.0[e] | 4.9 | 23.8 | - | 20.9 |
| Final Bed | 217.3 | 25.6[e] | 7.8 | 20.8 | 6.2 | 29.8 |
| Bed Withdrawal | 30.2 | 23.3 | 7.7 | 20.4 | 5.7 | 30.2 |
| First Stage Cyclone | - | - | - | - | - | - |
| Second Stage Cyclone | 83.9 | 4.3 | 2.9 | 8.4 | 27.9 | 0.7 |

TABLE G4. MINIPLANT CALCIUM AND SULFUR BALANCES

| Run No. | Calcium (%) | Sulfur (%) |
|---|---|---|
| 11.1 | 85 | 47 |
| 11.2 | 70 | 57 |
| 12.1 | 108 | 118 |
| 12.2 | 99 | 98 |
| 13.2 | 110 | 93 |
| 14.1 | 115 | 112 |
| 16.1 | 94 | -- |
| 19.3 | 88 | 90 |
| Average | 96 ± 15 (1S) | 88 ± 27 (1S) |

# APPENDIX H

# BATCH UNIT RUN SUMMARIES

Page

TABLE H1. SUMMARY OF BATCH COMBUSTOR OPERATING CONDITIONS 199

TABLE H2. SUMMARY OF BATCH COMBUSTOR EMISSIONS DATA 202

TABLE H3. BATCH COMBUSTOR BED AND OVERHEAD SOLIDS ANALYSES ( RUNS 145C, 2C-5C) 205

TABLE H4. BATCH COMBUSTOR BED AND OVERHEAD SOLIDS ANALYSIS 206

TABLE H5. SUMMARY OF PARTICULATE LOADINGS FOR BATCH UNIT 207

TABLE H6. BATCH COMBUSTOR CYCLONE COLLECTION EFFICIENCIES 209

TABLE H7. ANALYSIS OF ARKWRIGHT COAL ASH 210

## TABLE H1. SUMMARY OF BATCH COMBUSTOR OPERATING CONDITIONS

| Run No. | Sorbent | Pressure, kPa | Sup. Vel., m/s | Settled Bed Depth, m | Bed Temperature °C |  | Excess Air, % | Coal, kg./hr. | Run Length, hr. |
|---|---|---|---|---|---|---|---|---|---|
|  |  |  |  |  | Avg. | Range |  |  |  |
| 6-2690- |  |  |  |  |  |  |  |  |  |
| 112aC | 1C | 810 | 0.94 | 0.49 | 805 | 640-925 | 43 | 6.04 | 0.30 |
| 112b | 1C | 810 | 1.02 | 0.49 | 905 | 805-1035 | 23 | 7.04 | 0.48 |
| 127 | 2HC | 540 | 1.30 | 0.49 | 805 | 705-920 | 104 | 3.90 | 0.53 |
| 128 | 2HC | 540 | 1.40 | 0.49 | 850 | 760-1000 | 153 | 3.27 | 0.43 |
| 129 | 2HC | 870 | 0.92 | 0.49 | 845 | 730-905 | 130 | 3.90 | 0.55 |
| 133 | 1C | 660 | 1.70 | 0.17 | 870 | 815-975 | 43 | 8.40 | 2.00 |
| 134 | 1R | 660 | 1.66 | 0.29 | >1095 | 760-1150 | 8 | 9.08 | 0.33 |
| 136 | 1C | 610 | 1.46 | 0.09 | 740 | 675-815 | 97 | 5.68 | 0.50 |
| 138 | 1C | 660 | 1.65 | 0.23 | 975 | 805-1180 | 77 | 6.04 | 2.00 |
| 139 | 1C | 880 | 1.19 | 0.38 | 950 | 795-1075 | 27 | 8.31 | 1.00 |
| 141 | 2HC | 660 | 1.95 | 0.50 | 1095 | 680-1370 | 45 | 7.99 | 2.00 |
| 142 | 2HC | 660 | 1.67 | 0.50 | 955 | 860-1045 | 26 | 8.76 | 1.80 |
| 143 | 2HC | 660 | 1.50 | 0.50 | 795 | 595-830 | 110 | 5.36 | 1.00 |
| 145 | 2HC | 660 | 1.50 | 0.50 | 925 | 610-1000 | 88 | 5.40 | 4.50 |
| 675-1C | 2HC | 660 | 1.17 | 0.50 | 845 | 705-955 | 56 | 5.45 | 1.50 |
| 2 | 2HC | 640 | 1.41 | 0.50 | 875 | 730-1000 | 61 | 5.99 | 3.00 |
| 3 | 1R | 630 | 1.47 | 0.51 | 900 | 790-970 | 27 | 7.67 | 2.63 |
| 4 | 2HC | 630 | 1.17 | 0.50 | 925 | 760-1010 | 58 | 7.35W | 3.08 |
| 5 | 2HC | 630 | 1.34 | 0.50 | 805 | 650-960 | 43 | 7.95I | 1.02 |
| 6 | 1R | 840 | 1.43 | 0.52 | 880 | 790-980 | 43 | 8.99 | 1.97 |
| 8 | 2R | 700 | 1.56 | 0.50 | 875 | 705-945 | 44 | 7.26S | 2.00 |
| 9 | 1R | 800 | 1.14 | 1.03 | 690 | 480-980 | 8 | 11.30 | 1.25 |
|  |  |  |  |  | Vertical Coils Installed |  |  |  |  |
| 11 | 1R | 810 | 1.17-1.37 | 0.51 | 850 | 827-916 | 15 | 10.90 | 0.67 |
| 14 | 1R | 800 | 0.58 | 1.03 | 350 | 200-800 | 0 | 10.90 | 0.82 |
| 15 | 1R | 800 | 1.06 | 1.04 | 620 | 570-710 | 0 | 13.94(a) | 1.08 |
| 17 | 1R | 810 | 1.49 | 0.51 | 920 | 880-950 | 19 | 10.49 | 1.92 |
| 18 | 1R | 850 | 1.36 | 0.51 | 860 | 820-880 | 1 | 12.39 | 1.92 |

## TABLE H1. SUMMARY OF BATCH COMBUSTOR OPERATING CONDITIONS (Cont'd)

| Run No. | Sorbent | Pressure, kPa | Sup. Vel., m/s | Settled Bed Depth, m | Bed Temperature °C Avg. | Bed Temperature °C Range | Excess Air, % | Coal, kg./hr. | Run Length, hr. |
|---|---|---|---|---|---|---|---|---|---|
| 20 | 1R | 800 | 1.22 | 0.51 | 827 | 780-840 | 24 | 8.85 | 2.00 |
| 21 | 1R | 800 | 1.27 | 0.51 | 855 | 810-930 | 13 | 9.90 | 1.33 |
| 22 | Bed from 21C | 800 | 1.26 | 0.43 (est) | 850 | 820-910 | 15 | 9.72 | 2.92 |
| 23 | 2R | 800 | 1.25 | 0.51 | 920 | 890-970 | 30 | 7.72 | 2.50 |
| 25 | 2R | 800 | 1.28 | 0.51 | 910 | 875-950 | 42 | 7.57 | 5.10 |
| 26 | Bed from 25 | 800 | 1.23 | 0.27 | 975 | (b) | 138 | 4.13 | 4.50 |
| 28 | 1R | 800 | 1.07 | 0.55 | 840 | 785-890 | 29 | 7.35 | 4.50 |
| 29 | Bed from 28 | 810 | 1.10 | 0.46 | 870 | 750-890 | 46 | 6.54 | 5.08 |
| 31 | 2R | 800 | 1.58 | 0.88 | 895 | 855-950 | 5 | 12.71 | 2.12 |
| 32 | 1R | 800 | 1.58 | 0.82 | 885 | 865-945 | 0 | 14.12 | 2.67 |
| 34 | 3 | 800 | 1.10 | 0.52 | 870 | 860-895 | 16 | 8.17 | 5.58 |
| 36 | 3 | 790 | 1.23 | 0.52 | 863 | 825-895 | 27 | 8.35 | 3.83 |
| 37 | 3 | 800 | 1.20 | 0.52 | 893 | 875-930 | 24 | 8.04 | 1.50 |
| 38 | 3 | 800 | 1.25 | 0.52 | 860 | 815-900 | 34 | 8.17 | 1.67 |
| 46 | 1R | 800 | 1.14 | 0.46 | 911 | 872-963 | 32 | 7.25 | 2.00 |
| 50 | 1R | 800 | 1.40 | 0.77 | 887 | 825-965 | 31 | 9.08 | 3.50 |
| 51 | 1R | 811 | 1.43 | 0.77 | 850 | 795-915 | 14 | 11.26 | 3.83 |
| 53 | Bed from 51C | 800 | 1.45 | -- | 857 | 750-975 | 24 | 10.25 | 3.53 |
| 54 | 1R | 800 | 1.09 | 0.77 | 751 | 652-872 | 25 | 8.44 | 2.67 |
| 55 | 1R | 800 | 1.65 | 0.77 | 867 | 717-940 | 17 | 12.25 | 1.75 |
| 56 | 1R | 800 | 1.10 | 0.55 | 877 | 794-975 | 22 | 7.72 | 3.50 |

## TABLE H1. SUMMARY OF BATCH COMBUSTOR OPERATING CONDITIONS (Cont'd)

NOTES:

Coal: Arkwright Mine, W. Vir., 2.6% S, -16 mesh used unless otherwise noted.
S = Arkwright coal screened to remove fines less than 70 mesh.
W = Wyoming coal, 0.7% S.
I = Illinois coal, 4.1% S.

Stone: (1) = Grove limestone, 8 x 25 mesh (BCR No. 1359).
(2) = Tymochtee dolomite, 8 x 25 mesh.
(3) = Alundum
C = Calcined
HC = Half-calcined
R = Raw stone, not calcined.

(a) Coal probe positioned downward for 15C and all subsequent runs.

(b) Only one thermocouple in bed.

TABLE H2. SUMMARY OF BATCH COMBUSTOR EMISSIONS DATA

| | NO (Average) | | $SO_2$ (Average) | | | $SO_2$ (Final) | | | | | |
|---|---|---|---|---|---|---|---|---|---|---|---|
| Run No. | ppm | $\frac{lb\ NO_2}{10^6\ BTU}$ | ppm | $\frac{lb\ SO_2}{10^6\ BTU}$ | % Reduction | ppm | $\frac{lb\ SO_2}{10^6\ BTU}$ | % Reduction | % Sulfation | Combustion Efficiency (%) | % Sulfur Balance |
| Phase I<br>Sampling System | | | | | | | | | | | |
| 6-2690-112aC | 310 | 0.54 | 240 | 0.58 | 85 | | | | | | |
| 112b | 290 | 0.43 | 250 | 0.52 | 86 | | | | | | |
| 127 | 340 | 0.83 | 145 | 0.50 | 87 | 400 | 1.37 | 64 | | | |
| 128 | 450 | 1.36 | 250 | 1.05 | 72 | 550 | 2.32 | 39 | | | |
| 129 | 410 | 1.12 | 145 | 0.55 | 86 | | | | | | |
| 133 | 340 | 0.59 | n.m. | -- | -- | n.m. | -- | -- | | | |
| 134 | n.m. | -- | 1000 | 1.84 | 50 | | | | | | |
| 136 | 310 | 0.71 | 1100 | 3.50 | 8 | | | | | | |
| 138 | 300 | 0.64 | 860 | 2.56 | 34 | 1060 | 3.15 | 18 | | | |
| 139 | 380 | 0.59 | 240 | 0.52 | 87 | 400 | 0.86 | 78 | | | |
| 141 | 470 | 0.82 | 730 | 1.78 | 54 | 1250 | 3.05 | 22 | | | |
| 142 | 610 | 0.93 | 1700 | 3.62 | 6 | | | | | | |
| 143 | 300 | 0.76 | 120 | 0.43 | 89 | 225 | 0.78 | 79 | | | |
| 145 | 365 | 0.82 | 340 | 1.07 | 72 | 675 | 2.12 | 44 | 55 | 97.5 | 83 |
| 675-1C | 335 | 0.63 | 135 | 0.35 | 91 | 650 | 1.71 | 55 | | | |
| 2 | 370 | 0.73 | 150 | 0.42 | 89 | 600 | 1.63 | 57 | 43 | 95.3 | 93 |
| 3 | 240 | 0.37 | 545 | 1.17 | 69 | 900 | 1.93 | 49 | 6 | 92.3 | 67 |
| 4 | 250 | 0.47 | 40 | 0.10 | 91 | 75 | 0.17 | 83 | 13 | 98.1 | 106 |
| 5 | 230 | 0.41 | 1800 | 4.50 | 35 | 2110 | 4.33 | 24 | 3 | 94.2 | 81 |
| 6 | 220 | 0.38 | 200 | 0.48 | 87 | 640 | 1.54 | 60 | | 95.3 | |
| 8 | 160 | 0.28 | 24 | 0.06 | 98 | 880 | 2.13 | 44 | 34 | 82.8 | |
| 9 | 220 | 0.29 | 18 | 0.03 | 99 | 250 | 0.46 | 88 | | | |
| Vertical Coils | | | | | | | | | | | |
| 11 | 180 | 0.22 | 170 | 0.29 | 93 | 1100 | 1.85 | 52 | 8 | 86.6 | |
| 14 | 170 | 0.18 | 320 | 0.47 | 87 | 630 | 0.92 | 75 | | 76.0 | |
| 15 | 150 | 0.16 | n.m. | -- | -- | n.m. | -- | -- | | 59.7 | |
| 17 | 150 | 0.22 | 25 | 0.05 | 99 | 75 | 0.15 | 96 | 20 | 86.3 | 82 |
| 18 | 170 | 0.21 | 520 | 0.89 | 76 | 790 | 1.36 | 64 | 39 | 87.9 | 120 |

TABLE H2. SUMMARY OF BATCH COMBUSTOR EMISSIONS DATA (Cont'd)

| Run No. | NO (Average) |  | $SO_2$ (Average) |  |  | $SO_2$ (Final) |  |  |  |  |  |
|---|---|---|---|---|---|---|---|---|---|---|---|
|  | ppm | $\frac{\text{lb } NO_2}{10^6 \text{ BTU}}$ | ppm | $\frac{\text{lb } SO_2}{10^6 \text{ BTU}}$ | % Reduction | ppm | $\frac{\text{lb } SO_2}{10^6 \text{ BTU}}$ | % Reduction | % Sulfation | Combustion Efficiency (%) | % Sulfur Balance |
| Phase II Sampling System |  |  |  |  |  |  |  |  |  |  |  |
| 20 | 180 | 0.21 | 31 | 0.07 | 98 | 130 | 0.27 | 93 |  | 88.5 |  |
| 21 | 170 | 1.23 | 0 | 0.00 | 100 | 0 | 0.00 | 100 |  | 89.8 |  |
| 22 | 205 | 0.29 | 280 | 0.55 | 86 | 850 | 1.66 | 56 |  | 86.6 |  |
| 23 | 330 | 0.52 | 47 | 0.10 | 97 | 340 | 0.75 | 80 | 27 | 94.3 | 71 |
| 25 | n.m. | -- | 4 | 0.07 | 99 | 130 | 0.31 | 92 | 35 | 96.8 | 43 |
| 26 | 160 | 0.45 | 160 | 0.65 | 84 | 660 | 2.61 | 31 | 63 | 97.6 | 31 |
| 28 | n.m. | -- | 100 | 0.23 | 94 | 265 | 0.58 | 85 | 27 | 93.5 | 86 |
| 29 | n.m. | -- | 240 | 0.58 | 84 | 322 | 0.79 | 79 | 61 | 94.3 | 123 |
| 31 | n.m. | -- | 60 | 0.10 | 97 | 150 | 0.27 | 93 | 30 |  | 94 |
| 32 | n.m. | -- | 75 | 0.12 | 97 | 150 | 0.25 | 93 | 48 |  | 158 |
| 34 | 66 | 0.10 | 594 | 1.20 | 68 | 1130 | 2.29 | 40 |  |  |  |
| 36 | 150 | 0.23 | 830 | 1.79 | 53 | 1140 | 2.45 | 35 |  |  |  |
| 37 | 160 | 0.25 | 839 | 1.80 | 53 | 970 | 2.08 | 45 |  |  |  |
| 38 | 123 | 0.20 | 936 | 2.10 | 44 | 1140 | 2.58 | 32 |  |  |  |
| Phase III Sampling System |  |  |  |  |  |  |  |  |  |  |  |
| 46 | 201 | 0.33 | 545 | 1.21 | 66 | 790 | 1.76 | 51 | 15 |  |  |
| 50 | 176 | 0.28 | 636 | 1.41 | 63 | 870 | 1.94 | 49 |  |  |  |
| 51 | 153 | 0.21 | 772 | 1.50 | 60 | 1130 | 2.19 | 42 | 26 | 94.0 |  |
| 53 | 166 | 0.25 | 1021 | 2.15 | 44 | 1510 | 3.19 | 17 | 42 | 93.0 |  |
| 54 | 217 | 0.33 | 573 | 1.21 | 68 | 1170 | 2.49 | 34 | 54 | 87.0 |  |
| 55 | 160 | 0.23 | 749 | 1.48 | 61 | 1130 | 2.25 | 41 | 20 |  |  |
| 56 | 198 | 0.30 | 264 | 0.55 | 85 | 830 | 1.73 | 54 | 20 |  | 83 |

---

n.m. = not measured because of problems with equipment

## TABLE H-2. SUMMARY OF BATCH COMBUSTOR EMISSIONS DATA (CON'T)

| Run No. 3675- | CO (ppm) | Temperature (°C) | Excess Air (%) |
|---|---|---|---|
| 1C | 182 | 845 | 56 |
| 2 | 450 | 875 | 61 |
| 3 | 320 | 900 | 27 |
| 4 | 1190 | 925 | 58 |
| 5 | 2040 | 805 | 43 |
| 6 | 830 | 880 | 43 |
| 8 | 950 | 875 | 44 |
| 9 | 1610 | 690 | 8 |
| 11 | 4740 | 850 | 55 |
| 14 | 1400 | 350 | 0 |
| 15 | n.m. | 620 | 0 |
| 17 | 570 | 920 | 19 |
| 18 | 1900 | 860 | 1 |
| 20 | 3100 | 827 | 24 |
| 21 | 610 | 855 | 13 |
| 22 | 1230 | 850 | 15 |
| 23 | 47 | 920 | 30 |
| 25 | 105 | 910 | 42 |
| 26 | 4 | 975 | 58 |
| 28 | 430 | 840 | 29 |
| 29 | 129 | 870 | 46 |
| 31 | 700 | 895 | 5 |
| 32 | 700 | 885 | 0 |
| 34 | 710 | 870 | 16 |
| 36 | 470 | 863 | 27 |
| 37 | 407 | 893 | 24 |
| 38 | 710 | 860 | 34 |
| 46 | n.m. | 911 | 32 |
| 50 | 123 | 887 | 31 |
| 51 | 325 | 850 | 14 |
| 53 | 397 | 857 | 24 |
| 54 | 3642 | 751 | 25 |
| 55 | 71 | 867 | 17 |
| 56 | 165 | 877 | 22 |

### TABLE H3. BATCH COMBUSTOR BED AND OVERHEAD SOLIDS ANALYSIS (RUNS 145C, 2C-5C)

| | Run 145C | Run 2C | Run 3C | Run 4C | Run 5C |
|---|---|---|---|---|---|
| Bed | | | | | |
| $CaSO_4$ | 41.13 | 37.70 | 9.13 | 12.39 | 2.59 |
| $CaCO_3$ | 3.30 | 2.60 | 63.26 | 24.72 | 64.26 |
| CaO | 12.01 | 18.80 | 21.43 | 20.93 | 0.00 |
| MgO | 23.21 | 28.20 | <0.32 | 17.73 | 21.64 |
| $MgCO_3$ | | | | | 0.71 |
| $Al_2O_3$ | 2.96 | 4.40 | <0.41 | 2.65 | 1.02 |
| $SiO_2$ | 7.51 | 7.70 | 0.42 | 11.12 | 3.61 |
| $Fe_2O_3$ | 3.51 | 4.00 | 0.16 | 2.39 | 0.16 |
| NiO | | | <0.15 | <0.15 | <0.15 |
| $Na_2O$ | | | <0.12 | <0.31 | <0.31 |
| $V_2O_5$ | | | <1.82 | <1.82 | <1.82 |
| $H_2O$ | 3.01 | | | | |
| Overhead | | | | | |
| $CaSO_4$ | 7.49 | | 9.40 | 11.85 | 8.58 |
| $CaCO_3$ | 14.51 | | 10.21 | 16.82 | 13.91 |
| CaO | 12.57 | | 2.97 | 16.16 | 0.00 |
| MgO | 16.60 | | 1.65 | 15.43 | 4.72 |
| $MgCO_3$ | | | | | 5.99 |
| $Al_2O_3$ | 7.65 | | 11.32 | 7.24 | 7.34 |
| $SiO_2$ | 16.11 | | 18.63 | 16.47 | 19.05 |
| $Fe_2O_3$ | 4.31 | | 6.06 | 3.19 | 7.82 |
| NiO | | | <0.15 | <0.15 | <0.15 |
| $Na_2O$ | | | 0.68 | <0.31 | 0.81 |
| $V_2O_5$ | | | <1.82 | <1.82 | <1.82 |
| C | 11.00 | 19.00 | 36.08 | 6.18 | 21.78 |
| $H_2O$ | 2.30 | | | | |

---

All values are weight percent

TABLE H4. BATCH COMBUSTOR BED AND OVERHEAD SOLIDS ANALYSIS

| | Bed | | | Cyclone 1 | | | | Cyclone 2 | | | | Filter | | | |
|---|---|---|---|---|---|---|---|---|---|---|---|---|---|---|---|
| Run No. | $Ca^{++}$ | $SO_4^=$ | $CO_3^=$ | Total C[a] | Total S | $SO_4^=$ | $CO_3^=$ | Total C[a] | Total S | $SO_4^=$ | $CO_3^=$ | Total C[a] | Total S | $SO_4^=$ | $CO_3^=$ |
| 3675-14 | | | | 58.14 | | | 6.50 | 68.48 | | | 6.50 | | | | |
| 15 | | | | 64.33 | | | 2.76 | 65.88 | | | 2.85 | 47.19 | | | 9.51 |
| 17 | | 22.10 | 4.34 | 60.76 | | | 2.56 | 36.37 | | | 8.51 | 44.74 | | | 3.26 |
| 18 | 23.90 | 22.30 | | 48.62 | | | 3.60 | | | | | | | | |
| 20 | | 22.40 | | 53.50 | | | | | | | | | | | |
| 21 | | 21.00 | | 53.81 | | | | | | | | | | | |
| 22 | | 29.00 | | 67.03 | | | | | | | | | | | |
| 23 | 29.50 | 18.90 | 2.93 | 29.80 | | | 0.77 | | | | | | | | |
| 25 | 27.20 | 22.60 | | 22.62 | | | 1.85 | | | | | 11.66 | | | 0.43 |
| 26 | 20.00 | 30.30 | | 12.00 | | | 2.63 | | | | | | | | |
| 28 | 34.80 | 22.90 | 29.90 | 45.76 | | | 9.45 | 36.14 | | | 0.43 | 28.67 | | | 0.87 |
| 29 | 28.40 | 41.50 | | 29.32 | | 7.70 | | 39.63 | | 5.05 | | 46.29 | | 4.77 | |
| 31 | 26.80 | 19.20 | | 18.43 | | 11.30 | | | | | | 30.20 | | 11.90 | |
| 32 | 35.50 | 41.00 | | 46.68 | | 5.89 | | | | | | 41.75 | | 7.06 | |
| 34 | | | | 36.90 | 1.59 | 2.44 | | | | | | 31.80 | | 5.89 | |
| 36 | | | | 46.95 | 1.24 | 1.84 | | | | | | 42.31 | | 6.35 | |
| 37 | | | | | | | | | | | | | | | |
| 38 | | | | 45.51 | 1.28 | 1.83 | | | | | | | | | |
| 46 | 51.10 | 18.48 | | 51.41 | 1.75 | | 2.45 | | | | | 30.83 | 3.48 | | 1.41 |
| 50 | | | | | | | | | | | | | | | |
| 51 | 40.10 | 24.66 | 36.16 | 42.02 | 2.19 | | 1.41 | | | | | 40.56 | 2.53 | | 0.66 |
| 53 | 20.21 | 20.56 | | 52.22 | 2.20 | | | | | | | 39.64 | 3.21 | | |
| 54 | 18.81 | 24.55 | | 54.15 | 1.80 | | | | | | | 51.95 | 2.72 | | |
| 55 | 38.70 | 18.78 | 31.03 | 50.08 | 2.30 | | 0.71 | 27.94 | 2.49 | | | | | | |
| 56 | 46.30 | 21.87 | 8.17 | 35.01 | 1.30 | | | | | | | 58.33 | 2.02 | | |

---

All values are weight percent

[a] Includes carbon present as $CO_3^=$

TABLE H5. SUMMARY OF PARTICULATE LOADINGS FOR BATCH UNIT

| Run Number | Bed Outlet Loading (gr/scf) | Cyclone #1 Outlet Loading (gr/scf) | Cyclone #2 Outlet Loading (gr/scf) |
|---|---|---|---|
| 675-1C (T) | 7.83 | Particulates from Cyclones 2 and 3 filter not weighed. | |
| 2 (T) | 7.25 | 0.33 | 0.03 |
| 3 (G) | 8.24 | 1.16 | 0.38 (Cyclone #2 plugged) |
| 4 (T) | 7.91 | 0.01 | 0.01 |
| 5 (T) | 9.35 | 0.07 | 0.07 |
| 6 | No data available | | |
| 8 (T) | 6.[illegible] | 0.73 | 0.60 |
| 9 | No data available | | |
| 11 (G) | 11.54 | 11.54 (Cyclone #1 plugged) | 3.43 |
| 14 | Solids caught by filter burned | | |
| 15 (G) | 36.94 | 8.29 | 1.42 |
| 17 (G) | 9.23 | 0.76 | 0.19 |
| 18 (G) | 11.32 | 3.60 | 0.27 |
| 20 (G) | 7.83 | 0.72 | 0.10 |
| 21 (G) | 8.19 | 0.76 | 0.15 |
| 22 (G) | 8.23 | 0.35 | 0.10 |
| 23 (T) | 7.43 | 0.61 | 0.35 |
| 25 (T) | 5.48 | 0.87 | 0.78 |
| 26 (T) | 4.31 | 0.78 | 0.47 |
| 28 (G) | 5.75 | 1.64 | 0.84 |
| 29 (G) | 5.74 | 2.19 | 0.70 |
| 31 (T) | 12.48 | 3.42 | 3.22 (Cyclone #2 plugged) |
| 32 (G) | 12.26 | 4.93 | 4.62 (Cyclone #2 plugged) |
| 34 (A) | 4.85 | 1.66 | 1.49 (Cyclone #2 plugged) |
| 36 (A) | 5.22 | 1.11 | 0.61 |
| 37 (A) | 5.73 | 0.72 | 0.14 |
| 38 (A) | 5.40 | 0.60 | 0.12 |
| 46 (G) | 6.40 | 1.07 | 0.95 |

TABLE H5. (Continued) SUMMARY OF PARTICULATE LOADINGS FOR BATCH UNIT

| Run Number | Bed Outlet Loading (gr/scf) | Cyclone #1 Outlet Loading (gr/scf) | Cyclone #2 Outlet Loading (gr/scf) |
|---|---|---|---|
| 50 (G) | 8.30 | 3.58 | 3.12 |
| 51 (G) | 5.73 | 1.88 | 1.51 |
| 53 (G) | 5.59 | 2.21 | 0.55 |
| 54 (G) | 8.85 | 2.57 | 1.53 |
| 55 (G) | 7.92 | 1.26 | 0.09 |
| 56C (G) | 6.47 | 0.63 | 0.42 |

---

Note: Letters in parenthesis indicate bed material - (G) - Grove limestone
(T) - Tymochtee Dolomite
(A) - Alundum

## TABLE H6. BATCH COMBUSTOR CYCLONE COLLECTION EFFICIENCIES

| Run No. | Cyclone 1 | Cyclone 2 | Overall |
|---|---|---|---|
| 3675-2C | 0.95 | 0.90 | 1.00 |
| 8 | 0.90 | 0.18 | 0.91 |
| 15 | 0.78 | 0.83 | 0.97 |
| 17 | 0.92 | 0.75 | 0.98 |
| 18 | 0.68 | 0.93 | 0.98 |
| 20 | 0.91 | 0.86 | 0.99 |
| 21 | 0.91 | 0.80 | 0.98 |
| 22 | 0.96 | 0.71 | 0.99 |
| 23 | 0.92 | 0.43 | 0.95 |
| 25 | 0.84 | 0.10 | 0.86 |
| 26 | 0.82 | 0.40 | 0.89 |
| 28 | 0.72 | 0.48 | 0.85 |
| 29 | 0.62 | 0.68 | 0.87 |
| 31 | 0.73 | 0.10 | 0.74 |
| 32 | 0.58 | 0.10 | 0.61 |
| 34 | 0.66 | 0.10 | 0.69 |
| 36 | 0.79 | 0.45 | 0.88 |
| 37 | 0.88 | 0.80 | 0.98 |
| 38 | 0.89 | 0.80 | 0.98 |
| 46 | 0.83 | 0.11 | 0.85 |
| 50 | 0.57 | 0.12 | 0.62 |
| 51 | 0.67 | 0.20 | 0.74 |
| 53 | 0.60 | 0.75 | 0.90 |
| 54 | 0.71 | 0.41 | 0.83 |
| 55 | 0.84 | 0.93 | 0.99 |
| 56 | 0.90 | 0.33 | 0.94 |

---

$$\text{Efficiency} = \frac{\text{mass collected}}{\text{mass entering}}$$

## TABLE H7. ANALYSIS OF ARKWRIGHT COAL ASH

| Component | Wt. % | Mole % |
|---|---|---|
| CaO | 2.7 | 3.7 |
| $Fe_2O_3$ | 19.0 | 9.2 |
| $Al_2O_3$ | 32.1 | 24.5 |
| $SiO_2$ | 47.1 | 60.8 |
| $Na_2O$ | 1.5 | 1.9 |
| Other | -2.4 | — |

Total ash in coal = 7.3 wt. percent.